MycoKeys 87: 1–52 (2022)
doi: 10.3897/mycokeys.87.73082
https://mycokeys.pensoft.net

RESEARCH ARTICLE

A peer-reviewed open-access journal
MycoKeys
Launched to accelerate biodiversity research

Examination of the generic concept and species boundaries of the genus *Erioscyphella* (Lachnaceae, Helotiales, Ascomycota) with the proposal of new species and new combinations based on the Japanese materials

Yukito Tochihara[1,2], Tsuyoshi Hosoya[2]

1 *Department of Biological Sciences, Graduate School of Science, The University of Tokyo, Hongo 7-3-1, Bunkyo-ku, Tokyo 113-0033, Japan* **2** *Department of Botany, National Museum of Nature and Science, 4-1-1 Amakubo, Tsukuba, Ibaraki 305-0005, Japan*

Corresponding author: Yukito Tochihara (tochi@kahaku.go.jp)

Academic editor: Cecile Gueidan | Received 17 August 2021 | Accepted 10 January 2022 | Published 8 February 2022

Citation: Tochihara Y, Hosoya T (2022) Examination of the generic concept and species boundaries of the genus *Erioscyphella* (Lachnaceae, Helotiales, Ascomycota) with the proposal of new species and new combinations based on the Japanese materials. MycoKeys 87: 1–52. https://doi.org/10.3897/mycokeys.87.73082

Abstract

The genus *Erioscyphella* Kirschst., which was morphologically confused with *Lachnum*, was herein examined. Based on molecular phylogenetic analyses using a combined dataset of ITS, LSU, mtSSU, and RPB2 and morphological examinations, *Erioscyphella* was distinguished from *Lachnum* and redefined by longer ascospores and the presence of apical amorphous materials and/or resinous materials equipped on hairs. Species boundaries recognized by morphology/ecology and phylogenetic analyses were cross-checked using species delimitation analyses based on DNA barcode sequences downloaded from UNITE, resulting in that species' taxonomic problems being uncovered. Six new species (*E. boninensis*, *E. insulae*, *E. otanii*, *E. papillaris*, *E. paralushanensis*, and *E. sasibrevispora*) and two new combinations (*E. hainanensis* and *E. sinensis*) were proposed.

Keywords

ITS, morphology, phylogeny, species delimitation, species hypothesis, taxonomy, UNITE

Introduction

The genus *Erioscyphella* Kirschst belongs to the family Lachnaceae Raitv. (Helotiales, Ascomycota) and includes 11 species: *E. abnormis* (Mont.) Baral, Šandová & B. Perić [lectotype of *Erioscyphella* (Haines and Dumont 1984); as '*E. longispora* (P. Karst.) Kirschst.' in the original description (Kirschstein 1938)], *E. alba* Ekanayaka & K.D. Hyde, *E. aseptata* Ekanayaka & K.D. Hyde, *E. bambusina* (Bres.) Kirschst., *E. brasiliensis* (Mont.) Baral, Šandová & B. Perić, *E. curvispora* B. Perić & Baral, *E. euterpes* (S.A. Cantrell & J.H. Haines) Guatim., R.W. Barreto & Crous, *E. fusiformis* (Ekanayaka & K.D. Hyde) Ekanayaka & K.D. Hyde, *E. lunata* (W.Y. Zhuang & Spooner) B. Perić & Baral, *E. lushanensis* (W.Y. Zhuang & Zheng Wang) Guatim., R.W. Barreto & Crous, and *E. sclerotii* (A.L. Sm.) Baral, Šandová & B. Perić. (Index Fungorum 2021).

Erioscyphella has been suggested as a monophyletic group by molecular phylogenetic analyses by Cantrell and Hanlin (1997), Hosoya et al. (2010), Perić and Baral (2014), and Guatimosim et al. (2016). However, the morphological delimitation of the genus is currently ill-defined. In the original description (Kirschstein 1938), *Erioscyphella* was misleadingly defined based on features that are not taxonomically informative, such as filiform, colored, and pigmented ascospores and lanceolate paraphyses (Korf 1978; Perić and Baral 2014). After that, in the genus *Lachnum* Retz. [type genus of Lachnaceae], species of so-called 'long-spored *Lachnum*', which were characterized by longer ascospores and the occurrence in tropical areas, were suggested as members of *Erioscyphella* (Haines and Dumont 1984) and have been transferred into *Erioscyphella* based on molecular phylogenetic analyses by Perić and Baral (2014) and Guatimosim et al. (2016). However, in fact, as morphology of *Erioscyphella*, including 'long-spored *Lachnum*', is consecutive with that of the genus *Lachnum* especially regarding the ascospore length and shape of ectal excipular cells (Haines and Dumont 1984), the morphological delimitation of *Erioscyphella* has not been sufficiently discussed. Since much more potential species are thought to be included in *Erioscyphella*, its morphological concept must be discussed and updated based on a wider size of taxon sampling.

In the present study, the authors aimed to: a) clarify the generic boundaries of *Erioscyphella* using molecular and morphological/ecological data, and b) propose new species or new combinations based on more objectively defined species boundaries. To reach our first goal, we used specimens from the herbarium of the National Museum of Nature and Science (TNS) (Tsukuba, Japan) as most of them were accompanied by culture and/or DNA extracts. In TNS, only three identified species of *Erioscyphella* were recognized (*E. abnormis*, *E. brasiliensis*, and *E. sclerotii*); however, we presumed that many unidentified species of *Erioscyphella* were housed therein. To reach our second goal, for species recognition, we tested DNA barcoding using the internal transcribed spacer region of nuclear ribosomal DNA (ITS), widely accepted as fungal DNA barcode (Begerow et al. 2010; Schoch et al. 2012; Hosoya 2021). ITS-based species boundaries were explored based on multiple methods, and the results were compared to species boundaries based on morphology, ecology, and phylogenetic relationships.

Materials and methods

Taxon sampling

In TNS, specimens labeled as *Erioscyphella* were initially searched, and closely related specimens to *Erioscyphella* were searched based on the sequence similarities of ITS. Selected specimens were tentatively identified based on morphology following Dennis (1954), Haines (1980), Haines and Dumont (1984), Spooner (1987), and Perić and Baral (2014).

Morphological observation, DNA extraction, and sequencing

Micromorphology was examined using cotton blue (CB) dissolved in lactic acid (LA) (CB/LA; 0.5 g CB and 99.5 mL LA) as a mounting fluid. To check the ascal apex iodine reaction, Melzer's reagent (MLZ; 0.5 g I_2, 1.5 g KI, 20 g chloral hydrate, and 20 g water) was initially used without KOH pretreatment, and Lugol's iodine (IKI; 1 g I_2 and 1 g KI, and 100 mL H_2O) and MLZ with 3% KOH pretreatment were used when necessary. World Geodetic System 84 was used for the geographic coordinates. URLs herein shown were accessed on April 15, 2021, except for GBIF website accessed on Feb 10, 2020.

DNA was extracted from cultivated isolates in 2% malt extract broth (MEB) using the modified cetyltrimethylammonium bromide (CTAB) method (Hosaka and Castellano 2008; Tochihara and Hosoya 2019). When isolates are not available, DNA was extracted directly from a crushed apothecium using DNA extraction buffer following Tochihara and Hosoya (2019). The isolates from which DNA extracted were deposited in the NITE National Biological Resource Center (NBRC) (Kisarazu, Japan), except for isolates with restriction on transition by Japanese laws and those unavailable because of contracts with private companies.

Polymerase chain reaction (PCR) was used to amplify the following regions: ITS (= ITS1-5.8S-ITS2), the partial large subunit nuclear ribosomal RNA gene (LSU), the partial mitochondrial small subunit (mtSSU), and section '6–7' of the second largest subunit of the nuclear RNA polymerase II gene (RPB2). Primer pairs for PCR reactions of ITS, LSU and mtSSU were ITS1F (5'–CTTGGTCATTTAGAGGAAGTAA–3') (Gardes and Bruns 1993) or ITS1 (5'–TCCGTAGGTGAACCTCGGG–3') (White et al. 1990) and ITS4 (5'–TCCTCCGCTTATTGATATGC–3') (White et al. 1990), LR0R (5'–ACCCGCTGAACTTAAGC–3') and LR5 (5'–TCCTGAGGGAAACTTCG–3') (Vilgalys and Hester 1990), and mrSSU1 (5'–AGCAGTGAGGAATATTGGTC–3') and mrSSU3R (5'–ATGTGGCACGTCTATAGCCC–3') (Zoller et al. 1999) respectively. The PCR program consisted of an initial denaturation at 95 °C for 3 min, followed by 30 cycles of 94 °C for 35 s, 51 °C for 30 s, and 72 °C for 1 min, and a final extension at 72 °C for 10 min. When appropriate PCR products were not obtained, a modified PCR program was applied first, and then alternative primer pairs were tested. For RPB2, an alternative forward primer fRPB2-5F (5'–GAY-

GAYMGWGATCAYTTYGG–3') (Liu et al. 1999) or RPB2-P6Fa (5'–TGGGGRYTK GTBTGYCCKGCHGA–3') (Hansen et al. 2005) and a reverse primer bRPB2-7.1R2 (5'–CCCATNGCYTGYTTVCCCATDGC–3') (modified from bRPB2-7.1R) (Matheny 2005; Matheny et al. 2007; Gelardi et al. 2015) were used.

Sequencing was conducted on an ABI PRISM 3500xL Genetic Analyzer (Applied Biosystems; Thermo Fisher Scientific, Waltham, MA, USA) with a BigDye Terminator 3.1 Cycle Sequencing Kit (Applied Biosystems). The obtained sequences were assembled using ATGC 7 (Genetyx, Tokyo, Japan). Assembled sequences were deposited in the International Nucleotide Sequence Database Collaboration (INSDC) via the DNA Data Bank of Japan (DDBJ), and acquired INSDC accession numbers. Assembled ITS sequences were also deposited in the UNITE database (https://unite.ut.ee/) via the PlutoF workbench (https://plutof.ut.ee/) (Abarenkov et al. 2010) and acquired UNITE accession numbers.

Phylogenetic analyses

The specimens obtained from TNS were included in the phylogenetic analyses as candidate members of *Erioscyphella* ('‡' in Table 1). From other genera of the family Lachnaceae, four species of *Lachnum*, two species of *Albotricha*, *Brunnipila*, *Capitotricha*, *Dasyscyphella*, *Incrucipulum*, and *Lachnellula*, and one species of *Neodasyscypha* and *Proliferodiscus* were used ('†' in Table 1). Among the eight genera, seven of them (except *Proliferodiscus*) included type species. Three species of Helotiales were selected as outgroups following Tochihara and Hosoya (2019) (Table 1).

A concatenated dataset of ITS, LSU, mtSSU, and RPB2 was used in the phylogenetic analyses. Each region was aligned separately using MAFFT 7 (Katoh and Standley 2013). The Q-INS-i option was used for ITS, LSU, and mtSSU to accommodate the secondary structures of RNA, and the G-INS-1 option was used for RPB2 to assume global alignment using the entire region. The aligned sequences were edited manually using BioEdit 7.0.5.2 (Hall 1999).

Phylogenetic conflicts among gene partitions were checked before the phylogenetic analyses using the concatenated matrix. Maximum likelihood (ML) trees with 1,000 bootstrap replications (Felsenstein 1985) using the ITS, LSU, mtSSU, and RPB2 datasets separately were constructed using MEGA X (Kumar et al. 2018) with the GTR+G model; branches with bootstrap values > 70% were compared among trees. For mtSSU and RPB2, specimens containing missing data were excluded from the analyses.

The concatenated dataset was analyzed using ML, maximum parsimony (MP), and Bayesian inference (BI). For the ML and BI analyses, substitution models were estimated for each partition (ITS, LSU, mtSSU, and each codon position of RPB2) based on Akaike's information criterion (AIC) (Akaike 1974) using Modeltest-NG 0.1.6 (Darriba et al. 2019).

ML tree search (Felsenstein 1984) and bootstrapping (Felsenstein 1985; Lemoine et al. 2018) was performed using RAxML-NG 0.9.0 (Kozlov et al. 2019) with 1,000 bootstrap replications under the substitution model SYM+I+G4 for ITS, TIM1+I+G4

Table 1. Taxa analyzed in the phylogenetic analyses.

Specimen no. (TNS-F-)	Taxon[]	Collection site	Collected Date	Host plants and parts	Strain no. (NBRC[§])	UNITE/GenBank accession no.[#]			
						ITS	LSU	mtSSU	RPB2
†16740	*Albotricha acutipila* (P. Karst.) Raitv.	Japan, Nagano, Ueda, Sugadaira Montane Research Center	2006-06-17	culm of unidentified bamboo	104380	AB481234	LC438571	LC431751	AB481354
†16497	*Albotricha albotestacea* (Desm.) Raitv.	Japan, Nagano, Ueda, Sugadaira Montane Research Center	2005-05-18	culm of *Miscanthus sinensis*	101346	AB481235	LC424943	LC431747	AB481340
†16635	*Brunnipila fuscescens* (Pers.) Baral	Japan, Gunma, Higashi-Agatsuma	2006-04-27	leaf of unidentified tree	104365	AB481255	LC424945	LC431750	AB481348
†16690	*Brunnipila pseudocannabina* (Raitv.) Tochihara, Sasagawa & Hosoya	JAPAN, Akita, Kosaka	2006-05-26	stem of unidentified herb	104374	AB481272	LC533520	LC533522	LC533521
†65670	*Capitotricha bicolor* (Bull.) Baral	SWITZERLAND, Filisur	2016-06-06	twig of *Prunus spinosa*	(FC-6101)	LC424834	LC424942	LC533244	LC425011
†65752	*Capitotricha rubi* (Bres.) Baral	SWITZERLAND, Saicourt	2016-06-04	twig of *Rubus idaeus*	(FC-6075)	LC438560	LC438573	LC533243	LC440395
†16439	*Dasyscyphella longistipitata* Hosoya	JAPAN, Kanagawa, Yamakita	2005-04-17	cupule of *Fagus crenata*	101335	AB481239	LC424947	LC533228	AB481331
†16527	*Dasyscyphella montana* Raitv.	Japan, Nagano, Ueda, Sugadaira Montane Research Center	2005-05-21	wood of unidentified tree	102336	AB481242	LC438577	LC533241	AB481336
‡16556	*Erioscyphella abnormis* (Mont.) Baral, Šandová & B. Perić	Japan, Oita, Kokonoe	2005-05	wood of unidentified tree	114449	UDB0779051	LC533153	LC533257	LC533198
‡16582	*Erioscyphella abnormis* (Mont.) Baral, Šandová & B. Perić	Japan, Kanagawa, Yamakita	2005-07-02	wood of unidentified tree	104360	AB481249	LC533176	LC533233	LC533199
‡16606	*Erioscyphella abnormis* (Mont.) Baral, Šandová & B. Perić	Japan, Kanagawa, Yamakita	2005-07-03	wood of unidentified tree	114450	UDB0779053	LC533154	LC533258	LC533200
‡16609	*Erioscyphella abnormis* (Mont.) Baral, Šandová & B. Perić	Japan, Kanagawa, Yamakita	2005-07-03	wood of *Cephalotaxus harringtonia*	101350	††AB705234	LC533175	LC533256	LC533184
‡16639	*Erioscyphella abnormis* (Mont.) Baral, Šandová & B. Perić	Japan, Ibaraki, Tsukuba Botanical Garden	2006-05-01	twig of unidentified tree	114451	UDB0779054	LC533155	LC533259	LC533201
‡25579	*Erioscyphella abnormis* (Mont.) Baral, Šandová & B. Perić	Japan, Tokyo, Hongo	2009-05-25	twig of unidentified tree	(FC-1887)	UDB0779057	LC533146	LC533250	LC533191
‡32163	*Erioscyphella abnormis* (Mont.) Baral, Šandová & B. Perić	Japan, Kanagawa, Odawara	2010-05-14	twig of unidentified tree	114456	UDB0779062	LC533158	LC533260	LC533203
‡38452	*Erioscyphella abnormis* (Mont.) Baral, Šandová & B. Perić	Japan, Gunma, Naganohara	2013-06-27	wood of unidentified tree	114463	††UDB0779069	LC533171	LC533262	LC533210
‡46416	*Erioscyphella abnormis* (Mont.) Baral, Šandová & B. Perić	Taiwan, Taipei	2012-04-15	wood of unidentified tree	(FC-2906)	UDB0779067	LC533132	LC533277	LC549671
‡46841	*Erioscyphella abnormis* (Mont.) Baral, Šandová & B. Perić	Japan, Gifu, Gujo	2012-05-28	wood of unidentified tree	114462	UDB0779086	LC533170	LC533279	LC533209
‡61773	*Erioscyphella abnormis* (Mont.) Baral, Šandová & B. Perić	Japan, Kanagawa, Yokohama	2015-04-01	twig of unidentified tree	114464	††UDB0779074	LC533137	LC533264	LC533211
‡61931	*Erioscyphella abnormis* (Mont.) Baral, Šandová & B. Perić	Japan, Kanagawa, Zushi	2015-04-16	wood of unidentified tree	114466	UDB0779072	LC533139	LC533266	LC533213

Specimen no. (TNS-F-)	Taxon[|]	Collection site	Collected Date	Host plants and parts	Strain no. (NBRC[¶])	UNITE/GenBank accession no.[#]			
						ITS	LSU	mtSSU	RPB2
‡80478	*Erioscyphella abnormis* (Mont.) Baral, Šandová & B. Perić	Japan, Shizuoka, Oyama	2017-06-26	twig of unidentified tree	113934	LC424837	LC424949	LC533283	LC425009
†26520	*Erioscyphella boninensis* Tochihara & Hosoya	Japan, Tokyo, Chichijima Island	2009-06-28	trunk of unidentified tree	114447	UDB0779049	LC533151	LC533254	LC533196
‡46419	*Erioscyphella brasiliensis* (Mont.) Baral, Šandová & B. Perić	Taiwan, Taipei	2012-04-20	wood of unidentified tree	(FC-2910)	UDB0779068	LC533133	LC533278	LC549672
‡35049	*Erioscyphella hainanensis* (W.Y. Zhuang and Zheng Wang) Hosoya and Tochihara (←*Lachnum hainanense* W.Y. Zhuang and Zheng Wang)	Japan, Niigata, Minamiuonuma	2010-05-14	leaf of *Quercus glauca*	114457	UDB0779064	LC533168	LC533274	LC533205
‡35056	*Erioscyphella hainanensis* (W.Y. Zhuang and Zheng Wang) Hosoya and Tochihara (←*Lachnum hainanense* W.Y. Zhuang and Zheng Wang)	Japan, Niigata, Minamiuonuma	2010-05-14	leaf of *Quercus serrata*	114458	UDB0779065	LC533169	LC533275	LC533206
‡61775	*Erioscyphella hainanensis* (W.Y. Zhuang and Zheng Wang) Hosoya and Tochihara (←*Lachnum hainanense* W.Y. Zhuang and Zheng Wang)	Japan, Kanagawa, Hiratsuka	2015-04-12	leaf of *Quercus myrsinifolia*	114465	UDB0779071	LC533138	LC533265	LC533212
‡61941	*Erioscyphella hainanensis* (W.Y. Zhuang and Zheng Wang) Hosoya and Tochihara (←*Lachnum hainanense* W.Y. Zhuang and Zheng Wang)	Japan, Kanagawa, Kamakura	2015-04-24	leaf of *Quercus glauca*	112569	UDB0779073	LC533140	LC533280	LC533214
‡65722	*Erioscyphella hainanensis* (W.Y. Zhuang and Zheng Wang) Hosoya and Tochihara (←*Lachnum hainanense* W.Y. Zhuang and Zheng Wang)	Japan, Gunma, Midori	2016-04-24	leaf of *Quercus serrata* subsp. *Mongolicoides*	114469	UDB0779076	LC533142	LC533281	LC533215
‡80356	*Erioscyphella hainanensis* (W.Y. Zhuang and Zheng Wang) Hosoya and Tochihara (←*Lachnum hainanense* W.Y. Zhuang and Zheng Wang)	Japan, Kanagawa, Hiratsuka	2017-05-18	leaf of *Quercus glauca*	114470	UDB0779077	LC533172	LC533282	LC533186
‡80371	*Erioscyphella hainanensis* (W.Y. Zhuang and Zheng Wang) Hosoya and Tochihara (←*Lachnum hainanense* W.Y. Zhuang and Zheng Wang)	Japan, Kanagawa, Hiratsuka	2017-05-18	leaf of *Castanopsis sieboldii*	114472	UDB0779078	LC533135	LC533246	LC533188
‡26500	*Erioscyphella insulae* Tochihara & Hosoya	Japan, Tokyo, Hahajima Island	2009-06-24	wood of unidentified tree	114445	UDB0779060	LC533149	LC533252	LC533194
‡39720	*Erioscyphella insulae* Tochihara & Hosoya	Japan, Okinawa, Iriomote Island	2011-06-12	bark of unidentified tree	114459	UDB0779063	LC533177	LC533261	LC533207
‡61920	*Erioscyphella paralushanensis* Tochihara & Hosoya	Japan, Shizuoka, Atami	2015-06-08	culm of *Pleioblastus argenteostriatus*	114468	††UDB0779075	LC533141	LC533267	LC533220
†81472	*Erioscyphella otanii* Tochihara	Japan, Hokkaido, Horonobe, Teshio Experimental Forest, Hokkaido University	2018-07-11	leaf of *Sasa senanensis*	114476	UDB0779085	LC533179	LC533286	‖LC533226
‡81272	*Erioscyphella papillaris* Tochihara	Japan, Gunma, Minakami	2017-07-16	leaf of unidentified bamboo	113937	UDB0779081	LC533161	LC533285	LC533204
‡80399	*Erioscyphella sasibrevispora* Tochihara & Hosoya	Japan, Gunma, Higashi-Agatsuma	2017-06-06	sheath of *Sasa veitchii*	—	UDB0779082/ LC669470	LC533173	LC533268	LC533216

Specimen no. (TNS-F-)	Taxon[|]	Collection site	Collected Date	Host plants and parts	Strain no. (NBRC[¶])	UNITE/GenBank accession no.[#]			
						ITS	LSU	mtSSU	RPB2
‡81401	*Erioscyphella sasibrevispora* Tochihara & Hosoya	Japan, Hokkaido, Tomakomai	2018-06-16	culm of *Sasa nipponica*	114475	UDB0779084/ LC669472	LC533174	LC533269	LC533217
‡26492	*Erioscyphella sclerotii* (A.L. Sm.) Baral, Šandová & B. Perić	Japan, Tokyo, Hahajima Island	2009-06-24	wood of unidentified tree	114448	UDB0779050/ LC669438	LC533152	LC533255	LC533197
‡38480	*Erioscyphella sclerotii* (A.L. Sm.) Baral, Šandová & B. Perić	Taiwan, Wulai	2013-07-12	twig of unidentified tree	(FC-5208)	††UDB0779070	LC533134	LC533263	LC549673
‡16838	*Erioscyphella sinensis* (Z.H. Yu and W.Y. Zhuang) Sasagawa, Tochihara & Hosoya (←*Lachnum mapirianum* var. *sinense* Z.H. Yu and W.Y. Zhuang)	Japan, Ibaraki, Tsukuba Botanical Garden	2007-06-15	leaf of unidentified broad-leaved tree	104389	AB481280	LC533164	LC533235	AB481364
‡80354	*Erioscyphella sinensis* (Z.H. Yu and W.Y. Zhuang) Sasagawa, Tochihara & Hosoya (←*Lachnum mapirianum* var. *sinense* Z.H. Yu and W.Y. Zhuang)	Japan, Kanagawa, Manazuru	2017-05	leaf of *Castanopsis sieboldi*	114471	UDB0779083/ LC669471	LC533143	LC533245	LC533187
‡16841	*Erioscyphella sinensis* (Z.H. Yu and W.Y. Zhuang) Sasagawa, Tochihara & Hosoya (←*Lachnum mapirianum* var. *sinense* Z.H. Yu and W.Y. Zhuang)	Japan, Ibaraki, Mt. Tsukuba	2007-06-23	leaf of unidentified broad-leaved tree	104390	AB481281	LC533157	LC533236	LC533218
‡32161	*Erioscyphella sinensis* (Z.H. Yu and W.Y. Zhuang) Sasagawa, Tochihara & Hosoya (←*Lachnum mapirianum* var. *sinense* Z.H. Yu and W.Y. Zhuang)	Japan, Kanagawa, Odawara	2010-05-14	leaf of *Quercus myrsinifolia*	113715	UDB0779061/ LC669449	LC533167	LC533273	LC533219
‡16837	*Erioscyphella sinensis* (Z.H. Yu and W.Y. Zhuang) Sasagawa, Tochihara & Hosoya (←*Lachnum mapirianum* var. *sinense* Z.H. Yu and W.Y. Zhuang)	Japan, Ibaraki, Tsukuba Botanical Garden	2007-06-15	leaf of unidentified broad-leaved tree	114452	UDB0779055/ LC669443	LC533156	LC533272	LC533202
†81520	*Incrucipulum ciliare* (Schrad.) Baral	Japan, Shizuoka, Shizuoka	2018-08-18	leaf of *Quercus mongolica* subsp. *crispula*	113941	LC438566	LC438583	LC533284	LC438596
†17632	*Incrucipulum longispineum* Sasagawa & Hosoya	Japan, Miyagi, Sendai	2006-07-29	leaf of *Lyonia ovalifolia*	102347	AB481256	LC438579	LC533234	AB481362
†81248	*Lachnellula calyciformis* (Batsch) Dharne	Japan, Hokkaido, Engaru	2017-07-12	twig of *Abies sachalinensis*	113935	LC438561	LC438574	LC533247	LC438590
†16529	*Lachnellula suecica* (de Bary ex Fuckel) Nannf.	Japan, Nagano, Ueda, Sugadaira Montane Research Center	2005-05-21	twig of *Larix kaempferi*	101348	AB481248	LC424944	LC533231	AB481341
†16494	*Lachnum asiaticum* (Y. Otani) Raitv.	Japan, Nagano, Ueda, Sugadaira Montane Research Center	2005-05-18	culm of unidentified bamboo	101341	AB481251	LC533162	LC533229	AB481334
‡17249	*Lachnum mapirianum* (Pat. & Gaillard) M.P. Sharma	Malaysia, Gerik	2004-09-07	leaf of unidentified tree	—	UDB0779088/ LC669476	LC533182	—	LC533223
‡17245	*Lachnum mapirianum* (Pat. & Gaillard) M.P. Sharma	Malaysia, Gerik	2004-09-07	leaf of unidentified tree	—	UDB0779087/ LC669475	LC533181	—	LC533222
‡16442	*Lachnum novoguineense* var. *yunnanicum* W.Y. Zhuang	Japan, Nagano, Ueda, Sugadaira Montane Research Center	2005-05-18	culm of unidentified bamboo	102339	AB481270	LC533163	LC533232	AB481342
‡16642	*Lachnum novoguineense* var. *yunnanicum* W.Y. Zhuang	Japan, Ibaraki, Mt. Tsukuba	2006-05-02	culm of unidentified bamboo	104368	AB481271	LC533165	LC533227	§§LC533225
‡11197	*Lachnum palmae* sensu lato (←*Lachnum palmae* (Kanouse) Spooner)	Japan, Shizuoka, Shimoda	2004-07-26	leaf of *Livistona chinensis* var. *subglobosa*	106495	UDB0779047/ LC669435	LC533166	LC533248	LC533185

Specimen no. (TNS-F-)	Taxon[|]	Collection site	Collected Date	Host plants and parts	Strain no. (NBRC[¶])	UNITE/GenBank accession no.[#]			
						ITS	LSU	mtSSU	RPB2
‡13500	*Lachnum palmae* sensu lato (←*Lachnum palmae* (Kanouse) Spooner)	Japan, Kagoshima, Yakushima Island	2005-10-19	leaf of *Livistona chinensis* var. *subglobosa*	114441	††LC425039/ UDB779046	LC429382	LC533240	‡‡LC431718
‡17567	*Lachnum palmae* sensu lato (←*Lachnum palmae* (Kanouse) Spooner)	New Zealand	2005-05-28	leaf of unidentified palm	—	UDB0779089/ LC669477	LC533183	LC533288	—
‡24588	*Lachnum palmae* sensu lato (←*Lachnum palmae* (Kanouse) Spooner)	Japan, Kagoshima, Amami-Oshima	2009-02-24	leaf of *Livistona chinensis* var. *subglobosa*	114442	UDB0779052/ LC669440	LC533144	LC533270	LC533190
‡24600	*Lachnum palmae* sensu lato (←*Lachnum palmae* (Kanouse) Spooner)	Japan, Kagoshima, Amami-Oshima	2009-02-25	leaf of *Livistona chinensis* var. *subglobosa*	114443	UDB0779056/ LC669444	LC533145	LC533249	‖LC533224
‡26161	*Lachnum palmae* sensu lato (←*Lachnum palmae* (Kanouse) Spooner)	Japan, Tokyo, Chichijima Island	2009-06-27	leaf of *Livistona boninensis*	114446	UDB0779048/ LC669436	LC533150	LC533253	LC533195
‡26172	*Lachnum palmae* sensu lato (←*Lachnum palmae* (Kanouse) Spooner)	Japan, Tokyo, Kita-Iwojima Island	2009-06-17	leaf of *Livistona chinensis* var. *subglobosa*	(FC-1935)	UDB0779058/ LC669446	LC533147	LC533251	LC533192
‡26185	*Lachnum palmae* sensu lato (←*Lachnum palmae* (Kanouse) Spooner)	Japan, Tokyo, Kita-Iwojima Island	2009-06-18	leaf of *Livistona chinensis* var. *subglobosa*	114444	UDB0779059/ LC669447	LC533148	LC533271	LC533193
‡39729	*Lachnum palmae* sensu lato (←*Lachnum palmae* (Kanouse) Spooner)	Japan, Okinawa, Iriomote Island	2011-06-13	leaf of *Livistona chinensis* var. *subglobosa*	114460	UDB0779066/ LC669454	LC533178	LC533276	LC533208
†16501	*Lachnum pudibundum* (Quél.) J. Schröt.	Japan, Nagano, Ueda, Sugadaira Montane Research Center	2005-05-18	wood of unidentified tree	102335	AB481259	LC533160	LC533230	AB481335
†81229	*Lachnum rachidicola* J.G. Han, Raitv. & H.D. Shin	Japan, Hokkaido, Tomakomai, Tomakomai Experimental Forest	2017-08-09	petiole of *Juglans* sp.	114473	UDB0779079/ LC669467	LC533136	—	LC533189
†16583	*Lachnum virgineum* (Batsch) P. Karst.	Japan, Kanagawa, Yamakita	2005-07-02	wood of unidentified tree	104358	AB481268	AB926119	LC431748	AB481343
†65625	*Neodasyscypha cerina* (Pers.) Spooner	Switzerland, Saicourt	2016-06-08	twig of *Crataegus* sp.	(FC-6068)	LC424836	LC424948	LC533242	LC425013
†17436	*Proliferodiscus alboviridis* (Sacc.) Spooner	Japan, Ibaraki, Tsukuba Botanical Garden	2006-07-08	wood of unidentified tree	108594	LC438558	LC533159	LC533239	LC425014
§17909	*Hyaloscypha spiralis* (Velen.) J.G. Han, Hosoya & H.D. Shin	Japan, Kumamoto, Kikuchi	2005-10-10	wood of unidentified tree	108585	††LC438602	LC438604	LC533237	LC438606
§16472	*Hymenoscyphus varicosporoides* Tubaki	Japan, Ibaraki, Kasumigaura	2005-05-05	wood of unidentified tree	104355	AB926052	LC424952	LC431746	AB481329
§18014	*Urceolella carestiana* (Rabenh.) Dennis	Japan, Iwate, Hanamaki	2006-05-23	stem of *Parathelypteris nipponica*	108588	††LC438603	LC438605	LC533238	LC438607

† Lachnaceae except for Erioscyphella and its potential species tentatively identified based on morphology
‡ Erioscyphella or its potential species tentatively identified based on morphology
§ Outgroup
| Original taxon name labeled on the specimen is shown enclosed by "(←)" and is only shown when it is different from a name determined in this study.
¶ Cultures not donated in NBRC is beginning with "FC-", local suffix in TNS. '—' represents no culture exist and DNA was extracted from apothecia.
# UNITE accession no. is beginning with 'UDB'. GenBank accession no. is beginning with 'AB' or 'LC'.
†† Primer pair ITS1 and ITS4 was used. In ITS sequences without notes (††), primer pair ITS1F and ITS4 was used.
‡‡ Primer pair fRPB2-5F and RPB2-P7R was used.
§§ Primer pair RPB2-P6Fa and bRPB2-7.1R2 was used.
|| Primer pair RPB2-P6Fa and RPB2-P7R was used. In RPB2 sequences without any notes (‡‡, §§, ||), primer pair RPB2-P6F and RPB2-P7R was used.

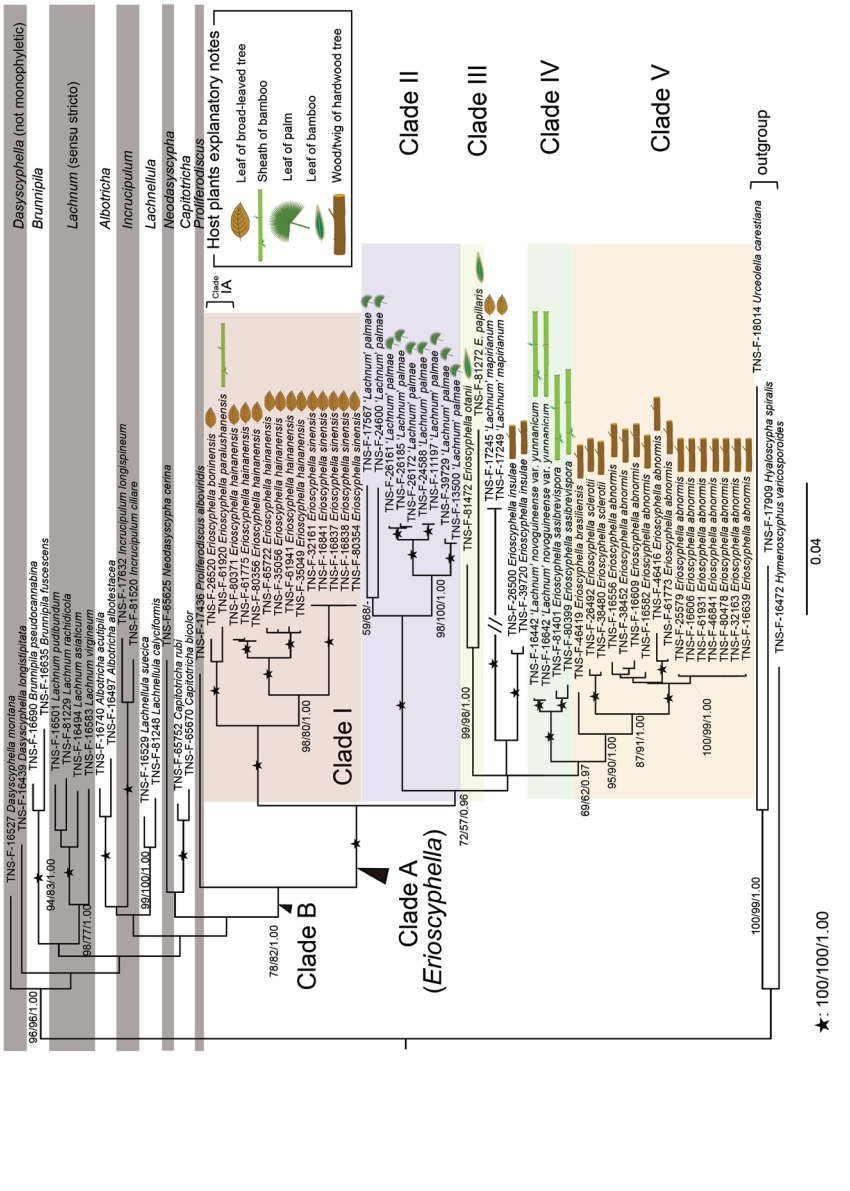

Figure 1. ML best-scored phylogenetic tree based on the concatenated dataset of ITS, LSU, mtSSU, and RPB2 constructed using RAxML-NG. MLBP/MPBP/BPP are represented on branches in this order. In MLBP/MPBP < 50% or BPP < 0.95, a hyphen appears. No evaluation values are shown on branches when MLBP and MPBP < 50% and BPP < 0.95. The branch of a clade TNS-F-17245 + 17249 to its most recent common ancestor is only one-third of the intended length due to space limitation.

for LSU, TPM1uf+I+G4 for mtSSU and RPB2 third codon position, GTR+I+G4 for RPB2 first codon position, and TPM3uf+I+G4 for RPB2 second codon position. Sequence matrix containing missing data typically yield multiple trees residing on a phylogenetic terrace (Sanderson et al. 2011; Biczok et al. 2018). Therefore, we checked if the best-scored-tree did not lie on a terrace using the Python tool called 'terraphy' implemented in RAxML-NG 0.9.0.

MP analysis was conducted using PAUP* 4.0a 167 (Swofford 2002). All substitutions were treated as unordered and of equal weights. All gaps were treated as missing data. A heuristic parsimony search was carried out with 1,000 replicates of random step addition, with a tree bisection reconnection (TBR) branch swapping algorithm, Multrees option on, Steepest descent modification option on, and branch collapse option set to MinBrlen. Bootstrap values (MPBP; Felsenstein 1985) were estimated from 1,000 replicates of heuristic searches, with random taxon addition, TBR branch swapping, and Multrees options off.

BI analysis was based on MrBayes 3.2.7a (Ronquist et al. 2012) under the substitution model SYM+I+G4 for ITS, GTR+I+G4 for LSU and RPB2 first codon positions, HKY+I+G4 for mtSSU and RPB2 third codon positions, and F81+I for RPB2 second codon position. Two separate Metropolis-Coupled Markov Chains of Monte Carlo (MCMCMC) ran simultaneously starting from random trees for 20 million generations, and trees were sampled every 500 generations. The average standard deviation of split frequencies (ASDSF) and effective sample size (ESS) were checked using Tracer 1.7.1 (Rambaut 2018a) as an indication of convergence. Using post-burn-in trees, a 50% majority rule consensus tree was generated, and Bayesian posterior probabilities (BPP) were calculated to evaluate node supports. Trees were visualized using FigTree 1.4.4 (Rambaut 2018b) based on the ML, MP, and BI analyses respectively. Branches with MLBP and MPBP > 90% and BPP > 0.95 were regarded as strongly supported.

ITS-based species delimitation analyses (Fig. 2)

To maximize the number of ITS sequences, we used the UNITE Species Hypotheses (SH) system provided by the UNITE database (Kõljalg et al. 2013; Nilsson et al. 2015; GBIF 2018; Kõljalg et al. 2020). In the UNITE SH system, all fungal ITS sequences are periodically divided into species-level clusters (species hypothesis; SH) at optional sequence-distance thresholds (0%–3% in 0.5% steps), each of which is assigned to a unique UNITE SH code represented by a digital objective identifier (DOI) accessible from internet (Kõljalg et al. 2016, 2020; Nilsson et al. 2015).

Based on the UNITE SH system, we collected ITS sequences of *Erioscyphella* in the following process: a) selectivity of closely related sequences: for every ITS sequence newly obtained from TNS specimens (= query sequences, 49 sequences), UNITE SH code at the 3% threshold value were searched in the UNITE database to gather sequences in wider scope, and all sequences within the UNITE SH code were downloaded. b) selectivity based on taxon names: using the UNITE search page, ITS sequences named *Erioscyphella* were searched, because only closely related sequences to query sequences are filtered under the a) criterion. Sequences with synonyms of *Eriosyphella* species were also searched, because the UNITE lookup function is not supported by any backbone taxonomies to integrate synonyms. Sequences satisfying criterion a) or

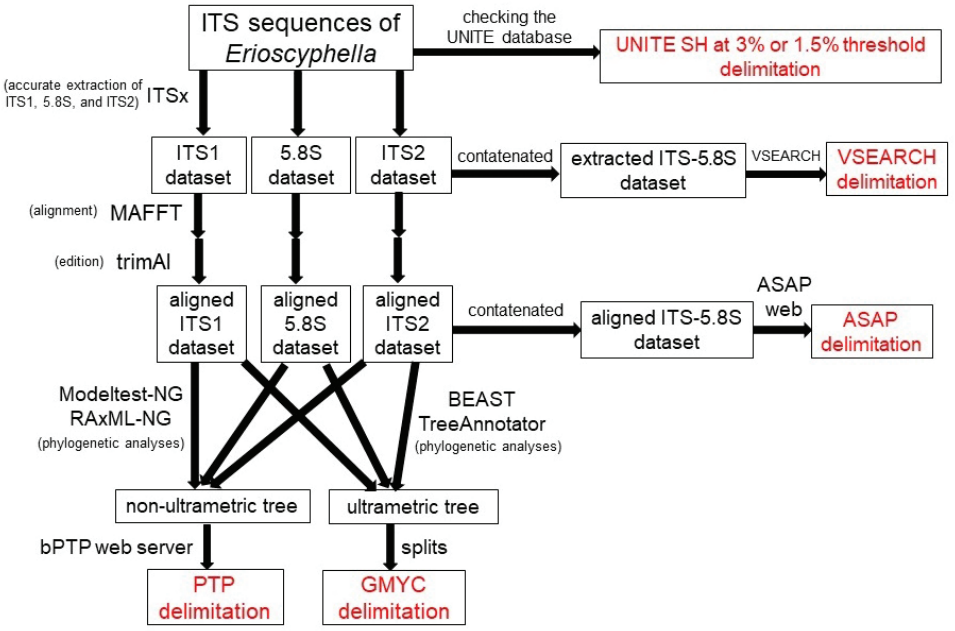

Figure 2. Diagrammatic representation showing the species delimitation analyses using ITS sequences.

b) were downloaded for ITS-based species recognition. The obtained ITS sequences were clustered into SHs based on an OTU clustering method, hierarchical clustering method, and two coalescent-based methods. For all ITS sequences, ITS1, 5.8S, and ITS2 regions were extracted using ITSx (Nilsson et al. 2010) to construct an accurate ITS dataset, because the inclusion of segments of adjacent regions (such as a small subunit of 18S rRNA or LSU) may decrease the accuracy of the calculation of ITS distances (Nilsson et al. 2010). OTU clustering was executed using VSEARCH v2.17.2 (Rognes et al. 2016) implemented in the Qiime 2 microbiome analysis platform (Bolyen et al. 2019).

The concatenated dataset of extracted ITS1, 5.8S, and ITS2 was incorporated into VSEARCH, and OTU clustering at 97% and 98.5% similarity thresholds were performed using the '-cluster_fast' option. Hierarchical clustering based on pairwise sequence distances was executed using the Assemble Species by Automatic Partitioning (ASAP) method (Puillandre et al. 2021). The datasets of extracted ITS1, 5.8S, and ITS2 were separately aligned using MAFFT 7 under the Q-INS-i option and edited using trimAl v1.2 (Capella-Gutiérrez et al. 2009) under the '-gappyout' option. The concatenated dataset of the three aligned partitions was analyzed using ASAP web (https://bioinfo.mnhn.fr/abi/public/asap/asapweb.html). Jukes-Cantor (JC69) was selected as a substitution model for computing pairwise distances of sequences. As phylogeny-based species delimitation methods, the generalized mixed Yule-coalescent (GMYC) model (Pons et al. 2006; Fujisawa and Barraclough 2013) and the Poisson Tree Processes (PTP) model (Zhang et al. 2013) were used. In both models, specia-

tion (species-level differentiation) and coalescence (population-level differentiation) are identified based on the length of phylogenetic trees. GMYC requires the use of phylogenetic trees following the molecular clock model (= ultrametric tree) because it detects transition points from speciation to coalescence focusing on the time axis, while PTP does not require ultrametric tree as it focuses on the number of nucleotide substitutions. Ultrametric trees were estimated using BEAST v2.6.3. (Bouckaert et al. 2019). The ITS dataset was divided into ITS1, 5.8S, and ITS2, and suitable substitution models GTR+G for ITS1 and JC+G for 5.8S and ITS2 estimated using Modeltest-NG 0.1.6. were applied. To estimate branch length, a Yule model and a relaxed clock with a log-normal distribution were selected. MCMC chains were run for 1.5×10^8 generations and sampled every 1,000 generations. After each run, convergence was checked using Tracer 1.7.1, and the first 10% were discarded as burn-in. A consensus tree was generated using TreeAnnotator v1.10.4 in BEAST package, from 150,000 generated trees except for the first 10% regarded as burn-in. A single-threshold species delimitation analysis based on GMYC was conducted using the R package 'splits' (Fujisawa and Barraclough 2013).

For the species delimitation analyses using PTP, an unrooted ML phylogenetic tree was constructed using RAxML-NG 0.9.0. The analysis used ITS1, 5.8S, and ITS2 partitions, aligned as previously described, under the substitution models TIM2+G4 for ITS1, TPM2+I+G4 for 5.8S, and GTR+I+G4 for ITS2, estimated using Modeltest-NG 0.1.6. based on the AIC. The species delimitation analysis was executed using the generated ML best-scored tree with the bPTP web server (https://species.h-its.org/). The MCMC run was set to 500,000 generations and burn-in rate was set to 0.1. The convergence of MCMC runs was visually checked. In ML and Bayesian results, a result generating fewer SHs was adopted to avoid excessive species division.

SHs generated in the species delimitation analyses and the UNITE SHs at 3% and 1.5% threshold values were compared with one another.

Species recognition

In the present study, we initially recognized species boundaries based on the two criteria:

1. Forming a monophyletic group in the phylogenetic analyses based on multigene data (Fig. 1).
2. Members can be distinguished based on morphological and/or common ecological features (such as host plants).

Species boundaries recognized by 1.and 2. were cross-checked based on the results of ITS-based species delimitation analyses. When the species boundaries are supported by the majority (= more than four methods) of the seven species delimitation methods (UNITE SH at 3% threshold, UNITE SH at 1.5% threshold, VSEARCH 97% similarity, VSEARCH 98.5% similarity, ASAP, GMYC, and PTP) (Fig. 3), we regard the species as reasonable and carry out taxonomic treatments if necessary.

Figure 3. Species delimitation analyses using ITS sequences of *Erioscyphella* and its potential members. Clusters based on UNITE SH at 3% and 1.5% threshold values at UNITE v8.2, VSEARCH at 97% and 98.5% threshold values, ASAP, GMYC, and PTP are displayed. Schematic phylogenetic relationships are shown using the ultrametric tree constructed for the GMYC analysis. The taxon names shown on the tree branches follow the results of the present study.

Results

Taxon sampling from TNS specimens

Forty-nine specimens in TNS were identified as candidates of *Erioscyphella* and morphologically identified as *E. abnormis*, *E. brasiliensis*, *E. sclerotii*, *Lachnum hainanense* W.Y. Zhuang & Zheng Wang, *L. mapirianum* (Pat. & Gaillard) M.P. Sharma, *Lachnum mapirianum* var. *sinense* Z.H. Yu, W.Y. Zhuang, *Lachnum novoguineense* var. *yunnanicum* W.Y. Zhuang, and *L. palmae* (Kanouse) Spooner (Table 1), together with six species of *Erioscyphella* described here as new ([*E. boninensis*, *E. insulae*, *E. otanii*, *E. papillaris*, *E. paralushanensis*, and *E. sasibrevispora*], Table 1).

Phylogenetic analyses

The molecular phylogenetic analyses were based on 70 specimens selected from TNS (Table 1). The concatenated sequence matrix was composed of 2488 bp (sites 1–332 for ITS, 333–1108 for LSU, 1109–1828 for mtSSU, and 1829–2488 for RPB2). In the matrix, the following parts were treated as missing data: TNS-F-17245, 17249, and 81229 for mtSSU, and TNS-F-17567 for RPB2. The matrix was registered in TreeBase (http://purl.org/phylo/treebase/phylows/study/TB2:S28477).

Among the four ML trees based on each region, no conflicts were found in clades with support > 70% (Suppl. material 1: Fig. S1). Therefore, we considered these four regions to be combinable, and phylogenetic analyses were based on the concatenated sequence matrix. In the ML analysis, the best-scored tree generated did not reside on the phylogenetic terrace. In the MP analysis, 766 nucleotide substitution sites were detected, 601 of which were parsimony-informative. A total of 182,630 equally parsimonious trees were generated with tree length = 2,985 steps, consistency index (CI) = 0.38, retention index (RI) = 0.73, and rescaled consistency index (RC) = 0.28. In the BI analysis, when two runs reached 20 million generations and the first 10,000 trees (25%) of generated trees were excluded, ASDSF was observed to fall below 0.004 and ESS of all parameters was over 200. The first 10,000 trees were discarded as burn-in. A 50% majority rule consensus tree was constructed and BPP was calculated based on the remaining 30,000 trees.

As no topological contradictions occurred among the ML best-scored tree, MP 50% majority-rule consensus tree, and BI 50% majority-rule consensus tree, only ML tree was illustrated, and MLBS, MPBS, and BPP were plotted on its branches (Fig. 1).

Based on the phylogenetic analyses, 49 candidates of *Erioscyphella* formed a strongly supported clade (= Clade A, MLBP = 100%/MPBP = 100%/BPP = 1.00), apart from the clade of *Lachnum* sensu stricto (= *L. asiaticum* (Y. Otani) Raitv., *L. pudibundum* (Quél.) J. Schröt., *L. rachidicola* J.G. Han, Raitv. & H.D. Shin, and *L. virgineum* (Batsch) P. Karst.) [type of *Lachnum*]) (Fig. 1). Clade A and *Proliferodiscus alboviridis* formed a relatively strongly supported clade (Clade B, MLBP = 78%, MPBP = 82%, BPP = 1.00).

Within Clade A, each morphologically identified species and variety formed strongly supported monophyletic groups of their own (Fig. 1), and five strongly supported

subclades were recognized (Clade I–V, Fig. 1). *Lachnum mapirianum* (TNS-F-17545, 17249) and *E. insulae* (TNS-F-26500, 39720) did not belong to any subclade. Clade I was composed of *E. boninensis*, *E. paralushanensis*, *L. hainanense*, and *L. mapirianum* var. *sinense*. Within Clade I, only *E. paralushanensis* occurred on bamboo sheaths, while others occurred on fallen leaves of broad-leaved trees. Clade II was composed only of *L. palmae*, which occurred on the palm petioles. Clade III was composed of *E. otanii* and *E. papillaris* occurring on bamboo leaves. Clade IV was composed of *L. novoguineense* var. *yunnanicum*, and *E. sasibrevispora*, occurring on bamboo sheaths. Clade V was composed of *E. abnormis*, *E. brasiliensis*, and *E. sclerotii*, occurring on wood.

Morphological characters within Clade A

Members of Clade A had totally and densely granulate, hyaline to brown, thin-walled hairs, fusiform to long filiform ascospores, ectal excipulum composed of *textura prismatica* to *textura angularis*, asci lacking croziers at the bases, and smooth walled ectal excipulum cells. Exceptionally, *E. sasibrevispora*, *L. hainanense* (Hosoya et al. 2013), and *L. novoguineense* var. *yunnanicum* W.Y. Zhuang had croziers and *E. boninensis* had granulated ectal excipulum.

Moreover, hairs of Clade A lacked crystals, but were equipped with apical amorphous materials and/or resinous materials. In the present study, "crystals" refers to amber colored materials that positioned near the hair apices and were regular-shaped (e.g. tetrahedral materials, masses of needle-like materials, or cross-shaped materials), described by Raitviir (2002), Suková (2005) or Tochihara and Hosoya (2019). "Resinous materials" refers to colored, refractive, irregular-shaped materials attached on any parts of hairs, described by Spooner (1987). Crystals and resinous materials are easily detatched from hairs and broken into fragments in the squash mount. "Apical amorphous materials" is termed uniquely in this study, and refers to hyaline to brown, refractive, irregular-shaped materials positioned outside the hair apices. They are usually small and inconspicuous cap-like shaped, and conspicuously globular in some species. Apical amorphous materials do not grow to big masses and are not easily detached from hairs in the squash mount.

In Clade A, members except for *E. boninensis*, *E. sasibrevispora* and *L. novoguineense* var. *yunnanicum* had apical amorphous materials, and *E. boninensis*, *E. paralushanensis*, and *L. palmae* complex also had resinous materials (see figures of described species and Suppl. material 1: Fig. S2).

ITS-based species delimitation analyses

In UNITE v8.3, 87 ITS sequences were clustered into 23 SHs at 3% and 26 SHs at 1.5% threshold values (Table 2, Fig. 3). The UNITE SH code for each SH is presented in Table 2. In OTU clustering using VSEARCH, 87 ITS sequences were clustered into 25 SHs at 97% similarity and 28 SHs at 98.5% similarity (Table 2, Fig. 3). VSEARCH SH codes (allocated in this study uniquely; VSH97_1 to VSH97_25, VSH985_1 to VSH985_28) are shown in Table 2.

Table 2. ITS sequences analyzed by the species delimitation analyses.

ITS sequence GenBank/UNITE accession no.	TNS-F specimen no.	Reference (initial appearance)	Taxon name (ultimately allocated in this study)	UNITE taxon name	INSDC taxon name	Country	Host plants and parts	UNITE SH code (DOI) at 3% threshold	UNITE SH code (DOI) at 1.5% threshold	VSEARCH SH at 97% similarity	VSEARCH SH at 98.5% similarity
AB267634		Miyoshi et al. (2007)	*E. abnormis*	*Lachnum abnorme*	*Lachnum abnorme*	JAPAN, Ehime	twig of *Citrus junos*	SH1155612.08FU	SH1522994.08FU	VSH97_1	VSH985_2
AB267636 (duplicate; AB267635)		Miyoshi et al. (2007)	*E. abnormis*	*Lachnum abnorme*	*Lachnum abnorme*	JAPAN, Ehime	twig of *Citrus junos*	SH1155612.08FU	SH1522994.08FU	VSH97_1	VSH985_2
AB267641 (duplicate; AB267639, AB267640)		Miyoshi et al. (2007)	*E. abnormis*	*Lachnum abnorme*	*Lachnum abnorme*	JAPAN, Tokushima	twig of *Citrus junos*	SH1155612.08FU	SH1522994.08FU	VSH97_1	VSH985_2
AB267642		Miyoshi et al. (2007)	*E. abnormis*	*Lachnum abnorme*	*Lachnum abnorme*	JAPAN, Tokushima	twig of *Citrus junos*	SH1155612.08FU	SH1522994.08FU	VSH97_1	VSH985_2
JF937578		Zhao and Zhuang (2011)	*E. abnormis*	*Lachnum abnorme*	*Lachnum abnorme*	CHINA	(unspecified)	SH1155612.08FU	SH1522994.08FU	VSH97_1	VSH985_2
JN033395		Han et al. (2014)	*E. abnormis*	*Lachnum abnorme*	*Lachnum abnorme*	KOREA	Wood	SH1155612.08FU	SH1522994.08FU	VSH97_1	VSH985_2
UDB0779067/ LC669455	46416	this study	*E. abnormis*	-	-	TAIWAN, Taipei	wood of unidentified tree	SH1155612.08FU	SH1522994.08FU	VSH97_1	VSH985_2
UDB0779074/ LC669462	61773	this study	*E. abnormis*	-	-	JAPAN, Kanagawa, Yokohama	twig of unidentified tree	SH1155612.08FU	SH1522994.08FU	VSH97_1	VSH985_2
MK584950		Ekanayaka et al. (2019)	*E. abnormis*	*E. abnormis*	*E. abnormis*	CHINA, Yunnan	(unspecified)	SH1155612.08FU	†SH1522994.08FU	VSH97_1	VSH985_2
AB267637		Miyoshi et al. (2007)	*E. abnormis*	*Lachnum abnorme*	*Lachnum abnorme*	JAPAN, Nara	Twig	SH1155612.08FU	SH1523013.08FU	VSH97_2	VSH985_1
AB267638		Miyoshi et al. (2007)	*E. abnormis*	*Lachnum abnorme*	*Lachnum abnorme*	JAPAN, Shizuoka	Twig	SH1155612.08FU	SH1523013.08FU	VSH97_2	VSH985_1
AB481249	16582	Hosoya et al. (2010)	*E. abnormis*	*Lachnum abnorme*	*Lachnum abnorme*	JAPAN, Kanagawa, Yamakita	wood of unidentified tree	SH1155612.08FU	SH1523013.08FU	VSH97_1	VSH985_1
AB705234	16609	Zhao et al. (2012)	*E. abnormis*	*Lachnum abnorme*	*Lachnum abnorme*	JAPAN, Kanagawa, Yamakita	wood of *Cephalotaxus harringtonia*	SH1155612.08FU	SH1523013.08FU	VSH97_1	VSH985_1
LC424837	80478	this study	*E. abnormis*	-	-	JAPAN, Shizuoka, Oyama	twig of unidentified tree	SH1155612.08FU	SH1523013.08FU	VSH97_2	VSH985_3
MG712307		unpublished	*E. abnormis*	*Lachnum abnorme*	*Lachnum abnorme*	CHINA	(unspecified)	SH1155612.08FU	SH1523013.08FU	VSH97_2	VSH985_3
MK282241		unpublished	*E. abnormis*	*Lachnum abnorme*	*Lachnum abnorme*	(unspecified)	(unspecified)	SH1155612.08FU	SH1523013.08FU	VSH97_2	VSH985_1
MK584957		Ekanayaka et al. (2019)	*E. abnormis*	*E. aseptata*	*E. aseptata*	THAILAND, Chiang Rai	(unspecified)	SH1155612.08FU	SH1523013.08FU	VSH97_2	VSH985_1
MN082536		unpublished	*E. abnormis*	*Lachnum abnorme*	*Lachnum abnorme*	(unspecified)	(unspecified)	SH1155612.08FU	SH1523013.08FU	VSH97_1	VSH985_1
MT995055		unpublished	*E. abnormis* (misregistered?)	*Chapsa patens*	*Chapsa patens*	(unspecified)	(unspecified)	SH1155612.08FU	SH1523013.08FU	VSH97_1	VSH985_1
MW007918		unpublished	*E. abnormis* (misregistered?)	*Chapsa patens*	*Chapsa patens*	(unspecified)	(unspecified)	SH1155612.08FU	SH1523013.08FU	VSH97_2	VSH985_3

ITS sequence GenBank/UNITE accession no.	TNS-F specimen no.	Reference (initial appearance)	Taxon name (ultimately allocated in this study)	UNITE taxon name	INSDC taxon name	Country	Host plants and parts	UNITE SH code (DOI) at 3% threshold	UNITE SH code (DOI) at 1.5% threshold	VSEARCH SH at 97% similarity	VSEARCH SH at 98.5% similarity
UDB0779051/ LC669439	16556	this study	*E. abnormis*	-	-	JAPAN, Oita, Kokonoe	wood of unidentified tree	SH1155612.08FU	SH1523013.08FU	VSH97_2	VSH985_1
UDB0779053/ LC669441	16606	this study	*E. abnormis*	-	-	JAPAN, Kanagawa, Yamakita	wood of unidentified tree	SH1155612.08FU	SH1523013.08FU	VSH97_2	VSH985_3
UDB0779054/ LC669442	16639	this study	*E. abnormis*	-	-	JAPAN, Ibaraki, Tsukuba Botanical Garden	twig of unidentified tree	SH1155612.08FU	SH1523013.08FU	VSH97_2	VSH985_3
UDB0779057/ LC669445	25579	this study	*E. abnormis*	-	-	JAPAN, Tokyo, Hongo	twig of unidentified tree	SH1155612.08FU	SH1523013.08FU	VSH97_2	VSH985_3
UDB0779062/ LC669450	32163	this study	*E. abnormis*	-	-	JAPAN, Kanagawa, Odawara	twig of unidentified tree	SH1155612.08FU	SH1523013.08FU	VSH97_2	VSH985_3
UDB0779069/ LC669457	38452	this study	*E. abnormis*	-	-	JAPAN, Gunma, Naganohara	twig of unidentified tree	SH1155612.08FU	SH1523013.08FU	VSH97_1	VSH985_1
UDB0779072/ LC669460	61931	this study	*E. abnormis*	-	-	JAPAN, Kanagawa, Zushi	twig of unidentified tree	SH1155612.08FU	SH1523013.08FU	VSH97_2	VSH985_3
UDB0779086/ LC669474	46841	this study	*E. abnormis*	-	-	JAPAN, Gifu, Gujo	twig of unidentified tree	SH1155612.08FU	SH1523013.08FU	VSH97_1	VSH985_1
AB481250	16617	Hosoya et al. (2010)	*E. abnormis*	*Lachnum abnorme*	*Lachnum abnorme*	JAPAN, Kanagawa, Yamakita	twig of unidentified tree	‡SH1155612.08FU	‡SH1523013.08FU	VSH97_1	VSH985_1
UDB0779055/ LC669443	16837	this study	*E. sinensis* (←*Lachnum mapirianum* var. *sinense*)	-	-	JAPAN, Ibaraki, Tsukuba Botanical Garden	leaf of unidentified broad-leaved tree	SH1155682.08FU	SH1523107.08FU	VSH97_4	VSH985_5
AB481280	16838	Hosoya et al. (2010)	*E. sinensis* (←*Lachnum mapirianum* var. *sinense*)	*Lachnum* sp.	*Lachnum* (*Lachnum* sp. FC-2355)	JAPAN, Ibaraki, Tsukuba Botanical Garden	leaf of unidentified broad-leaved tree	SH1155682.08FU	SH1523107.08FU	VSH97_4	VSH985_5
AB481281	16841	Hosoya et al. (2010)	*E. sinensis* (←*Lachnum mapirianum* var. *sinense*)	*Lachnum* sp.	*Lachnum* (*Lachnum* sp. FC-2358)	JAPAN, Ibaraki, Mt. Tsukuba	leaf of unidentified broad-leaved tree	SH1155682.08FU	SH1523107.08FU	VSH97_4	VSH985_5
UDB0779061/ LC669449	32161	this study	*E. sinensis* (←*Lachnum mapirianum* var. *sinense*)	-	-	JAPAN, Kanagawa, Odawara	leaf of *Quercus myrsinifolia*	SH1155682.08FU	SH1523107.08FU	VSH97_4	VSH985_5
UDB0779083/ LC669471	80354	this study	*E. sinensis* (←*Lachnum mapirianum* var. *sinense*)	-	-	JAPAN, Kanagawa, Manazuru	leaf of *Castanopsis sieboldii*	†SH1155682.08FU	†SH1523107.08FU	VSH97_4	VSH985_5

ITS sequence GenBank/UNITE accession no.	TNS-F specimen no.	Reference (initial appearance)	Taxon name (ultimately allocated in this study)	UNITE taxon name	INSDC taxon name	Country	Host plants and parts	UNITE SH code (DOI) at 3% threshold	UNITE SH code (DOI) at 1.5% threshold	VSEARCH SH at 97% similarity	VSEARCH SH at 98.5% similarity
UDB023346		unpublished	*E. curvispora*	*E. curvispora*	-	MONTENEGRO, Žijevo Mountains	needle of *Pinus heldreichii*	SH1155703.08FU	SH1523136.08FU	VSH97_12	VSH985_14
MH190414		Perić and Baral (2014)	*E. curvispora*	*E. curvispora*	*E. curvispora*	MONTENEGRO, Žijevo Mountains	needle of *Pinus heldreichii*	†SH1155703.08FU	†SH1523136.08FU	VSH97_12	VSH985_14
JF937580		Zhao and Zhuang (2011)	*E. brasiliensis*	*Lachnum brasiliense*	*Lachnum brasiliense*	CHINA	(unspecified)	SH1155705.08FU	SH1523142.08FU	VSH97_6	VSH985_7
MK584953		Ekanayaka et al. (2019)	*E. brasiliensis*	*E. brasiliensis*	*E. brasiliensis*	(unspecified)	(unspecified)	SH1155705.08FU	SH1523142.08FU	VSH97_6	VSH985_7
MK584967		Ekanayaka et al. (2019)	*E. brasiliensis*	*E. brasiliensis*	*E. brasiliensis*	THAILAND, Chiang Rai	(unspecified)	SH1155705.08FU	SH1523142.08FU	VSH97_6	VSH985_7
UDB0779068/ LC669456	46419	this study	*E. brasiliensis*	-	-	TAIWAN, Taipei	wood of unidentified tree	SH1155705.08FU	SH1523142.08FU	VSH97_6	VSH985_7
JF937579		Zhao and Zhuang (2011)	*E. brasiliensis*	*Lachnum brasiliense*	*Lachnum brasiliense*	CHINA	(unspecified)	†SH1155705.08FU	†SH1523142.08FU	VSH97_6	VSH985_7
KX501132		Tello and Baral (2016)	*E. lunata*	*E. lunata*	*E. lunata*	SPAIN, Andalucía	needle of *Pinus nigra* subsp. *nigra*	†SH1155760.08FU	†SH1523257.08FU	VSH97_18	VSH985_19
JX984680		unpublished	*E. hainanensis* (←*Lachnum hainanense*)	Hyaloscyphaceae	Fungi (uncultured fungus)	KOREA, Seoul	(Total suspended particulate matter (TSP) in urban air during non-Asian dust days)	SH1155844.08FU	SH1523423.08FU	VSH97_3	VSH985_4
UDB0779064/ LC669452	35049	this study	*E. hainanensis* (←*Lachnum hainanense*)	-	-	JAPAN, Niigata, Minamiuonuma	leaf of *Quercus glauca*	SH1155844.08FU	SH1523423.08FU	VSH97_3	VSH985_4
UDB0779065/ LC669453	35056	this study	*E. hainanensis* (←*Lachnum hainanense*)	-	-	JAPAN, Niigata, Minamiuonuma	leaf of *Quercus serrata*	SH1155844.08FU	SH1523423.08FU	VSH97_3	VSH985_4
UDB0779073/ LC669461	61941	this study	*E. hainanensis* (←*Lachnum hainanense*)	-	-	JAPAN, Kanagawa, Kamakura	leaf of *Quercus glauca*	SH1155844.08FU	SH1523423.08FU	VSH97_3	VSH985_4
UDB0779076/ LC669464	65722	this study	*E. hainanensis* (←*Lachnum hainanense*)	-	-	JAPAN, Gunma, Midori	leaf of *Quercus serrata* subsp. *mongolicoides*	SH1155844.08FU	SH1523423.08FU	VSH97_3	VSH985_4

ITS sequence GenBank/UNITE accession no.	TNS-F specimen no.	Reference (initial appearance)	Taxon name (ultimately allocated in this study)	UNITE taxon name	INSDC taxon name	Country	Host plants and parts	UNITE SH code (DOI) at 3% threshold	UNITE SH code (DOI) at 1.5% threshold	VSEARCH SH at 97% similarity	VSEARCH SH at 98.5% similarity
MK282242		unpublished	*E. hainanensis* (←*Lachnum hainanense*)	*Lachnum* sp.	*Lachnum albidulum*	KOREA	(unspecified)	SH1155844.08FU	†SH1523423.08FU	VSH97_3	VSH985_4
UDB0779077/ LC669465	80356	this study	*E. hainanensis* (←*Lachnum hainanense*)	-	-	JAPAN, Kanagawa, Hiratsuka	leaf of *Quercus glauca*	SH1155844.08FU	SH3597461.08FU	VSH97_3	VSH985_9
UDB0779078/ LC669466	80371	this study	*E. hainanensis* (←*Lachnum hainanense*)	-	-	JAPAN, Kanagawa, Hiratsuka	leaf of *Castanopsis sieboldii*	SH1155844.08FU	SH3597461.08FU	VSH97_3	VSH985_9
UDB0779071/ LC669459	61775	this study	*E. hainanensis* (←*Lachnum hainanense*)	-	-	JAPAN, Kanagawa, Hiratsuka	leaf of *Quercus myrsinifolia*	†SH1155844.08FU	†SH3597461.08FU	VSH97_3	VSH985_9
UDB0779050/ LC669438	26492	this study	*E. sclerotii*	-	-	JAPAN, Tokyo, Hahajima Island	wood of unidentified tree	SH1155848.08FU	SH1523429.08FU	VSH97_5	VSH985_6
JF937584		Zhao and Zhuang (2011)	*E. sclerotii*	*Lachnum sclerotii*	*Lachnum sclerotii*	CHINA	(unspecified)	SH1155848.08FU	SH1523429.08FU	VSH97_5	VSH985_6
MK584951		Ekanayaka et al. (2019)	*E. sclerotii*	*E. sclerotii*	*E. sclerotii*	THAILAND, Chiang Rai	(unspecified)	SH1155848.08FU	SH1523429.08FU	VSH97_5	VSH985_6
UDB0779070/ LC669458	38480	this study	*E. sclerotii*	-	-	TAIWAN, Wulai	twig of unidentified tree	SH1155848.08FU	SH1523429.08FU	VSH97_5	VSH985_6
MK584969		Ekanayaka et al. (2019)	*E. sclerotii*	*E. sclerotii*	*E. sclerotii*	THAILAND, Chiang Rai	(unspecified)	†SH1155848.08FU	†SH1523429.08FU	VSH97_5	VSH985_6
AB481271	16642	Hosoya et al. (2010)	*Lachnum novoguineense* var. *yunnanicum*	*Lachnum* sp.	*Lachnum* sp. (*Lachnum* sp. FC-2211)	JAPAN, Ibaraki, Mt. Tsukuba	culm of unidentified bamboo	SH1236904.08FU	SH1648536.08FU	VSH97_10	VSH985_12
AB481270	16442	Hosoya et al. (2010)	*Lachnum novoguineense* var. *yunnanicum*	*Lachnum* sp.	*Lachnum* sp. (*Lachnum* sp. FC-2117)	JAPAN, Nagano, Ueda, Sugadaira Montane Research Center	culm of unidentified bamboo	†SH1236904.08FU	†SH1648536.08FU	VSH97_10	VSH985_12
MK584965		Ekanayaka et al. (2019)	*E. alba*	*E. alba*	*E. alba*	THAILAND, Chiang Mai	(unspecified)	†SH2596405.08FU	†SH2712425.08FU	VSH97_22	VSH985_25
AB267647		Miyoshi et al. (2007)	*Lachnum palmae* sensu lato	*Lachnum palmae*	*Lachnum palmae*	JAPAN, Oita	leaf of *Livistona chinensis*	SH1149764.08FU	SH1515235.08FU	VSH97_7	VSH985_8

ITS sequence GenBank/UNITE accession no.	TNS-F specimen no.	Reference (initial appearance)	Taxon name (ultimately allocated in this study)	UNITE taxon name	INSDC taxon name	Country	Host plants and parts	UNITE SH code (DOI) at 3% threshold	UNITE SH code (DOI) at 1.5% threshold	VSEARCH SH at 97% similarity	VSEARCH SH at 98.5% similarity
LC425039 (duplicate; UDB0779046)	13500	Johnston et al. (2019)	*Lachnum palmae* sensu lato	*Lachnum palmae*	*Lachnum palmae*	JAPAN, Kagoshima, Yakushima Island	leaf of *Livistona chinensis* var. *subglobosa*	SH1149764.08FU	SH1515235.08FU	VSH97_7	VSH985_8
UDB0779066/ LC669454	39729	this study	*Lachnum palmae* sensu lato	-	-	JAPAN, Okinawa, Iriomote Island	leaf of *Livistona chinensis* var. *subglobosa*	SH1149764.08FU	SH1515235.08FU	VSH97_7	VSH985_8
MG283320		Zhao et al. (2018)	*Lachnum palmae* sensu lato	*Lachnum palmae*	*Lachnum palmae*	CHINA, Linzhou	root of *Przewalskia tangutica* (endophyte)	†SH1149764.08FU	†SH1515235.08FU	VSH97_7	VSH985_8
UDB0779089/ LC669477	17567	this study	*Lachnum palmae* sensu lato	-	-	NEW ZEALAND	leaf of unidentified palm	SH2594271.08FU	SH2709065.08FU	VSH97_15	VSH985_16
MH921862		unpublished	*Lachnum palmae* sensu lato	*Lachnum palmae*	*Lachnum palmae*	NEW ZEALAND	unidentified part of *Rhopalostylis sapida*	†SH2594271.08FU	†SH2709065.08FU	VSH97_15	VSH985_16
UDB0779052/ LC669440	24588	this study	*Lachnum palmae* sensu lato	-	-	JAPAN, Kagoshima, Amami-Oshima	leaf of *Livistona chinensis* var. *subglobosa*	SH3569651.08FU	SH3597456.08FU	VSH97_9	VSH985_17
UDB0779047/ LC669435	11197	this study	*Lachnum palmae* sensu lato	-	-	JAPAN, Shizuoka, Shimoda	leaf of *Livistona chinensis* var. *subglobosa*	†SH3569651.08FU	†SH3597456.08FU	VSH97_9	VSH985_17
UDB0779048/ LC669436	26161	this study	*Lachnum palmae* sensu lato	-	-	JAPAN, Tokyo, Chichijima Island	leaf of *Livistona boninensis*	SH3569651.08FU	SH3597457.08FU	VSH97_9	VSH985_11
UDB0779058/ LC669446	26172	this study	*Lachnum palmae* sensu lato	-	-	JAPAN, Tokyo, Kita-Iwojima Island	leaf of *Livistona chinensis* var. *subglobosa*	SH3569651.08FU	SH3597457.08FU	VSH97_16	VSH985_11
UDB0779059/ LC669447	26185	this study	*Lachnum palmae* sensu lato	-	-	JAPAN, Tokyo, Kita-Iwojima Island	leaf of *Livistona chinensis* var. *subglobosa*	SH3569651.08FU	†SH3597457.08FU	VSH97_16	VSH985_11
UDB0779056/ LC669444	24600	this study	*Lachnum palmae* sensu lato	-	-	JAPAN, Kagoshima, Amami-Oshima	leaf of *Livistona chinensis* var. *subglobosa*	†SH3569653.08FU	†SH3597459.08FU	VSH97_25	VSH985_28
U58640		Cantrell and Hanlin (1997)	*E. euterpes*	*Lachnum euterpes*	*Lachnum euterpes*	PUERTO RICO	(unspecified)	†SH1236906.08FU	†SH1648538.08FU	VSH97_21	VSH985_24
KT384413		Ekanayaka et al. (2019)	*E. fusiformis*	*Lachnum fusiforme*	*Lachnum fusiforme*	THAILAND	dead stems	‡SH1236907.08FU	‡SH1648539.08FU	VSH97_11	VSH985_13
MK584948		Ekanayaka et al. (2019)	*E. fusiformis*	*Lachnum fusiforme*	*Lachnum fusiforme*	CHINA	dead stems	SH1236907.08FU	SH1648539.08FU	VSH97_11	VSH985_13

ITS sequence GenBank/UNITE accession no.	TNS-F specimen no.	Reference (initial appearance)	Taxon name (ultimately allocated in this study)	UNITE taxon name	INSDC taxon name	Country	Host plants and parts	UNITE SH code (DOI) at 3% threshold	UNITE SH code (DOI) at 1.5% threshold	VSEARCH SH at 97% similarity	VSEARCH SH at 98.5% similarity
UDB0779049/ LC669437	26520	this study	*E. boninensis*	-	-	JAPAN, Tokyo, Hahajima Island	wood of unidentified tree	†SH3569652.08FU	†SH3597458.08FU	VSH97_20	VSH985_21
UDB0779060/ LC669448	26500	this study	*E. insulae*	-	-	JAPAN, Tokyo, Hahajima Island	wood of unidentified tree	SH3569654.08FU	SH3597460.08FU	VSH97_14	VSH985_15
UDB0779063/ LC669451	39720	this study	*E. insulae*	-	-	JAPAN, Okinawa, Iriomote Island	bark of unidentified tree	†SH3569654.08FU	†SH3597460.08FU	VSH97_14	VSH985_15
UDB0779075/ LC669463	61920	this study	*E. paralushanensis*	-	-	JAPAN, Shizuoka, Atami	culm of *Pleioblastus argenteostriatus*	†SH3569655.08FU	†SH3597462.08FU	VSH97_19	VSH985_20
AF505515			*E. lushanensis*	*Lachnum lushanense*	*Lachnum lushanense*	(unspecified)	(unspecified)	†SH1155706.08FU	†SH1523143.08FU	VSH97_8	VSH985_10
JF937582		Zhao and Zhuang (2011)	*E. lushanensis*	*Lachnum lushanense*	*Lachnum lushanense*	CHINA	(unspecified)	SH1155706.08FU	SH1523143.08FU	VSH97_8	VSH985_10
MG434782		unpublished	*E. lushanensis*	*Erioscyphella* sp.	*E. lushanensis*	INDIA, Tangmarg	root tips of *Pinus wallichiana* (ectomycorrhiza)	(unassigned)	(unassigned)	VSH97_8	VSH985_10
UDB0779081/ LC669469	81272	this study	*E. papillaris*	-	-	JAPAN, Gunma, Minakami	leaf of unidentified bamboo	†SH3569656.08FU	†SH3597463.08FU	VSH97_23	VSH985_26
UDB0779084/ LC669472	81401	this study	*E. sasibrevispora*	-	-	JAPAN, Hokkaido, Tomakomai	culm of *Sasa nipponica*	SH3569657.08FU	SH3597464.08FU	VSH97_13	VSH985_23
UDB0779082/ LC669470	80399	this study	*E. sasibrevispora*	-	-	JAPAN, Gunma, Higashi-Agatsuma	sheath of *Sasa veitchii*	†SH3569657.08FU	†SH3597464.08FU	VSH97_13	VSH985_22
UDB0779085/ LC669473	81472	this study	*E. otanii*	-	-	JAPAN, Hokkaido, Horonobe, Teshio Experimental Forest, Hokkaido University	leaf of *Sasa senanensis*	†SH3569658.08FU	†SH3597465.08FU	VSH97_24	VSH985_27
UDB0779087/ LC669475	17245	this study	*Lachnum mapirianum*	-	-	MALAYSIA, Gerik	leaf of unidentified tree	†SH3569659.08FU	†SH3597466.08FU	VSH97_17	VSH985_18
UDB0779088/ LC669476	17249	this study	*Lachnum mapirianum*	-	-	MALAYSIA, Gerik	leaf of unidentified tree	SH3569659.08FU	SH3597466.08FU	VSH97_17	VSH985_18

† Representative sequence of each SH
‡ Reference sequence of each SH

The extracted and aligned ITS sequences were composed of three partitions, ITS1 (162 bp), 5.8S (157 bp), and ITS2 (142 bp). The concatenated ITS sequence matrix was registered in TreeBase (http://purl.org/phylo/treebase/phylows/study/TB2:S28473). In the ASAP analysis, the concatenated dataset of these partitions (461 bp) was input, and 87 ITS sequences were clustered into 18 SHs with the lowest asap-score, reflecting better partitioning (Suppl. material 1: Fig. S3). In the GMYC analysis, 29 SHs were delimited (Suppl. material 1: Fig. S4). The ultrametric tree constructed for the GMYC analysis is available in TreeBase (http://purl.org/phylo/treebase/phylows/study/TB2:S28473). For the PTP analyses, an ML best-scored tree was constructed (Suppl. material 1: Fig. S5). PTP analyses delimited 23 SHs in the Bayesian support and 26 SHs in the ML support (Suppl. material 1 Fig. S6), and the former was adopted.

Comparing the number of SHs generated by different clustering methods and applied thresholds, 18 SHs by ASAP, and 23 SHs by UNITE SH at 3% threshold represented the lowest SH numbers (Fig. 3; Table 2). The ASAP results were too rough to delimit the boundaries of *E. abnormis*, *E. boninensis*, *E. brasiliensis*, *E. curvispora*, and *E. sclerotii*. SH-classification recognized by UNITE SH at 3% threshold mostly corresponded to taxon names originally assigned to sequences.

Comparing the results of seven species delimitation methods (UNITE SH at 3% threshold, UNITE SH at 1.5% threshold, VSEARCH 97% similarity, VSEARCH 98.5% similarity, ASAP, GMYC, and PTP), sequences labeled as *E. alba*, *E. brasiliensis*, *E. curvispora*, *E. euterpes*, *E. fusiformis*, *E. lunata*, *E. sclerotii*, *L. mapirianum*, *L. mapirianum* var. *sinense*, *L. novoguineense* var. *yunnanica*, and six new species candidates were distinguished as separate clusters by more than four delimitation methods (Fig. 3). These species clusters did not contradict with morphological/ecological and phylogenetic relationships (Fig. 1). Seven sequences labeled as *L. hainanense* were clustered into one SH by four species delimitation analyses, and part of the SHs included a sequence labeled as *Lachnum albidulum* (Fig. 3).

Erioscyphella abnormis, *E. aseptate*, and *L. palmae* did not form separate clusters supported by majority of four species delimitation analyses (Fig. 3). Sequences labeled as *E. abnormis* were clustered into one to four SHs, and some SHs included sequences labeled as *Chapsa patens* (Nyl.) Frisch, *E. aseptata*, *E. brasiliensis*, and *E. sclerotii* (Fig. 3). Twelve sequences labeled as *L. palmae* were clustered into four to six SHs (Fig. 3).

Discussion

Generic delimitation and generic concept of *Erioscyphella*

We accepted Clade A as a monophyletic unit for *Erioscyphella* which is supported by morphology. Although Clade B comprised Clade A together with *P. alboviridis*, Clade B should not be regarded as a genus delimitation of *Erioscyphella*, because *Proliferodiscus* differs from members of Clade A in having apothecia proliferating from the margins continuously and thick-walled and coarsely warted hairs (Haines and Dumont 1983; Spooner 1987). All members of Clade A are distinguishable from the other

lachnacenous genera. In contrast to *Erioscyphella*, *Albotricha* and *Dasyscyphella* are distinguished by hair apices with no granulation (Hosoya et al. 2010), *Brunnipila*, *Capitotricha*, and *Incrucipulum* by hair-crystals (Baral and Krieglsteiner 1985; Tochihara and Hosoya 2019), and *Lachnellula* by ectal excipulum composed of *textura globose* to *textura oblita* (Dharne 1965). Typical members of Clade A can be easily segregated from *Neodasyscypha*, because the characteristic features of *Neodasyscypha*, such as dark-brown hairs, ectal-excipulum structure, and ellipsoid to fusoid ascospores < 10 μm long (Spooner 1987), are rare in Clade A. Among members of Clade A and *Lachnum* sensu stricto, the shape and length of ascospores were continuous (Fig. 4), as indicated by Haines and Dumont (1984). However, ascospores longer than 15–20 μm were restricted to Clade A (Fig. 4). Moreover, most members of Clade A have hairs with apical amorphous materials, which are not seen in *Lachnum* sensu stricto. Members of Clade A usually also have hairs not swelling at the apices and distantly septate, as Perić and Baral (2014) pointed out for three tropical members, while members of *Lachnum* have swelling apices. The combination of such characters allows us to differentiate typical members of *Erioscyphella* from *Lachnum*.

In summary, *Erioscyphella* is still difficult to define solely based on morphology because of multiple exceptional characters continuous to other genera, but its typical members could be recognizable mainly by the hair structures and ascospore length. Based on members of Clade A, *Erioscyphella* is tentatively described as follows: apothecia occurring on dead hardwood leaves, rotten wood, bamboo sheaths, bamboo leaves or palm leaves; asci mostly arising from simple septa, but occasionally from croziers; ascospores fusiform to long needle-shaped, aseptate to multi-septate; paraphyses filiform to narrowly lanceolate, shortly exceeding the asci, but rarely lanceolate and long exceeding the asci; hairs straight or irregularly curved, usually not swollen at the apices, thin-walled, hyaline, but sometimes brown, totally and densely granulated, usually distantly septate, without needle-like or three-dimensional shaped crystals but mostly equipped with hyaline to brown apical amorphous materials, and/or resinous materials at any part of hairs; walls of ectal excipulum cells smooth but granulate in one species.

Perić and Baral (2014) pointed out that "yellow hymenium derived from carotenoid" is one of the common characters of *Erioscyphella*. This feature was not discussed in this study because some specimens were not observed when fresh; the hymenium color is variable (usually white hymenium becomes yellow) between fresh and dried states in lachnaceous species.

Host selectivity of *Erioscyphella*

In *Erioscyphella*, the tendency of selectivity of species to host plants or parts occurs across the genus. Each subclade within *Erioscyphella* (Clade I–V) generally shared tendencies toward host selectivity as follows: Clade I on leaves of broad-leaved trees, except for *E. paralushanensis* occurring on bamboo sheaths, Clade II on palm leaves, Clade III on bamboo leaves, Clade IV on bamboo sheaths, and Clade V on rotten wood (Fig. 1). The results showed that selectivity to host plants, and parts of *Erioscyphella*, was acquired as apomorphic characters during speciation.

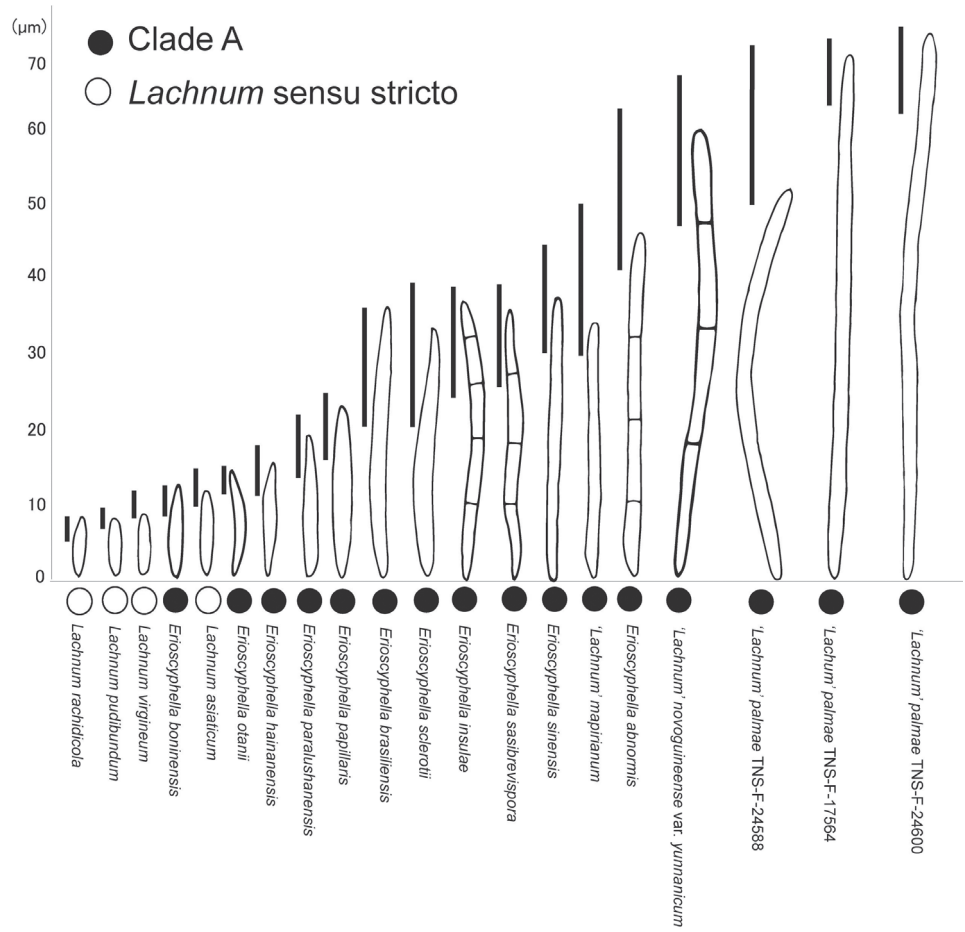

Figure 4. Comparison of ascospores of Clade A (= *Erioscyphella*) and the clade of *Lachnum* sensu stricto in Fig. 1. Subclade numbers for members of Clade A in Fig. 1 are shown in parentheses. Bars show variation of ascospore length within each species.

Is *Erioscyphella* limited to 'tropical' zones?

Erioscyphella (long-spored *Lachnum*) has long been known as the tropical genus in Lachnaceae (Dennis 1954; Spooner 1987; Guatimosim et al. 2016). Most long-spored species were described from tropical areas of Latin America (Dennis 1954) and tropical to temperate areas of Australasia (Spooner 1987). However, the new species or new combinations proposed in this study were reported from Japan in subtropical areas (*E. boninensis* and *E. insulae*), temperate area (*E. hainanensis*, *E. palalushanensis*, and *E. sinensis*) and cool-temperate to subarctic areas (*E. otanii*, *E. papillaris*, and *E. sasibrevispora*), showing that *Erioscyphella* is not limited to tropical zones, but is also distributed in temperate to subarctic zones in the northern hemisphere.

Ascal iodine reactions seen in *E. papillaris*

Iodine reactions of the ascus apical apparatus have been classified into several types (inamyloid, hemiamyloid [Type RB and RR, and euamyloid Type BB]) (Baral 2009), and the reaction 'MLZ- without KOH pretreatment and MLZ+ with KOH pretreatment', observed in *E. papillaris* (Fig. 11E1 and Fig. E2) has been restricted to the type of hemiamyloid. However, the apical apparatus of *E. papillaris* showed a dark blue reaction in IKI without KOH pretreatment (Fig. 11E3), while the hemiamyloid apparatus usually shows a red reaction under these conditions. The hemiamyloid ascal apparatus could show IKI-blue without KOH pretreatment due to long storage in the herbarium (Baral 2009), but this is not applicable for the material of *E. papillaris*, which has been maintained for only two years in herbarium until observed. Therefore, we assessed the iodine reaction of *E. papillaris* as a new type, and color reactions with various solutions of the species should be further examined using new materials, because there are few apothecia in the type specimen.

Species-level taxonomic treatment of *Erioscyphella*

In this study, we carried out taxonomic treatment for species which were distinguished by morphology/ecology and phylogenetic analyses, and formed single clusters in species delimitation analyses. Based on this criteria, six undescribed species of *Erioscyphella* have been proposed as new species of *Erioscyphella* [*E. boninensis*, *E. insulae*, *E. otanii*, *E. papillaris*, *E. paralushanensis*, and *E. sasibrevispora*], and *Lachnum hainanense* and *L. mapirianum* var. *sinense* have been proposed as new members of *Erioscyphella*. Interpretation of species boundaries of *L. hainanense* was discussed in the taxonomy chapter. For new species and new combinations, Japanese names were also denominated for wider use of Japanese mycologists or amateurs.

In the phylogenetic analyses, Malaysian materials of *L. mapirianum* (TNS-F-17245, 17249) and Japanese materials of *L. novoguineense* var. *yunnanicum* (TNS-F-16442, 16642) were also found to be members of *Erioscyphella* (Fig. 1). However, we hesitate to transfer the two species into *Erioscyphella*, as we cannot guarantee the identification accuracy of the materials, because of inadequate type information of the two species.

Taxonomic assessments of *E. abnormis*, *L. aseptate*, and *L. palmae*, which were not accepted as independent species in species delimitation analyses, are discussed below.

Taxonomy of *E. abnormis* and its related species

In the species delimitation analyses, sequences labeled as *E. abnormis* formed a single SH at UNITE SH 3% threshold (DOI: SH1155612.08FU) and divided into two to four SHs at UNITE SH 1.5% threshold, VSEARCH, and GMYC (Fig. 3).

In ASAP, sequences labeled as *E. abnormis* belong to a single SH, but the SH also contained sequences labeled as *Chapsa patens*, *E. aseptata*, *E. brasiliensis*, *E. curvispora*,

and *E. sclerotii* (Fig. 3). However, the phylogenetic analyses revealed that *E. brasiliensis*, and *E. sclerotii* are separate from the clade of *E. abnormis* (Fig. 1), suggesting that the two species are different from *E. abnormis*. Although *E. curvispora* was not included in the phylogenetic analyses (Fig. 1), the apparent morphological and ecological differentiation (Perić and Baral 2014) and low similarity of ITS (< 97%) with members of *E. abnormis* (Fig. 3) suggest that *E. curvispora* is different from *E. abnormis*.

Erioscyphella aseptata was originally described in Thailand and characterized by having aseptate ascospores, unlike *E. abnormis* or *E. sclerotii* with septate ascospores (Ekanayaka et al. 2019). However, the species delimitation analyses in this study suggested the difficulty of delimiting *E. aseptata* (MK584957) from *E. abnormis* (Fig. 3), suggesting that *E. aseptata* is a morphologically atypical (aseptate-ascospored) individual of *E. abnormis*.

Although two ITS sequences of *C. patens* (MT995055 = specimen no. FJ19131 and MW007918 = specimen no. FJ19049) were positioned in SHs dominated by *E. abnormis*, LSU and mtSSU sequences of FJ19131 and LSU sequence of FJ19049 were closely related to *Chapsa* spp. [Graphidaceae, Ostropales]. Since Lachnaceae and Graphidaceae are phylogenetically distant, the two ITS sequences MT995055 and MW007918 have been misidentified.

Considering that the monophyly of *E. abnormis* is strongly supported (Fig. 1) and members of the species share high ITS similarities (> 97%, compiled into SH1155612.08FU) (Fig. 3, Table 2), *E. abnormis* is accepted here as a species with some intraspecific morphological and phylogenetic variation.

Taxonomy of '*Lachnum*' *palmae*

Lachnum palmae formed a strongly supported clade in the phylogenetic analyses (Clade II in Fig. 1). They also shared strong selectivity to palm leaves and characteristic morphology such as thick-walled asci, hairs with resinous materials and apical amorphous materials (Suppl. material 1: Fig. S2) and ectal excipulum composed of thick-walled prismatic cells and interwoven hyphae. However, sequences labeled as *L. palmae* were divided into 4 to 7 SHs in all species delimitation analyses (Fig. 3), indicating that *L. palmae* is a species complex that includes multiple potential sister species. At present, we avoid creating new species from the complex, because the morphological and ecological differences detected among SHs are not enough to delimit species boundaries, although the size of asci and ascospores differ among some SHs, as shown in Fig. 4. Phylogenetic analyses revealed that members of the *L. palmae* complex belonged to *Erioscyphella* (Fig. 1). However, we could not judge which SH within the complex is equivalent to *L. palmae* as originally described from Honduras by Kanouse (1941) and redescribed by Spooner (1987) from the type plus another specimen from New Zealand. There are no *L. palmae* sequences from the tropical American type locality, so phylogenetic characterization and recombination of the species were avoided in the present study.

Taxonomy

***Erioscyphella boninensis* Tochihara & Hosoya, sp. nov.**
MycoBank No: 835702
Figs 5, 6

Diagnosis. Differs from all other *Erioscyphella* species by the granulate walls of the ectal excipular cells.

Holotype. Japan, Bonin Islands, Chichijima Island, Mt. Tsutsujiyama, 27.060556, 142.222500, ca 270 m, 28 Jun. 2009, on fallen leaves of *Pittosporum boninense*, T.Hosoya (TNS-F-26520).

GenBank/UNITE no. ex holotype. LC669437/UDB0779049 (ITS), LC533151 (LSU), LC533254 (mtSSU), LC533196 (RPB2).

Etymology. Referring to the type locality Bonin Islands.

Japanese name. Ogasawara-cha-hina-no-chawantake.

Description. Apothecia scattered, superficial, 0.5–1.0 mm in diameter, having well-developed stipes, up to 1.5 mm high, cream to pale brown, externally covered with short and shiny hairs. Disc concave, cream to pale yellow. Ectal excipulum *textura prismatica* composed of long elongated cells to *textura angularis*, 6–25 × 5–13 µm, hyaline to relatively brown colored, somewhat thick-walled; cell walls covered by granules with a similar appearance to those on hairs. Stipe composed of *textura prismatica* with a granulate surface as ectal excipular cells. Medullary excipulum *textura intricata* of hyaline hyphae up to 3 µm wide. Hairs straight, cylindrical, 38–62 × 2.5–4.0 µm, hyaline, completely covered by brown granules, 2–3-septate, thin-walled, arising from swelling cells completely covered by granules; apex lacking crystals or apical amorphous materials, equipped with amber-colored resinous materials dissolvable with CB/LA at a little below the apex. Asci (36–)37.7–44(–46) × (3.5–)3.6–4.2(–4.5) µm (av. 41 ±3.2 × 3.9 ± 0.3 µm, n = 16), 8-spored, cylindrical-clavate; pore blue in MLZ without 3% KOH pretreatment; croziers absent at the basal septa. Ascospores (9–)10–12.3(–13) × 1.2–1.7(–1.8) µm (av. 11 ± 1.2 × 1.5 ± 0.2 µm, n = 16), Q = (6.3–)6.9–9.2(–10) (av. 7.8 ± 1.5, n = 16), fusiform, aseptate. Paraphyses straight, up to 2.5 µm wide, septate, exceeding the asci up to 5 µm, narrowly lanceolate.

Culture characteristics. Colony of NBRC 114447/TNS-F-26520 on PDA umbonate forming a dome-shape, slightly sulcate. Context not shiny, velvety, buff at the center, paler toward the margin, dark buff from the reverse. Sectors and zonation absent. Aerial mycelium white or buff, dense cottony, forming white mycelium strands except in the margin. Margin distinct, entire, flat. Asexual morph absent.

Distribution. Japan. (Bonin Islands). Known only from the type locality.

Notes. Granulation on the surface of the ectal excipular cells has been observed only in *Incrucipulum* in Lachnaceae (Baral and Krieglsteiner 1985; Tochihara and Hosoya 2019), and *E. boninensis* is the first report for such a character in *Erioscyphella*

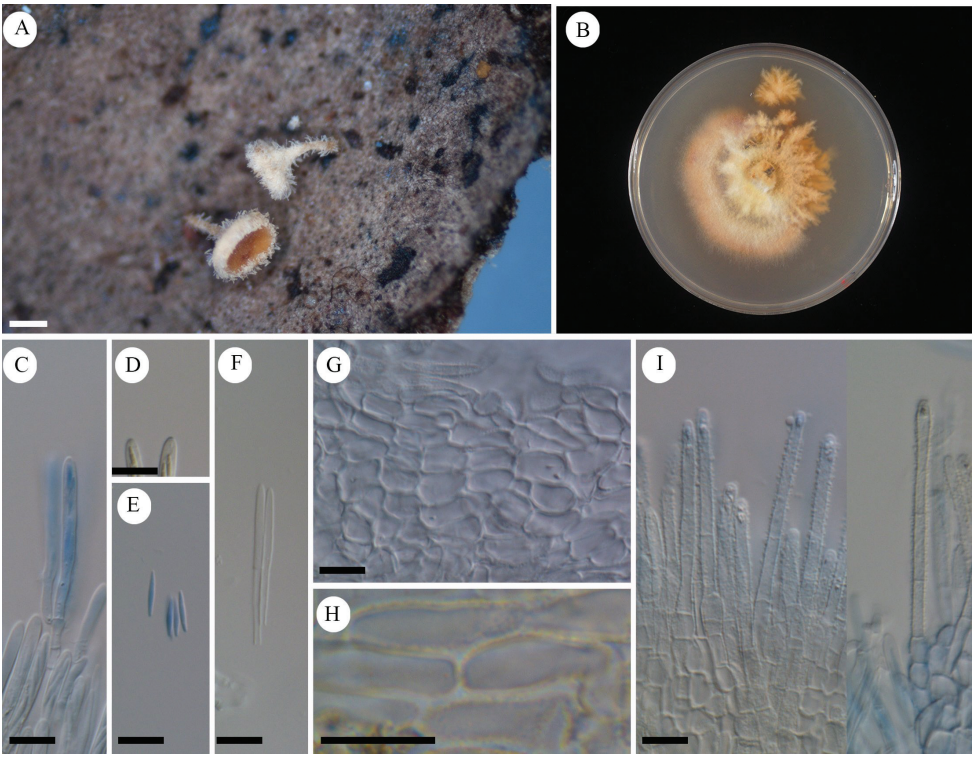

Figure 5. *Erioscyphella boninensis* TNS-F-26520 (Holotype) **A** dried apothecia **B** pure culture on PDA (NBRC 114447) **C** ascus **D** ascal pore MLZ (+) **E** ascospores **F** paraphyses **G** ectal excipular cells **H** ectal excipular cells with red granules **I** hairs with resinous matters arising from ectal excipular cells. Mounted in CB/LA (**C, E–I**), MLZ (**D**). Scale bars: 1 mm (**A**); 10 μm (**C–I**).

(Fig. 5H, 6E). Phylogenetic analysis revealed that *E. boninensis* is closely related to *E. paralushanensis* (Fig. 1). The two species (Clade IA, Fig. 1) have colored granules on hairs and forming red mycelia on PDA. However, granulation of ectal excipulum is seen only in *E. boninensis*.

***Erioscyphella hainanensis* (W.Y. Zhuang and Zheng Wang) Hosoya and Tochihara, comb. nov.**
MycoBank No: 835707

≡ *Lachnum hainanense* W.Y. Zhuang & Zheng Wang, Mycotaxon 67: 25 (1998).

Diagnosis. Forming apothecia with long stipes and long hairs. Differing *E. sinensis* in much shorter ascospores.

Japanese name. Shii-Kashi-hina-no-chawantake.

Specimens examined. Japan, Niigata, Minamiuonuma, 37.056808, 138.80705, ca 720 m, 14 May 2010, on fallen leaves of *Quercus glauca*, T.Hosoya

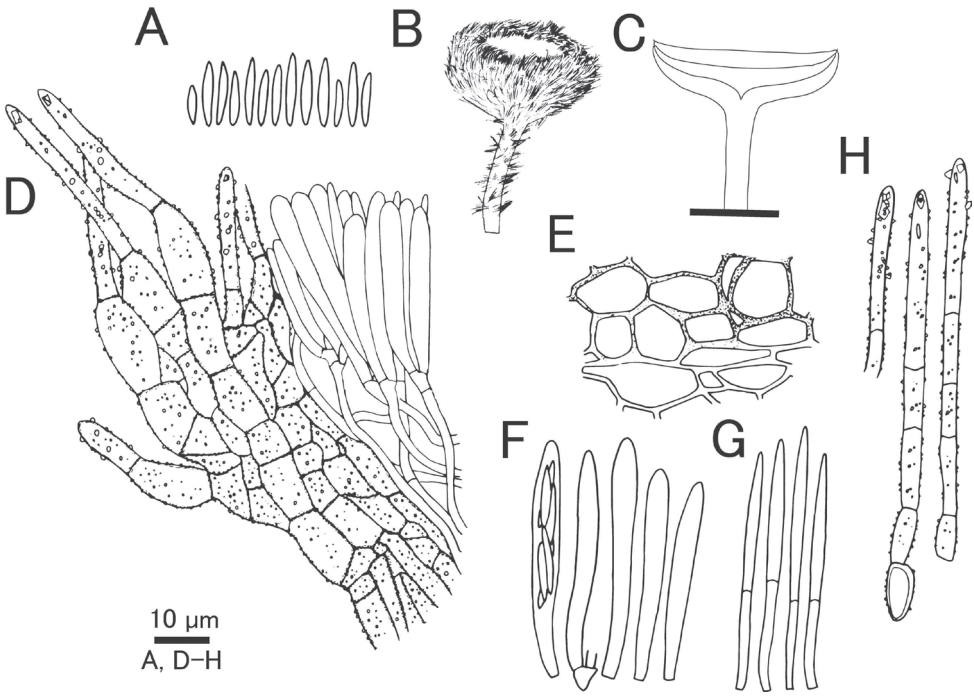

Figure 6. *Erioscyphella boninensis* TNS-F-26520 (Holotype) **A** ascospores **B** apothecium **C** vertical section of an apothecium **D** expansion of a vertical section of an apothecium **E** ectal excipular cells **F** asci **G** paraphyses **H** hairs.

(TNS-F-35049). Ibid (TNS-F-35056). Japan, Kanagawa, Hiratsuka, 35.33861111, 139.285, ca 80 m, 12 Apr. 2015, on fallen leaves of *Q. myrsinifolia*, M.Nakajima (TNS-F-61775). JAPAN, Kanagawa, Kamakura, 35.30756, 139.51958, ca 40 m, 24 Apr. 2015, on fallen leaves of *Q. serrata*, M.Nakajima (TNS-F-61941). Japan, Gunma, Midori, 36.476684, 139.242771, ca 510 m, 9 May 2016, on fallen leaves of *Q. serrata*, K.Furuya (TNS-F-65722). Japan, Kanagawa, Hiratsuka, 35.340139, 139.287167, ca 60 m, 18 May 2017, on fallen leaves of *Q. glauca*, Y.Tochiara (TNS-F-80356). The same locality, on fallen leaves of *Castanopsis sieboldii*, Y. Tochihara (TNS-F-80371).

Distribution. China (Hainan), Japan (Honshu: Kanto region).

Notes. Based on the UNITE SH system at a 3% threshold, ITS sequences of this species were integrated into a single SH (DOI: SH1155844.08FU). SH1155844.08FU included sequences labeled as 'Hyaloscyphaceae' (JX984680) in UNITE and '*L. albidulum*' (MK282242) in INSDC (Table 2). JX984680 was sequenced from air samples in Seoul, South Korea, and was not tied to any fungal specimens or cultures. *Lachnum albidulum* is common on leathery dicot leaves of the old and new world tropics (Haines 1992). *Erioscyphella hainanensis* resembles *L. albidulum* in morphology, but *L. albidulum* has yellow resinous substances at the tip of apothecial hairs and occurs on dead leaves of Rubiaceae (Haines 1992), whereas *E. hainanensis* lacks resinous sub-

stances and occurs on leaves of broad-leaved trees (Zhuang and Wang 1998b; Hosoya et al. 2013). Therefore, we presume that MK282242, coexisting with *L. hainanense* in every SH, was misidentified as *L. albidulum*. No sequences are available for *L. albidulum* specimens from the type locality. *Lachnum hainanense* was therefore judged as acceptable species, and recombined into *Erioscyphella*.

Erioscyphella hainanensis resembles *E. sinensis* in occurring on dead leaves of *Quercus* spp. or *Castanopsis* spp. However, *E. hainanensis* has much shorter ascospores than *E. sinensis*. In this study, presence of minute, hyaline apical amorphous materials and absence of any crystals or resinous materials were confirmed in both species (Suppl. material 1: Fig. S2).

Erioscyphella insulae Tochihara & Hosoya, sp. nov.

MycoBank No: 835703
Figs 7, 8

Diagnosis. Characterized by pure white apothecia unlike related species *Lachnum nothofagi*, and two-layered ectal excipulum.

Holotype. Japan, Okinawa, Yaeyama, Taketomi, Iriomote Island, Otomi, 24.297458, 123.866128, ca 50 m, 12 Jun. 2011, on fallen bark of unidentified tree, T.Fukiharu (TNS-F-39720).

GenBank/UNITE no. ex holotype. LC669451/UDB0779063 (ITS), LC533177 (LSU), LC533261 (mtSSU), LC533207 (RPB2).

Other specimens examined. Japan, Bonin Islands, Hahajima Island, Sekimon, 26.666686, 142.152222, ca 260 m, 24 Jun. 2009, on fallen bark of unidentified tree, T.Hosoya (TNS-F-26485, 26500).

Etymology. Referring to the occurrence of the species on remote islands in Japan.

Japanese name. Shima-hina-no-chawantake.

Description. Apothecia gregarious, superficial, 0.7–1.4(–2.5) mm in diameter, short- and thick-stipitate, up to 0.8 mm high, externally white to cream throughout but sometimes pale brown in the lower parts, covered with white hairs. Disc concave, cream to pale yellow (fresh state not observed). Ectal excipulum composed of two layers: outer layer *textura angularis*, up to 20 µm thick, 3–28 × 2–8 µm, hyaline, thin to relatively thick-walled, with cell walls smooth; inner layer up to 15 µm thick, *textura porrecta* composed of hyaline hyphae up to 5 µm wide. Medullary excipulum up to 100 µm thick, composed of hyaline hyphae forming *textura intricata*; hyphae up to 3 µm wide. Hairs straight or irregularly curved, cylindrical, sometimes branched, up to 125 × 2.5–3.0 µm, hyaline, completely granulate, thin-walled; lacking crystals or resinous materials; apex usually equipped with hyaline apical amorphous materials. Asci (88–)92–101(–106) × 6–7.3(–8) µm (av. 96 ± 4.5 × 6.7 ± 0.6 µm, n = 18), 8-spored, thick-walled, cylindrical-clavate, arising from ascogenous hyphae branching several times; pore blue in MLZ without 3% KOH pretreatment; croziers absent at the basal septa. Ascospores (24–)26.7–34.5(–39) × (1.8–)1.9–2.3(–2.5) µm (av. 31 ± 3.9 × 2.1 ± 0.2 µm, n = 18), Q = (11–)12.5–17(–20)

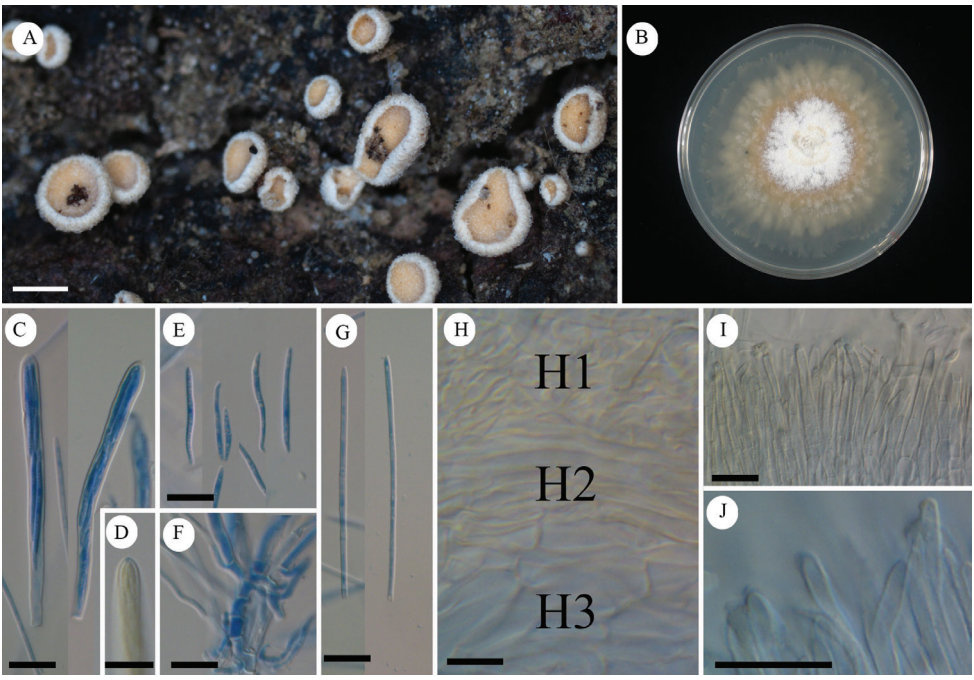

Figure 7. *Erioscyphella insulae* TNS-F-39720 (Holotype) **A** dried apothecia **B** a pure culture on PDA (NBRC 114459) **C** asci **D** ascal pore MLZ (+) **E** ascospores **F** ascogenous hyphae **G** paraphyses **H** layer structures of excipulum **H1** medullary excipulum **H2** inner layer of ectal excipulum composed of hyphae **H3** outer layer of ectal excipulum composed of *textura angularis* **I, J** hairs with apical amorphous materials. Mounted in CB/LA (**C, E–J**), MLZ (**D**). Scale bars: 1 mm (**A**); 10 µm (**A–J**).

(av. 14.7 ± 2.3, n = 18), showing various shapes and lengths, usually long fusiform and sometimes hypsiloid or sigmoid due to bending of both ends, sometimes swelling or constricted irregularly, aseptate or one- to three-septate (usually one-septate). Paraphyses straight, narrowly lanceolate, up to 2.5 µm wide, septate, exceeding the asci up to 7.5 µm.

Culture characteristics. Colony of NBRC 114445/TNS-F-26500 and NBRC 114459/TNS-F-39720 on PDA relatively thick-planar, pruinose, white to cream, ivory at the margin, pale sepia. Sectors and zonation absent. Aerial mycelium white to pale ocher, mainly developed except in the margin, not forming mycelial strands. Soluble pigment amber colored produced at the center. Margin unclear, flat and immersed into agar, radially undulate. Anamorph not seen.

Distribution. Japan (Bonin Islands, Yaeyama Islands).

Notes. This fungus resembles *Lachnum nothofagi* (Dennis) Spooner in the size and shape of apothecia, ascospores, asci, and hairs. However, *E. insulae* has completely hyaline hairs and ectal excipulum, and hairs are equipped with apical materials (Fig. 7J, 8A), whereas *L. nothofagi* has partly to totally brown hairs and ectal excipulum (Spooner 1987). *Lachnum nothofagi* is currently known only from New Zealand and Australia and mainly arises from *Nothofagus* spp., which are native in the southern hemisphere (Spooner 1987).

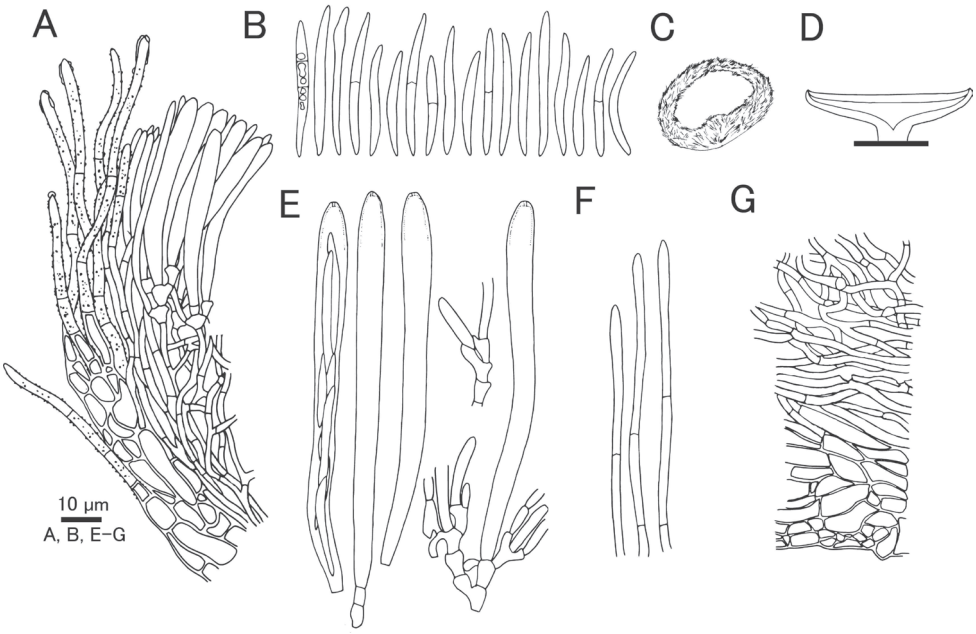

Figure 8. *Erioscyphella insulae* TNS-F-39720 (Holotype) **A** expansion of a vertical section of an apothecium **B** ascospores **C** apothecium **D** vertical section of an apothecium **E** asci **F** paraphyses **G** layer structures of excipulum.

Erioscyphella otanii **Tochihara, sp. nov.**
MycoBank No: 835704
Figs 9, 10

Diagnosis. Characterized by pure white minute apothecia (< 0.3 mm in diameter) unlike *L. diminutum* with rather colored apothecia, and smaller asci compared to similar species *Lachnum minutum*.

Holotype. Japan, Hokkaido, Horonobe, Toikambetsu, Teshio Experimental Forest, Field Science Center for Northern Biosphere, Hokkaido University, 44.993978, 142.130125, ca 400 m, 11 Jul. 2018, on fallen leaves of *Sasa senanensis*, Y.Tochihara & K.Kaneko (TNS-F-81472).

GenBank/UNITE no. ex holotype. LC669471/UDB0779083 (ITS), LC533179 (LSU), LC533286 (mtSSU), LC533226 (RPB2).

Other specimen examined. Japan, Hokkaido, Sapporo, Mt. Moiwa, 43.024718, 141.318427, ca 530 m, 21 Jun. 1965, on fallen leaves of *Sasa kurilensis*, Y.Otani (TNS-F-50482, in poor condition).

Etymology. Referring to the name of Dr Yoshio Otani, the first discoverer of this species.

Japanese name. Kita-sasaba-hina-no-chawantake.

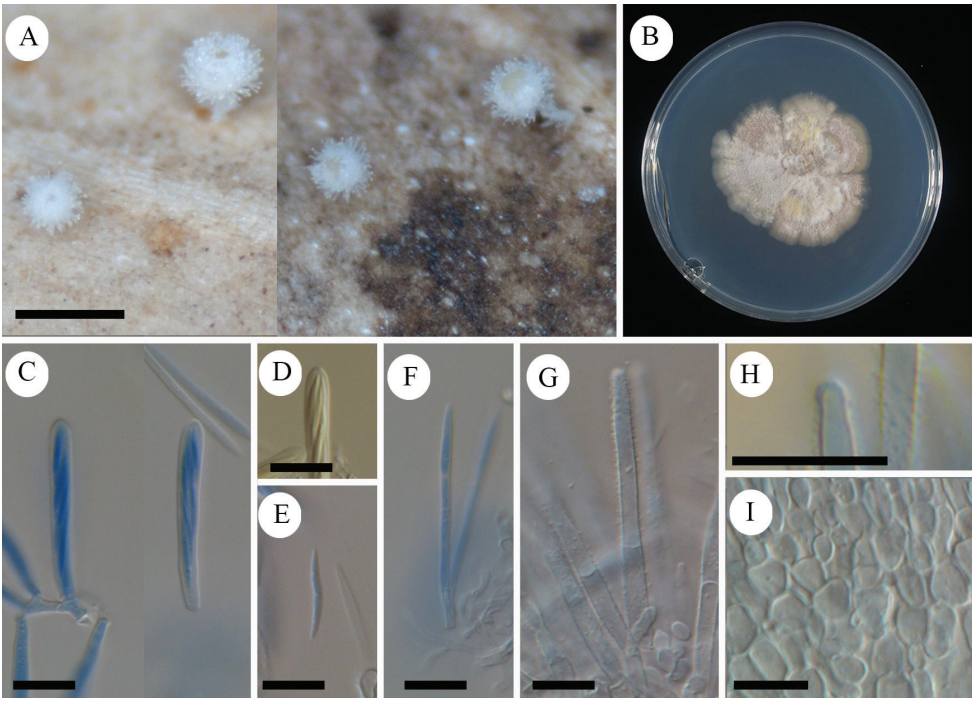

Figure 9. *Erioscyphella otanii* TNS-F-81472 (Holotype) **A** dried apothecia **B** pure culture on PDA (NBRC 114476) **C** asci **D** ascal pore MLZ (+) **E** ascospore **F** paraphyses **G** a hair **H** hair-apex with a apical amorphous material **I** ectal excipular cells. Mounted in CB/LA (**C, E–I**), MLZ (**D**). Scale bars: 0.5 mm (**A**); 10 µm (**C–I**).

Description. Apothecia scattered, superficial, minute, 0.1–0.3 mm in diameter, at first spherical and later urceolate, having well-developed stipes, up to 0.3 mm high, pure white, externally covered with short white hairs, never colored brown. Disc concave, almost enclosed by an incurving margin when fresh and dry, cream to pale yellow when dry (not observed when fresh). Ectal excipulum *textura prismatica* like stone pavings arranged in rows, 3–25 × 3–8 µm, hyaline, relatively thick-walled; cell walls smooth. Medullary excipulum *textura intricata*; hyphae up to 2.5 µm wide. Hairs straight, cylindrical or tapering toward the apices, up to 60 µm long, up to 5 µm wide near the bases and 2.5–3.0 µm wide near the apices, arising from swollen ectal excipular cells, hyaline, up to 3-septate (usually 1- or 2-septate), thin-walled, completely granulated; granules dense near the apices and coarse toward the bases; apex sometimes with a hyaline and inconspicuous apical amorphous materials not dissolved with CB/LA, lacking any crystals or resinous materials. Asci (33–)34–38.8(–41) × 4–5 µm (av. 37 ± 2.2 × 4.4 ± 0.4 µm, n = 15), 8-spored, cylindrical-clavate, relatively thick-walled; pore blue in MLZ without 3% KOH pretreatment; croziers absent at the basal septa. Ascospores (11.5–)12.3–14.6(–15) × (1.2–)1.36–1.7(–1.8) µm (av. 13.4 ± 1.2 × 1.6 ± 0.2 µm, n = 15), Q = (6.7–)7.8–9.6(–10.8) (av. 8.7 ± 0.9, n = 15),

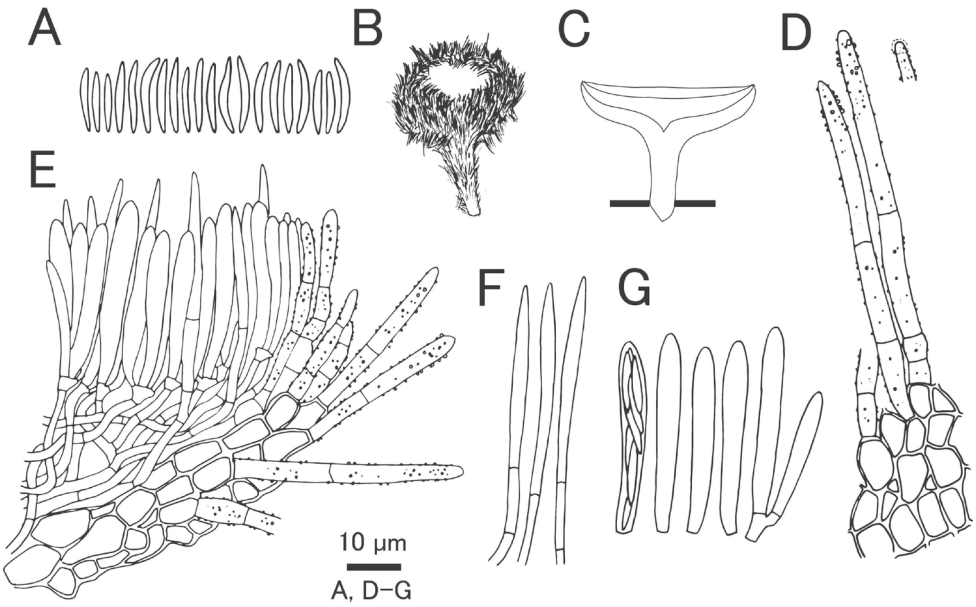

Figure 10. *Erioscyphella otanii* TNS-F-81472 (Holotype) **A** ascospores **B** apothecium **C** vertical section of an apothecium **D** hairs with cap-like structures arising from ectal excipular cells **E** expansion of a vertical section of an apothecium **F** paraphyses **G** asci.

fusiform, aseptate. Paraphyses straight, narrowly lanceolate to lanceolate, up to 2.5 µm wide, septate, exceeding the asci up to 10 µm.

Culture characteristics. Colony of NBRC 114476/TNS-F-81472 on PDA flat, partially protruding and forming mycelial mass, divided into two sectors. One sector flat, wooly to velvety, white to cream; dark ocher from the reverse. The other sector with wooly context, white and partly yellow; pale ocher from the reverse. Aerial mycelia developed throughout the colony, white, sparse to cottony, not forming mycelium strands. Margin distinct, flat and immersed into the agar. Soluble pigment absent. Asexual morph absent.

Distribution. Japan (Hokkaido; subarctic zone).

Notes. *Erioscyphella otanii* was first collected and documented by Otani (1967) under the misapplied name *Dasyscyphus diminutus* (TNS-F-50482). Based on the description, we concluded that the specimen was the same species as TNS-F-81472. The present species is very similar to *Lachnum diminutum* (Roberge ex Desm.) Rehm in the minute apothecia, ascospore size, and narrow paraphyses; however, *E. otanii* is pure white when fresh and dry (Fig. 9A, in dried state) and occurs on bamboo leaves, while *L. diminutum* is somewhat brown in the exterior parts of apothecia and occurs on sheaths of *Juncus* spp. (Dennis 1949). In the mature state, the apothecia of *E. otanii* become urceolate (Fig. 9A and Fig. 10B), whereas the apothecia of *L. diminutum* are flat (Dennis 1949). The ITS sequence of TNS-F-81472 showed low similarity (< 80%) with that of *L. diminutum* collected in France (GenBank accession number: MH857306). Based on the French sequence, *L. diminutum* is phylogenetically a good *Lachnum*.

The appearance of *E. otanii* is also similar to that of the graminicolous species *Lachnum minutum* W.Y. Zhuang and M. Ye documented in China (Ye and Zhuang 2003). *Erioscyphella otanii* is distinguished from *L. minutum* in having smaller asci, although DNA sequences of the species are not available.

***Erioscyphella papillaris* Tochihara, sp. nov.**
MycoBank No: 835705
Figs 11, 12

Diagnosis. Characterized by protruding papillary hairs with hyaline apical amorphous materials.

Holotype. Japan, Gunma, Minakami, Yubiso, Mt. Tanigawadake, 36.064014, 141.344653, ca 710 m, 16 Jul. 2017, on both sides of a fallen leaf of bamboo, Y.Tochihara (TNS-F-81272).

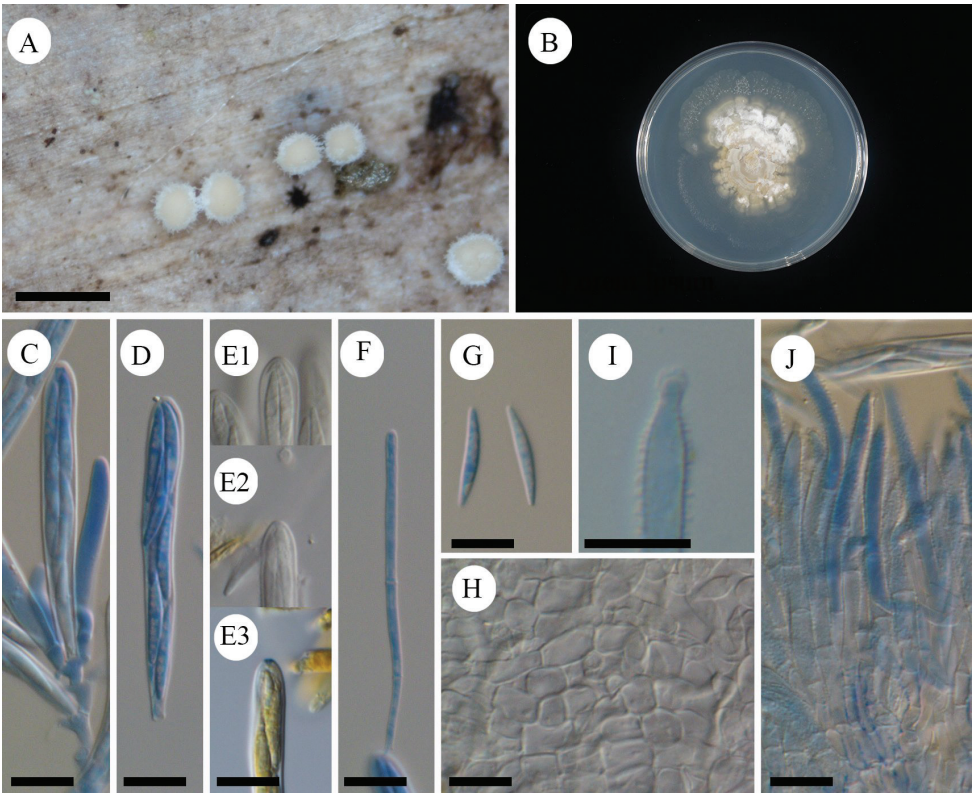

Figure 11. *Erioscyphella papillaris* TNS-F-81272 (Holotype) **A** dried apothecia **B** pure culture on PDA (NBRC 113937) **C** Ascus arising from ascogenous hyphae **D** an ascus **E** ascal pore iodine reactions **E1** MLZ (-) without 3% KOH pretreatment **E2** MLZ (-) with 3% KOH pretreatment **E3** IKI (+) without 3% KOH pretreatment **F** paraphysis **G** ascospores with guttules **H** ectal excipulum **I** hair-apex with a apical amorphous material **J** hairs. Mounted in CB/LA (**C, D, F–J**), MLZ (**E1, E2**), IKI (**E3**). Scale bars: 0.5 mm (**A**); 10 µm (**C–J**).

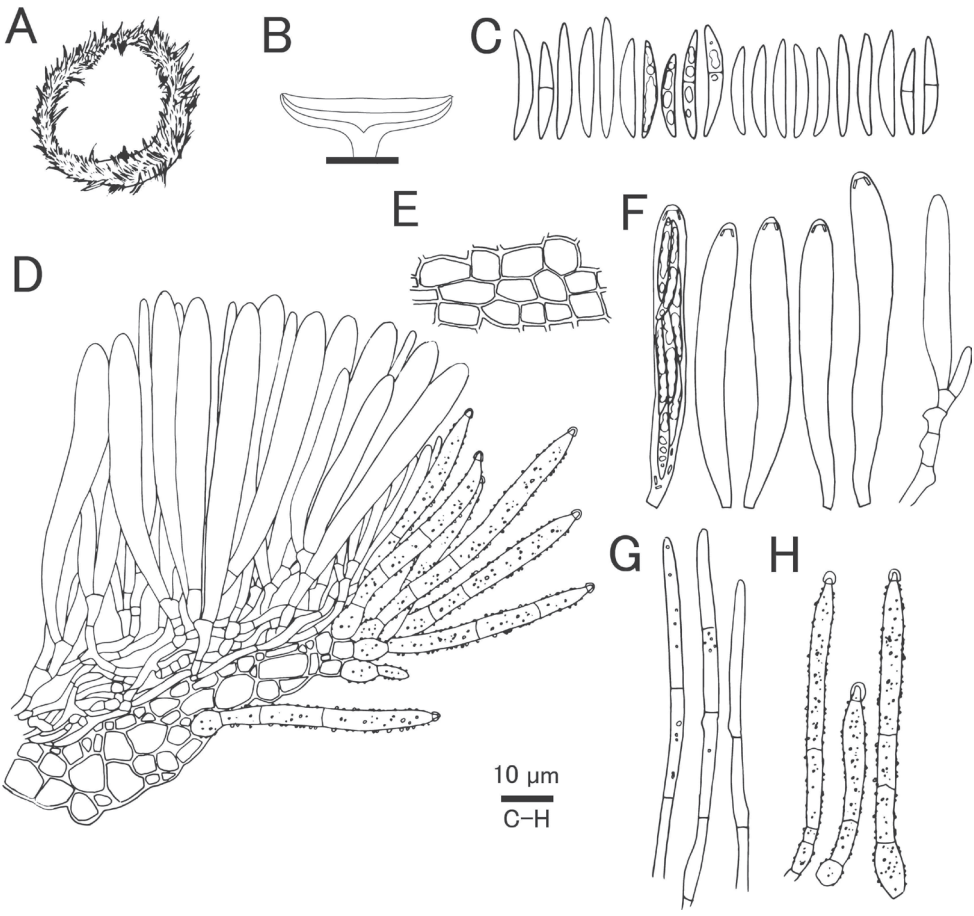

Figure 12. *Erioscyphella papillaris* TNS-F-81272 (Holotype) **A** apothecium **B** vertical section of an apothecium **C** ascospores **D** expansion of an vertical section of an apothecium **E** ectal excipular cells **F** asci **G** paraphyses **H** hairs with cap-like structures.

GenBank/UNITE no. ex holotype. LC669473/UDB0779085 (ITS), LC533161 (LSU), LC533285 (mtSSU), LC533204 (RPB2).

Etymology. Referring to papillate hair apices.

Japanese name. Sasaba-hina-no-chawantake.

Description. Apothecia gregarious, superficial, minute, 0.1–0.3 mm in diameter, short-stipitate, up to 0.25 mm high, externally densely covered with pure white short hairs. Disc concave, white to lemon yellow when fresh and dry. Ectal excipulum *textura prismatica* composed of cuboid cells, 3–13 × 2.5–7 µm, hyaline, thin-walled, lacking carotenoid pigments; cell walls smooth. Medullary excipulum *textura intricata* of hyaline hyphae up to 3 µm wide. Hairs straight, cylindrical, 45–75 × 3–5 µm, 2–3-septate, hyaline, totally granulate, thin-walled, arising from swollen cells; apical cells rather longer than other cells, 30–40 µm long, with papillate at the apex, sometimes swelling,

equipped with hyaline and globose apical amorphous materials not dissolved with CB/LA, lacking any crystals or resinous matters. Asci (59–)59.8–66(–69) × (7.5–)7.6–8.3(–9) µm (av. 63 ± 2.9 × 8.0 ± 0.4 µm, n = 16), 8-spored, cylindrical-clavate; pore inamyloid with MLZ without 3% KOH pretreatment, faint blue with MLZ with 3% KOH pretreatment, dark blue with IKI with and without KOH pretreatment; vesicle apparatus inverted-v-shaped present near the apices; croziers absent at the basal septa; base sympodially branched. Ascospores (16–)17.5–21.7(–24) × (2–)2.3–2.8(–3) µm (av. 20 ± 2.1 × 2.6 ± 0.3 µm, n = 20), Q = (6.4–)6.8–8.9(–9.8) (av. 7.8 ± 1.0, n = 20), fusiform, aseptate, or one-septate (rarely two-septate), filled with hyaline oil drops. Paraphyses straight, cylindrical, up to 3 µm wide, septate, containing small hyaline lipid bodies, equal or scarcely exceeding the asci.

Culture characteristics. Colony of NBRC 113937/TNS-F-81272 on PDA divided into two semicircular zones. The first zone umbonate, pruinose, white, producing white aerial mycelia densely, presenting wooly appearance; margin distinct, entire, flat. The second zone flat, glutinous, white to beige with concentric patterns, producing few aerial mycelia; margin entire, flat and immersed into agar, irregularly undulate. The reverse uniform unrelated to the zoning position, beige to pale dark brown throughout. Soluble pigment and asexual morph absent throughout the colony.

Distribution. Japan (Mt. Tanigawa). Currently known only from the type locality.

Notes. This species is similar to *Lachnum sclerotii* var. *microascum* in the dimension and shape of asci and ascospores, habitats, and inconspicuous ascus apex reaction in MLZ (Zhuang 2004). However, *E. papillaris* has ascospores containing conspicuous guttules in any mount (Fig. 11G) and filiform paraphyses rarely exceeding the asci (Fig. 11F, Fig. 12D, and Fig. 12G), whereas *L. sclerotii* var. *microascum* has non-guttulate asci and narrowly lanceolate to lanceolate paraphyses exceeding the asci by 15–18 µm (Zhuang 2004). Although DNA sequences of *L. sclerotii* var. *microascum* are not available, we judged the present fungus as different from it, because the presence or absence of guttules in ascospores is a significant taxonomic character at the species level (Baral 2015).

Papillate hairs are also shown in the line drawings of *Lachnum gahniae* Spooner (Spooner 1987), suggesting the relationship of the present fungus to Australasian species. However, *L. gahniae* can be distinguished by having longer hairs, occurring on different substrates (leaves of Cyperaceae) and showing different ascal-iodine reactions (MLZ+) (Spooner 1987), although DNA sequences of *L. gahnia* are not available.

Erioscyphella paralushanensis Tochihara and Hosoya, sp. nov.

MycoBank No: 839618
Figs 13, 14

Diagnosis. Characterized by throughout red apothecia occurring on bamboo sheaths. Similar to *E. lushanensis* in macro- and micromorphology and habitats, but has larger asci and ascospores.

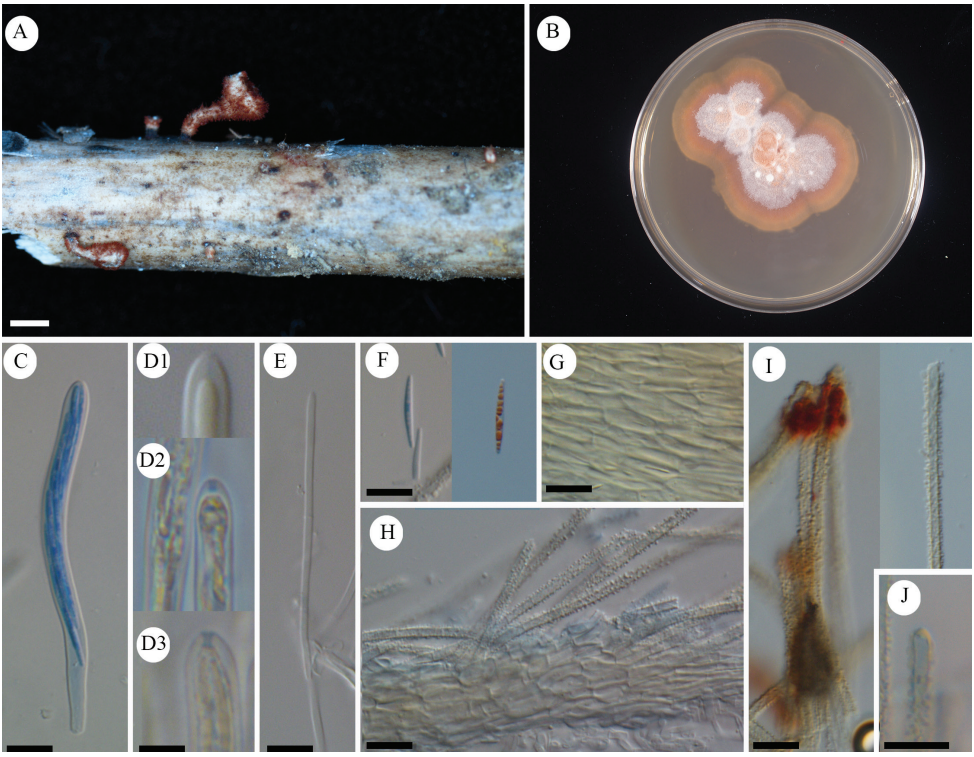

Figure 13. *Erioscyphella paralushanensis* TNS-F-61920 (Holotype) **A** apothecia **B** pure culture on PDA (NBRC 114468) **C** ascus **D** ascal pore iodine reactions **D1** MLZ (faintly +) without 3% KOH pretreatment **D2** MLZ (+) with 3% KOH pretreatment **D3** IKI (+) without 3% KOH pretreatment **E** paraphysis **F** ascospores **G** ectal excipular cells **H** marginal section of an apothecium generating hairs **I** hairs with red resinous materials **J** apical amorphous materials of hairs. Mounted in CB/LA (**C, E–J**), MLZ (**D1, D2**), IKI (**D3**). Scale bars: 0.5 mm (**A**); 10 μm (**C–J**).

Holotype. Japan, Shizuoka, Atami, Izusan, 35.128834, 139.051194, ca 620 m, 8 Jun. 2015, on fallen sheaths of *Pleioblastus argenteostriatus*, M.Nakajima (TNS-F-61920).

GenBank/UNITE no. ex holotype. LC669463/UDB0779075 (ITS), LC533141 (LSU), LC533267 (mtSSU), LC533220 (RPB2).

Etymology. Referring to the similarity with *E. lushanensis*.

Japanese name. Akage-hina-no-chawantake.

Description. Apothecia scattered, superficial, 0.7–1.5 mm in diameter, long-stipitate, up to 2.0 mm high, externally covered with dark-red hairs. Disc concave, cream to pale yellow. Ectal excipulum well-developed *textura prismatica* and partly *t. angularis*, 6–13 × 2.0–2.5 *μm*, *hyaline*, *relatively* thick-walled, with smooth walls. Medullary excipulum *textura intricata* of hyaline hyphae up to 2 μm wide. Hairs straight, cylindrical, up to 160 *μm long*, *2.0*–3.0 μm wide, pale brown but hyaline near the bases; hair cells narrowly septate, > 7 μm long, covered by big and amber-colored granules; gran-

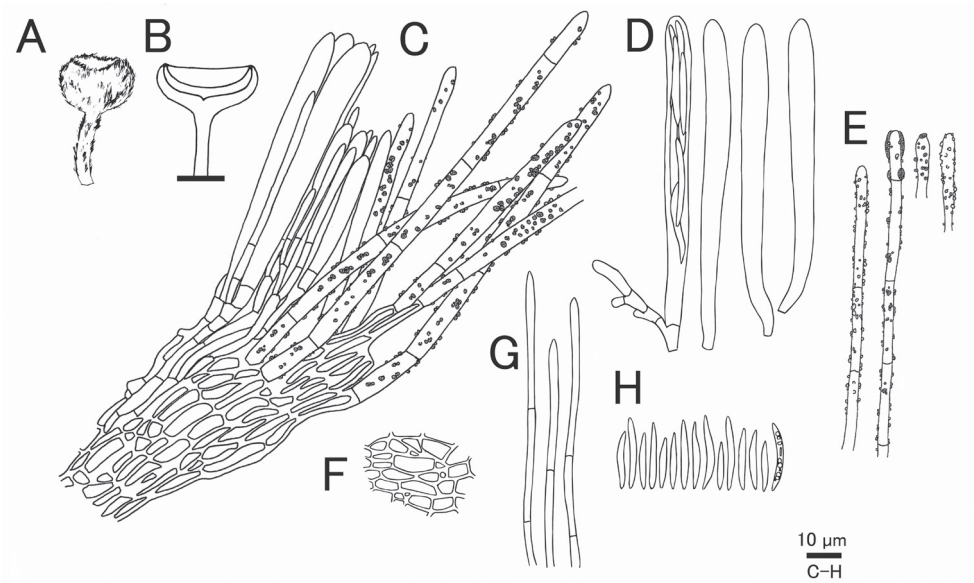

Figure 14. *Erioscyphella paralushanensis* TNS-F-61920 (Holotype) **A** apothecia **B** vertical section of an apothecium **C** expansion of an vertical section of an apothecium **D** asci **E** hairs **F** ectal excipulum **G** paraphyses **H** ascospores.

ules big and dense near the apices and smaller and sparse near the bases, up to 2 µm in diameter near the apices, equipped with amber-colored resinous materials that dissolves in CB/LA at any position of hairs; apices with amber-colored apical amorphous materials, lacking any crystals. Asci (59–)61.4–70.2(–73) × (4.5–)4.7–5.6(–6) µm (av. 65.8 ± 4.4 × 5.2 ± 0.4 µm, n = 15), Q = (11.5–)12–13.6(–14.6) (av. 12.8 ± 0.8, n = 15), 8-spored, cylindrical-clavate; pore faintly blue in MLZ without 3% pretreatment, clear blue in MLZ with 3% KOH pretreatment and IKI without 3% KOH pretreatment. Ascospores (14–)15.8–20.7(–22) × (1.5–)1.7–2.0 µm (av. 18.2 ± 2.5 × 1.8 ± 0.2 µm, n = 15), Q = (7.5–)8.7–11.2(–12.6) (av. 9.9 ± 1.3, n = 15), septate, sometimes bent to U-shaped or S-shaped, containing conspicuous guttules; guttules hyaline but sometimes red. Paraphyses straight, up to 2 µm wide, septate, exceeding the asci 5–10 *µm*, initially cylindrical to clavate, later becoming narrowly lanceolate.

Culture characteristics. Colony of NBRC 114468/TNS-F-61920 on PDA flat, sparse, dendritically spread. Context wooly, ocher to pale buff, dark buff from the reverse. Sectors and zonation absent. Aerial mycelium ocher to pale buff, dense cottony, developed near the center, forming white mycelium strands; margin distinct, flat and partly immersed into the agar. Asexual morph absent. Soluble pigments present, buff, dyeing agar without colony pale buff.

Distribution. Japan (Shizuoka). Currently known only from the type locality.

Notes. *Erioscyphella paralushanensis* is closely related to *E. lushanensis* in having red hairs (Fig. 13I) and the ectal excipulum composed of well-developed rectangular cells

in common (Fig. 13H, Fig. 14C, and Fig. 14F) (Zhuang and Wang 1998a). Compared with *E. lushanensis*, *E. paralushanensis* has slightly larger asci, ascospores and hairs. Red guttules in ascospores were observed only in *E. paralushanensis* (Fig. 13F). In this study, we proposed the present fungus as a new species, because species delimitation analyses based on ITS sequences strongly supported that *E. paralushanensis* is different from *E. lushanensis* (Fig. 3).

Erioscyphella sasibrevispora Tochihara & Hosoya, sp. nov.

MycoBank No: 835706
Figs 15, 16

Diagnosis. Characterized by wooly appearance and yellow to orange discs, and distinguished from similar species *Lachnum novoguineense* var. *yunnanicum* in having shorter ascospores.

Holotype. Japan, Hokkaido, Tomakomai, Utonai, 42.705314, 141.7346, ca 10 m, 16 Jun. 2018, on fallen sheaths of *Sasa nipponica*, Y.Tochihara & T.Hosoya (TNS-F-81401).

GenBank/UNITE no. ex holotype. LC669470/UDB0779082 (ITS), LC533174 (LSU), LC533269 (mtSSU), LC533217 (RPB2).

Other specimen examined. Japan, Gunma, Higashiagatsuma, 36.562253, 138.724139, ca 1330 m, 6 Jun. 2017, on fallen sheaths of *Sasa veitchii*, Y.Tochihara & T.Hosoya (TNS-F-80399, in bad condition).

Etymology. "sasi" means bamboo [host plants] and "brevispora" means shorter ascospores compared to *L. novoguineense* var. *yunnanicum*.

Japanese name. Sasa-no-youmou-chawantake.

Description. Apothecia gregarious, superficial, 0.6–1.3 mm in diameter, short-stipitate, up to 0.8 mm high, pure white, externally covered with long white hairs. Disc concave, yellow to pale orange when fresh and dry. Ectal excipulum *textura prismatica* to *t. angularis*, 3–16 × 2–10 µm, hyaline, thin-walled; surface smooth. Medullary excipulum *textura intricata* of hyaline hyphae up to 2 µm wide. Hairs straight, delicate, cylindrical with relatively acute apices, up to 190 × 2–3 µm, hyaline, totally granulate, thin-walled; apical cell a little longer than other cells, lacking any crystals, resinous materials, or apical amorphous materials. Asci (79–)82.5–90(–95) × (6–)6.6–8.1(–9) µm (av. 86 ± 4.0 × 7.4 ± 0.8 µm, n = 15), 8-spored, cylindrical-clavate; lateral parts sometimes swelling irregularly; pore blue in MLZ without 3% KOH pretreatment; croziers with perforation present at the basal septa. Ascospores (26–)27.9–36.1(–39) × (1.5–)1.7–2 µm (av. 32 ± 4.1 × 1.8 ± 0.2 µm, n = 17), Q = (13–)15–19.7(–21) (av. 17.5 ± 2.3, n = 17), long fusiform, usually 3-septate, rarely 0- to 2-septate (only observed in TNS-F-81401 because TNS-F-80399 was immature). Paraphyses straight, lanceolate, 2.5–4 µm wide, densely septate, exceeding the asci up to 15 µm. Note that the description is solely based on the holotype because another examined specimen TNS-F-80399 was in bad condition.

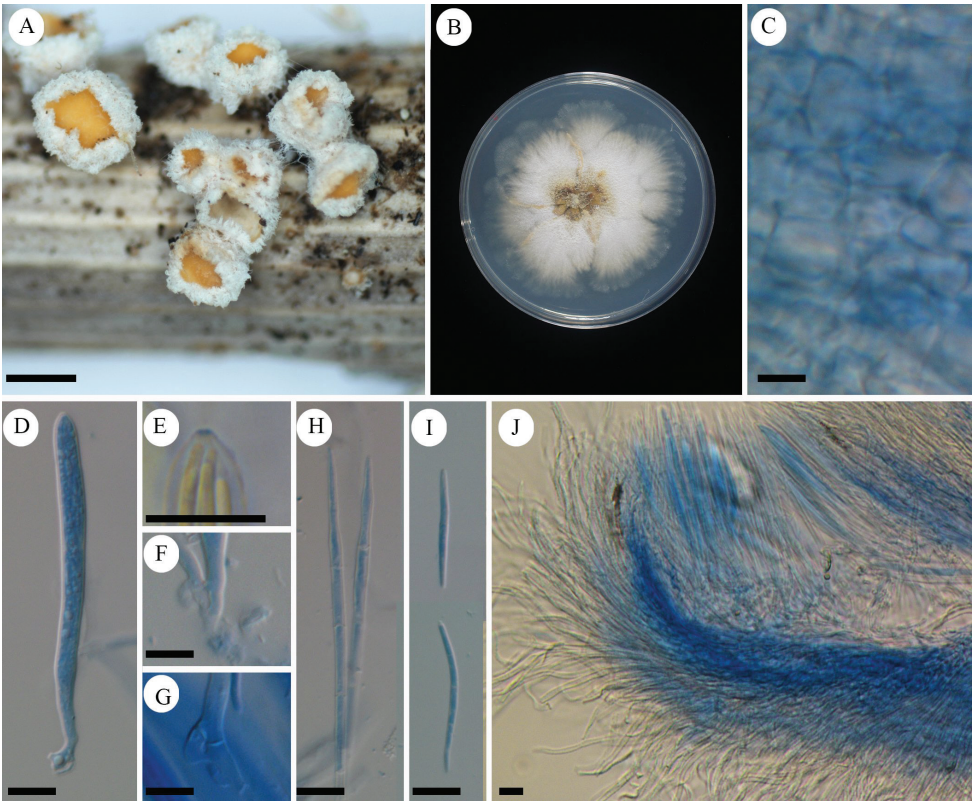

Figure 15. *Erioscyphella sasibrevispora* TNS-F-81401 (Holotype, **A–F, H–J**). *Lachnum novoguineense* var. *yunnanicum* TNS-F-16442 (**G**) **A** dried apothecia **B** a pure culture on PDA (NBRC 114475) **C** ectal excipular cells **D** ascus **E** an ascal pore MLZ (+) **F** ascal base with a perforated crozier **G** ascal base with a perforated crozier **H** septated paraphyses **I** ascospores **J** vertical section through the apothecium. Mounted in CB/LA (**D, F–J**), MLZ (**E**). Scale bars: 1 mm (**A**); 10 µm (**C–J**).

Culture characteristics. Colony of NBRC 114475/TNS-F-81401 on PDA wrinkled. Context cottony and partially funiculose, white, turning ocher at the center; almost ocher except for the white margin from the reverse. Sectors and zonation absent. Aerial mycelium developed throughout the colony, concolous, forming mycelium strands. Margin indistinct, flat and immersed into agar. Soluble pigment absent. Asexual morph absent.

Distribution. Japan (cool-temperate zone, subarctic zone).

Notes. *Erioscyphella sasibrevispora* is closely related to *L. novoguineensis* var. *yunnanicum* (TNS-F-16442, 16642) (Fig. 1) and occurs in the same habitats (that is, bamboo sheaths) but has shorter asci and ascospores. The ascal bases of the two species are very characteristic, in that they have croziers with perforations (Fig. 15G and Fig. 16E). In Lachnaceae, this type of crozier has only been reported in *Lachnel-*

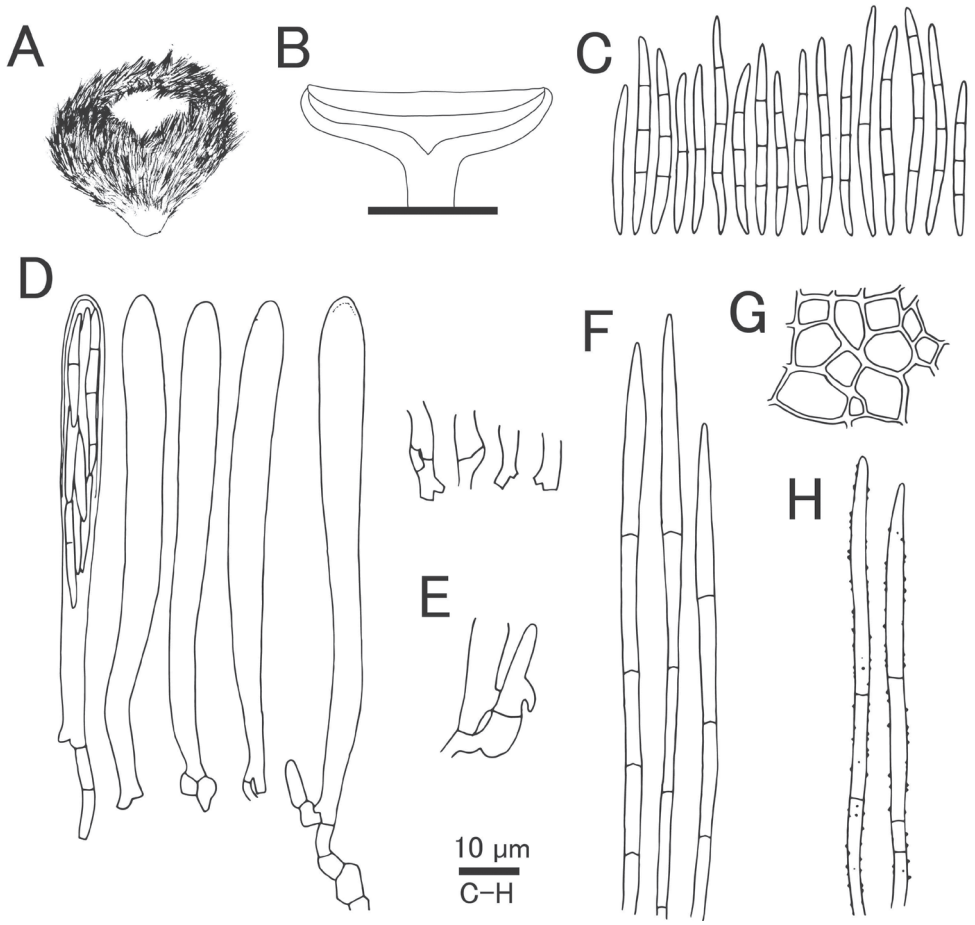

Figure 16. *Erioscyphella sasibrevispora* TNS-F-81401 (Holotype **A–D, F, G**). *Lachnum novoguineense* var. *yunnanicum* TNS-F-16642 (**E**) **A** apothecium **B** vertical section of an apothecium **C** ascospores **D** asci (with basal structures sometimes with perforation) **E** ascal base arising from a crozier with perforation **F** paraphyses **G** ectal excipular cells **H** hairs.

lula (Baral 1984). Additionally, both species exceptionally lack any hair materials in *Erioscyphella*.

The tropical species *E. bambusina* and *Lachnum albidum* var. *americanum* (Dennis) W.Y. Zhuang also occur on bamboo sheaths. However, compared with the present fungus, the former has smaller ascospores and filiform paraphyses (Dennis 1954), and the latter has extremely large asci and ascospores (Dennis 1960). In cool-temperate to subarctic zones, *L. asiaticum* and *Lachnum sasae* Raitv. occur on bamboo sheaths (Otani 1967; Raitviir 1985), but their ascospores are much shorter than those of the present fungus.

The wooly appearance and yellow disc of this species (Fig. 15A) resemble those of *Capitotricha rubi* (Bres.) Baral; however, microscopic observations easily distinguish the two species.

***Erioscyphella sinensis* (Z.H. Yu and W.Y. Zhuang) Sasagawa, Tochihara & Hosoya, comb. et stat. nov.**
MycoBank No: 835709

≡ *Lachnum mapirianum* var. *sinense* Z.H. Yu and W.Y. Zhuang, Nova Hedwigia 74(3-4): 422 (2002).

Diagnosis. Occurring on fallen leaves of of *Quercus* spp. or *Castanopsis* spp. in early summer and having needle-like ascospores.

Japanese name. Shii-Kashi-hina-no-chawantake-modoki.

Specimen examined. Japan, Ibaraki, Tsukuba, Mt. Tsukuba, 36.228539, 140.103504, ca 870 m, 23 Jun. 2007, on fallen leaves of *Castanopsis sieboldii*, R.Sasagawa (TNS-F-16841). Japan, Ibaraki, Tsukuba, Amakubo, Tsukuba Botanical Garden, 36.101472, 140.110944, ca 20 m, 15 Jun. 2007, on fallen leaves of *C. sieboldii*, R.Sasagawa (TNS-F-16838). JAPAN, Tottori, Yonago, Yonago Castle, 35.42437, 133.325472, ca 50 m, 3 Jun. 2018, on fallen leaves of *C. sieboldii*, Y.Tochihara (TNS-F-81383).

Distribution. China (Hainan, Yunnan; Yu and Zhuang 2003). Japan (warm-temperate zone).

Notes. The present fungus was treated as *Lachnum* sp. 13 by Hosoya et al. (2010). This fungus occurs in the same habitats as *E. hainanensis*, but it is easily distinguished in having longer and needle-like ascospores. *Erioscyphella sinensis* resembles *L. mapirianum* in the shape of ascospores, but the two species are different in that *L. mapirianum* has long slender apothecial stipes, larger asci, longer ascospores, and wider paraphyses.

In the present study, we transferred this fungus to *Erioscyphella* and upgraded it from variety to species level, because this fungus is not phylogenetically related to '*L*'. *mapirianum* (Fig. 1). The presence of apical amorphous materials of hairs was confirmed in this study (Suppl. material 1: Fig. S2).

Acknowledgements

We thank Dr Shimpei Hiruta at the National Museum of Nature and Science for his kind support in the species delimitation analyses. We also thank Dr Toshimitsu Fukiharu at the Natural History Museum and Institute, Chiba, Ms Michiru Fujisaki and Rei Sasagawa at the Faculty of Life and Environmental Sciences, University of Tsukuba, and Mr Minoru Nakajima at Kanagawa Kinoko no Kai for collecting and donating their significant fungal specimens to TNS.

References

Abarenkov K, Tedersoo L, Nilsson RH, Vellak K, Saar I, Veldre V, Parmasto E, Prous M, Aan A, Ots M, Kurina O, Ostonen I, Jõgeva J, Halapuu S, Põldmaa K, Toots M, Truu J, Larsson K-H, Kõljalg U (2010) PlutoF – a web based workbench for ecological and taxonomic

research, with an online implementation for fungal ITS sequences. Evolutionary Bioinformatics 6: 189–196. https://doi.org/10.4137/EBO.S6271

Akaike H (1974) A new look at the statistical model identification. IEEE Transactions on Automatic Control 19(6): 716–723. https://doi.org/10.1109/TAC.1974.1100705

Baral HO (1984) Taxonomische und ökologische Studien über die Koniferen bewohnenden europäischen Arten der Gattung *Lachnellula* Karsten. Beiträge zur Kenntnis der Pilze Mitteleuropas 1: 143–156. [in German]

Baral HO (2009) Iodine reaction in Ascomycetes: why is Lugol's solution superior to Melzer's reagent? http://www.gbif-mycology.de/HostedSites/Baral/IodineReaction.htm [Accessed on: 2021-03-15]

Baral HO (2015) *Hymenoscyphus menthae*, *H. macroguttatus* and *H. scutula*, a comparative taxonomic study emphasizing the value of spore guttulation and croziers. Ascomycete.org 7(6): 255–287. https://doi.org/10.25664/art-0147

Baral HO, Krieglsteiner GJ (1985) Bausteine zu einer Askomyzeten-Flora der Bundersrepublik Deutschland. In: Süddeutchland gefundene inoperculte Diskomyceten mit taxonomischen, ökologischen, chorologischen Hinweisen und einer Farbtafel. Beiheften zur Zeitschrift für Mykologie 6: 1–160. [in German]

Begerow D, Nilsson H, Unterseher M, Maier W (2010) Current state and perspectives of fungal DNA barcoding and rapid identification procedures. Applied Microbiology and Biotechnology 87: 99–108. https://doi.org/10.1007/s00253-010-2585-4

Biczok R, Bozsoky P, Eisenmann P, Ernst J, Ribizel T, Scholz F, Trefzer A, Weber F, Hamann M, Stamatakis A (2018) Two C++ libraries for counting trees on a phylogenetic terrace. Bioinformatics 34(19): 3399–3401. https://doi.org/10.1093/bioinformatics/bty384

Bolyen E, Rideout JR, Dillon MR, Bokulich NA, Abnet CC, Al-Ghalith GA, Alexander H, Alm EJ, Arumugam M, Asnicar F, Bai Y, Bisanz JE, Bittinger K, Brejnrod A, Brislawn CJ, Brown CT, Callahan BJ, Caraballo-Rodríguez AM, Chase J, Cope EK, Da Silva R, Diener C, Dorrestein PC, Douglas GM, Durall DM, Duvallet C, Edwardson CF, Ernst M, Estaki M, Fouquier J, Gauglitz JM, Gibbons SM, Gibson DL, Gonzalez A, Gorlick K, Guo J, Hillmann B, Holmes S, Holste H, Huttenhower C, Huttley GA, Janssen S, Jarmusch AK, Jiang L, Kaehler BD, Kang KB, Keefe CR, Keim P, Kelley ST, Knights D, Koester I, Kosciolek T, Kreps J, Langille MGI, Lee J, Ley R, Liu YX, Loftfield E, Lozupone C, Maher M, Marotz C, Martin BD, McDonald D, McIver LJ, Melnik AV, Metcalf JL, Morgan SC, Morton JT, Naimey AT, Navas-Molina JA, Nothias LF, Orchanian SB, Pearson T, Peoples SL, Petras D, Preuss ML, Pruesse E, Rasmussen LB, Rivers A, Robeson MS 2nd, Rosenthal P, Segata N, Shaffer M, Shiffer A, Sinha R, Song SJ, Spear JR, Swafford AD, Thompson LR, Torres PJ, Trinh P, Tripathi A, Turnbaugh PJ, Ul-Hasan S, van der Hooft JJJ, Vargas F, Vázquez-Baeza Y, Vogtmann E, von Hippel M, Walters W, Wan Y, Wang M, Warren J, Weber KC, Williamson CHD, Willis AD, Xu ZZ, Zaneveld JR, Zhang Y, Zhu Q, Knight R, Caporaso JG (2019) Reproducible, interactive, scalable and extensible microbiome data science using QIIME 2. Nature Biotechnology 37: 852–857. https://doi.org/10.1038/s41587-019-0209-9

Bouckaert R, Vaughan TG, Barido-Sottani J, Duchêne S, Fourment M, Gavryushkina A, Heled J, Jones G, Kühnert D, Maio ND, Matschiner M, Mendes FK, Müller NF, Ogilvie HA, Plessis L, Popinga A, Rambaut A, Rasmussen D, Siveroni I, Suchard MA, Wu C-H,

Xie D, Zhang C, Stadler T, Drummond AJ (2019) BEAST 2.5: An advanced software platform for Bayesian evolutionary analysis. PLOS Computational Biology 15(4): e1006650. https://doi.org/10.1371/journal.pcbi.1006650

Cantrell SA, Hanlin RT (1997) Phylogenetic relationships in the family Hyaloscyphaceae inferred from sequences of ITS regions, 5.8S ribosomal DNA and morphological characters. Mycologia 89(5): 745–755. https://doi.org/10.1080/00275514.1997.12026841

Capella-Gutiérrez S, Silla-Martínez JM, Gabaldón T (2009) trimAl: a tool for automated alignment trimming in large-scale phylogenetic analyses. Bioinformatics 25(15): 1972–1973. https://doi.org/10.1093/bioinformatics/btp348

Darriba D, Posada D, Kozlov AM, Stamatakis A, Morel B, Flouri T (2019) ModelTest-NG: A new and scalable tool for the selection of DNA and protein evolutionary models. Molecular Biology and Evolution 37(1): 291–294. https://doi.org/10.1093/molbev/msz189

Dennis RWG (1949) A revision of the British Hyaloscyphaceae with notes on related European species. Mycological Papers 32: 1–97.

Dennis RWG (1954) Some inoperculate discomycetes of tropical America. Kew Bulletin 9(2): 289–348. https://doi.org/10.2307/4114399

Dennis RWG (1960) Fungi venezuelani: III. Kew Bulletin 14(3): 418–458. https://doi.org/10.2307/4114758

Dharne CG (1965) Taxonomic investigations on the discomycetous genus *Lachnellula* Karst. Phytopathologische Zeitschrift 53(2): 101–144. https://doi.org/10.1111/j.1439-0434.1965.tb02194.x

Ekanayaka AH, Hyde KD, Gentekaki E, McKenzie EHC, Zhao Q, Bulgakov TS, Camporesi E (2019) Preliminary classification of Leotiomycetes. Mycosphere 10: 310–489. https://doi.org/10.5943/mycosphere/10/1/7

Felsenstein J (1984) Distance methods for inferring phylogenies: a justification. Evolution 38: 16–24. https://doi.org/10.1111/j.1558-5646.1984.tb00255.x

Felsenstein J (1985) Confidence limits on phylogenies: an approach using the bootstrap. Evolution 39: 783–791. https://doi.org/10.2307/2408678

Fujisawa T, Barraclough TG (2013) Delimiting species using single-locus data and the Generalized Mixed Yule Coalescent approach: a revised method and evaluation on simulated data sets. Systematic Biology 62(5): 707–724. https://doi.org/10.1093/sysbio/syt033

Gardes M, Bruns TD (1993) ITS primers with enhanced specificity for basidiomycetes-application to the identification of mycorrhizae and rusts. Molecular Ecology 2(2): 113–118. https://doi.org/10.1111/j.1365-294X.1993.tb00005.x

GBIF (2018) Adding sequence-based identifiers to backbone taxonomy reveals 'dark taxa' fungi. https://www.gbif.org/news/2LrgV5t3ZuGeU2WIymSEuk/adding-sequence-based-identifiers-to-backbonetaxonomy-reveals-dark-taxa-fungi [Accessed on: 2020-02-10]

Gelardi M, Vizzini A, Ercole E, Horak E, Ming Z, Li TH (2015) Circumscription and taxonomic arrangement of *Nigroboletus roseonigrescens* Gen. Et Sp. Nov., a new member of Boletaceae from tropical South-Eastern China. PloS ONE 10: e0134295. https://doi.org/10.1371/journal.pone.0134295

Guatimosim E, Schwartsburd PB, Barreto RW, Crous PW (2016) Novel fungi from an ancient niche: cercosporoid and related sexual morphs on ferns. Persoonia 37: 106–141. https://doi.org/10.3767/003158516X690934

Haines JH (1980) Studies in the Hyaloscyphaceae. I: Some species of *Dasyscyphus* on tropical ferns. Mycotaxon 11(1): 189–216.

Haines JH (1992) Studies in the Hyaloscyphaceae. VI: The genus *Lachnum* (ascomycetes) of the Guayana Highlands. Nova Hedwigia 54: 97–112.

Haines JH, Dumont KP (1983) Studies in the Hyaloscyphaceae II: *Proliferodiscus*, A new genus of Arachnopezizoideae. Mycologia 75(3): 535–543. https://doi.org/10.1080/00275514.1983.12023717

Haines JH, Dumont KP (1984) Studies in the Hyaloscyphaceae III: The long-spored, lignicolous species of *Lachnum*. Mycotaxon 19: 1–39.

Hall TA (1999) BioEdit: a user-friendly biological sequence alignment editor and analysis program for Windows 95/98/NT. Nucleic Acids Symposium Series 41: 95–98.

Han JG, Hosoya T, Sung GH, Shin HD (2014) Phylogenetic reassessment of Hyaloscyphaceae sensu lato (Helotiales, Leotiomycetes) based on multigene analyses. Fungal Biology 118: 150–167. https://doi.org/10.1016/j.funbio.2013.11.004

Hansen K, LoBuglio KF, Pfister DH (2005) Evolutionary relationships of the cup-fungus genus *Peziza* and Pezizaceae inferred from multiple nuclear genes: RPB2, β-tubulin, and LSU rDNA. Molecular Phylogenetics and Evolution 36(1): 1–23. https://doi.org/10.1016/j.ympev.2005.03.010

Hosaka K, Castellano MA (2008) Molecular phylogenetics of Geastrales with special emphasis on the position of Sclerogaster. Bulletin of the National Science Museum. Series B, Botany 34(4): 161–173. https://www.kahaku.go.jp/research/publication/botany/download/34_4/BNMNS_B340403.pdf [Accessed on: 2021-03-21]

Hosoya T (2021) Systematics, ecology, and application of Helotiales: Recent progress and future perspectives for research with special emphasis on activities within Japan. Mycoscience 62(1): 1–9. https://doi.org/10.47371/mycosci.2020.05.002

Hosoya T, Saito Y, Sasagawa R (2013) Enumeration of remarkable Japanese discomycetes (7): Notes on one operculate discomycete and one inoperculate discomycete. Bulletin of the National Science Museum. Series B, Botany 39(4): 151–158. https://www.kahaku.go.jp/research/publication/botany/download/39_4/BNMNS_B39-4_151-158.pdf [Accessed on: 2020-03-12]

Hosoya T, Sasagawa R, Hosaka K, Gi-Ho S, Hirayama Y, Yamaguchi K, Toyama K, Kakishima M (2010) Molecular phylogenetic studies of *Lachnum* and its allies based on the Japanese material. Mycoscience 51(3): 170–180. https://doi.org/10.1007/S10267-009-0023-1

Index Fungorum (2021) Index Fungorum. http://www.indexfungorum.org/names/Names.asp [Accessed on: 2021-04-15]

Johnston PR, Quijada L, Smith CA, Baral HO, Hosoya T, Baschien C, Pärtel K, Zhuang WY, Haelewaters D, Park D, Carl S, López-Giráldez F, Wang Z, Townsend JP (2019) A multigene phylogeny toward a new phylogenetic classification of Leotiomycetes. IMA Fungus 10: e1. https://doi.org/10.1186/s43008-019-0002-x

Kanouse BB (1941) New and unusual species of discomycetes. Mycologia 33: 461–467. https://doi.org/10.1080/00275514.1941.12020841

Katoh K, Standley DM (2013) MAFFT multiple sequence alignment software version 7: improvements in performance and usability. Molecular Biology and Evolution 30(4): 772–780. https://doi.org/10.1093/molbev/mst010

Kirschstein W (1938) Über neue, seltene und kritische Ascomyceten und Fungi imperfecti. I. Annales Mycologici 36(5–6): 367–400.

Kõljalg U, Tedersoo L, Nilsson RH, Abarenkov K (2016) Digital identifiers for fungal species. Science 352(6290): 1182–1183. https://doi.org/10.1126/science.aaf7115

Kõljalg U, Nilsson RH, Abarenkov K, Tedersoo L, Taylor AF, Bahram M, Bates ST, Bruns TD, Bengtsson-Palme J, Callaghan TM, Douglas B, Drenkhan T, Eberhardt U, Dueñas M, Grebenc T, Griffith GW, Hartmann M, Kirk PM, Kohout P, Larsson E, Lindahl BD, Lücking R, Martín MP, Matheny PB, Nguyen NH, Niskanen T, Oja J, Peay KG, Peintner U, Peterson M, Põldmaa K, Saag L, Saar I, Schüßler A, Scott JA, Senés C, Smith ME, Suija A, Taylor DL, Telleria MT, Weiss M, Larsson KH (2013) Towards a unified paradigm for sequence-based identification of fungi. Molecular Ecology 22: 5271–5277. https://doi.org/10.1111/mec.12481

Kõljalg U, Nilsson HR, Schigel D, Tedersoo L, Larsson K-H, May TW, Taylor AFS, Jeppesen TS, Frøslev TG, Lindahl BD, Põldmaa K, Saar I, Suija A, Savchenko A, Yatsiuk I, Adojaan K, Ivanov F, Piirmann T, Pöhönen R, Zirk A, Abarenkov K (2020) The Taxon Hypothesis Paradigm – On the Unambiguous Detection and Communication of Taxa Microorganisms 8(12): e1910. https://doi:10.3390/microorganisms8121910

Korf RP (1978) Nomenclatural and taxonomic notes on *Lasiobelonium*, *Erioscypha* and *Erioscyphella*. Mycotaxon 7(2): 399–406.

Kozlov AM, Darriba D, Flouri T, Morel B, Stamatakis A (2019) RAxML-NG: a fast, scalable and user-friendly tool for maximum likelihood phylogenetic inference. Bioinformatics 35(21): 4453–4455. https://doi.org/10.1093/bioinformatics/btz305

Kumar S, Stecher G, Li M, Knyaz C, Tamura K (2018) MEGA X: Molecular evolutionary genetics analysis across computing platforms. Molecular Biology and Evolution 35(6): 1547–1549. https://doi.org/10.1093/molbev/msy096

Lemoine F, Entfellner JBD, Wilkinson E, Correia D, Felipe MD, Oliveira TD, Gascuel O (2018) Renewing Felsenstein's phylogenetic bootstrap in the era of big data. Nature 556: 452–456. https://doi.org/10.1038/s41586-018-0043-0

Liu YL, Whelen S, Hall BD (1999) Phylogenetic relationships among ascomycetes: evidence from an RNA polymerase II subunit. Molecular Biology and Evolution 16: 1799–1808. https://doi.org/10.1093/oxfordjournals.molbev.a026092

Matheny PB (2005) Improving phylogenetic inference of mushrooms with RPB1 and RPB2 nucleotide sequences (Inocybe, Agaricales). Molecular Phylogenetics and Evolution 35: 1–20. https://doi.org/10.1016/j.ympev.2004.11.014

Matheny PB, Wang Z, Binder M, Curtis JM, Lim YW, Nilsson RH, Hughes KW, Hofstetter V, Ammirati JF, Schoch CL, Langer E, Langer G, McLaughlin DJ, Wilson AW, Frøslev T, Ge ZW, Kerrigan RW, Slot JC, Yang ZL, Baroni TJ, Fischer M, Hosaka K, Matsuura K, Seidl MT, Vauras J, Hibbett DS (2007) Contributions of rpb2 and tef1 to the phylogeny of mushrooms and allies (Basidiomycota, Fungi). Molecular Phylogenetics and Evolution 43(2): 430–451. https://doi.org/10.1016/j.ympev.2006.08.024

Miyoshi T, Ono Y, Shimizu S (2007) Occurrence of concave stem canker of citrus in Ehime prefecture [Japan] and detection of the pathogenic fungus *Lachnum abnorme* by PCR. Japanese Journal of Phytopathology 73(1): 9–14. https://doi.org/10.3186/jjphytopath.73.9 [in Japanese]

Nilsson RH, Abarenkov K, Veldre V, Nylinder S, De Wit P, Brosché S, Alfredsson JF, Ryberg M, Kristiansson E (2010). An open source chimera checker for the fungal ITS region. Molecular Ecology Resources 10(6): 1076– 1081. https://doi.org/10.1111/j.1755-0998.2010.02850.x

Nilsson RH, Tedersoo L, Ryberg M, Kristiansson E, Hartmann M, Unterseher M, Porter TM, Bengtsson-Palme J, Walker DM, de Sousa F, Gamper HA, Larsson E, Larsson KH, Kõljalg U, Edgar RC, Abarenkov K (2015) A comprehensive, automatically updated fungal ITS sequence dataset for reference-based chimera control in environmental sequencing efforts. Microbes and Environments 30(2): 145–150. https://doi.org/10.1264/jsme2.ME14121

Otani Y (1967) Notes on some cup fungi of the Hyaloscyphaceae collected in Hokkaido, Japan. Transactions of the Mycological Society of Japan 8: 33–42.

Perić B, Baral HO (2014) *Erioscyphella curvispora* spec. nov. from Montenegro. Mycologia Montenegrina 17: 89–104. https://www.etis.ee/File/DownloadPublic/ab9f7b44-b094-4148-8508-a48479be0ba9? [Accessed on: 2020-02-15]

Pons J, Barraclough TG, Gomez-Zurita J, Cardoso A, Duran DP, Hazell S, Kamoun S, Sumlin WD, Vogler AP (2006) Sequence-based species delimitation for the DNA taxonomy of undescribed insects. Systematic Biology 55(4): 595–609. https://doi.org/10.1080/10635150600852011

Puillandre N, Brouillet S, Achaz G (2021) ASAP: assemble species by automatic partitioning. Molecular Ecology Resources 21(2): 609–620. https://doi.org/10.1111/1755-0998.13281

Raitviir A (1985) Species Hyaloscyphacearum in *Sasa* spp. inventae. Novosti Sistematiki Nizshikh Rastenii 22: 157–162.

Raitviir A (2002) A revision of the genus *Dasyscyphella* (Hyaloscyphaceae, Helotiales). Polish Botanical Journal 47(2): 227–241.

Rambaut A (2018a) Tracer. Molecular evolution, phylogenetics and epidemiology, Edinburgh. http://beast.community/tracer [Accessed on: 2021-03-15]

Rambaut A (2018b) FigTree. Molecular evolution, phylogenetics and epidemiology, Edinburgh. http://tree.bio.ed.ac.uk/software/figtree/ [Accessed on: 2020-03-15]

Rognes T, Flouri T, Nichols B, Quince C, Mahé F (2016) VSEARCH: a versatile open source tool for metagenomics. PeerJ 4: e2584. https://doi.org/10.7717/peerj.2584

Ronquist F, Teslenko M, van der Mark P, Ayres DL, Darling A, Höhna S, Larget B, Liu L, Suchard MA, Huelsenbeck JP (2012) MrBayes 3.2: efficient Bayesian phylogenetic inference and model choice across a large model space. Systematic Biology 61: 539–542. https://doi.org/10.1093/sysbio/sys029

Sanderson MJ, McMahon MM, Steel M (2011) Terraces in phylogenetic tree space. Science 333(6041): 448–450. https://doi.org/10.1126/science.1206357

Schoch CL, Seifert KA, Huhndorf S, Robert V, Spouge JL, Levesque CA, Chen W, Fungal Barcoding Consortium (2012) Nuclear ribosomal internal transcribed spacer (ITS) region as a universal DNA barcode marker for Fungi. PNAS 109(16): 6241–6246. https://doi.org/10.1073/pnas.1117018109

Suková M (2005) A revision of selected material of lignicolous species of *Brunnipila*, *Capitotricha*, *Dasyscyphella* and *Neodasyscypha* from the Czech Republic. Czech Mycology 57(1–2): 139–172. https://doi.org/10.33585/cmy.57108

Spooner BM (1987) Helotiales of Australasia: Geoglossaceae, Orbiliaceae, Sclerotiniaceae, Hyaloscyphaceae. Bibliotheca Micologica 116: 1–711.

Swofford DL (2002) PAUP*. Phylogenetic analysis using parsimony (* and other methods). Version 4.0 b10. Sinauer Associates, Sunderland, MA.

Tello S, Baral HO (2016) *Erioscyphella lunata* (Lachnaceae), a rare discomycete collected in Spain. Ascomycete.org 8(4): 157–162. https://doi.org/10.25664/ART-0183

Tochihara Y, Hosoya T (2019) Three new species of *Incrucipulum* (Lachnaceae, Helotiales, Ascomycota) from Japan. Phytotaxa 403: 25–38. https://doi.org/10.11646/phytotaxa.403.1.2

Vilgalys R, Hester M (1990) Rapid genetic identification and mapping of enzymatically amplified ribosomal DNA from several *Cryptococcus* species. Journal of Bacteriology 172: 4238–4246. https://doi.org/10.1128/jb.172.8.4238-4246.1990

White T, Bruns TD, Lee A, Taylor JW (1990) Amplification and direct sequencing of fungal ribosomal RNA genes for phylogenetics. In: Innis MA, Gelfand DH, Snisky JJ, White TJ (Eds) PCR Protocols: A Guide to Methods and Applications. Academic Press, San Diego, 315–322. https://doi.org/10.1016/B978-0-12-372180-8.50042-1

Ye M, Zhuang WY (2003) New taxa of *Lachnum* (Helotiales, Hyaloscyphaceae) from temperate China. Nova Hedwigia 76(3–4): 443–450. https://doi.org/10.1127/0029-5035/2003/0076-0443

Zhao M, Yuan LY, Guo DL, Ye Y, Da-Wa ZM, Wang XL, Ma FW, Chen L, Gu YC, Ding LS, Zhou Y (2018) Bioactive halogenated dihydroisocoumarins produced by the endophytic fungus *Lachnum palmae* isolated from *Przewalskia tangutica*. Phytochemistry 148: 97–103. https://doi.org/10.1016/j.phytochem.2018.01.018

Zhao P, Zhuang WY (2011) Evaluation of ITS region as a possible DNA barcode for the genus *Lachnum* (Helotiales). Mycosystema 30(6): 932–937.

Zhao YJ, Hosoya T, Baral HO, Hosaka K, Kakishima M (2012) *Hymenoscyphus pseudoalbidus*, the correct name for *Lambertella albida* reported from Japan. Mycotaxon 122: 25–41. https://doi.org/10.5248/122.25

Zhuang WY (2004) New taxa of *Lachnum* (Ascomycetes, Helotiales) on bamboo and a key to the bambusicolous species of the genus. Nova Hedwigia 78(3–4): 425–433. https://doi.org/10.1127/0029-5035/2004/0078-0425

Zhuang WY, Wang Z (1998a) Some new species and new records of discomycetes in China. VIII. Mycotaxon 66: 429–438.

Zhuang WY, Wang Z (1998b) Discomycetes of tropical China. I. Collections from Hainan Island. Mycotaxon 67: 21–31.

Zhang J, Kapli P, Pavlidis P, Stamatakis A (2013) A general species delimitation method with applications to phylogenetic placements. Bioinformatics 15(29): 2869–2876. https://doi.org/10.1093/bioinformatics/btt499

Zoller S, Scheidegger C, Sperisen C (1999) PCR primers for the amplification of mitochondrial small subunit ribosomal DNA of lichen-forming ascomycetes. The Lichenologist 31: 511–516. https://doi.org/10.1006/lich.1999.0220

Supplementary material 1

Figure S1. ML trees

Authors: Yukito Tochihara, Tsuyoshi Hosoya

Data type: Image.

Explanation note: ML trees based on ITS (**A**), LSU (B), mtSSU (**C**) and RPB2 (**D**) constructed using MEGA X. Bootstrap values > 50% are indicated on branches and branches with MLBS > 70% are shown bold.

Link: https://doi.org/10.3897/mycokeys.87.73082.suppl1

Supplementary material 2

Figure S2. Hair apices

Authors: Yukito Tochihara, Tsuyoshi Hosoya

Data type: Image.

Explanation note: Hair apices of members of Clade **A** *Erioscyphella abnormis* TNS-F-32163 **B** *E. abnormis* TNS-F-61773 **C** *E. brasiliensis* TNS-F-46419 **D** *E. sclerotii* TNS-F-26492 **E** 'Lachnum' mapirianum TNS-F-17245 **F** 'Lachnum' palmae TNS-F-17567 **F1** Hair with resinous matters **F2** Hair with apical amorphous material **G** 'Lachnum' palmae TNS-F-24600 **G1** Hair with a resinous matter **G2** Hair with apical amorphous materials **H** *E. hainanensis* TNS-F-80371 **I** *E. sinensis* TNS-F-80354. Mounted in CB/LA. Scale bars: 10 mm. Arrowheads show hair apical materials.

Link: https://doi.org/10.3897/mycokeys.87.73082.suppl2

Supplementary material 3

Figure S3. Result of the ASAP species delimitation analysis

Authors: Yukito Tochihara, Tsuyoshi Hosoya

Data type: Image.

Explanation note: The graph shows the distribution of ASAP scores according to partitioning results, and the phylogenetic tree shows the way of partitioning.

Link: https://doi.org/10.3897/mycokeys.87.73082.suppl3

Supplementary material 4

Figure S4. Result of the GMYC species delimitation analysis

Authors: Yukito Tochihara, Tsuyoshi Hosoya

Data type: Image.

Explanation note: Number with each node shows the support value that each cluster is an independent species.

Link: https://doi.org/10.3897/mycokeys.87.73082.suppl4

Supplementary material 5

Figure S5. ML best-scored phylogenetic tree based on concatenated dataset of ITS1, 5.8S, and ITS2 constructed by RAxML-NG

Authors: Yukito Tochihara, Tsuyoshi Hosoya

Data type: Image.

Explanation note: GenBank/UNITE accession number and TNS specimen number (if any) is shown for each taxon. MLBP > 50% were attached on branches.

Link: https://doi.org/10.3897/mycokeys.87.73082.suppl5

Supplementary material 6

Figure S6. Results of PTP species delimitation analyses

Authors: Yukito Tochihara, Tsuyoshi Hosoya

Data type: Image.

Explanation note: Number with each node shows the probability of the likelihood that each cluster is an independent species. Clusters showed by red branches are regarded as species.

Link: https://doi.org/10.3897/mycokeys.87.73082.suppl6

MycoKeys 87: 53–76 (2022)
doi: 10.3897/mycokeys.87.72941
https://mycokeys.pensoft.net

RESEARCH ARTICLE

A peer-reviewed open-access journal
MycoKeys
Launched to accelerate biodiversity research

Diversity of *Fusarium* associated banana wilt in northern Viet Nam

Loan Le Thi[1*], Arne Mertens[2,10*], Dang Toan Vu[1], Tuong Dang Vu[1], Pham Le Anh Minh[13], Huy Nguyen Duc[9], Sander de Backer[2], Rony Swennen[3,10], Filip Vandelook[2], Bart Panis[4], Mario Amalfi[2,11], Cony Decock[12], Sofia I.F. Gomes[5,6], Vincent S.F.T. Merckx[5,7], Steven B. Janssens[2,8]

1 *Plant Resources Center, Hanoi, Vietnam* **2** *Meise Botanic Garden, Nieuwelaan 38, BE-1860 Meise, Belgium* **3** *IITA-Tanzania, c/o Nelson Mandela African Institution of Science and Technology, Duluti, Arusha, Tanzania* **4** *Bioversity International, Willem de Croylaan 42, BE-3001 Leuven, Belgium* **5** *Naturalis Biodiversity Center, Leiden, The Netherlands* **6** *Plant Ecology and Nature Conservation Group, Wageningen University, PO Box 47, NL-6700 AA Wageningen, The Netherlands* **7** *Department of Evolutionary and Population Biology, Institute for Biodiversity and Ecosystem Dynamics, University of Amsterdam, Amsterdam, The Netherlands* **8** *Department of Biology, KU Leuven, Belgium* **9** *Department of Plant Pathology, Faculty of Agronomy, Vietnam National University of Agriculture (VNUA), Vietnam* **10** *Laboratory of Tropical Crop Improvement, Department of Biosystems, KU Leuven, Belgium* **11** *Fédération Wallonie–Bruxelles, Service général de l'Enseignement universitaire et de la Recherche scientifique, Rue A. Lavallée 1, 1080 Bruxelles, Belgium* **12** *Mycothèque de l'Université catholique de Louvain (MUCL, MBLA), Place Croix du Sud 3, B-1348 Louvain-la-Neuve, Belgium* **13** *Faculty of Biotechnology, Vietnam National University of Agriculture (VNUA), Hanoi, Vietnam*

Corresponding author: Steven B. Janssens (steven.janssens@botanicgardenmeise.be)

Academic editor: Kevin D. Hyde | Received 18 August 202 | Accepted 22 December 2021 | Published 10 February 2022

Citation: Le Thi L, Mertens A, Vu DT, Vu TD, Anh Minh PL, Duc HN, de Backer S, Swennen R, Vandelook F, Panis B, Amalfi M, Decock C, Gomes SIF, Merckx VSFT, Janssens SB (2022) Diversity of *Fusarium* associated banana wilt in northern Viet Nam. MycoKeys 87: 53–76. https://doi.org/10.3897/mycokeys.87.72941

Abstract

Fusarium is one of the most important fungal genera of plant pathogens that affect the cultivation of a wide range of crops. Agricultural losses caused by *Fusarium oxysporum* f. sp. *cubense* (*Foc*) directly affect the income, subsistence, and nourishment of thousands of farmers worldwide. For Viet Nam, predictions on the impact of *Foc* for the future are dramatic, with an estimated loss in the banana production area of 8% within the next five years and up to 71% within the next 25 years. In the current study, we applied a combined morphological-molecular approach to assess the taxonomic identity and phylogenetic position of the different *Foc* isolates collected in northern Viet Nam. In addition, we aimed to estimate the proportion of the different *Fusarium* races infecting bananas in northern Viet Nam. The morphology of

* These authors contributed equally to this publication.

the isolates was investigated by growing the collected *Fusarium* isolates on four distinct nutritious media (PDA, SNA, CLA, and OMA). Molecular phylogenetic relationships were inferred by sequencing partial *rpb1*, *rpb2*, and *tef1a* genes and adding the obtained sequences into a phylogenetic framework. Molecular characterization shows that c. 74% of the *Fusarium* isolates obtained from infected banana pseudostem tissue belong to *F. tardichlamydosporum*. Compared to *F. tardichlamydosporum*, *F. odoratissimum* accounts for c.10% of the Fusarium wilt in northern Viet Nam, demonstrating that *Foc* TR4 is not yet a dominant strain in the region. *Fusarium cugenangense* – considered to cause Race 2 infections among bananas – is only found in c. 10% of the tissue material that was obtained from infected Vietnamese bananas. Additionally, one of the isolates cultured from diseased bananas was phylogenetically not positioned within the *F. oxysporum* species complex (FOSC), but in contrast, fell within the *Fusarium fujikuroi* species complex (FFSC). As a result, a possible new pathogen for bananas may have been found. Besides being present on several ABB 'Tay banana', *F. tardichlamydosporum* was also derived from infected tissue of a wild *Musa lutea*, showing the importance of wild bananas as a possible sink for *Foc*.

Keywords

AAA Cavendish, ABB Tay banana, banana disease, *Foc*-Race 1, *Foc*-TR4, FOSC, fungal diversity, *Musa lutea*, Viet Nam

Introduction

For millions of people, bananas are an important food crop. With an annual global production of 153 million tons produced on 5.6 million hectares of land, a revenue of more than 26.5 billion Euro was generated in 2017 (FAO 2018). Particularly in Asia, Africa, Latin America, and the Caribbean, bananas support rural livelihood as most grown bananas are self-consumed or locally traded. As a result, any reduction in crop harvest directly affects the income, subsistence, and nourishment of thousands of smallholders.

One of the most important fungal plant pathogens impacting the cultivation of numerous agricultural crops is the ascomycete *Fusarium* (e.g., rice, coffee, tomato, melon, wheat; Dean et al. 2012). *Fusarium* has a considerable economic, social and biological impact on the daily livelihood of millions of people worldwide. Within the genus, *F. oxysporum* is one of the two most devastating pathogens, besides *F. graminearum*. The *F. oxysporum* species complex (FOSC) is responsible for wilt diseases of various crops (e.g., cotton and tomato wilt) but is mainly known from its massive impact on the banana industry (Panama disease). For more than 100 years, the fungus has affected banana production worldwide (Ploetz and Pegg 1997; Ploetz 2015a).

Nowadays, the worldwide banana export is still seriously affected by *Foc*, as most of its current production depends on the cultivation of members of the Cavendish subgroup (Buddenhagen 2009; Ploetz 2009). Although the triploid 'AAA' Cavendish cultivars were selected in the past century for their resistance against *F. oxysporum* f. sp. *cubense* Race 1 (*Foc*-Race 1), to which the initially grown Gros Michel cultivars were highly susceptible (Stover 1962a), Cavendish cultivars (e.g., Grand Naine, Williams) are highly susceptible to *Foc*-TR4. All *Foc* strains currently known (e.g., Race 1, Race 2, STR4, TR4) pose a huge threat for banana cultivation worldwide. Moreover,

knowing that nearly half of the global banana production is derived from Cavendish clones and has become more popular for domestic use, a *Foc*-TR4 pandemic is still not averted to date (Ploetz 2015b; Zheng et al. 2018).

In the near future, *Foc* will further intensively spread in Asia, thereby significantly affecting important banana-producing countries such as China, the Philippines, Pakistan, and Viet Nam (Scheerer et al. 2018). For Viet Nam, the predictions are dramatic, estimating a loss in the banana production area for the country of 8% within the next five years and up to 71% within the next 25 years (Scheerer et al. 2018).

As a soil-borne fungus, *Foc* invades the root system from where it subsequently moves into the vascular tissue that gradually deteriorates. When reaching the corm, wilt occurs eventually, resulting in the death of the contaminated plant (Stover 1962a). A particular problem that arises with *Foc* infections is the remaining presence of *Foc* spores (microconidia, macroconidia, and chlamydospores) in the soil surrounding the infected plants for at least 20 years after the complete removal of all infected plants or plant tissue (Stover 1962b; Buddenhagen 2009; Dita et al. 2018). As a result, reinfection of new banana accessions in the same area is very likely to happen in the absence of complete soil disinfection or if one has not waited long enough for planting new *Musa* cultivars (Moore et al. 2001; Huang et al. 2012). Therefore, Fusarium wilt not only has an impact on the overall yield during the time of infection but also on the land use for banana cultivars during the coming 20 years.

Whereas pathogenic *Foc* lineages were usually classified into three races (*Foc* 1, 2 & 4) based on the different *Musa* cultivars they had infected, the development of the Vegetative Compatibility Group (VCG) system resulted in a more in-depth identification tool of *Foc* strains into 24 unique entities (Fourie et al. 2011; O'Donnell et al. 2009; Perez-Vicente et al. 2014; Mostert et al. 2017). The fact that isolated *Foc* lineages could already be split up into compatible vegetative groups already indicated that there are more natural lineages in the FOSC than can be reflected by the number of races. In addition, the polyphyletic nature of *F. oxysporum* f. sp. *cubense* isolates is also demonstrated by Maryani et al. (2019a), who used a combined molecular phylogenetic approach to delineate natural lineages within the FOSC (O'Donnell and Cigelnik 1997), thereby describing 11 new *Fusarium* species which were formerly considered as *F. oxysporum*. A result of Maryani et al. (2019a) also indicated that the VCG system is perhaps slightly prone to an oversimplification of the categorization of different *Foc* strains that cause Fusarium wilt in bananas and plantains.

In 1968, Vakili and coworkers published the first survey on *Fusarium* infecting bananas in Southern Viet Nam (Vakili et al. 1968). Later studies showed that by the end of the 20th century, *Foc* infections were omnipresent in the whole country (Mai Van Tri 1997; Bentley et al. 1998; Vinh et al. 2001). The characterization of the *Fusarium* isolates in the studies mentioned above demonstrated that Fusarium wilt on bananas in Viet Nam was derived from different *Foc* VCG's (e.g., VCG 0123, VCG 0124, VCG 0124/5, VCG 0125). Hung et al. (2017) reported the first observation of *Foc*-TR4 (VCG 01213/16) on Cavendish bananas in Viet Nam using a combined molecular (polymerase chain reaction (PCR) approach) and morphological characterization. However, Zheng et

al. (2018) claimed that they made the earliest collected records of *Foc*-TR4 in Viet Nam in 2016 by assessing the pathogenicity of the collected strains and characterizing them molecularly using whole-genome sequencing methodology. The study of Mostert et al. (2017) also used a molecular-morphological characterization approach to determine the origin of the different *Fusarium* infections in Viet Nam. Their results showed the presence of at least five different VCG's (VCG 0123, VCG 0124, VCG 0124/5, VCG 0128, VCG 01221), of which the latter two were not yet detected in earlier studies.

In the current study, we aim to assess the overall diversity of *Foc* wilt in northern Viet Nam by using a combined morphological-molecular phylogenetic approach in which the different VCG's are included. With this approach, we provide the overall species identity and phylogenetic position of *Foc* infections in the northern Vietnamese region and examine the genetic diversity between the different *Foc* isolates (from wild and cultivated bananas) collected from various provinces in northern Viet Nam. Furthermore, our results will indicate the proportion of the different *Foc* strains (and linked VCGs) that are currently infecting bananas in northern Viet Nam.

Material and methods

Sampling

From April 2018 until December 2019, several field trips were carried out focusing on the presence of banana Fusarium wilt in northern Viet Nam. During these surveys, banana Fusarium wilt samples were collected at 19 locations in three large geographic regions; North-eastern region, North Central region and Red River Delta, with most specimens collected in the latter region (Table 1, Fig. 1). *Fusarium* infected banana plants were identified by following a set of diagnostic characters in which (mostly older) leaves were clearly yellow (initiated from the leaf margin) or even completely collapsed, halfway along the petiole forming a ring of dead leaves around a dying plant, combined with brown discoloration and longitudinally fissuring of the pseudostems leaf sheaths (Fig. 2). From symptomatic plants observed in the field, discoloured brownish vascular tissue was collected from pseudostems and roots. Subsequent to the collection, infected tissue samples were stored in paper bags and put in a refrigerator or cooling box to avoid quality loss upon the further analysis in the molecular lab. For each sample collected, notes were taken about the altitude, longitude and latitude, site location, and the host specimen. Collected *Fusarium* samples were stored at the Plant Resources Center (PRC), Ha Noi, Viet Nam (Table 1).

Isolate cultivation

In order to observe possible morphological differences between the Fusarium wilt isolates collected from the wild and cultivated northern Vietnamese *Musa* accessions, we followed the approach of Groenewald et al. (2006) in which different *Foc* isolates were

Table 1. List of collected *Fusarium* (*Foc*) wilt samples on bananas in northern Viet Nam.

Isolate	Locality	Cultivar or Species	Altitude (m)	Latitude	Longitude
FOC1	Yen Binh town, Quang Binh district, Ha Giang province	Tay banana (ABB)	78	2254.0'104°32 ,"5.28'23°"	
FOC2	Dong Cay village, Yen Thang commune, Luc Yen district, Yen Bai province	Tay banana (ABB)	188	22°05'46.2",	104°45'34.0"
FOC4	Khe Chao village, Ngoi A commune, Van Yen district, Yen Bai province	Tay banana (ABB)	76	21°54'21.4",	104°43'48.3"
FOC5	No 7 village, Dai Son commune, Van Yen district, Yen Bai province	*Musa lutea*	351	21°48'17.6",	104°36'01.0"
FOC6-1	No 4 village, Dai Son commune, Van Yen district, Yen Bai province	Tay banana (ABB)	352	21°48'16.9",	104°36'02.5"
FOC7	No 18 village, Lam Giang commune, Van Yen district, Yen Bai province	Tay banana (ABB)	137	22°02'35.3",	104°30'52.3"
FOC10	Hai Son 1 village, Phu Nhuan commune, Bao Thang district, Lao Cai province	Tay banana (ABB)	370	22°13'58.6",	104°08'14.9"
FOC11	Khanh Yen town, Van Ban district, Lao Cai province	Tay banana (ABB)	383	22°06'53.9",	104°14'37.9"
FOC16	Hoang An commune, Hiep Hoa district, Bac Giang province	Tay banana (ABB)	20	21°23'00.2",	105°58'40.5"
FOC18	Hoang Thanh commune, Hiep Hoa district, Bac Giang provinse	Tay banana (ABB)	18	21°23'22.1",	106°00'24.9"
FOC21	Thinh Long town, Hai Hau district, Nam Dinh province	Tay banana (ABB)	4	20°01'59",	106°12'49.0"
FOC23-2	Thanh Chau commune, Phu Ly district, Ha Nam province	Tay banana (ABB)	7	20°31'24.2",	105°55'31.1"
FOC24	Hung Thanh commune, Tuyen Quang city, Tuyen Quang province	Tay banana (ABB)	26	21°48'19.4",	105°11'39.7"
FOC25-1	Le Chi commune, Gia Lam district, Ha Noi province	Tay banana (ABB)	11	21°18'20.5",	106°00'24.6"
FOC25-2	Le Chi commune, Gia Lam district, Ha Noi province	Tay banana (ABB)	11	21°18'20.5",	106°00'24.6"
FOC38	Quan Mia village, Nghia Tan commune, Nghia Dan district, Nghe An province	Tay banana (ABB)	85	19°19'07.5",	105°21'53.7"
FOC56	Agriculture University,Trau Quy town, Gia Lam district, Ha Noi province	Tay banana (ABB)	11	21°18'20.5",	106°00'24.6"
FOC58	Nui Ngam, Minh Tan commune, Vu Ban district, Nam Dinh province	Tay banana (ABB)	3	20°21'59.1"N,	106°04'02.9"E
FOC 61	Hong Chau commune, Yen Lac district, Vinh Phuc province	Cavendish (AAA)	3	21°10'17.1"N,	105°34'37.0"E

grown on different media. Infected discoloured pseudostem tissue samples were cut into 2–3 cm pieces and placed on the Komada medium (Komada 1975). After a few days, fungal *Fusarium* colonies were transferred to plates with different media and then put in a growing chamber at 25 °C until the colonies reached 2–3 cm. The different isolates were grown on four distinct nutritious media to observe the Fusarium wilt in different culture conditions: PDA (Potato Dextrose Agar), SNA (Spezieller Nährstoffarmer Agar), CLA (Carnation Leaf Agar), and OMA (Oatmeal Agar) (Nirenberg 1976). The PDA medium consisted of 200g potato dextrose, 20g D-glucose, and 20g agar dissolved in 1000ml distilled water, whereas the SNA medium consisted of 1g KH_2PO_4,

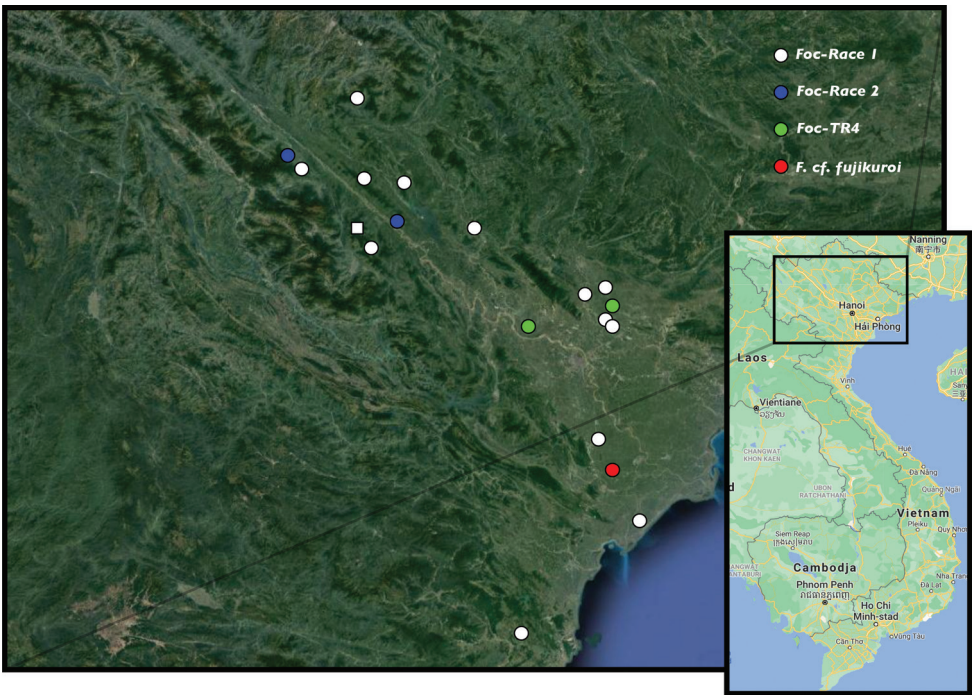

Figure 1. Distribution map of localities in northern Viet Nam where Fusarium wilt was observed. Colours indicate different *Fusarium* strains or species. Squares indicate *Fusarium* infections of wild bananas; circles indicate infections of cultivated bananas.

1g KNO_3, 0.5g $MgSO_4$•$7H_2O$, 0.5g KCl, 0.2g D-glucose and 0.2g D-sucrose dissolved in 1000ml distilled water. The CLA medium contained aseptic carnation leaves and 20g agar dissolved in 1000ml distilled water. The OMA medium consisted of 50g oatmeal and 20g agar dissolved in 1000ml distilled water. The growth of the *Fusarium* isolates on the different media took place under in-vitro conditions with temperatures between 23 and 27 °C (Pérez et al. 2003). After seven days of incubation, the developing colonies were morphologically investigated under a light microscope (400x magnification). The coloration of the colony, the morphology, and the size of the conidia were determined. The colony reverse colour was determined on PDA medium after incubation at room temperature, using the colour charts of Rayner (1970). In addition to colony colour, the aroma of the different cultures was assessed as a strong rank odour generated by mature cultures which is a typical characteristic for TR4 infections. In the first stage of culturing, we characterized the isolates as *Fusarium* spp. emanated from mycelium morphology and the presence of different types of conidia. The study of Maryani et al. (2019a) was used as a reference to classify the Foc lineages into different sublineages further. All obtained *Fusarium* isolates were stored in the Plant Resources Center (PRC), Ha Noi, Viet Nam.

Figure 2. A overall view of a banana plant infected by *Fusarium* wilt **B** detailed view of wilted plant **C** radial cutting of *Fusarium*-infected banana pseudostem **D** tangential cutting of *Fusarium*-infected banana pseudostem.

Molecular protocols

In order to extract high-quality DNA from the Fusarium wilt isolates collected and cultured, we used the pure mycelium cultures generated for the morphological characterization of the banana wilt. Total genomic DNA was isolated using a modified CTAB protocol based on the study of Lin et al. (2008) and Dellaporte et al. (1983). After the addition of 5ml TNE buffer (100 mM Tris-HCl, 50 mM EDTA, 50 mM NaCl, 8 µM β-mercaptoethanol, 1% SDS, pH 8.0) to the sampled mycelium, the samples were incubated for 1 h (65 °C). Subsequent to the lysis phase, 1.66ml NaOAc (5M) was added and centrifuged. Chloroform-isoamylalcohol (24/1 v/v) extraction was done twice, followed by isopropanol precipitation at -32 °C for 12h. After centrifugation at 4 °C, the pellet was washed twice (75% ethanol), air-dried, and dissolved in 100µl TE buffer (10mM TrisHCl, 0.1mM EDTA; pH 8)

Amplification reactions of *rpb1*, *rpb2*, and *tef1a* were carried out using standard PCR (20µl). Reactions were initiated with a 3 min heating at 95 °C followed by 30 cycles consisting of 95 °C for 30s, 55–65 °C (*rpb1* and *rpb2*) and 53°-59 °C (*tef1a*) for 60s, and 72 °C for 60s. Reactions ended with a 3 min incubation at 72 °C. Primers designed by O'Donnell et al. (1998) were used to sequence *tef1a*, whereas primers for *rpb1* and *rpb2* were adopted from O'Donnell et al. (2010). PCR products were purified using an ExoSap purification protocol. Purified amplification products were sequenced by the Macrogen sequencing facilities (Macrogen, Seoul, South Korea).

Phylogenetic analyses

Raw sequences were assembled using Geneious Prime (Biomatters, New Zealand). Automatic alignment was conducted with MAFFT (Katoh et al. 2002) using an E-INS-i algorithm, a 100PAM/k = 2 scoring matrix, a gap open penalty of 1.3, and an offset value of 0.123. Manual fine-tuning of the aligned dataset was performed in Geneious Prime.

Fusarium sequence data of *rpb1*, *rpb2*, and *tef1a* was extracted from GenBank (September 20, 2020) using the 'NCBI Nucleotide extraction' tool in Geneious Prime. Together with the newly generated sequences for the 19 Vietnamese Fusarium wilt accessions, the total sequence data matrix consisted of 529 specimens divided over 201 species (Suppl. material 1: Table S1). Of those, 72 species belong to different closely related genera of *Fusarium* within the Nectriaceae family were chosen as outgroup (*Albonectria*, *Bisifusarium*, *Cosmospora*, *Cyanonectria*, *Cylindrocarpon*, *Fusicolla*, *Geejayessia*, *Luteonectria*, *Macroconia*, *Microcera*, *Neocosmospora*, *Pycnofusarium*, *Rectifusarium*, *Setofusarium*; sensu Crous et al. 2021). Newly generated sequences were deposited in the GenBank sequence database (Table 1). Furthermore, in order to compare the newly collected Vietnamese *Foc* accessions with the known VCGs, the sequence dataset included *Foc* samples representing all VCGs (see Table S1; Ordonez et al. 2015), except for VCG01212 and VCG0129, from which only one locus was available, thereby causing phylogenetic biases due to the occurrence of too much missing data.

Possible incongruency between the different datasets was inferred by conducting an ILD test (Farris et al. 1995) as implemented in PAUP* v.4.0b10 (Swofford 2003) with the following parameters applied: simple taxon addition, TBR branch swapping, and heuristic searches of 1000 repartitions of the data. Despite the well-known sensitivity of the ILD test (Barker and Lutzoni 2002), the results of this test were compared in light of the resolution and support values for each of the single gene topologies. As a result, the possible conflict between data matrices was visually inspected by searching for conflicting relationships within each topology (obtained per single sequence data matrix) that were supported by a Maximum Likelihood (ML) support value > 70% (hard vs. soft incongruence; Johnson and Soltis 1998; Pirie 2015). A conflict was assumed to be significant if two different relationships for the same set of taxa (one being monophyletic and the other non-monophyletic) were observed in rival trees. ML analyses were conducted under the RAxML search algorithm (Stamatakis 2014) with the GTRGAMMAI approximation of rate heterogeneity for each gene. ML bootstrapping was carried out on five hundred bootstrapped datasets using the RAxML Rapid bootstrap algorithm (ML-BS).

The best-fit nucleotide substitution model for each dataset was selected using jModelTest 2.1.4. (Posada 2008) out of 88 possible models under the Akaike information criterion (AIC). The GTR+I+G, TVM+G, and HKY+I+G were determined as the best-fit substitution models for *rpb1*, *tef1a*, and *rpb2* markers, respectively. Consequently, we used a mixed-model approach to apply different evolutionary models on each DNA region of the combined dataset (Ronquist and Huelsenbeck 2003). Bayesian inference analyses were conducted with MrBayes v3.2.6 (Ronquist et al. 2012) on three individual data partitions and a combined data matrix. Each analysis was run twice for 20 million generations. Trees were sampled every 5000th generation. Chain convergence and ESS parameters were inspected with TRACER v.1.4 (Rambaut and Drummond 2007). Only nodes with Bayesian posterior probabilities (BPP) above 0.95 were considered as well supported by the data (Suzuki et al. 2002).

Results

Fusarium wilt infections are prevalent in most of northern Viet Nam as they have been observed in all provinces of northern Viet Nam that were sampled in this study. The 19 Fusarium wilt infections collected based on the typical plant Fusariosis symptoms (old leaves turning yellow, leaves gradually collapsing, petioles broken close to the midrib with dead leaves remaining attached to the pseudostem, pseudostem sheaths longitudinally splitting near the base, and vascular necrosis) (Fig. 2) were cultured and further morphologically and molecularly analysed. Despite the fact that tissue which showed signs of Fusariosis disease symptoms was used to further morphologically and molecularly characterize the *Fusarium* wilt, we cannot draw eminent conclusions on the pathogenicity of the isolates as no real pathogenicity test was carried out and therefore Koch's postulates were not fully fulfilled.

Morphological characterization of the cultured pathogenic Fusarium wilt isolates showed that when the isolates were grown on CLA medium, they produced macroconidia that were uniform in size and form. On SNA medium, the morphology of the macroconidia was sometimes less uniform in size than when SLA medium was used. Except for two accessions (FOC56 and FOC61), no aroma was observed among the *Fusarium* isolates collected in northern Viet Nam. In general, for all isolates, we observed that macroconidia are sickle-shaped, 3–7 septate, and thin-walled. Microconidia are oval to kidney-shaped, 0–1 septate. Chlamydospores were round and thick-walled. Subtle differences have been observed in the colony morphology and coloration. Based on these morphological differences, we tried to identify different groups within the *Fusarium* isolates analysed.

The first group, consisting of 14 isolates (FOC1, 2, 5, 6–1, 7, 11, 16, 18, 21, 23–2, 24, 25–1, 25–2, 38), is characterized by a purple reverse in the centre, white-greyish towards the periphery. The colony surface is dry and is filamentous at the edge. On CLA medium, it produces ample macroconidia, yet only little microconidia. On PDA and SNA medium, it produces prolific microconidia. The second group has a reverse colony colour containing a small touch of dark purple in the centre, gradually discolouring to white towards the edge. This type is observed for isolates FOC 4 and 10. The surface of these colonies is also dry and filamentous at the margin. On CLA medium, ample macroconidia are produced, whereas on PDA and SNA medium, the presence of macroconidia is less profound. On the latter two media, prolific microconidia are produced. The third group of isolates (FOC56 and 61) is characterized by an unpigmented, white colony reverse and a dry colony surface with a filamentous margin. On CLA medium, many macroconidia are produced, while on PDA and SNA medium, macroconidia are hardly formed. On PDA and SNA, prolific microconidia are produced, whereas on CLA medium, only a few microconidia were observed. In addition, FOC 56 and 61 isolates are characterized by a typical strong odour of the older cultures. FOC 58 falls a bit amidst the first and second group, containing a pale purple colony reverse colour that becomes whitish towards the periphery and with a dry colony surface appearance.

Table 2. Alignment and sequence characteristics of the different partitions (including outgroup specimens).

	rpb1	*rpb2*	*tef1a*
N° taxa	457	525	271
Sequence length range	558–1574	597–859	343–636
Aligned sequence range	1578	917	797
Variable characters	1103 (70%)	572 (62%)	529 (66%)
Constant characters	474	345	268

Phylogenetic analyses of *Fusarium* wilt isolates from northern Viet Nam

Sequence characteristics of all data matrices analysed are summarized in Table 2. Despite the fact that sometimes not all gene markers could be sequenced, their absence did not influence the overall phylogenetic results, as sufficient nucleotide variation was present. The partition homogeneity test found no significant incongruence between all three sequence datasets (with all P-values being larger than 0.05). Visual examination of the two different partitions of the combined dataset corroborates this congruency analysis.

Phylogenetic analyses of the 19 Fusarium wilt isolates found in various northern Vietnamese bananas showed that although overall morphological characterisation pointed towards *F. oxysporum* f. sp. *cubense*, it was clear that they had various evolutionary origins (Fig. 3c, d). Of the 19 accessions analysed, two (FOC61 and FOC56) were placed within the *F. odoratissimum* clade (as defined by Maryani et al. 2019a, Fig. 3d) and for which pathogenicity tests by Maryani et al. (2019a) showed that the members of this group caused infections in Cavendish and Gros Michel AAA banana varieties. In addition, VCG 01213 and VCG 01216 are positioned close to FOC61 and FOC56. As a result, two of the 19 (10.5%) northern Vietnamese Fusarium wilt isolates are assumed to be *Foc*-TR4 (also taking the morphological characterization into account). Interestingly, one of the two isolates characterised as *Foc*-TR4 (FOC61) infected a Cavendish plantation in Vinh Phuc province, whereas the other infection of *Foc*-TR4 (FOC56) took place on ABB Tay banana cultivars situated on a smallholder farm in Nam Dinh province (Table 1). The largest group (13 accessions; 68.5%) of Fusarium wilt isolates in northern Vietnamese bananas belong to the recently delineated *F. tardichlamydosporum* clade (Fig. 3d). Pathogenicity tests carried out for this clade by Maryani et al. (2019a) have indicated a large infection rate in Gros Michel cultivars for this lineage, and therefore members of the *F. tardichlamydosporum* clade are consequently classified as *Foc*-Race 1. Furthermore, the isolates that fell within the *F. tardichlamydosporum* were also most closely related to VCG 0125, a known *Foc*-Race 1 representative. In northern Viet Nam, infections of *Foc*-Race 1 occurred both on wild and cultivated accessions. For the cultivated accessions, the *Foc*-Race 1 was only found on the ABB Tay banana cultivar, yet was clearly spread in northern Viet Nam as it was found in eight different provinces (Ha Giang, Yen Bai, Lao Cai, Bac Giang, Nam Dinh, Ha Nam, Tuyen Quang, Ha Noi; Table 1). Most interestingly, *Foc*-Race 1 was also identified (isolate FOC5) in an individual of the wild banana *Musa lutea* (section Callimusa). Here the infected accession grew sympatrically with other indi-

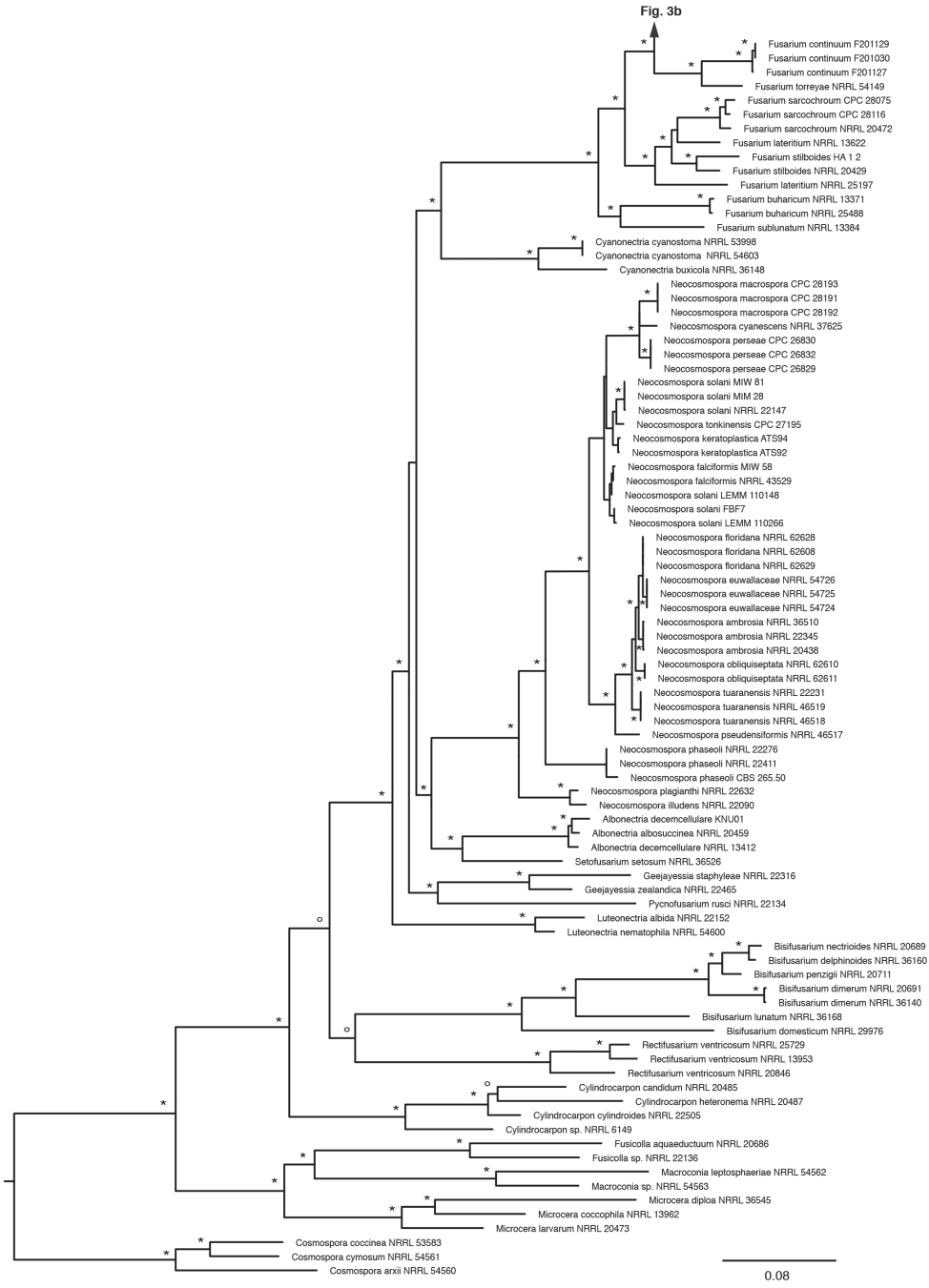

Figure 3. Maximum Likelihood topology obtained via heuristic search algorithm of the combined *rpb1*, *rpb2* and *tef1a* data matrix. Bootstrap support (ML-BS) values above 50 are indicated with a dot, ML-BS values above 75 are indicated with an asterisk. No indication above the branches indicates a ML-BS value below 50. Newly included accessions are indicated in red. FOSC: *Fusarium oxysporum* species complex, FFSC: *Fusarium fujikuroi* species complex.

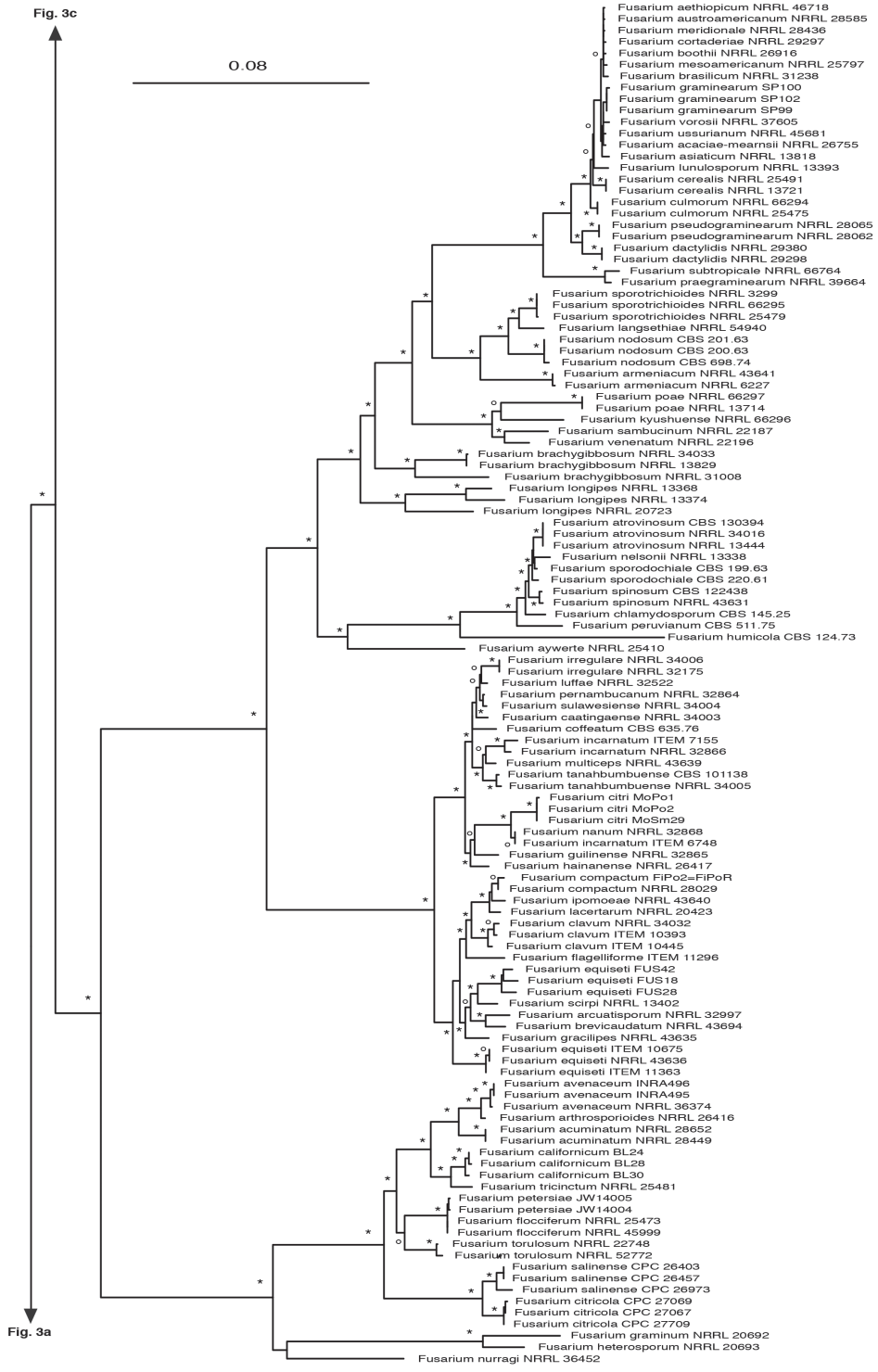

Figure 3. Continuation.

Figure 3. Continuation.

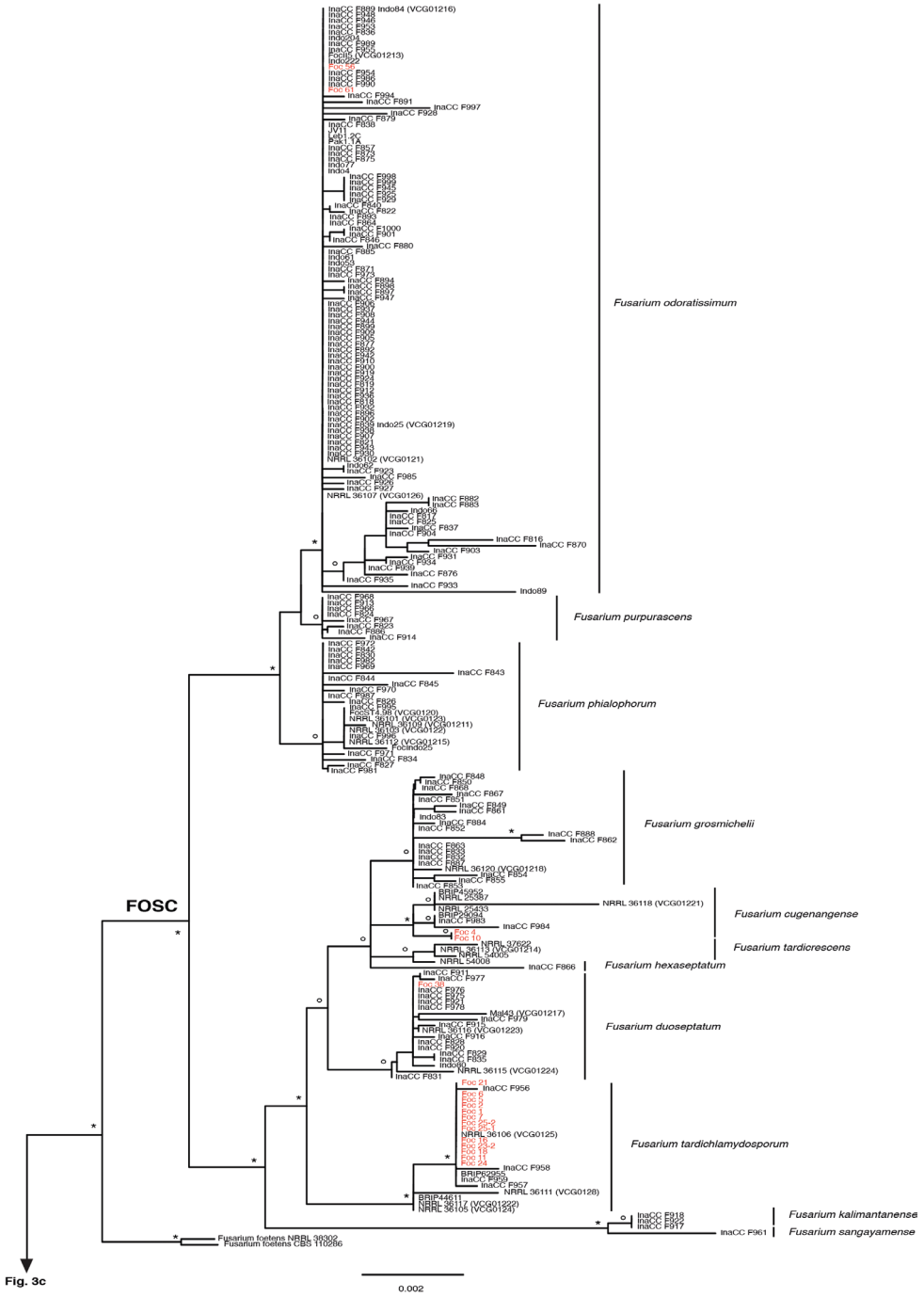

Figure 3. Continuation.

viduals of *M. lutea* as well as with *M. itinerans*. The area where this infection occurred was a steep, abandoned rice terrace in Yen Bai province where hundreds of individuals of both wild species co-occurred and were rather close to one of the smallholder farms where *Foc*-Race 1 was also detected (isolate FOC6-1). In addition to the *Foc*-Race 1 infections caused by *Fusarium tardichlamydosporum*, *F. duoseptatum* is also classified as a *Foc*-Race 1 Fusarium wilt (see Maryani et al. 2019a). An infection of this latter *Foc* isolate (FOC38) was found only once in northern Viet Nam (Nghe An province; c. 5% of the Fusarium wilt infections), where it infected the ABB Tay banana cultivars that were grown on a smallholder farm. The VCGs that occurred in the same clade as FOC38 are VCG 01223 and VCG 01217, with the latter being known as a *Foc*-Race 1 representative (e.g., Katan 1999; Fraser-Smith et al. 2014).

In addition to the *Foc*-Race 1 and *Foc*-TR4 infections, two *Foc* isolates (FOC4 and FOC10) were found in northern Viet Nam (10.5%) that belong to the recently described *F. cugenangense* (Maryani et al. 2019a; Fig. 3d). Hitherto, this *Fusarium* species was considered to be strictly Indonesian (see Maryani et al. 2019a). Pathogenicity tests conducted for representatives of *F. cugenangense* by Maryani et al. (2019a) have demonstrated that it only causes a mild infection in Gros Michel and Cavendish and is regarded as non-pathogenic for the above-mentioned AAA cultivars. However, our results clearly show that the infection of this isolate also occurred on ABB Tay banana cultivars in northern Viet Nam, where it had a large impact on the fitness of the infected host plants. Although additional confirmation is needed, Maryani et al. (2019a) assume that representatives of the *F. cugenangense* clade should be considered as *Foc*-Race 2 (Maryani et al. 2019a; Fig. 3d), yet more thorough analyses need to be carried out in order to further confirm this hypothesis. The VCG that occurred in the same clade as FOC4 and FOC10 is VCG 01221.

A final Fusarium wilt infection (FOC58) that was regarded upon collection in the field and during morphological screening as a *Foc* infection (c. 5% of the Fusarium wilt infections observed in this study) was not situated in the *F. oxysporum species complex* (FOSC) but was a distinct lineage sister to *F. fujikuroi* (Fig. 3c), a well-known pathogen of rice (e.g., Wulff et al. 2010; Choi et al. 2018). This *Fusarium* isolate was the prime infection source of ABB Tay bananas cultivated on a small plantation for local use in Nam Dinh province (Fig. 1).

Discussion

Fusarium wilt in Vietnam: lineage identification

To better manage the significant threat of *Foc* dispersion in northern Viet Nam, the correct identification and abundance of the *Foc* strains that cause Fusarium wilt in bananas in the region are necessary. This is the basis for eradication-confinement and suppression-contention measures (Perez-Vicente et al. 2014). Since the survey of Vakili

et al. (1968), *Foc* Race 1 has been considered as the main *Foc* infecting edible bananas in Viet Nam. With the emergence of *Foc* TR4 it remained unclear how abundant this new pathogenic *Foc* strain had become in Viet Nam. Although officially present in Viet Nam for only a few years (Hung et al. 2017; Zheng et al. 2018), *Foc* TR4 was already observed on Cavendish bananas in 1998 in Southern China (Hu et al. 2006). A few years later, in 2002, *Foc* TR4 was also found in Chinese regions adjacent to northern Viet Nam (Hu et al. 2006; Li et al. 2013). With the current shift of Cavendish cultivation in Asia from China to its neighbouring countries Laos, Myanmar, and Viet Nam, there is also an active spread of *Fusarium* pathogens through transportation of planting material, farming equipment, and contaminated soil from China (Zheng et al. 2018), so that *Foc* TR4 can quickly become the most dominant *Foc* race in Viet Nam affecting banana cultivation.

The present study applies the FOSC species delimitation concept of Maryani et al. (2019) to delineate the *Foc* lineages sampled in northern Viet Nam more thoroughly. Furthermore, incorporating the different VCGs in the current phylogenetic dataset allowed us to link the Vietnamese *Foc* isolates with one of the currently known VCGs that have been assessed in the past. Based on the compatibility of the novel material with the VCGs present in the same clade and their specific species allocation following the species delineation concept of Maryani et al. (2019), we linked the northern Vietnamese *Foc* isolates to one of the known *Foc* Races. Accordingly, our results show that *Foc* isolates that are phylogenetically situated within a lineage containing *Foc* Race 1 are among the most common isolates in northern Viet Nam, causing 74% of all the infections. A more in-depth molecular characterisation shows that of these, 13 out of 14 isolates are representatives of *F. tardichlamydosporum*, whereas one isolate is a representative of *F. duoseptatum*. Whereas *F. tardichlamydosporum* is commonly present throughout the northernly oriented Northeastern region and Red River Delta, *F. duoseptatum* is not present in these more northerly oriented geographic regions but occurs in the more centrally oriented North Central region in Viet Nam. Also, from a global distributional perspective, *F. tardichlamydosporum* is much more widespread than *F. duoseptatum*, with the first species located in Australia, Indonesia, Malaysia, Honduras, and Brazil, and the latter is only known to date from Indonesia and Malaysia (Maryani et al. 2019a).

Interestingly, the *Foc* isolates that are phylogenetically situated within the *F. odoratissimum* species lineage (linked to *Foc*-TR4 infections; Maryani et al. 2019a) account for only 10% of the Fusarium wilt in northern Viet Nam, demonstrating that *Foc-TR4* has not yet become a dominant banana pathogen, unlike other countries in Asia where there is a tendency to grow Cavendish cultivars as large monocultures, such as in China, the Philippines, and Taiwan. The *F. odoratissimum* accessions found in the current study were located in the River Delta region of northern Vietnam, provinces Vinh Phuc and Nam Dinh, which are rather distant from *Foc*-TR4 infected regions in Southern China. This indicates a gradual spreading in Viet Nam of *F. odoratissimum* (=*F. oxysporum* f. sp. *cubense* TR4) towards the south as the TR4 isolates analysed by Zheng et al. (2018) were collected in the upper North of Viet Nam in the Lao Cai

province at only a few kilometres from the border with China (Yunnan). At the moment, it is unclear whether the occurrence of *Foc*-TR4 in Viet Nam is still in an initial lag phase, with the potential of largely increasing its distribution range in the country if conditions would enable the disease to spread (Pegg et al. 2019). Especially the replacement of citrus plantations and maize fields by Cavendish monocultures provides an ideal basis for *Foc*-TR4 to rapidly spread as plants available for infection become less limited. A more worrying observation is that *Foc*-TR4 is not only found in Cavendish bananas in Viet Nam, but it also poses a threat to local banana varieties as is observed in the current study where *F. odoratissimum* is found in ABB Tay banana cultivars.

The current study demonstrates that the presence of *F. cugenangense* (linked to *Foc*-Race 2 infections; Maryani et al. 2019a) also accounts for 10% of the Fusarium wilt in northern Viet Nam. In general, *Foc*-Race 2 infections occur on triploid ABB Bluggoe varieties and its closely related cooking cultivars (Jones, 2000). Besides Bluggoe cooking bananas, *Foc*-Race 2 also infects the tetraploid AAAA Bodles Altafort hybrid between Gros Michel (AAA) and Pisang Lilin (AA) (Stover and Simmonds 1987). In addition, experimental infection of *Ensete ventricosum* demonstrated that this important Ethiopian crop is highly susceptible to *Foc*-Race 2 (Ploetz, 2005). With the confirmation of *F. cugenangense* also present in representatives of infected ABB Tay banana cultivars, it is clear that Fusarium wilt caused by *Foc*-Race 2 is potentially more widespread than has often been assumed.

Fusarium cf. fujikuroi; a new *Fusarium* lineage found within bananas

In addition to the *Fusarium* isolates collected from northern Vietnamese bananas belonging to FOSC, an infection with symptoms similar to *Foc* wilt was observed, yet the cultured isolate did not belong to FOSC. The morphological colony characteristics were comparable to those observed for FOSC cultures through having a pale purple colony reverse colour that became whitish towards the periphery with a dry colony surface appearance. However, when considering its phylogenetic position within the *Fusarium* genus, this isolate did not fall within *F. oxysporum* representatives, but was a member of the *F. fujikuroi* species complex (FFSC) where it is the sister lineage of *F. fujikuroi*. It is not uncommon that several *Fusarium* species cause the same disease pattern as this phenomenon has also been identified in mango deformity (Lima et al. 2009) and sugar beet wilt (Burlakoti et al. 2012). Within the FFSC, some species are known to be pathogenic for some *Musa* cultivars (*F. proliferatum*, *F. verticillioides*, *F. sacchari*, *F. lumajangense*, *F. desaboruense* and *F. musae*; Maldonado-Bonilla et al. 2019; Van Hove et al. 2002; Huang et al. 2019; Maryani et al. 2019b), yet to date, no other species of the FFSC - except for the above-mentioned - was identified as a pathogen for *Musa*. From a phylogenetic point of view, the novel *Fusarium* isolate that was obtained from the infected tissue of a triploid ABB Tay banana cultivar in Nam Dinh province is sister to *F. fujikuroi*. *Fusarium fujikuroi* is a widespread phytopathogen causing the bakanae disease in various *Oryza sativa* cultivars (rice), but it is also known to have a major impact on many other economically important crops (e.g., maize, wheat). This

result increases our knowledge of the diversity of the *Fusarium* species that cause wilt symptoms on bananas. More importantly, it also demonstrates the urgent need to accurately identify plant pathogens that are morphologically very difficult to distinguish from each other in the field.

Fusarium wilt on wild bananas

Although mainly observed on cultivated bananas, *Foc* has also been rarely recorded on wild *Musa* species (Ploetz and Pegg 2000). Waite (1954) noticed that Fusarium wilt also occurred on *M. acuminata*, *M. balbisiana*, *M. schizocarpa* and *M. textilis*. Since these specific *Musa* species belong to different sections in the genus - section *Musa* and *Callimusa* (*Australimusa*) - it is therefore likely that *Foc* can also infect other wild bananas. The current finding of a *Foc* isolate - phylogenetically situated within a *Foc*-Race 1 lineage - on a wild representative of *M. lutea*, could indicate that wild species are perhaps more susceptible to Fusarium wilt than previously assumed. Besides the visual symptoms of Fusarium wilt on this single specimen of *M. lutea*, none of the hundreds of individuals of *M. itinerans* and *M. lutea* surveyed in the same population showed any sign of *Foc* infection. This lack of visual symptoms either implies that *F. oxysporum* f. sp. *cubense* could have been absent from all those other wild accessions or that this *Fusarium* isolate related to *Foc*-Race 1 was present but failed to cause the disease in the other wild bananas. If the latter assumption is true, this could indicate that the pathogen has not necessarily co-evolved together with its host in Southeast Asia as postulated by Vakili, (1965). Nevertheless, it is evident that *F. oxysporum* is omnipresent throughout the native distribution range of the *Musa* genus, and its infections take place when the plant is weakened due to external biotic or abiotic stressors, and the endophytic equilibrium is disturbed.

The current study demonstrates that bananas in northern Viet Nam which are infected by Fusarium wilt are characterised by a various range of *Fusarium* species (*F. cugenangense*, *F. odoratissimum*, *F. duoseptatum* and *F. tardichlamydosporum*) that belong to the *Fusarium oxysporum* species complex. Of these, the latter was most commonly present in cultivated bananas infected by Fusarium wilt, whereas the other species are less prominently present, yet in equal amounts. *Fusarium tardichlamydosporum* also occurred in a wild accession of *Musa lutea*, indicating that wild bananas might function as a sink for *Foc*.

Acknowledgements

This study was funded by a bilateral grant between the Research Foundation - Flanders (FWO) and the Vietnamese National Foundation for Science and Technology Development (NAFOSTED) G0D9318N / FWO.106-NN.2017.02. This work was also supported by the University of Queensland via the Bill & Melinda Gates Foundation project ‘BBTV mitigation: Community management in Nigeria, and screening wild

banana progenitors for resistance' [OPP1130226]. We are grateful for the technical laboratory work carried out at Meise Botanic Garden by Wim Baert, Pieter Asselman, Lynn Delgat and Annelies Heylen. The authors thank all donors who supported this work, also through their contributions to the CGIAR Fund (http://www.cgiar.org/who-we-are/cgiar-fund/fund-donors-2/), and in particular to the CGIAR Research Program Roots, Tubers and Bananas (RTB-CRP).

References

Barker FK, Lutzoni FM (2002) The utility of the incongruence length difference test. Systematic Biology 51: 625–637. https://doi.org/10.1080/10635150290102302

Bentley S, Pegg KG, Moore NY, Davis RD, Buddenhagen IW (1998) Genetic variation among vegetative compatibility groups of *Fusarium oxysporum f.sp. cubense* by DNA fingerprinting. Phytopathology 88: 1283- 1293. https://doi.org/10.1094/PHYTO.1998.88.12.1283

Buddenhagen I (2009) Understanding strain diversity in *Fusarium oxysporum* f. sp. *cubense* and history of introduction of 'Tropical Race 4' to better manage banana production. In: Jones DR, Van den Bergh I (Eds) Proceedings of International ISHS-ProMusa Symposium on Recent Advances in Banana Crop Protection for Sustainable Production and Improved Livelihoods, White River, South Africa, 2007/09/10-14. Acta Horticulturae 828. ISHS, Leuven, 193–204. https://doi.org/10.17660/ActaHortic.2009.828.19

Burlakoti P, Rivera V, Secor GA, Qi A, Del Rio-Mendoza LE, Khan MFR (2012) Comparative pathogenicity and virulence of Fusarium species on sugar beet. Plant Disease 96: 1291–1296. https://doi.org/10.1094/PDIS-10-11-0908-RE

Choi J-H, Lee S, Nah J-Y, Kim H-K, Paek J-S, Lee S, Ham H, Hong SK, Yun S-H, Lee T (2018) Species composition of and fumonisin production by the Fusarium fujikuroi species complex isolated from Korean cereals. International Journal of Food Microbiology 267: 62–69. https://doi.org/10.1016/j.ijfoodmicro.2017.12.006

Crous PW, Lombard L, Sandoval-Denis M, Seifert KA, Schroers H-J, Chaverri P, Gené J, Guarro J, Hirooka Y, Bensch K, Kema GHJ, Lamprecht SC, Cai L, Rossman AY, Stadler M, Summerbell RC, Taylor JW, Ploch S, Visagie CM, Yilmaz N, Frisvad JC, Abdel-Azeem AM, Abdollahzadeh J, Abdolrasouli A, Akulov A, Alberts JF, Araújo JPM, Ariyawansa HA, Bakhshi M, Bendiksby M, Ben Hadj Amor A, Bezerra JDP, Boekhout T, Câmara MPS, Carbia M, Cardinali G, Castañeda-Ruiz RF, Celis A, Chaturvedi V, Collemare J, Croll D, Damm U, Decock CA, de Vries RP, Ezekiel CN, Fan XL, Fernández NB, Gaya E, González CD, Gramaje D, Groenewald JZ, Grube M, Guevara-Suarez M, Gupta VK, Guarnaccia V, Haddaji A, Hagen F, Haelewaters D, Hansen K, Hashimoto A, Hernández-Restr M, Houbraken J, Hubka V, Hyde KD, Iturriaga T, Jeewon R, Johnston PR, Jurjević Ž, Karalti İ, Korsten L, Kuramae EE, Kušan I, Labuda R, Lawrence DP, Lee HB, Lechat C, Li HY, Litovka YA, Maharachchiku SSN, Marin-Felix Y, Matio Kemkuigno B, Matočec N, McTaggart AR, Mlčoch P, Mugnai L, Nakashima C, Nilsson RH, Noumeur SR, Pavlov IN, Peralta MP, Phillips AJL, Pitt JI, Polizzi G, Quaedvlieg W, Rajeshkumar KC, Restrepo S, Rhaiem A, Robert J, Robert V, Rodrigues AM, Salgado-Salazar C, Sam-

son RA, Santos ACS, Shivas RG, Souza-Motta CM, Sun GY, Swart WJ, Szoke S, Tan YP, Taylor JE, Taylor PWJ, Tiago PV, Váczy KZ, van de Wiele N, van der Merwe NA, Verkley GJM, Vieira WAS, Vizzini A, Weir BS, Wijayawardene NN, Xia JW, Yáñez-Morales MJ, Yurkov A, Zamora JC, Zare R, Zhang CL, Thines M (2021) *Fusarium*: more than a node or a foot-shaped basal cell. Studies in Mycology 98: e100116. https://doi.org/10.1016/j.simyco.2021.100116

Dean R, van Kan JAL, Pretorius ZA, Hammond-Kosack KE, Di Pietro A, Spanu PD, Rudd JJ, Dickman M, Kahmann R, Ellis J, Foster GD (2012) The top 10 fungal pathogens in molecular plant pathology. Molecular Plant Pathology 13: 414–430. https://doi.org/10.1111/j.1364-3703.2011.00783.x

Dellaporta SL, Wood J, Hicks JB (1983) A plant DNA mini-preparation: version II. Plant Molecular Biology Reporter 1: 19–21. https://doi.org/10.1007/BF02712670

Dita M, Barquero M, Heck D, Mizubuti ESG, Staver CP (2018) Fusarium wilt of banana: current knowledge on epidemiology and research needs toward sustainable disease management. Frontiers in Plant Sciences 9: e1468. https://doi.org/10.3389/fpls.2018.01468

FAO (2018). Banana facts and figures. FAOSTAT EST: Banana Facts. http://www.fao.org/economic/est/est-commodities/bananas/bananafacts/en/#.W--lHTgzbIU%0A [Last accessed 01/12/2020]

Farris JD, Källersjö M, Kluge AG, Bult C (1995) Constructing a significance test for incongruence. Systematic Biology 44: 570–572. https://doi.org/10.2307/2413663

Fourie G, Steenkamp ET, Ploetz RC, Gordon TR, Viljoen A (2011) Current status of the taxonomic position of *Fusarium oxysporum* formae specialis *cubense* within the *Fusarium oxysporum* complex. Infection, Genetics and Evolution 11: 533–542. https://doi.org/10.1016/j.meegid.2011.01.012

Fraser-Smith S, Czislowski E, Meldrum RA, Zander M, Balali GR, Aitken EAB (2014) Sequence variation in the putative effector gene SIX8 facilitates molecular differentiation of *Fusarium oxysporum* f. sp. *cubense*. Plant Pathology 63: 1044–1052. https://doi.org/10.1111/ppa.12184

Garcia RO, Rivera-Vargas LI, Ploetz R, Correll JC, Irish BM (2018) Characterization of Fusarium spp. isolates recovered from bananas (Musa spp.) affected by Fusarium wilt in Puerto Rico. European Journal of Plant Pathology 2018. 152: 599–611. https://doi.org/10.1007/s10658-018-1503-y

Groenewald S, van den Berg N, Marasas WFO, Viljoen A. (2006). Biological, physiological and pathogenic variation in a genetically homogenous population of *Fusarium oxysporum f.sp. cubense*. Australian Plant Pathology 35: 401–409. https://doi.org/10.1071/AP06041

Hu L, Dou M, Xie JH, Cai SZ (2006) Progress of Banana *Fusarium* wilt resistance research. Guangxi Tropical Agriculture 1: 16–18.

Huang SP, Wei JG, Guo TX, Li QL, Tang LH, Mo J-Y, Wei J-F, Yang X-B (2019) First report of sheath rot caused by *Fusarium proliferatum* on Pisang Awak Banana (Musa ABB) in China. Journal of Plant Pathology 101:1271–1272. https://doi.org/10.1007/s42161-019-00329-z

Huang YH, Wang RC, Li CH, Zuo CW, Wei YR, Zhang L, Yi GJ (2012) Control of *Fusarium* wilt in banana with Chinese leek. European Journal of Plant Pathology 134: 87–95. https://doi.org/10.1007/s10658-012-0024-3

Hung TN, Hung, NQ, Mostert D, Viljoen A, Chao C-P, Molina G (2017). First report of *Fusarium* wilt on Cavendish bananas, caused by *Fusarium oxysporum f. sp. cubense* tropical race 4 (VCG 01213/16), in Viet Nam. Plant Disease 102: e448. https://doi.org/10.1094/PDIS-08-17-1140-PDN

Johnson LA, Soltis, DE (1998) Assessing congruence: empirical examples from molecular data. In: Molecular systematics of plants II, 297–348. Springer, Boston. https://doi.org/10.1007/978-1-4615-5419-6_11

Jones DR (2000) Diseases of banana, Abacá and Enset. CABI Publishing, Wallingford.

Katan T (1999) Current status of vegetative compatibility groups in *Fusarium oxysporum*. Phytoparasitica 27: 51–64. https://doi.org/10.1007/BF02980727

Katoh K, Misawa K, Kuma K, Miyata T (2002) MAFFT: a novel method for rapid multiple sequence alignment based on fast Fourier transform. Nucleic Acids Research 30: 3059–3066. https://doi.org/10.1093/nar/gkf436

Komada, H (1975) Development of a selective medium for quantitative isolation of Fusarium oxysporum from natural soils. Review of Plant Protection Research 8: 114–125

Li CY, Mostert G, Zuo CW, Beukes I, Yang QS, Sheng O, Kuang RB, Wei YR, Hu CH, Rose L, Karangwa P, Yang J, Deng GM, Liu SW, Gao J, Viljoen A, Yi GJ (2013) Diversity and Distribution of the Banana Wilt Pathogen *Fusarium oxysporum f. sp. cubense* in China. Fungal Genomics and Biology 3: e111.

Lima CS, Pfenning LH, Costa SS, Campos MA, Leslie JF (2009) A new Fusarium lineage within the *Gibberella fujikuroi* species complex is the main causal agent of mango malformation disease in Brazil. Plant Pathology 58: 33–42. https://doi.org/10.1111/j.1365-3059.2008.01946.x

Lin YH, Chang JY, Liu ET, Chao CP, Huang JW, Chang PFL, (2008. Development of a molecular marker for specific detection of *Fusarium oxysporum f. sp. cubense* race 4. European Journal of Plant Pathology 123: 353–365. https://doi.org/10.1007/s10658-008-9372-4

Mai Van Tri (1997) Vegetative Compatibility of isolates of *Fusarium oxysporum f. sp. cubense* in the MeKong Delta. Journal of Agriculture and Food Industry 6: 255–256.

Maldonado-Bonilla LD, MA Calderón-Oropeza, JL Villarruel-Ordaz and AC Sánchez-Espinosa (2019) Identification of novel potential causal agents of Fusarium Wilt of Musa sp. AAB in Southern México. Journal of Plant Pathology and Microbiology 10: e479. https://doi.org/10.35248/2157-7471.10.479

Maryani N, Lombard L, Poerba YS, Subandiyah S, Crous PW, Kema GHJ (2019a) Phylogeny and genetic diversity of the banana *Fusarium* wilt pathogen *Fusarium oxysporum f. sp. cubense* in the Indonesian centre of origin. Studies in Mycology 92: 155–194. https://doi.org/10.1016/j.simyco.2018.06.003

Maryani N, Sandoval-Denis M, Lombard L, Crous PW, Kema GHJ (2019b) New endemic *Fusarium* species hitch-hiking with pathogenic *Fusarium* strains causing Panama disease in smallholder banana plots in Indonesia. Persoonia 43: 48–69. https://doi.org/10.3767/persoonia.2019.43.02

Moore NY, Bentley S, Smith LJ (2001) *Fusarium* wilt of banana: global problems and perspectives. In: Molina AB, Nik Masdek NNH, Liew KW (Eds) Banana Fusarium wilt management: Towards sustainable cultivation. INIBAP, Los Baños, 11-30.

Mostert D, Molina AB, Daniells J, Fourie G, Hermanto C, Chao CP, Fabreagr E, Sinohin VG, Masdek N, Thangvelu R, Li C, Yi G, Mostert L, Viljoen A (2017) The distribution and host range of the banana *Fusarium* wilt fungus, *Fusarium oxysporum f. sp. cubense*, in Asia. PLoS ONE 12: e0181630. https://doi.org/10.1371/journal.pone.0181630

Nirenberg HI (1981) A simplified method for identifying Fusarium spp. occurring on wheat Canadian Journal of Botany 59: 1599–1609. https://doi.org/10.1139/b81-217

O'Donnell K, Cigelnik E (1997) Two divergent intra-genomic rDNAITS2 types with in a monophyletic lineage are non-orthologous. Molecular Phylogenetics and Evolution 7: 103–116. https://doi.org/10.1006/mpev.1996.0376

O'Donnell K, Gueidan C, Sink S, Johnston PR, Crous PW, Glenn A, Riley R Zitomer NC, Colyer P, Waalwijk C, van der Lee T, Moretti A, Kang S,Kim H-S, Geiser DM, Juba JH, Baayen RP, Cromey MG, Bithell S, Sutton DA, Skovgaard K, Ploetz R, Kistler HC, Elliott M, Davis M, Sarver BAJ (2009) A two-locus DNA sequence database for typing plant and human pathogens within the *Fusarium oxysporum* species complex. Fungal Genetics and Biology 46: 936–948. https://doi.org/10.1016/j.fgb.2009.08.006

O'Donnell K, Kistler HC, Cigelnik E, Ploetz RC (1998) Multiple evolutionary origins of the fungus causing Panama disease of banana: concordant evidence from nuclear and mitochondrial gene genealogies. Proceedings of the National Academy of Science USA 95: 2044–2049. https://doi.org/10.1073/pnas.95.5.2044

O'Donnell K, Sutton DA, Rinaldi MG, Sarver BAJ, Balajee SA, Schroers H-J, Summerbell RC, Robert VARG, Crous PW, Zhang N, Aoki T, Jung K, Park J, Lee Y-H, Kang S, Park B, Geiser DM (2010) An internet-accessible DNAsequence database for identifying fusaria from human and animal infections. Journal of Clinical Microbiology 48: 3708–3718. https://doi.org/10.1128/JCM.00989-10

Ordonez N, Seidl MF, Waalwijk C, Drenth A, Kilian A, Thomma BPHJ, Ploetz RC, Kema G (2015) Worse comes to worst: bananas and Panama disease - when plant and pathogen clones meet. PLoS Pathogen 11: e1005197. https://doi.org/10.1371/journal.ppat.1005197

Pegg KG, Coates LM, O'Neill WT, Turner DW (2019) The epidemiology of Fusarium wilt of banana. Frontiers in Plant Sciences 10: 1395. https://doi.org/10.3389/fpls.2019.01395

Pérez-Vicente L, Dita MA, Martínez-de la Parte E (2014) Technical Manual Prevention and diagnostic of Fusarium Wilt (Panama disease) of banana caused by *Fusarium oxysporum f. sp. cubense* Tropical Race 4 (TR4). FAO, Rome.

Pérez L, Batlle A, Fonseca J (2003) *Fusarium oxysporum* f. sp. *cubense* en Cuba: biología de las poblaciones, reacción de los clones híbridos de la FHIA y biocontrol. En: Memorias del Taller "Manejo convencional y alternativo de la Sigatoka negra, nematodos y otras plagas asociadas al cultivo de Musáceas" Rivas, G. y Rosales, F (Eds) Guayaquil, Ecuador, 11- 13 de Agosto. Pp: 141–155.

Pirie MD (2015) Phylogenies from concatenated data: Is the end nigh? Taxon 64: 421–423. https://doi.org/10.12705/643.1

Ploetz RC (2005) Panama disease: An old nemesis rears its ugly head part 2. The Cavendish era and beyond. Plant Health Progress 23: 1–17. https://doi.org/10.1094/APSnetFeature-2005-1005

Ploetz, RC (2015a) *Fusarium* wilt of banana. Phytopathology 105: 1512–1521. https://doi.org/10.1094/PHYTO-04-15-0101-RVW

Ploetz, RC. (2015b) Management of Fusarium wilt of banana: a review with special reference to tropical race 4. Crop Protection 73: 7–15. https://doi.org/10.1016/j.cropro.2015.01.007

Ploetz RC, Pegg K (1997) *Fusarium* wilt of banana and Wallace's line: was the disease originally restricted to his Indo-Malayan region? Australasian Plant Pathology 26: 239–249. https://doi.org/10.1071/AP97039

Ploetz RC, Pegg, KG (2000) Fusarium wilt. In: Jones DR (Ed.) Diseases of Banana, Abaca and Enset. CABI Publishing, Wallingford, 143–159.

Ploetz RC (2009) Assessing threats posed by destructive banana pathogens. In: Jones DR, Van den Bergh I (Eds) Proceedings of International ISHS-ProMusa Symposium on Recent Advances in Banana Crop Protection for Sustainable Production and Improved Livelihoods, White River, South Africa, 2007/09/10-14. Acta Horticulturae 828. ISHS, Leuven, 245–252. https://doi.org/10.17660/ActaHortic.2009.828.25

Posada D (2008) jModelTest: phylogenetic model averaging. Molecular Biology and Evolution 25: 1253–1256. https://doi.org/10.1093/molbev/msn083

Rambaut A, Drummond AJ (2007) Tracer v1.4 (http:// beast.bio.ed.ac.uk/Tracer)

Rayner RW (1970) A Mycological Colour Chart. Commonwealth Mycological Institute & British Mycological Society, Kew.

Ronquist F, Huelsenbeck JP (2003) Mr. Bayes 3: Bayesian phylogenetic inference under mixed models. Bioinformatics 19: 1572–1574. https://doi.org/10.1093/bioinformatics/btg180

Ronquist F, Teslenko M, van der Mark P, Ayres DL, Darling A, Höhna S, Larget B, Liu L, Suchard MA, Huelsenbeck JP (2012) MrBayes 3.2: efficient Bayesian phylogenetic inference and model choice across a large model space. Systematic Biology 61: 539–542. https://doi.org/10.1093/sysbio/sys029

Scheerer L, Pemsl D, Dita M, Perez-Vicente L, Staver C (2018) A quantified approach to projecting losses caused by *Fusarium* Wilt Tropical Race 4. Acta Horticulturae, 1196: 211–218. https://doi.org/10.17660/ActaHortic.2018.1196.26

Stamatakis A (2014) RAxML Version 8: A tool for Phylogenetic Analysis and Post-Analysis of Large Phylogenies. Bioinformatics 30: 1312–1313. https://doi.org/10.1093/bioinformatics/btu033

Stover RH (1962a) *Fusarium* wilt (Panama disease) of Bananas and Other *Musa* Species. Commonwealth Mycological Institute, Kew.

Stover RH (1962b) Studies on *Fusarium* wilt of bananas: VIII. Differentiation of clones by cultural interaction and volatile substances. Canadian. Journal of Botany 40: 1467–1471. https://doi.org/10.1139/b62-142

Stover RH, Simmonds NW (1987) Bananas, 3rd edn. Longmans, London.

Suzuki Y, Glazko GV, Nei M (2002) Over credibility of molecular phylogenies obtained by Bayesian phylogenetics. Proceedings of the National Academy of Science USA 99: 16138–16143. https://doi.org/10.1073/pnas.212646199

Swofford DL (2003) PAUP*: Phylogenetic Analysis Using Parsimony (*and Other Methods), Version 4. Sunderland, MA: Sinauer Associates

Vakili N, Thai LV, Dinh VN (1968) Chuoi Viet Nam - Phuong phap trong tia, cai thien. Vien khao nghien cuu Nong nghiep Saigon.

Vakili NG (1965) Fusarium wilt resistance in seedlings and mature plants of Musa species. Phytopathology 55: 135–140.

Van Hove F, Waalwijk C, Logrieco A, Munaut F, Moretti A (2011) *Gibberella musae* (*Fusarium musae*) sp. nov.: a new species from banana is sister to *F. verticillioides*. Mycologia 103: 570–585. https://doi.org/10.3852/10-038

Vinh DN, Khiem NV, Phuc CB, Ham LH (2001) Vegetative compatibility groups of the populations of *Fusarium oxysporum f. sp. cubense* in Viet Nam. Infomusa 10: 32–33.

Waite BH (1963) Wilt of *Heliconia* spp. caused by *Fusarium oxysporum f. sp. cubense* race 3. Tropical Agriculture Trinidad 40: 299–305.

Wulff EG, Sorensen JL, Lubeck M, Nielsen KF, Thrane U, Torp J (2010) Fusarium spp. associated with rice Bakanae: ecology, genetic diversity, pathogenicity and toxigenicity. Environmental Microbiology 12: 649–657. https://doi.org/10.1111/j.1462-2920.2009.02105.x

Zheng SJ, García-Bastidas FA, Li X, Zeng L, Bai T, Xu S, Yin K, Fu H, Yu Y, Yang L, Nguyen HC, Douangboupha B, Khaing AA, Drenth A, Seidl MF, Meijer HJG, Kema GHJ (2018) New geographical insights of the latest expansion of Fusarium oxysporum f. sp. cubense tropical race 4 into the greater Mekong subregion. Frontiers in Plant Sciences 9: e457. https://doi.org/10.3389/fpls.2018.00457

Supplementary material 1

Table S1

Authors: Loan Le Thi, Arne Mertens, Dang Toan Vu, Dang Tuong Vu, Pham Le Anh Minh, Huy Nguyen Duc, Sander de Backer, Rony Swennen, Filip Vandelook, Bart Panis, Mario Amalfi, Cony Decock, Sofia I.F. Gomes, Vincent S.F.T. Merckx, Steven B. Janssens

Data type: Docx file.

Explanation note: List of accessions used for the phylogenetic analyses, including voucher information and GenBank numbers. Asterisks indicate accessions for which new sequences were generated in the current study.

Link: https://doi.org/10.3897/mycokeys.87.72941.suppl1

MycoKeys 87: 77–98 (2022)
doi: 10.3897/mycokeys.87.79433
https://mycokeys.pensoft.net

RESEARCH ARTICLE

A peer-reviewed open-access journal
MycoKeys
Launched to accelerate biodiversity research

Pleocatenata chiangraiensis gen. et. sp. nov. (Pleosporales, Dothideomycetes) from medicinal plants in northern Thailand

Ya-Ru Sun[1,2,3], Ning-Guo Liu[2,5], Kevin D. Hyde[2,3,4], Ruvishika S. Jayawardena[2,3], Yong Wang[1]

1 *Department of Plant Pathology, College of Agriculture, Guizhou University, Guiyang 550025, China* **2** *Center of Excellence in Fungal Research, Mae Fah Luang University, Chiang Rai 57100, Thailand* **3** *School of Science, Mae Fah Luang University, Chiang Rai 57100, Thailand* **4** *Innovative Institute of Plant Health, Zhongkai University of Agriculture and Engineering, Haizhu District, Guangzhou 510000, China* **5** *School of Life Science and Technology, Center for Informational Biology, University of Electronic Science and Technology of China, Chengdu 611731, China*

Corresponding author: Yong Wang (yongwangbis@aliyun.com)

Academic editor: Nalin Wijayawardene | Received 16 December 2021 | Accepted 19 January 2022 | Published 11 February 2022

Citation: Sun Y-R, Liu N-G, Hyde KD, Jayawardena RS, Wang Y (2022) *Pleocatenata chiangraiensis* gen. et. sp. nov. (Pleosporales, Dothideomycetes) from medicinal plants in northern Thailand. MycoKeys 87: 77–98. https://doi.org/10.3897/mycokeys.87.79433

Abstract

Pleocatenata, a new genus, is introduced with its type species, *Pleocatenata chiangraiensis*, which was isolated from withered twigs of two medicinal plants, *Clerodendrum quadriloculare* (Blanco) Merr (Verbenaceae) and *Tarenna stellulata* (Hook.f.) Ridl (Rubiaceae) in northern Thailand. The genus is characterized by mononematous, septate, brown or dark brown conidiophores, monotretic conidiogenous cells and catenate, obclavate, olivaceous to blackish brown conidia. Phylogenetic analysis of combined LSU, SSU, *tef1-α*, *rpb2* and ITS sequence data showed *Pleocatenata* forms a distinct phylogenetic lineage in Pleosporales, Dothideomycetes. Therefore, we treat *Pleocatenata* as Pleosporales genera *incertae sedis* based on morphology and phylogenetic analyses. Descriptions and illustrations of the new taxa are provided, and it is compared with morphologically similar genera.

Keywords

Genera *incertae sedis*, hyphomycetes, multi-gene phylogeny, taxonomy

Introduction

Medicinal plants are a rich source of natural products with biological and chemical properties. They are used in health care or treatment of human ailments and have been used since prehistoric times worldwide (Rasool-Hassan 2012). Many fungi have been found on medicinal plants and are members of Dothideomycetes and Sordariomycetes (Bhagat et al. 2012; Long et al. 2019; Ma et al. 2019; Hyde et al. 2020; Tennakoon et al. 2021). They form important associations with medicinal plants and as pathogens or saprobes (Long et al. 2019; Tennakoon et al. 2021), sources of medicines (Strobel et al. 1993; Huang et al. 2008; Hyde et al. 2019), involved in nutrient recycling (Bonnardeaux et al. 2007) and some are used in biological control (Hyde et al. 2019).

Pleosporales is the largest order in Dothideomycetes, which accounts for about a quarter of the class (Zhang et al. 2012; Hyde et al. 2013; Hongsanan et al. 2020a). They have a worldwide distribution with diverse lifestyles, including saprobes, pathogens of plants and humans, endophytes, epiphytes and hyperparasites (Ramesh 2003; Kirk et al. 2008; Zhang et al. 2012; Hyde et al. 2013; Sun et al. 2019; Ferdinandez et al. 2021). Many species in *Alternaria* Nees, *Curvularia* Boedijn and *Corynespora* Güssow, can invade medicinal plants and cause leaf spots and other diseases, as economically important plant pathogens (Mathiyazhagan et al. 2004; Abtahi and Nourani 2017; Zhang et al. 2020), and some also pose a threat to human health (Hyde et al. 2018; Iturrieta-González et al. 2020). Endophytes in Pleosporales also show important biocontrol value (Su et al. 2014; De Silva et al. 2019; Hyde et al. 2019), for example, an extract from *Cochliobolus spicifer* R.R. Nelson has mosquito-larvicidal activity (Abutaha et al. 2015).

The sexual morph of Pleosporales is characterized by uniloculate ascomata typically with papillae, ostioles and pseudoparaphyses, generally fissitunicate asci bearing mostly septate ascospores of different colours and shapes (Ramesh 2003; Kirk et al. 2008; Zhang et al. 2012; Hyde et al. 2013). Coelomycetes and hyphomycetes are the asexual morphs of pleosporalean taxa (Zhang et al. 2012; Hongsanan et al. 2020a). Recent comprehensive studies on Dothideomycetes treated 91 families in Pleosporales (Hongsanan et al. 2020a). More than 40 genera are recognized as genera *incertae sedis* in Pleosporales (Hongsanan et al. 2020a; Wijayawardene et al. 2020, 2021). This uncertainty in genetic placement occurs for the following reasons: 1) some genera lack sufficient collections even though molecular data is available, they are not included in any families in phylogenetic analyses, eg. *Aegeanispora* E.B.G. Jones & Abdel-Wahab, *Antealophiotrema* A. Hashim. & Kaz. Tanaka and *Perthomyces* Crous (Li et al. 2016; Abdel-Wahab et al. 2017; Crous et al. 2017); 2) due to the diverse morphology of hyphomycetous asexual morphs, it is difficult to determine their familial placement without the sexual morph and molecular data. Examples are *Briansuttonia* R.F. Castañeda, Minter & Saikawa, *Cheiromoniliophora* Tzean & J.L. Chen, *Dangeardiella* Sacc. & P. Syd and *Pleosphaerellula* Naumov & Czerepan (Obrist 1959; Tóth 1975; Tzean and Chen 1990; Castañeda-Ruiz et al. 2004).

During the examination of collections from medicinal plants in northern Thailand (Sun et al. 2021), two isolates representing a new species were obtained from

Clerodendrum quadriloculare and *Tarenna stellulata.* Morphology and phylogenetic analyses confirmed that it was distinct in Pleosporales, but its familial placement was uncertain. Thus, we introduced a new genus, *Pleocatenata* (Pleosporales, genera *incertae sedis*) to accommodate the new species, *P. chiangraiensis*.

Materials and methods

Collection, examination and isolation

The isolates used in this study were collected from decaying twigs of *Clerodendrum quadriloculare* and *Tarenna stellulata* from Mae Fah Luang University, Chiang Rai, Thailand during June to July 2020 in terrestrial habitat. The samples were packaged in envelopes and returned to the laboratory as described in Senanayake et al. (2020). The fruiting bodies on natural substrates were observed and photographed using a stereo-microscope (SteREO Discovery, V12, Carl Zeiss Microscopy GmBH, Germany). Morphological characters were observed using a Nikon ECLIPSE Ni compound microscope (Nikon, Japan) and photographed with a Nikon DS-Ri2 digital camera (Nikon, Japan). The Adobe Photoshop CS6 Extended v. 13.0 software was used to make photo-plates. Measurements were done with the Tarosoft (R) Image Frame Work software.

Single spore isolations were used to obtain pure cultures following the methods described by Senanayake et al. (2020). Germinated conidia were transferred to new potato dextrose agar (PDA) plates and incubated at 26 °C for four weeks. The pure cultures obtained were deposited in Mae Fah Luang University Culture Collection (MFLUCC), Chiang Rai, Thailand. Herbaria materials were deposited in the herbarium of Mae Fah Luang University (MFLU), Chiang Rai, Thailand. Facesoffungi (FoF) and Index Fungorum numbers were acquired as described in Jayasiri et al. (2015) and Index Fungorum (2022).

DNA extraction, PCR amplification and sequencing

Fresh fungal mycelia grown on PDA medium for 4 weeks at 26 °C were scraped with a sterile scalpel. Genomic DNA was extracted from scraped mycelia using the BIOMIGA Fungus Genomic DNA Extraction Kit (GD2416, BIOMIGA, San Diego, California, USA) following the manufacture's protocol. Five genes were selected in this study: the 28S subunit rDNA (LSU), the 18S subunit rDNA (SSU), the internal transcribed spacers (ITS), the translation elongation factor 1 (*tef1-α*), and the RNA polymerase II subunit 2 (*rpb2*). Polymerase chain reaction (PCR) was carried out in 20 µL reaction volume which contained 10 µL 2 × PCR Master Mix, 7 µL ddH_2O, 1 µL of each primer, and 1 µL template DNA. The PCR thermal cycle program and primers are given (Table 1). Purification and sequencing of PCR products were carried out at SinoGenoMax (Beijing) Co., China.

Table 1. Primers and PCR procedures used in this study.

Locus	Primers		PCR procedures	References
	Name	Sequence (5'–3')		
Large subunit (LSU)	LR0R	ACCCGCTGAACTTAAGC	94 °C 3 min; 35 cycles of 94 °C 30 s, 52 °C 30 s, 72 °C 1 min; 72 °C 8 min; 4 °C on hold	Vilgalys and Hester (1990), Rehner and Samuels (1994)
	LR5	TCCTGAGGGAAACTTCG		
Small subunit (SSU)	NS1	GTAGTCATATGCTTGTCTC		White et al. (1990)
	NS4	CTTCCGTCAATTCCTTTAAG		
Internal transcribed spacer (ITS)	ITS5	GGAAGTAAAAGTCGTAACAAGG		
	ITS4	TCCTCCGCTTATTGATATGC		
Elongation factor-1 alpha (*tef1-α*)	EF1-983F	GCYCCYGGHCAYCGTGAYTTYAT	94 °C 2 min; 36 cycles of 66 °C – 56 °C (touchdown 9 cycles), 94 °C 30 sec, 56 °C 1 min, 72 °C 1 min; 72 °C 10 min; 4 °C on hold	Rehner and Buckley (2005)
	EF1-2218R	ATGACACCRACRGCRACRGTYTG		
RNA polymerase II subunit (*rpb2*)	fRPB2-5F	GAYGAYMGWGATCAYTTYGG	94 °C 3 min; 40 cycles of 94 °C 20 sec, 55 °C 30 sec, 72 °C 1 min; 72 °C 10 min; 4 °C on hold	Liu et al. 1999
	fRPB2-7cR	CCCATRGCTTGYTTRCCCAT		

Phylogenetic analyses

BLASTn (https://blast.ncbi.nlm.nih.gov//Blast.cgi) was used to evaluate closely related strains to our new taxa. Other sequences used in this study were obtained from GenBank referring to Zhang et al. (2012, 2018) and Hongsanan et al. (2020a, 2021) (Table 2). The single gene sequences were viewed using BioEdit v. 7.0.9.0 (Hall 1999). Alignments for each locus were generated with MAFFT v.7 (https://mafft.cbrc.jp/alignment/server/) and manually improved using AliView (Larsson 2014) for maximum alignment and minimum gaps. The final single gene alignments were combined by SequenceMatrix 1.7.8 (Vaidya et al. 2011).

The single locus and combined analyses were carried out for maximum likelihood (ML) and Bayesian posterior probability (BYPP). The ML analyses were carried out using IQ-TREE (Nguyen et al. 2015; Trifinopoulos et al. 2016) on the IQ-TREE web server (http://iqtree.cibiv.univie.ac.at, 30 September 2021) under partitioned models. The best-fit substitution models were determined by WIQ-TREE (Chernomor et al. 2016): SYM+I+G4 for LSU and SSU; TIM+F+I+G4 for *tef1-α*; GTR+F+I+G4 for *rpb2*; TIM2+F+I+G4 for ITS. Ultrafast bootstrap analysis was implemented with 1,000 replicates (Minh et al. 2013; Hoang et al. 2018).

The BYPP analyses were performed in CIPRES (Miller et al. 2010) with MrBayes on XSEDE 3.2.7a (Ronquist et al. 2012). The best nucleotide substitution model for each data partition was evaluated by MrModeltest 2.2 (Nylander 2004). The substitution model GTR+I+G was decided for LSU, SSU, ITS, *tef1-α* and *rpb2* sequences. The Markov chain Monte Carlo (MCMC) sampling approach was used to calculate posterior probabilities (PP) (Rannala and Yang 1996). Six simultaneous Markov chains were run for 10 million generations and trees were sampled every 1,000th generation. The first 20% of trees, representing the burn-in phase of the analyses, were discarded and the remaining trees were used for calculating posterior probabilities (PP) in the majority rule consensus tree.

Table 2. Taxa of Pleosporales used in the phylogenetic analysis with the corresponding GenBank accession numbers. The newly generated strains are indicated in bold. N/A: Not available.

Species names	Strain number	LSU	SSU	ITS	*tef1-α*	*rpb2*
Acrocalymma aquatica	MFLUCC 11-0208	JX276952	JX276953	JX276951	N/A	N/A
Acrocalymma pterocarpi	MFLUCC 17-0926	MK347949	MK347840	MK347732	MK360040	N/A
Acuminatispora palmarum	MFLUCC 18-0264	MH390437	MH390401	NR_163327	MH399248	N/A
	MFLUCC 18-0460	MH390438	MH390402	MN749106	MH399249	N/A
Aigialus grandis	BCC 20000	GU479775	GU479739	N/A	GU479839	N/A
Alternaria alternata	AFTOL ID-1610	DQ678082	KC584507	KF465761	KC584634	KC584375
Amniculicola aquatica	MFLUCC 16-1123	MK106096	MK106108	N/A	MK109800	N/A
Amorocoelophoma cassia	MFLUCC 17-2283	MK347956	NG_065775	MK347739	MK360041	MK434894
Angustimassarina lonicerae	MFLUCC 15-0087	KY496724	N/A	KY496759	N/A	N/A
Anteaglonium parvulum	SMH5223	GQ221909	N/A	N/A	GQ221918	N/A
Aquasubmersa japonica	HHUF 30469	NG_057138	NG_062426	NR_154739	LC194384	LC194421
Aquasubmersa mircensis	MFLUCC 11-0401	NG_042699	NG_061141	JX276954	N/A	N/A
Ascocylindrica marina	MD6011	KT252905	KT252907	N/A	N/A	N/A
	MF416	MK007123	MK007124	N/A	N/A	N/A
Astragalicola vasilyevae	MFLUCC 17-0832	MG828986	MG829098	NR_157504	MG829193	MG829248
Astrosphaeriella fusispora	MFLUCC 10-0555	KT955462	KT955443	N/A	KT955425	KT955413
Atrocalyx acutisporus	KT 2436	LC194341	LC194299	LC194475	LC194386	LC194423
Bahusandhika indica	GUFCC 18001	KF460274	N/A	KF460273	N/A	N/A
Bambusicola bambusae	MFLUCC 11-0614	JX442035	JX442039	JX442031	N/A	KP761718
Berkleasmium crunisia	BCC 17023	DQ280271	N/A	DQ280265	N/A	N/A
Berkleasmium typhae	BCC 12536	DQ280275	N/A	DQ280264	N/A	N/A
Brevicollum hyalosporum	MFLUCC 17-0071	MG602200	MG602202	MG602204	MG739516	N/A
Brevicollum versicolor	HHUF 30591	NG_058716	NG_065124	NR_156335	LC271246	LC271250
Camarosporidiella caraganicola	MFLUCCC 14-0605	KP711381	KP711382	KP711380	N/A	N/A
Camarosporium quaternatum	CPC 31081	NG_064442	KY929123	NR_159756	KY929201	N/A
Camarosporomyces flavigenus	CBS 314.80	GU238076	NG_061093	MH861266	N/A	N/A
Coniothyrium palmarum	CBS 400.71	JX681084	EU754054	MH860184	N/A	KT389592
Corynespora cassiicola	CBS 100822	GU301808	GU296144	N/A	GU349052	GU371742
Corynespora torulosa	CPC 15989	KF777207	N/A	NR_145181	N/A	N/A
Crassiperidium octosporum	MAFF 246406	LC373116	LC373092	LC373104	LC373128	LC373140
Cryptocoryneum japonicum	HHUF 30482	NG_059035	NG_065118	NR_153938	LC096144	LC194438
Cryptocoryneum pseudorilstonei	CBS 113641	NG_059036	LC194322	NR_153941	LC096152	LC194446
Cucurbitaria berberidis	MFLUCC 11-0387	KC506796	KC506800	N/A	N/A	N/A
Cyclothyriella rubronotata	CBS 141486	KX650544	NG_061252	NR_147651	KX650519	KX650574
Cylindroaseptospora leucaenicola	MFLUCC 17-2424	MK347966	MK347856	NR_163333	MK360047	N/A
Dacampia engeliana	Hafellner 72868	KT383791	N/A	N/A	N/A	N/A
Dacampia hookeri	Hafellner 73897	KT383792	N/A	N/A	N/A	N/A
Delitschia chaetomioides	SMH 3253.2	GU390656	N/A	N/A	GU327753	N/A
Delitschia winteri	AFTOL ID-1599	DQ678077	DQ678026	N/A	DQ677922	DQ677975
Dendryphion fluminicola	MFLUCC 17-1689	MG208141	N/A	NR_157490	MG207992	N/A
Dictyocheirospora bannica	KH 332	AB807513	AB797223	LC014543	AB808489	N/A
Dictyosporium elegans	NBRC 32502	DQ018100	DQ018079	DQ018087	N/A	N/A
Didymella exigua	CBS 183.55	MH868977	GU296147	MH857436	N/A	N/A
Didymella rumicicola	CBS 683.79	MH873007	N/A	KT389503	N/A	KT389622
Didymosphaeria rubi-ulmifolii	MFLUCC 14-0023	KJ436586	KJ436588	MK646049	N/A	N/A
Dimorphosporicola tragani	CBS 570.85	KU728536	N/A	KU728497	N/A	N/A
Dothidotthia aceris	MFLUCC 16-1183	MK751816	MK751761	MK751726	N/A	N/A
Fissuroma calami	MFLUCC 13-0836	MF588993	NG_062430	N/A	MF588975	N/A
Flammeascoma bambusae	MFLU 11-0143	NG_059553	KP753952	NR_132915	N/A	N/A
Flavomyces fulophazii	CBS 135761	NG_058131	NG_061191	NR_137960	N/A	N/A
Foliophoma fallens	CBS 161.78	GU238074	GU238215	KY940772	N/A	KC584502
	CBS 284.70	GU238078	GU238218	MH859609	N/A	N/A
Fuscostagonospora cytisi	MFLUCC 16-0622	KY770978	KY770977	N/A	KY770979	N/A

Species names	Strain number	LSU	SSU	ITS	*tef1-α*	*rpb2*
Fuscostagonospora sasae	HHUF 29106	AB807548	AB797258	AB809636	AB808524	N/A
Fusculina eucalypti	CBS 120083	DQ923531	N/A	DQ923531	N/A	N/A
Fusculina eucalyptorum	CBS 145083	MK047499	N/A	NR_161140	N/A	N/A
Halojulella avicenniae	BCC 20173	GU371822	GU371830	N/A	GU371815	GU371786
Halotthia posidoniae	BBH 22481	GU479786	GU479752	N/A	N/A	N/A
Hazslinszkyomyces aloes	CBS 136437	KF777198	N/A	KF777142	N/A	N/A
Helminthosporium velutinum	L131	KY984352	KY984432	KY984352	KY984463	KY984413
Hermatomyces iriomotensis	HHUF 30518	LC194367	LC194325	LC194483	LC194394	LC194449
Hermatomyces tectonae	MFLUCC 14-1140	KU764695	KU712465	KU144917	KU872757	KU712486
Hypsostroma caimitalense	GKM1165	GU385180	N/A	N/A	N/A	N/A
Hypsostroma saxicola	SMH5005	GU385181	N/A	N/A	N/A	N/A
Hysterium angustatum	CBS 123334	FJ161207	N/A	N/A	N/A	N/A
Hysterobrevium smilacis	CBS 114601	FJ161174	FJ161135	N/A	FJ161091	FJ161114
Latorua caligans	CBS 576.65	NG_058180	N/A	N/A	N/A	N/A
Latorua grootfonteinensis	CBS 369.72	NG_058181	N/A	N/A	N/A	N/A
Lentimurispora urniformis	MFLUCC 18-0497	MH179144	MH179160	N/A	MH188055	N/A
Lentithecium clioninum	HHUF 28199	NG_059391	NG_064845	NR_154137	AB808515	N/A
Lentithecium pseudoclioninum	HHUF 29055	NG_059392	NG_064847	AB809633	AB808521	N/A
Lepidosphaeria nicotiae	AFTOL ID-1576	DQ678067	N/A	N/A	DQ677910	DQ677963
Leptosphaeria cichorium	MFLUCC 14-1063	KT454712	KT454728	KT454720	N/A	N/A
Leucaenicola phraeana	MFLUCC 18-0472	MK348003	NG_065784	MK347785	MK360060	MK434867
Libertasomyces myopori	CPC 27354	NG_058241	N/A	KX228281	N/A	N/A
Ligninsphaeria jonesii	MFLUCC 15-0641	NG_059642	N/A	N/A	N/A	N/A
Lindgomyces cigarospora	G619	KX655804	KX655805	KX655794	N/A	N/A
Lindgomyces ingoldianus	ATCC 200398	AB521736	NG_016531	NR_119938	N/A	N/A
Longiostiolum tectonae	MFLUCC 12-0562	KU764700	N/A	KU712447	N/A	N/A
Longipedicellata aptrootii	MFLU 10-0297	KU238894	KU238895	KU238893	KU238892	KU238891
Lophiostoma macrostomum	KT508	AB619010	AB618691	N/A	LC001751	N/A
Lophiotrema eburnoides	KT 1424.1	LC001707	LC001706	LC001709	LC194403	LC194458
Macrodiplodiopsis desmazieri	CBS 140062	NG_058182	N/A	NR_132924	N/A	N/A
Massaria anomia	CBS 59178	GU301839	GU296169	N/A	N/A	GU371769
Massaria inquinans	M19	N/A	HQ599444	HQ599402	HQ599342	HQ599460
Melanomma japonicum	MAFF 239634	NG_060360	NG_065122	NR_154215	LC203367	LC203395
Melanomma pulvis pyrius	CBS 124080	MH874873	GU456302	MH863349	GU456265	GU456350
Misturatosphaeria aurantonotata	GKM 1238	NG_059927	N/A	N/A	GU327761	N/A
Morosphaeria muthupetensis	NFCCI4219	MF614796	MF614797	MF614795	MF614798	N/A
Morosphaeria velatispora	KH221	AB807556	AB797266	LC014572	AB808532	N/A
Multilocularia bambusae	MFLUCC 11-0180	KU693438	KU693442	KU693446	N/A	N/A
Murispora galii	MFLUCC 13-0819	KT709175	KT709182	KT736081	KT709189	N/A
Neocamarosporium goegapense	CPC 23676	KJ869220	N/A	KJ869163	N/A	N/A
Neoconiothyrium persooniae	CBS 143175	MG386094	N/A	MG386041	N/A	N/A
Neomassaria fabacearum	MFLUCC 16-1875	KX524145	NG_061245	N/A	KX524149	N/A
Neomassaria formosana	NTUCC 17-007	MH714756	MH714759	N/A	MH714762	MH714765
Neomassarina thailandica	MFLU 11-0144	NG_059718	N/A	NR154244	N/A	N/A
	MFLUCC 17-1432	MT214467	MT214420	MT214373	N/A	N/A
Neopaucispora rosaecae	MFLUCC 17-0807	MG829033	NG_061293	MG828924	MG829217	N/A
Neophaeosphaeria agaves	CPC 21264	KF777227	N/A	KF777174	N/A	N/A
Neophaeosphaeria filamentosa	CBS 102202	GQ387577	GQ387516	JF740259	GU349084	GU371773
Neophaeosphaeria phragmiticola	KUMCC 16-0216	MG837009	NG_065735	N/A	MG838020	N/A
Neoplatysporoides aloes	CPC 36068	MN567619	N/A	NR_166316	N/A	N/A
Neopyrenochaeta cercidis	MFLUCC 18-2089	MK347932	MK347823	MK347718	N/A	MK434908
Neopyrenochaetopsis hominis	UTHSC DI16 238	LN907381	N/A	LT592923	N/A	LT593061
Neoroussoella bambusae	MFLUCC 11-0124	KJ474839	N/A	KJ474827	KJ474848	KJ474856
Neotestudina rosatii	CBS 690.82	DQ384107	DQ384069	N/A	N/A	N/A
Neoyrenochaeta acicola	CBS 812.95	GQ387602	GQ387541	NR_160055	N/A	LT623271
Nigrograna fuscidula	CBS 141556	KX650550	N/A	NR_147653	KX650525	N/A

Species names	Strain number	LSU	SSU	ITS	*tef1-α*	*rpb2*
Nigrograna mackinnonii	CBS 674.75	GQ387613	NG_061081	NR_132037	KF407986	KF015703
Occultibambusa bambusae	MFLUCC 13-0855	KU863112	N/A	KU940123	KU940193	KU940170
Occultibambusa jonesii	GZCC 16-0117	KY628322	KY628324	N/A	KY814756	KY814758
Parabambusicola bambusina	KH 139	AB807537	AB797247	LC014579	AB808512	N/A
Paradictyoarthrinium aquatica	MFLUCC 16-1116	NG_064501	N/A	NR_158861	N/A	N/A
Paradictyoarthrinium diffractum	MFLUCC 13-0466	KP744498	KP753960	KP744455	N/A	KX437764
Paralophiostoma hysterioides	PUFNI 17617	MT912850	MN582762	MN582758	N/A	MT926117
Parapyrenochaeta protearum	CBS 131315	JQ044453	N/A	JQ044434	N/A	LT717683
Periconia delonicis	MFLUCC 17-2584	NG_068611	NG_065770	N/A	N/A	MK434901
Periconia pseudodigitata	KT 1395	AB807564	AB797274	LC014591	N/A	N/A
Phaeoseptum mali	MFLUCC 17-2108	MK625197	N/A	MK659580	MK647990	MK647991
Phaeoseptum terricola	MFLUCC 10-0102	MH105779	MH105780	MH105778	MH105781	MH105782
Phaeosphaeria oryzae	CBS 110110	KF251689	GQ387530	KF251186	N/A	KF252193
Phaeosphaeriopsis triseptata	MFLUCC 13-0271	KJ522479	KJ522484	KJ522475	MG520919	KJ522485
Plenodomus salvia	MFLUCC 13-0219	KT454717	KT454732	KT454725	N/A	N/A
Pleocatenatium chiangraiense	**MFLUCC 21-0222**	**OL986398**	**N/A**	**OL986396**	**OM240638**	**OM117709**
	MFLUCC 21-0223	**OL986399**	**N/A**	**OL986397**	**OM240637**	**OM117708**
Pleohelicoon richonis	CBS 282.54	N/A	AY856952	MH857332	N/A	N/A
Pleomonodictys descalsii	FMR 12716	KY853522	N/A	KY853461	N/A	N/A
Preussia funiculate	CBS 659.74	GU301864	GU296187	N/A	GU349032	GU371799
Pseudoastrosphaeriella longicolla	MFLUCC 11-0171	KT955476	N/A	N/A	KT955438	KT955420
Pseudoastrosphaeriella thailandensis	MFLUCC 11-0144	KT955478	KT955457	N/A	KT955440	KT955416
Pseudoberkleasmium chiangmaiense	MFLUCC 17-1809	MK131260	N/A	MK131259	MK131261	N/A
Pseudoberkleasmium pandanicola	KUMCC 17-0178	MH260304	MH260344	MH275071	N/A	N/A
Pseudocoleodictyospora tectonae	MFLUCC 12-0385	KU764709	NG_061232	NR_154338	N/A	KU712491
Pseudocoleodictyospora thailandica	MFLUCC 12-0565	KU764701	NG_062417	NR_154337	N/A	KU712494
Pseudodidymosphaeria spartii	MFLUCC 13-0273	KP325436	KP325438	KP325434	N/A	N/A
Pseudopyrenochaeta lycopersici	FMR 15746	EU754205	NG_062728	NR_103581	N/A	LT717680
Pseudopyrenochaeta terretris	FMR 15327	LT623216	N/A	LT623228	N/A	LT623287
Pseudotetraploa longissima	HC 4933	AB524612	AB524471	AB524796	AB524827	N/A
Pseudoxylomyces elegans	KT 2887	AB807598	AB797308	LC014593	AB808576	N/A
Pyrenochaetopsis leptospora	CBS 101635	GQ387627	NG_063097	JF740262	MF795881	LT623282
Pyrenochaetopsis tabarestanensis	IBRC M 30051	KF803343	NG_065034	NR_155636	N/A	N/A
Quadricrura bicornis	yone 153	AB524613	AB524472	AB524797	AB524828	N/A
Quercicola fusiformis	MFLUCC 18-0479	MK348009	MK347898	MK347790	MK360085	MK434864
Quercicola guttulospora	MFLUCC 18-0481	MK348010	MK347899	MK347791	MK360086	N/A
Quixadomyces cearensis	HUEFS 238438	MG970695	N/A	NR_160606	N/A	N/A
Roussoella nitidula	MFLUCC 11-0634	KJ474842	N/A	KJ474834	KJ474851	KJ474858
Salsuginea phoenicis	MFLU 19-0015	MK405280	N/A	N/A	MK404650	N/A
Salsuginea ramicola	KT 2597.2	GU479801	GU479768	N/A	GU479862	GU479834
Seltsamia ulmi	CBS 143002	MF795794	MF795794	MF795794	MF795882	MF795836
Shiraia bambusicola	GZAAS2.629	KC460980	N/A	GQ845415	N/A	N/A
Splanchnonema platani	CBS 222.37	KR909316	KR909318	MH855895	KR909319	KR909322
Sporormia fimetaria	UPS Dissing Gr.81.194	GQ203729	N/A	GQ203769	N/A	N/A
Sporormiella isomera	CBS 166.73	MH872355	N/A	AY943053	N/A	N/A
Stemphylium herbarum	CBS 191.86	GU238160	GU238232	NR_111243	KC584731	DQ247794
Striatiguttula nypae	MFLUCC 18-0265	MK035992	MK035977	MK035969	MK034432	MK034440
Striatiguttula phoenicis	MFLUCC 18-0266	MK035995	MK035980	MK035972	MK034435	MK034442
Sublophiostoma thailandica	MFLUCC 11-0185	KX534216	KX534222	MW136275	KX550080	MW088718
	MFLUCC 11-0207	KX534212	KX534218	MW136257	KX550077	MW088714
Subplenodomus violicola	CBS 306.68	MH870849	GU238231	MH859138	N/A	N/A
Sulcatispora acerina	KT 2982	LC014610	LC014605	LC014597	LC014615	N/A
Sulcatispora berchemiae	KT 1607	AB807534	AB797244	AB809635	AB808509	N/A
Sulcosporium thailandica	MFLUCC 12-0004	KT426563	KT426564	MG520958	N/A	N/A
Teichospora trabicola	C134	KU601591	N/A	KU601591	KU601601	KU601600
Tetraplosphaeria sasicola	KT 563	AB524631	AB524490	AB524807	AB524838	N/A

Species names	Strain number	LSU	SSU	ITS	*tef1-α*	*rpb2*
Thyridaria acaciae	CBS 138873	NG_058127	N/A	KP004469	N/A	N/A
Thyridaria broussonetiae	TB1	KX650568	KX650515	KX650568	KX650539	KX650586
Torula aquatica	MFLUCC 16-1115	MG208146	N/A	MG208167	N/A	MG207977
Torula pluriseptata	MFLUCC 14-0437	KY197855	KY197862	MN061338	KY197875	KY197869
Trematosphaeria grisea	CBS 332.50	NG_057979	NG_062930	NR_132039	KF015698	KF015720
Trematosphaeria pertusa	CBS 122368	NG_057809	FJ201991	NR_132040	KF015701	FJ795476
Tzeanania taiwanensis	NTUCC 17-006	MH461121	MH461127	MH461124	MH461131	N/A
Wicklowia aquatica	CBS 125634	MH875044	NG_061099	N/A	N/A	N/A
Wicklowia submersa	MFLUCC 18-0373	MK637644	MK637643	N/A	N/A	N/A
Xenopyrenochaetopsis pratorum	CBS 445.81	GU238136	NG_062792	MH861363	N/A	KT389671

Phylogenetic trees were viewed using FigTree v1.4.0 (Rambaut and Drummond 2008) and modified in Microsoft Office PowerPoint 2010 and converted to jpg file using Adobe Photoshop CS6 Extended 10.0 (Adobe Systems, San Jose, CA, USA). The new sequences derived from this study were deposited in GenBank. The final alignment and tree were deposited in TreeBase (http://purl.org/phylo/treebase/phylows/study/TB2:S29199).

Results

Phylogenetic analyses

Blast searches of LSU, *tef1-α*, *rpb2* and ITS sequences data in NCBI showed that our sequences were related to Acrocalymmaceae, Amorosiaceae, Sporormiaceae and Sublophiostomataceae. One hundred and seventy-six taxa, representing all families in Pleosporales, with *Hysterium angustatum* Alb. & Schwein (CBS 123334) and *Hysterobrevium smilacis* (Schwein.) E. Boehm & C.L. Schoch (CBS 114601) as the outgroups, were selected for the analyses. The final combined dataset consisted of 4,953 characters (LSU: 1–850 bp, SSU: 851–1,851 bp, *tef1-α*: 1,852–2,720 bp, *rpb2*: 2,721–3,701 bp, ITS: 3,702–4,953 bp), including alignment gaps. Among them, 2,336 characters were constant, 608 variable characters were parsimony-uninformative, and 2,009 characters were parsimony informative. The most likely tree (-ln = 98,965.704) is presented (Figure. 1) to show the phylogenetic placement of the newly introduced genus and its relationship with other members in Pleosporales.

Analyses of both ML and BYPP (not shown) yielded almost identical results, and the topology of the trees were similar to previous studies (Zhang et al. 2018; Hongsanan et al. 2020a, 2021). The combined analyses showed that two suborders Massarineae and Pleosporineae were well-supported and formed an upper clade in Pleosporales. Our two newly obtained fungal isolates (MFLUCC 21-0222 and MFLUCC 21-0223) clustered together and formed a distinct clade with maximum support (ML-BS = 100%, BYPP = 1.00) and they grouped with Amorosiaceae, Sporormiaceae and Sublophiostomataceae with weak support.

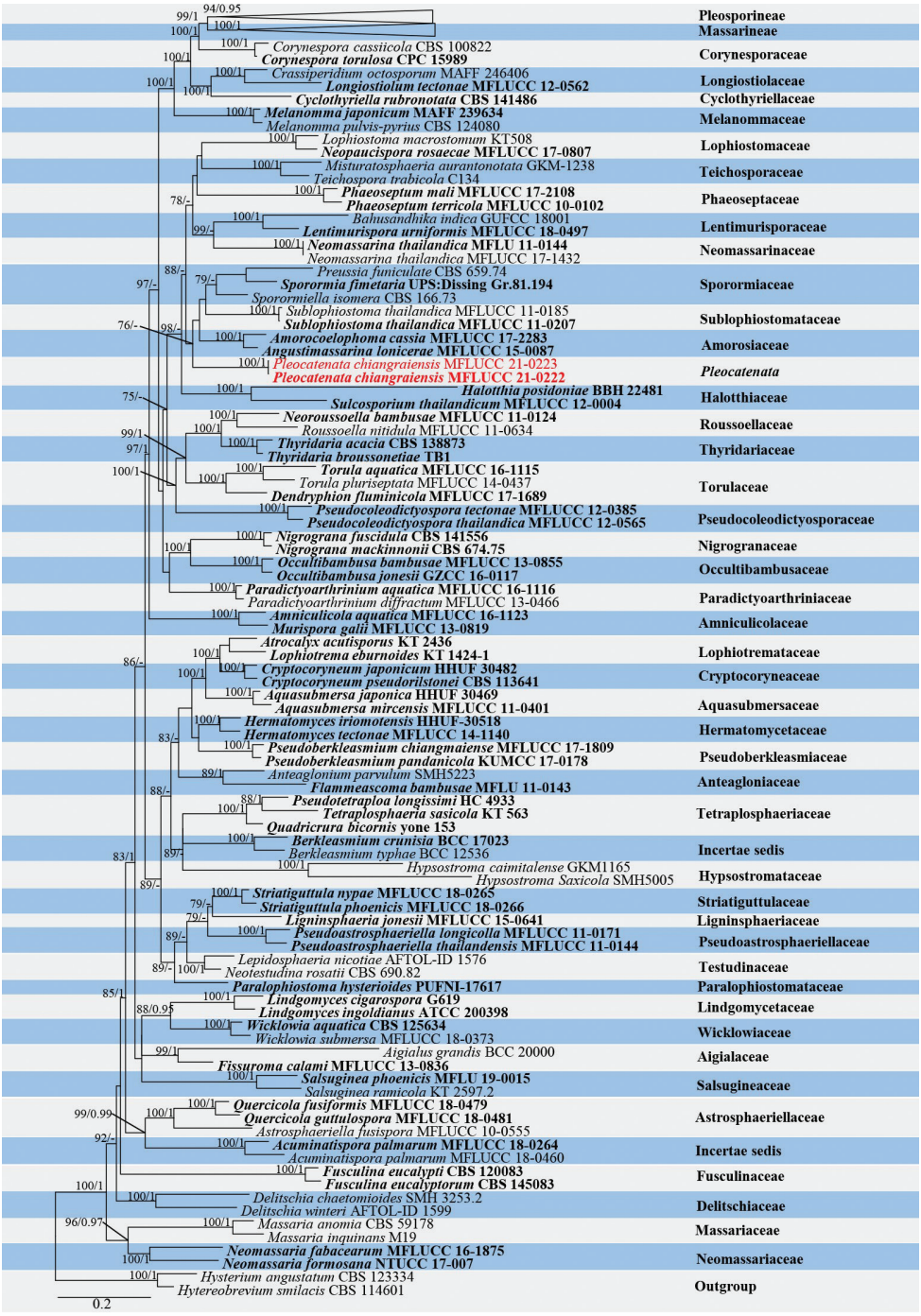

Figure 1. Maximum likelihood tree generated by IQ-Tree, based on analysis of a combined dataset of LSU, SSU, *tef1-α*, *rpb2* and ITS sequence data. Bootstrap support values for ML greater than 75% and Bayesian posterior probabilities greater than 0.95 are given near nodes, respectively. Ex-type strains are in bold, the new isolates are in red.

Taxonomy

Pleocatenata **Y.R. Sun, Yong Wang bis & K.D. Hyde, gen. nov.**
Index Fungorum number: IF559457
Facesoffungi number: FoF 10630

Etymology. "Pleo-" an abbreviation of Pleosporales, the order in which this fungus is classified; "*-catenata*" refers to the catenate conidia of this fungus.

Description. *Saprobic* on decaying twigs in terrestrial habitats. **Asexual morph:** Hyphomycetous. *Colonies* on natural substrate effuse, dark, velvety. *Conidiophores* macronematous, mononematous, straight or slightly curved, cylindrical, unbranched, septate, brown or dark brown. *Conidiogenous cells* monotretic, integrated, terminal, cylindrical, brown to dark brown. *Conidia* catenate, formed in acropetal chains, straight or bent, obclavate, olivaceous to dark brown, multi-euseptate, slightly constricted at septa, distal conidia rounded at apex, truncate at base, intercalary conidia truncate at both ends, with thickened and darkened scars at base or both ends. **Sexual morph:** Undetermined.

Type species. *Pleocatenata chiangraiensis* Y.R. Sun, Yong Wang bis & K.D. Hyde

Notes. The morphology of *Pleocatenata* is distinguished from members in other families in Pleosporales by its tretic conidiogenous cells and catenate, euseptate conidia, and phylogenic analyses indicated it does not belong to any existing families. To avoid establishing a new family with only one species, *Pleocatenata* is introduced as a new genus and assigned to Pleosporales, genera *incertae sedis*. *Pleocatenata* is a monotypic genus reported from terrestrial habitats but without a known sexual morph. Further discovery of other species in *Pleocatenata* or phylogenetic related genera with supported monophyly will determine the familial level of *Pleocatenata*.

Pleocatenata chiangraiensis **Y.R. Sun, Yong Wang bis & K.D. Hyde, sp. nov.**
Index Fungorum number: IF559458
Facesoffungi number: FoF 10631
Fig. 2

Etymology. The epithet referring to the location in which the fungus was collected.

Holotype. MFLU: 22-0002

Description. *Saprobic* on twigs of *Clerodendrum quadriloculare* and *Tarenna stellulata*. **Asexual morph:** Hyphomycetous. *Colonies* on natural substrate effuse, dark, velvety. *Mycelium* immersed, composed of septate, branched, hyaline to subhyaline hyphae. *Conidiophores* macronematous, mononematous, erect, straight or slightly curved, cylindrical, unbranched, robust, 4–6-septate, brown or dark brown, rough, 35–100 μm long, 5.5–8.5 μm wide. *Conidiogenous cells* monotretic, integrated, terminal, determinate, cylindrical, dark brown. *Conidia* catenate, formed in acropetal chains of 2–3, straight or curved, obclavate, olivaceous to brown when young, blackish brown

Figure 2. *Pleocatenata chiangraiensis* (MFLU 22-0002, holotype) **a** host (*Tarenna stellulata*) **b, c** colonies on natural substrate **d, e** conidiophores with conidia **f** conidiogenous cells **g–k** conidia **l** germinated conidium **m, n** colonies on PDA (upper view and lower view). Scale bars: 1 mm (**b**); 100 μm (**c**); 20 μm (**d–l**).

when mature, 5–8-euseptate, slightly constricted at septa, distal conidia rounded at apex, truncate at base, intercalary conidia truncate at both ends, with thickened and darkened scars at base or both ends, 34–70 μm long, 6.5–12 μm at the widest. **Sexual morph:** Unknown.

Culture characteristics. Conidia germinated on PDA within 12 hours at 26 °C. Germ tubes were produced from both ends. Colony reached 20–25 mm diameter after 4 weeks at room temperature on PDA media. Mycelia superficial, irregularly circular, entire edge, dark brown from above, black from below, pigment produced which turns the media reddish brown.

Material examined. Thailand, Chiang Rai Province, Mae Fah Luang University, on twigs of *Tarenna stellulata*, 3 July 2020, Y.R. Sun, MFU5 (MFLU 22-0002, **holotype**, ex-type living culture MFLUCC 21-0222). Thailand, Chiang Rai Province, Medicinal Plants Garden, on twigs of *Clerodendrum quadriloculare*, 7 June 2020, Y.R. Sun, B45 (MFLU 22-0001, living culture MFLUCC 21-0223).

Notes. Two isolates collected from different hosts share similar morphology and clustered together in the phylogenic tree. There are no base pair differences in LSU and *tef1-α* genes between these two isolates. One base pair and two base pair differences (without gaps) are observed in ITS and *rpb2*, respectively. Therefore, the two isolates MFLUCC 21-0222 and MFLUCC 21-0223 are identified as conspecific.

Discussion

Pleocatenata is phylogenetically related to Amorosiaceae, Sporormiaceae, and Sublophiostomataceae in our multi-gene analyses, but their monophyly was not well-supported, indicating their uncertain phylogenetic affinities. No hyphomycetous asexual morph has been reported in Sporormiaceae or Sublophiostomataceae (Hongsanan et al. 2020a, 2021). However, in Amorosiaceae, only two known hyphomycetous genera, *Amorosia* and *Angustimassarina*, are characterized by micronematous to semimacronematous, pale brown conidiophores, monoblastic conidiogenous cells, and single, elongate-clavate conidia (Mantle et al. 2006; Thambugala et al. 2015; Hongsanan et al. 2020a). *Pleocatenata* can be distinguished from these two genera by having monotretic conidiogenous cells and catenate, obclavate conidia.

A recently introduced species, *Corynespora sinensis* Jian Ma, X.G. Zhang & R.F. Castañeda, resembles *Pleocatenata* in its unbranched, cylindrical conidiophores and monotretic, terminal conidiogenous cells that produce catenate, obclavate conidia (Xu et al. 2020). Morphologically, *Corynespora sinensis* is more similar to *P. chiangraiensis* than to the type species of *Corynespora*, *C. cassiicola* (Berk. & M.A. Curtis) C.T. Wei (Wei 1950). Since *Corynespora* (Corynesporascaceae, Pleosporales) is a polyphyletic genus (Schoch et al. 2009; Voglmayr and Jaklitsch 2017), and there is no available sequence data for *C. sinensis*, we presume that *C. sinensis* may belong to *Pleocatenata*. However, due to lack of molecular data, and since morphology-based classification is not reliable for many hyphomycetous genera (Shenoy et al. 2006; Su et al. 2016; Yang

Table 3. Comparison between *Corynespora cassiicola*, *C. sinensis*, and *Pleocatenata chiangraiensis*.

Species	Conidiophores	Conidiogenous cells	Conidia	References
Corynespora cassiicola	Unbranched, cylindrical proliferations, pale to mid brown, up to 9 septate, 110–850 × 4–11 µm	Monotretic, cylindrical, pale to mid brown	Solitary or in chains of 2–6, obclavate to cylindrical, subhyaline to pale olivaceous brown or brown, 4–20 distoseptate, 40–220 × 9–22 µm	Wei 1950
Corynespora sinensis (HJAUP M0156)	Unbranched, cylindrical, brown to dark, 4–8-septate, 53–96.5 × 7–8.5 µm	Monotretic, cylindrical, brown,	In chains of 2, primary conidia obclavate or fusiform, 3(–4)-distoseptate, 31.5–42 × 8–9.5 µm. secondary conidia ellipsoid, 3-distoseptate, 21–28.5 × 8–9.5 µm	Xu et al. 2020
Pleocatenata chiangraiensis (MFLU 21-0222)	Unbranched, cylindrical, brown or dark brown, 4–6-septate, 35–100 × 5.5–8.5 µm	Monotretic, cylindrical, dark brown	In chains of 2–3, obclavate, olivaceous to brown when young, blackish brown when mature, 5–8-euseptate, 34–70 µm × 6.5–12 µm	This study

et al. 2018), we retain the current classification. Sequences of *C. sinensis* are needed to resolve its phylogenetic placement. Detailed morphological comparison among *C. cassiicola*, *C. sinensis* and *P. chiangraiensis* is provided (Table 3).

Pleocatenata is similar to *Sporidesmium sensu stricto*, which is characterized by distinctive, unbranched conidiophores, monoblastic, determinate or proliferating conidiogenous cells, and acrogenous, solitary, transversely septate conidia (Ellis 1958, 1971; Shenoy et al. 2006; Boonmee et al. 2012; Su et al. 2016; Yang et al. 2018). However, *Pleocatenata* is different from *Sporidesmium* by having catenate conidia. Additionally, *Pleocatenata* is phylogenetically distinct from *Sporidesmium*, supporting the introduction of the new genus.

The catenate, obclavate phragmoconidia of *P. chiangraiensis* are similar to capnodendron asexual morph of *Antennulariella* Woron (Antennulariellaceae, Capnodiales) (Hughes 1976, 2000; Seifert et al. 2011). Although sequence data of *Antennulariella* is not available, morphological characters, such as holoblastic conidiogenous cells and branched conidiophores of *Antennulariella*, support its separation from *P. chiangraiensis* (Hughes 1976, 2000; Seifert et al. 2011). *Pleocatenata* is also similar to *Corynesporina* Subram (Pezizomycotina, *incertae sedis*) in having unbranched, robust conidiophores and catenate conidia (Seifert et al. 2011). However, they differ in that the distoseptate conidia form in basipetal chains in *Corynesporina* and euseptate conidia form in acropetal chains in *Pleocatenata*.

Acknowledgements

We would like to thank Dr. Shaun Pennycook for checking the nomenclature. Ya-Ru Sun thanks Mae Fah Luang University for the award of a fee-less scholarship. Ya-Ru Sun also thanks the director of the Mae Fah Luang University Botanical Garden, the botanist Dr. Jantrararuk Tovaranonte for her support. The study was funded by Guizhou Science Technology Department International Cooperation Basic project ([2018]5806), National Natural Science Foundation of China (No.31972222,

31560489), Program of Introducing Talents of Discipline to Universities of China (111 Program, D20023), and Talent project of Guizhou Science and Technology Cooperation Platform ([2017]57885, [2019]5641 and [2020]5001).

References

Abtahi F, Nourani SL (2017) The most important fungal diseases associated with some useful medicinal plants. In: Ghorbanpour M, Varma A (Eds) Medicinal plants and environmental challenges. Springer International Publishing, Cham, 279–293. https://doi.org/10.1007/978-3-319-68717-9_16

Abutaha N, Mashaly AM, Al-Mekhlafi FA, Farooq M, Al-shami M, Wadaan MA (2015) Larvicidal activity of endophytic fungal extract of *Cochliobolus spicifer* (Pleosporales: Pleosporaceae) on *Aedes caspius* and *Culex pipiens* (Diptera: Culicidae). Applied Entomology and Zoology 50: 405–414. https://doi.org/10.1007/s13355-015-0347-6

Barghoorn ES (1944) Marine fungi: their taxonomy and biology. Farlowia 1: 395–467. https://doi.org/10.5962/p.315987

Barr ME (1987) Prodromus to class Loculoascomycetes. Amherst. University of Massachusetts, Massachusetts.

Bhagat J, Kaur A, Sharma M, Saxena AK, Chadha BS (2012) Molecular and functional characterization of endophytic fungi from traditional medicinal plants. World Journal of Microbiology and Biotechnology 28: 963–971. https://doi.org/10.1007/s11274-011-0894-0

Bonnardeaux Y, Brundrett M, Batty A, Dixon K, Koch J, Sivasithamparam K (2007) Diversity of mycorrhizal fungi of terrestrial orchids: compatibility webs, brief encounters, lasting relationships and alien invasions. Mycological Research 111: 51–61. https://doi.org/10.1016/j.mycres.2006.11.006

Boonmee S, Ko TWK, Chukeatirote E, Hyde KD, Chen H, Cai L, McKenzie EHC, Jones EBG, Kodsueb R, Hassan BA (2012) Two new *Kirschsteiniothelia* species with *Dendryphiopsis* anamorphs cluster in *Kirschsteiniotheliaceae* fam. nov. Mycologia 104: 698–714. https://doi.org/10.3852/11-089

Castañeda-Ruiz RF, Heredia GP, Arias RM, Saikawa M, Minter DW, Stadler M, Guarro J, Decock C (2004) Two new hyphomycetes from rainforests of México, and *Briansuttonia*, a new genus to accommodate *Corynespora alternarioides*. Mycotaxon 89: 297–305.

Chernomor O, Von Haeseler A, Minh BQ (2016) Terrace aware data structure for phylogenomic inference from supermatrices. Systematic Biology 65: 997–1008. https://doi.org/10.1093/sysbio/syw037

Chomnunti P, Hongsanan S, Aguirre-Hudson B, Tian Q, Peršoh D, Dhami MK, Alias AS, Xu JC, Liu XZ, Stadler M, Hyde KD (2014) The sooty moulds. Fungal Diversity 66: 1–36. https://doi.org/10.1007/s13225-014-0278-5

Crous PW, Wingfield MJ, Burgess TI, Hardy GESJ, Barber PA, Alvarado P, Barnes CW, Buchanan PK, Heykoop M, Moreno G, Thangavel R, van der Spuy S, Barili A, Barrett S, Cacciola SO, Cano-Lira JF, Crane C, Decock C, Gibertoni TB, Guarro J, Guevara-Suarez

M, Hubka V, Kolařík M, Lira CRS, Ordoñez ME, Padamsee M, Ryvarden L, Soares AM, Stchigel AM, Sutton DA, Vizzini A, Weir BS, Acharya K, Aloi F, Baseia IG, Blanchette RA, Bordallo JJ, Bratek Z, Butler T, Cano-Canals J, Carlavilla JR, Chander J, Cheewangkoon R, Cruz RHSF, da Silva M, Dutta AK, Ercole E, Escobio V, Esteve-Raventós F, Flores JA, Gené J, Góis JS, Haines L, Held BW, Jung MH, Hosaka K, Jung T, Jurjević Ž, Kautman V, Kautmanova I, Kiyashko AA, Kozanek M, Kubátová A, Lafourcade M, La Spada F, Latha KPD, Madrid H, Malysheva EF, Manimohan P, Manjón JL, Martín MP, Mata M, Merényi Z, Morte A, Nagy I, Normand AC, Paloi S, Pattison N, Pawłowska J, Pereira OL, Petterson ME, Picillo B, Raj KNA, Roberts A, Rodríguez A, Rodríguez-Campo FJ, Romański M, Ruszkiewicz-Michalska M, Scanu B, Schena L, Semelbauer M, Sharma R, Shouche YS, Silva V, Staniaszek-Kik M, Stielow JB, Tapia C, Taylor PWJ, Toome-Heller M, Vabeikhokhei JMC, van Diepeningen AD, Van Hoa N, M VT, Wiederhold NP, Wrzosek M, Zothanzama J, Groenewald JZ (2017) Fungal Planet description sheets: 558–624. Persoonia 38: 240–384. https://doi.org/10.3767/003158517X698941

Ellis MB (1958) *Clasterosporium* and some allied Dematiaceae Phragmosporae: I. Mycological Papers 7: 1–89.

Ellis MB (1971) Dematiaceous hyphomycetes. Commonwealth Mycological Institute, Kew.

Ferdinandez HS, Manamgoda DS, Udayanga D, Deshappriya N, Munasinghe MS, Castlebury LA (2021) Molecular phylogeny and morphology reveal three novel species of *Curvularia* (Pleosporales, Pleosporaceae) associated withcereal crops and weedy grass hosts. Mycological Progress 20: 431–451. https://doi.org/10.1007/s11557-021-01681-0

Hall TA (1999) BioEdit: a user-friendly biological sequence alignment editor and analysis program for Windows 95/98/NT. In, 95–98.

Hashimoto A, Matsumura M, Hirayama K, Tanaka K (2017) Revision of *Lophiotremataceae* (*Pleosporales*, *Dothideomycetes*): *Aquasubmersaceae*, *Cryptocoryneaceae*, and *Hermatomycetaceae* fam. nov. Persoonia 39: 51–73. https://doi.org/10.3767/persoonia.2017.39.03

Hoang DT, Chernomor O, Von Haeseler A, Minh BQ, Vinh LS (2018) UFBoot2: improving the ultrafast bootstrap approximation. Molecular Biology and Evolution 35: 518–522. https://doi.org/10.1093/molbev/msx281

Hongsanan S, Hyde KD, Phookamsak R, Wanasinghe DN, McKenzie EHC, Sarma VV, Boonmee S, Lücking R, Bhat DJ, Liu NG, Tennakoon DS, Pem D, Karunarathna A, Jiang SH, Jones EBG, Phillips AJL, Manawasinghe IS, Tibpromma S, Jayasiri SC, Sandamali DS, Jayawardena RS, Wijayawardene NN, Ekanayaka AH, Jeewon R, Lu YZ, Dissanayake AJ, Zeng XY, Luo ZL, Tian Q, Phukhamsakda C, Thambugala KM, Dai DQ, Chethana KWT, Samarakoon MC, Ertz D, Bao DF, Doilom M, Liu JK, Pérez-Ortega S, Suija A, Senwanna C, Wijesinghe SN, Konta S, Niranjan M, Zhang SN, Ariyawansa HA, Jiang HB, Zhang JF, Norphanphoun C, de Silva NI, Thiyagaraja V, Zhang H, Bezerra JDP, Miranda-González R, Aptroot A, Kashiwadani H, Harishchandra D, Sérusiaux E, Aluthmuhandiram JVS, Abeywickrama PD, Devadatha B, Wu HX, Moon KH, Gueidan C, Schumm F, Bundhun D, Mapook A, Monkai J, Chomnunti P, Suetrong S, Chaiwan N, Dayarathne MC, Yang J, Rathnayaka AR, Bhunjun CS, Xu JC, Zheng JS, Liu G, Feng Y, Xie N (2020a) Refined families of Dothideomycetes: Dothideomycetidae and Pleosporomycetidae. Mycosphere 11: 1553–2107. https://doi.org/10.5943/mycosphere/11/1/13

Hongsanan S, Hyde KD, Phookamsak R, Wanasinghe DN, McKenzie EHC, Sarma VV, Lücking R, Boonmee S, Bhat JD, Liu NG, Tennakoon DS, Pem D, Karunarathna A, Jiang SH, Jones GEB, Phillips AJL, Manawasinghe IS, Tibpromma S, Jayasiri SC, Sandamali D, Jayawardena RS, Wijayawardene NN, Ekanayaka AH, Jeewon R, Lu YZ, Phukhamsakda C, Dissanayake AJ, Zeng XY, Luo ZL, Tian Q, Thambugala KM, Dai D, Samarakoon MC, Chethana KWT, Ertz D, Doilom M, Liu JK, Pérez-Ortega S, Suija A, Senwanna C, Wijesinghe SN, Niranjan M, Zhang SN, Ariyawansa HA, Jiang HB, Zhang J-F, Norphanphoun C, de Silva NI, Thiyagaraja V, Zhang H, Bezerra JDP, Miranda-González R, Aptroot A, Kashiwadani H, Harishchandra D, Sérusiaux E, Abeywickrama PD, Bao D-F, Devadatha B, Wu HX, Moon KH, Gueidan C, Schumm F, Bundhun D, Mapook A, Monkai J, Bhunjun CS, Chomnunti P, Suetrong S, Chaiwan N, Dayarathne MC, Yang J, Rathnayaka AR, Xu JC, Zheng J, Liu G, Feng Y, Xie N (2020b) Refined families of Dothideomycetes: orders and families incertae sedis in Dothideomycetes. Fungal Diversity 105: 17–318. https://doi.org/10.1007/s13225-020-00462-6

Hongsanan S, Phookamsak R, Goonasekara ID, Thambugala KM, Hyde KD, Bhat JD, Suwannarach N, Cheewangkoon R (2021) Introducing a new pleosporalean family Sublophiostomataceae fam. nov. to accommodate *Sublophiostoma* gen. nov. Scientific Reports 11: e9496. https://doi.org/10.1038/s41598-021-88772-w

Huang WY, Cai YZ, Hyde KD, Corke H, Sun M (2008) Biodiversity of endophytic fungi associated with 29 traditional Chinese medicinal plants. Fungal Diversity 33: 61–75.

Hughes SJ (1976) Sooty moulds. Mycologia 68: 693–820. https://doi.org/10.2307/3758799

Hughes SJ (2000) *Antennulariella batistae* n. sp. and its *Capnodendron* and *Antennariella* synanamorphs, with notes on *Capnodium capsuliferum*. Canadian Journal of Botany 78: 1215–1226. https://doi.org/10.1139/b00-098

Hyde KD, Jones EBG, Liu JK, Ariyawansa H, Boehm E, Boonmee S, Braun U, Chomnunti P, Crous PW, Dai DQ, Diederich P, Dissanayake A, Doilom M, Doveri F, Hongsanan S, Jayawardena R, Lawrey JD, Li YM, Liu YX, Lücking R, Monkai J, Muggia L, Nelsen MP, Pang KL, Phookamsak R, Senanayake IC, Shearer CA, Suetrong S, Tanaka K, Thambugala KM, Wijayawardene NN, Wikee S, Wu HX, Zhang Y, Aguirre-Hudson B, Alias SA, Aptroot A, Bahkali AH, Bezerra JL, Bhat DJ, Camporesi E, Chukeatirote E, Gueidan C, Hawksworth DL, Hirayama K, De Hoog S, Kang JC, Knudsen K, Li WJ, Li XH, Liu ZY, Mapook A, McKenzie EHC, Miller AN, Mortimer PE, Phillips AJL, Raja HA, Scheuer C, Schumm F, Taylor JE, Tian Q, Tibpromma S, Wanasinghe DN, Wang Y, Xu JC, Yacharoen S, Yan JY, Zhang M (2013) Families of Dothideomycetes. Fungal Diversity 63: 1–313. https://doi.org/10.1007/s13225-013-0263-4

Hyde KD, Chaiwan N, Norphanphoun C, Boonmee S, Camporesi E, Chethana KWT, Dayarathne MC, de Silva NI, Dissanayake AJ, Ekanayaka AH, Hongsanan S, Huang SK, Jayasiri SC, Jayawardena RS, Jiang HB, Karunarathna A, Lin CG, Liu JK, Liu NG, Lu YZ, Luo ZL, Maharachchimbura SSN, Manawasinghe IS, Pem D, Perera RH, Phukhamsakda C, Samarakoon MC, Senwanna C, Shang QJ, Tennakoon DS, Thambugala KM, Tibpromma S, Wanasinghe DN, Xiao YP, Yang J, Zeng XY, Zhang JF, Zhang SN, Bulgakov TS, Bhat DJ, Cheewangkoon R, Goh TK, Jones EBG, Kang JC, Jeewon R, Liu ZY, Lumyong S,

Kuo CH, McKenzie EHC, Wen TC, Yan JY, Zhao Q (2018) Mycosphere notes 169–224. Mycosphere 9: 271–430. https://doi.org/10.5943/mycosphere/9/2/8

Hyde KD, Xu JC, Rapior S, Jeewon R, Lumyong S, Niego AGT, Abeywickrama PD, Aluthmuhandiram JVS, Brahamanage RS, Brooks S, Chaiyasen A, Chethana KWT, Chomnunti P, Chepkirui C, Chuankid B, de Silva NI, Doilom M, Faulds C, Gentekaki E, Gopalan V, Kakumyan P, Harishchandra D, Hemachandran H, Hongsanan S, Karunarathna A, Karunarathna SC, Khan S, Kumla J, Jayawardena RS, Liu JK, Liu NG, Luangharn T, Macabeo APG, Marasinghe DS, Meeks D, Mortimer PE, Mueller P, Nadir S, Nataraja KN, Nontachaiyapoom S, O'Brien M, Penkhrue W, Phukhamsakda C, Ramanan US, Rathnayaka AR, Sadaba RB, Sandargo B, Samarakoon BC, Tennakoon DS, Siva R, Sriprom W, Suryanarayanan TS, Sujarit K, Suwannarach N, Suwunwong T, Thongbai B, Thongklang N, Wei D, Wijesinghe SN, Winiski J, Yan J, Yasanthika E, Stadler M (2019) The amazing potential of fungi: 50 ways we can exploit fungi industrially. Fungal Diversity 97: 1–136. https://doi.org/10.1007/s13225-019-00430-9

Hyde KD, Dong Y, Phookamsak R, Jeewon R, Bhat DJ, Jones EBG, Liu NG, Abeywickrama PD, Mapook A, Wei DP, Perera RH, Manawasinghe IS, Pem D, Bundhun D, Karunarathna A, Ekanayaka AH, Bao DF, Li JF, Samarakoon MC, Chaiwan N, Lin CG, Phutthacharoen K, Zhang SN, Senanayake IC, Goonasekara ID, Thambugala KM, Phukhamsakda C, Tennakoon DS, Jiang HB, Yang J, Zeng M, Huanraluek N, Liu JK, Wijesinghe SN, Tian Q, Tibpromma S, Brahmanage RS, Boonmee S, Huang SK, Thiyagaraja V, Lu YZ, Jayawardena RS, Dong W, Yang EF, Singh SK, Singh SM, Rana S, Lad SS, Anand G, Devadatha B, Niranjan M, Sarma VV, Liimatainen K, Aguirre-Hudson B, Niskanen T, Overall A, Alvarenga RLM, Gibertoni TB, Pfliegler WP, Horváth E, Imre A, Alves AL, da Silva Santos AC, Tiago PV, Bulgakov TS, Wanasinghe DN, Bahkali AH, Doilom M, Elgorban AM, Maharachchikumbura SSN, Rajeshkumar KC, Haelewaters D, Mortimer PE, Zhao Q, Lumyong S, Xu J, Sheng J (2020) Fungal diversity notes 1151–1276: taxonomic and phylogenetic contributions on genera and species of fungal taxa. Fungal Diversity 100: 5–277. https://doi.org/10.1007/s13225-020-00439-5

Iturrieta-González I, Pujol I, Iftimie S, García D, Morente V, Queralt R, Guevara-Suarez M, Alastruey-Izquierdo A, Ballester F, Hernández-Restrepo M (2020) Polyphasic identification of three new species in *Alternaria* section Infectoriae causing human cutaneous infection. Mycoses 63: 212–224. https://doi.org/10.1111/myc.13026

Jayasiri SC, Hyde KD, Ariyawansa HA, Bhat J, Buyck B, Cai L, Dai YC, Abd-Elsalam KA, Ertz D, Hidayat I, Jeewon R, Jones EBG, Bahkali AH, Karunarathna SC, Liu JK, Luangsa-ard JJ, Lumbsch HT, Maharachchikumbura SSN, McKenzie EHC, Moncalvo JM, Ghobad-Nejhad M, Nilsson H, Pang KL, Pereira OL, Phillips AJL, Raspé O, Rollins AW, Romero AI, Etayo J, Selçuk F, Stephenson SL, Suetrong S, Taylor JE, Tsui CKM, Vizzini A, Abdel-Wahab MA, Wen TC, Boonmee S, Dai DQ, Daranagama DA, Dissanayake AJ, Ekanayaka AH, Fryar SC, Hongsanan S, Jayawardena RS, Li WJ, Perera RH, Phookamsak R, de Silva NI, Thambugala KM, Tian Q, Wijayawardene NN, Zhao RL, Zhao Q, Kang JC, Promputtha I (2015) The Faces of Fungi database: fungal names linked with morphology, phylogeny and human impacts. Fungal Diversity 74: 3–18. https://doi.org/10.1007/s13225-015-0351-8

Kirk PM, Cannon PF, Minter DW, Staplers JA (2008) Dictionary of the Fungi 10th edn. CABI Bioscience, UK.

Larsson A (2014) AliView: a fast and lightweight alignment viewer and editor for large datasets. Bioinformatics 30: 3276–3278. https://doi.org/10.1093/bioinformatics/btu531

Li GJ, Hyde KD, Zhao RL, Hongsanan S, Abdel-Aziz FA, Abdel-Wahab MA, Alvarado P, Alves-Silva G, Ammirati JF, Ariyawansa HA, Baghela A, Bahkali AH, Beug M, Bhat DJ, Bojantchev D, Boonpratuang T, Bulgakov TS, Camporesi E, Boro MC, Ceska O, Chakraborty D, Chen JJ, Chethana KWT, Chomnunti P, Consiglio G, Cui BK, Dai DQ, Dai YC, Daranagama DA, Das K, Dayarathne MC, De Crop E, De Oliveira RJV, de Souza CAF, de Souza JI, Dentinger BTM, Dissanayake AJ, Doilom M, Drechsler-Santos ER, Ghobad-Nejhad M, Gilmore SP, Góes-Neto A (2016) Fungal diversity notes 253–366: taxonomic and phylogenetic contributions to fungal taxa. Fungal Diversity 78: 1–237. https://doi.org/10.1007/s13225-016-0366-9

Li H, Sun G, Batzer JC, Crous PW, Groenewald JZ, Karakaya A, Gleason ML (2011) *Scleroramularia* gen. nov. associated with sooty blotch and flyspeck of apple and pawpaw from the Northern Hemisphere. Fungal Diversity 46: 53–66. https://doi.org/10.1007/s13225-010-0074-9

Liu YJ, Whelen S, Hall BD (1999) Phylogenetic relationships among Ascomycetes: evidence from an RNA polymerse II subunit. Molecular Biology and Evolution 16: 1799–1808. https://doi.org/10.1093/oxfordjournals.molbev.a026092

Long H, Zhang Q, Hao YY, Shao XQ, Wei XX, Hyde KD, Wang Y, Zhao DG (2019) *Diaporthe* species in south-western China. MycoKeys 57: 113–127. https://doi.org/10.3897/mycokeys.57.35448

Luttrell ES (1955) The ascostromatci Ascomycetes. Mycologia 47: 511–532. https://doi.org/10.2307/3755666

Ma XY, Maharachchikumbura SSN, Chen BW, Hyde KD, McKenzie EHC, Chomnunti P, Kang JC (2019) Endophytic pestalotiod taxa in *Dendrobium orchids*. Phytotaxa 419: 268–286. https://doi.org/10.11646/phytotaxa.419.3.2

Mantle PG, Hawksworth DL, Pazoutova S, Collinson LM, Rassing BR (2006) *Amorosia littoralis* gen. sp. nov., a new genus and species name for the scorpinone and caffeine-producing hyphomycete from the littoral zone in The Bahamas. Mycological Research 110: 1371–1378. https://doi.org/10.1016/j.mycres.2006.09.013

Mathiyazhagan S, Kavitha K, Nakkeeran S, Chandrasekar G, Manian K, Renukadevi P, Krishnamoorthy AS, Fernando WGD (2004) PGPR mediated management of stem blight of *Phyllanthus amarus* (Schum and Thonn) caused by *Corynespora cassiicola* (Berk and Curt) Wei. Archives of Phytopathology and Plant Protection 37: 183–199. https://doi.org/10.1080/03235400410001730658

Miller MA, Pfeiffer W, Schwartz T (2010) "Creating the CIPRES Science Gateway for inference of large phylogenetic trees" in Proceedings of the Gateway Computing Environments Workshop (GCE), 14 Nov. 2010, New Orleans, LA, 1–8. https://doi.org/10.1109/GCE.2010.5676129

Minh BQ, Nguyen MAT, von Haeseler A (2013) Ultrafast approximation for phylogenetic bootstrap. Molecular Biology and Evolution 30: 1188–1195. https://doi.org/10.1093/molbev/mst024

Nguyen LT, Schmidt HA, Von Haeseler A, Minh BQ (2015) IQ-TREE: a fast and effective stochastic algorithm for estimating maximum-likelihood phylogenies. Molecular Biology and Evolution 32: 268–274. https://doi.org/10.1093/molbev/msu300

Nylander JAA (2004) MrModeltest v2.2. Program distributed by the author: 2. Evolutionary Biology Centre, Uppsala University, 1–2.

Obrist W (1959) Untersuchungen über einige" dothideale" Gattungen. Phytopathologische Zeitschrift 35: 357–388. https://doi.org/10.1111/j.1439-0434.1959.tb01833.x

Ramesh C (2003) *Loculoascomycetes* from India. Rao GP, Manoharachari C, Bhat DJ (Eds) Frontiers of Fungal Diversity in India, International Book Distributing Company, Lucknow, India, 457–479.

Rambaut A, Drummond A (2008) FigTree: Tree figure drawing tool, version 1.2. 2. Institute of Evolutionary Biology, University of Edinburgh.

Rannala B, Yang ZH (1996) Probability distribution of molecular evolutionary trees: A new method of phylogenetic inference. Journal of Molecular Evolution 43: 304–311. https://doi.org/10.1007/BF02338839

Rasool-Hassan BA (2012) Medicinal plants (importance and uses). Pharmaceut Anal Acta 3: 2153–2435. https://doi.org/10.4172/2153-2435.1000e139

Rehner SA, Samuels GJ (1994) Taxonomy and phylogeny of *Gliocladium* analysed from nuclear large subunit ribosomal DNA sequences. Mycological Research 98: 625–634. https://doi.org/10.1016/S0953-7562(09)80409-7

Rehner SA, Buckley E (2005) A beauveria phylogeny inferred from nuclear ITS and EF1-α sequences: evidence for cryptic diversification and links to *Cordyceps teleomorphs*. Mycologia 97(1): 84–98. https://doi.org/10.1080/15572536.2006.11832842

Ronquist F, Teslenko M, Van Der Mark P, Ayres DL, Darling A, Höhna S, Larget B, Liu L, Suchard MA, Huelsenbeck JP (2012) MrBayes 3.2: efficient Bayesian phylogenetic inference and model choice across a large model space. Systematic Biology 61: 539–542. https://doi.org/10.1093/sysbio/sys029

Schoch C, Crous PW, Groenewald JZ, Boehm E, Burgess TI, De Gruyter J, De Hoog GS, Dixon L, Grube M, Gueidan C (2009) A class-wide phylogenetic assessment of Dothideomycetes. Studies in Mycology 64: 1–15. https://doi.org/10.3114/sim.2008.61.08

Seifert K, Morgan-Jones G, Gams W, Kendrick B (2011) The genera of hyphomycetes. CBS–KNAW Fungal Biodiversity Centre, Utrecht.

Senanayake IC, Rathnayake AR, Marasinghe DS, Calabon MS, Gentekaki E, Lee HB, Hurdeal VG, Pem D, Dissanayake LS, Wijesinghe SN, Bundhun D, Nguyen TT, Goonasekara ID, Abeywickrama PD, Bhunjun CS, Jayawardena RS, Wanasinghe DN, Jeewon R, Bhat DJ, Xiang MM (2020) Morphological approaches in studying fungi: collection, examination, isolation, sporulation and preservation. Mycosphere 11: 2678–2754. https://doi.org/10.5943/mycosphere/11/1/20

Shenoy BD, Jeewon R, Wu WP, Bhat DJ, Hyde KD (2006) Ribosomal and *RPB2* DNA sequence analyses suggest that *Sporidesmium* and morphologically similar genera are polyphyletic. Mycological Research 110: 916–928. https://doi.org/10.1016/j.mycres.2006.06.004

Strobel G, Stierle A, Stierle D, Hess WM (1993) *Taxomyces andreanae*, a proposed new taxon for a bulbilliferous hyphomycete associated with Pacific Yew (*Taxus brevifolia*). Mycotaxon. 47: 71–80.

Su H, Kang JC, Cao JJ, Mo L, Hyde KD (2014) Medicinal plant endophytes produce analogous bioactive compounds. Chiang Mai Journal Science 41: 1–13.

Su HY, Hyde KD, Maharachchikumbura SSN, Ariyawansa HA, Luo ZL, Promputtha I, Tian Q, Lin CG, Shang QJ, Zhao YC, Chai HM, Liu XY, Bahkali AH, Bhat JD, McKenzie EHC, Zhou DQ (2016) The families *Distoseptisporaceae* fam. nov., *Kirschsteiniotheliaceae*, *Sporormiaceae* and *Torulaceae*, with new species from freshwater in Yunnan Province, China. Fungal Diversity 80: 375–409. https://doi.org/10.1007/s13225-016-0362-0

Sun JZ, Liu XZ, McKenzie EHC, Jeewon R, Liu JK, Zhang XL, Zhao Q, Hyde KD (2019) Fungicolous fungi: terminology, diversity, distribution, evolution, and species checklist. Fungal Diversity 95: 337–430. https://doi.org/10.1007/s13225-019-00422-9

Sun YR, Jayawardena RS, Hyde KD, Wang Y (2021) *Kirschsteiniothelia thailandica* sp. nov. (Kirschsteiniotheliaceae) from Thailand. Phytotaxa 490(2): 172–182. https://doi.org/10.11646/phytotaxa.490.2.3

Tan YP, Crous PW, Shivas RG (2016) Eight novel *Bipolaris* species identified from John L. Alcorn's collections at the Queensland Plant Pathology Herbarium (BRIP). Mycological Progress 15: 1203–1214. https://doi.org/10.1007/s11557-016-1240-6

Tennakoon DS, Kuo CH, Maharachchikumbura SSN, Thambugala KM, Gentekaki E, Phillips AJL, Bhat DJ, Wanasinghe DN, de Silva NI, Promputtha I, Hyde KD (2021) Taxonomic and phylogenetic contributions to *Celtis formosana*, *Ficus ampelas*, *F. septica*, *Macaranga tanarius* and *Morus australis* leaf litter inhabiting microfungi. Fungal Diversity 108: 1–215. https://doi.org/10.1007/s13225-021-00474-w

Thambugala KM, Hyde KD, Tanaka K, Tian Q, Wanasinghe DN, Ariyawansa HA, Jayasiri SC, Boonmee S, Camporesi E, Hashimoto A, Hirayama K, Schumacher RK, Promputtha I, Liu ZY (2015) Towards a natural classification and backbone tree for Lophiostomataceae, Floricolaceae, and Amorosiaceae fam. nov. Fungal Diversity 74: 199–266. https://doi.org/10.1007/s13225-015-0348-3

Tóth S (1975) Some new microscopic fungi, III. Annales Historico-naturales Musel nationalis Hungarici 67: 31–35.

Trifinopoulos J, Nguyen LT, von Haeseler A, Minh BQ (2016) W-IQ-TREE: a fast online phylogenetic tool for maximum likelihood analysis. Nucleic Acids Research 44: W232–W235. https://doi.org/10.1093/nar/gkw256

Tzean SS, Chen JL (1990) *Cheiromoniliophora elegans* gen. et sp. nov. (Hyphomycetes). Mycological Research 94: 424–427. https://doi.org/10.1016/S0953-7562(09)80373-0

Vaidya G, Lohman DJ, Meier R (2011) SequenceMatrix: concatenation softwarefor the fast assembly of multi-gene datasets with character set and codon information. Cladistics 27: 171–180. https://doi.org/10.1111/j.1096-0031.2010.00329.x

Vilgalys R, Hester M (1990) Rapid genetic identification and mapping of enzymatically amplified ribosomal DNA from several *Cryptococcus* species. Journal of Bacteriology 172: 4238–4246. https://doi.org/10.1128/jb.172.8.4238-4246.1990

Voglmayr H, Jaklitsch WM (2017) *Corynespora*, *Exosporium* and *Helminthosporium* revisited – New species and generic reclassification. Studies in Mycology 87: 43–76. https://doi.org/10.1016/j.simyco.2017.05.001

Wei CT (1950) Notes on *Corynespora*. Mycological Papers 34, 10 pp.

White TJ, Bruns T, Lee SJWT, Taylor J (1990) Amplification and direct sequencing of fungal ribosomal RNA genes for phylogenetics. In: Innis M, Gelfand D, Shinsky J, White T (Eds) PCR protocols: a guide to methods and applications. Academic Press, New York, 315–322. https://doi.org/10.1016/B978-0-12-372180-8.50042-1

Wijayawardene NN, Crous PW, Kirk PM, Hawksworth DL, Boonmee S, Braun U, Dai DQ, D'souza MJ, Diederich P, Dissanayake A, Doilom M, Hongsanan S, Jones EBG, Groenewald JZ, Jayawardena R, Lawrey JD, Liu JK, Lücking R, Madrid H, Manamgoda DS, Muggia L, Nelsen MP, Phookamsak R, Suetrong S, Tanaka K, Thambugala KM, Wanasinghe DN, Wikee S, Zhang Y, Aptroot A, Ariyawansa HA, Bahkali AH, Bhat DJ, Gueidan C, Chomnunti P, De Hoog GS, Knudsen K, Li WJ, McKenzie EHC, Miller AN, Phillips AJL, Piątek M, Raja HA, Shivas RS, Slippers B, Taylor JE, Tian Q, Wang Y, Woudenberg JHC, Cai L, Jaklitsch WM, Hyde KD (2014) Naming and outline of Dothideomycetes–2014 including proposals for the protection or suppression of generic names. Fungal Diversity 69: 1–55. https://doi.org/10.1007/s13225-014-0309-2

Wijayawardene NN, Hyde KD, Al-Ani LKT, Tedersoo L, Haelewaters D, Rajeshkumar KC, Zhao RL, Aptroot A, Leontyev D, Saxena RK, Tokarev YS, Dai DQ, Letcher PM, Stephenson SL, Ertz D, Lumbsch HT, Kukwa M, Issi IV, Madrid H, Phillips AJL, Selbmann L, Pfliegler WP, Horváth E, Bensch K, Kirk PM, Kolaříková K, Raja HA, Radek R, Papp V, Dima V, Ma J, Malosso E, Takamatsu S, Rambold G, Gannibal PB, Triebel D, Gautam AK, Avasthi S, Suetrong S, Timdal E, Fryar SC, Delgado G, Réblová M, Doilom M, Dolatabadi S, Pawłowska JZ, Humber RA, Kodsueb R, Sánchez-Castro I, Goto BT, Silva DKA, de Souza FA, Oehl F, da Silva GA, Silva IR, Błaszkowski J, Jobim K, Maia LC, Barbosa FR, Fiuza PO, Divakar PK, Shenoy BD, Castañeda-Ruiz RF, Somrithipol S, Lateef AA, Karunarathna SC, Tibpromma S, Mortimer PE, Wanasinghe DN, Phookamsak R, Xu J, Wang Y, Tian F, Alvarado P, Li DW, Kušan I, Matočec N, Mešić A, Tkalčec Z, Maharachchikumbura SSN, Papizadeh M, Heredia G, Wartchow F, Bakhshi M, Boehm E, Youssef N, Hustad VP, Lawrey JD, Santiago ALCMA, Bezerra JDP, Souza-Motta CM, Firmino AL, Tian Q, Houbraken J, Hongsanan S, Tanaka K, Dissanayake AJ, Monteiro JS, Grossart HP, Suija A, Weerakoon G, Etayo J, Tsurykau A, Vázquez V, Mungai P, Damm U, Li QR, Zhang H, Boonmee S, Lu YZ, Becerra AG, Kendrick B, Brearley FQ, Motiejūnaitė J, Sharma B, Khare R, Gaikwad S, Wijesundara DSA, Tang LZ, He MQ, Flakus A, Rodriguez-Flakus P, Zhurbenko MP, McKenzie EHC, Stadler M, Bhat DJ, Liu JK, Raza M, Jeewon R, Nassonova ES, Prieto M, Jayalal RGU, Erdoğdu M, Yurkov A, Schnittler M, Shchepin ON, Novozhilov YK, Silva-Filho AGS, Gentekaki E, Liu P, Cavender JC, Kang Y, Mohammad S, Zhang LF, Xu RF, Li YM, Dayarathne MC, Ekanayaka AH, Wen TC, Deng CY, Pereira OL, Navathe S, Hawksworth DL, Fan XL, Dissanayake LS, Kuhnert E, Grossart HP, Thines M (2020) Outline of Fungi and fungus-like taxa. Mycosphere 11: 1060–1456. https://doi.org/10.5943/mycosphere/11/1/8

Wijayawardene NN, Hyde KD, Anand G, Dissanayake LS, Tang LZ, Dai DQ (2021) Towards incorporating asexually reproducing fungi in the natural classification and notes for pleomorphic genera. Mycosphere 12: 238–405. https://doi.org/10.5943/mycosphere/12/1/4

Xu ZH, Kuang WG, Qiu L, Zhang XG, Castañeda-Ruíz RF, Ma J (2020) *Corynespora sinensis* sp. nov. from Jiangxi, China. Mycotaxon 135: 803–809. https://doi.org/10.5248/135.803

Yang J, Maharachchikumbura SSN, Liu JK, Hyde KD, Jones EBG, Al-Sadi AM, Liu ZY (2018) *Pseudostanjehughesia aquitropica* gen. et sp. nov. and *Sporidesmium sensu lato* species from freshwater habitats. Mycological Progress 17: 591–616. https://doi.org/10.1007/s11557-017-1339-4

Zhang Q, Yang ZF, Cheng W, Wijayawardene NN, Hyde KD, Chen Z, Wang Y (2020) Diseases of *Cymbopogon citratus* (Poaceae) in China: *Curvularia nanningensis* sp. nov. MycoKeys 63: 49–67. https://doi.org/10.3897/mycokeys.63.49264

Zhang SN, Hyde KD, Gareth Jones EB, Cheewangkoon R, Liu JK (2018) *Acuminatispora palmarum* gen. et sp. nov. from mangrove habitats. Mycological Progress 17: 1173–1188. https://doi.org/10.1007/s11557-018-1433-2

Zhang Y, Crous PW, Schoch CL, Hyde KD (2012) Pleosporales. Fungal Diversity 53: 1–221. https://doi.org/10.1007/s13225-011-0117-x

MycoKeys 87: 99–132 (2022)
doi: 10.3897/mycokeys.87.72614
https://mycokeys.pensoft.net

RESEARCH ARTICLE

A peer-reviewed open-access journal
MycoKeys
Launched to accelerate biodiversity research

Revision of *Immersaria* and a new lecanorine genus in Lecideaceae (lichenised Ascomycota, Lecanoromycetes)

Cong-Miao Xie[1], Li-Song Wang[2], Zun-Tian Zhao[1], Yan-Yun Zhang[2], Xin-Yu Wang[2], Lu-Lu Zhang[3]

1 *Key Laboratory of Plant Stress Research, College of Life Sciences, Shandong Normal University, Jinan, Shandong, 250014, China* **2** *CAS Key Laboratory for Plant Diversity and Biogeography of East Asia, Kunming Institute of Botany, Heilongtan, Kunming, Yunnan, 650204, China* **3** *Institute of Environment and Ecology, Shandong Normal University, Jinan, Shandong, 250014, China*

Corresponding authors: Xin-Yu Wang (wangxinyu@mail.kib.ac.cn), Lu-Lu Zhang (612038@sdnu.edu.cn)

Academic editor: Gerhard Rambold | Received 5 August 2021 | Accepted 17 January 2022 | Published 15 February 2022

Citation: Xie C-M, Wang L-S, Zhao Z-T, Zhang Y-Y, Wang X-Y, Zhang L-L (2022) Revision of *Immersaria* and a new lecanorine genus in Lecideaceae (lichenised Ascomycota, Lecanoromycetes). MycoKeys 87: 99–132. https://doi.org/10.3897/mycokeys.87.72614

Abstract

The species *Immersaria cupreoatra* has been included in *Bellemerea*. This caused us to reconsider the relationships between *Bellemerea* and the lecanorine species of *Immersaria* and to question the monophyly of *Immersaria*. Amongst 25 genera of the family Lecideaceae, most have lecideine apothecia, the exceptions being *Bellemerea* and *Koerberiella*, which have lecanorine apothecia. According to previous classifications, *Immersaria* included species with both lecanorine and lecideine apothecia. A five-loci phylogenetic tree (nrITS, nrLSU, RPB1, RPB2, and mtSSU) for Lecideaceae showed that *Immersaria* was split into two clades: firstly, all the lecideine apotheciate species and secondly, all the lecanorine apotheciate species. The latter clade was closely related to the remaining lecanorine apotheciate genera: *Bellemerea* and *Koerberiella*. Therefore, the genus concept of *Immersaria* is revised accordingly and a new lecanorine genus *Lecaimmeria* is proposed. Furthermore, four new species for *Immersaria* and seven new species and three new combinations for the new genus *Lecaimmeria* are proposed. Keys to *Immersaria* and the new genus *Lecaimmeria* are provided.

Keywords

China, generic classification, lecanorine apothecia, lichen, phylogeny, taxonomy

Introduction

The lichen genus *Immersaria* Rambold & Pietschm. (Rambold 1989) was originally split from the genus *Lecidea* Ach. in order to accommodate the species *Immersaria athroocarpa* (Ach.) Rambold & Pietschm. The genus *Immersaria* was characterised by its brown thallus with an epinecral layer, a pruinose margin and an amyloid medulla, immersed apothecia with a somewhat reduced proper margin and *Porpidia*-type asci with eight, simple, halonate ascospores (Rambold 1989). Subsequently, Calatayud and Rambold (1998) enlarged the scope of the genus by including the lecanorine species, *Immersaria mehadiana* Calat. & Rambold and *I. cupreoatra* (Nyl.) Calat. & Rambold, based on morphological characters only. Currently, eight species of *Immersaria* are known worldwide (Lücking et al. 2017), three of which have lecanorine apothecia. Four of these species were previously reported from China (Hertel 1977; Zhang et al. 2015).

The species *Immersaria cupreoatra* (Nyl.) Calat. & Rambold (= *Lecanora cupreoatra* Nyl.) was previously included in *Bellemerea* Hafellner & Cl. Roux (Clauzade and Roux 1984), then into *Immersaria* by Calatayud and Rambold (1998). This caused us to reconsider the relationships between *Bellemerea* and the lecanorine species of *Immersaria* and to question the monophyly of *Immersaria*. The family Lecideaceae Chevall originally included all the crustose lecideoid genera, but now only 25 genera have been retained. Most of these are monospecific genera or small genera with under five species (Fryday and Hertel 2014; McCune et al. 2017). Most genera in Lecideaceae have lecideine apothecia. Three exceptions are *Bellemerea*, *Immersaria* and *Koerberiella* Stein, which have lecanorine apothecia. Only *Immersaria* has both lecanorine and lecideine apothecia, according to the previous circumscription (Calatayud and Rambold 1998; Valadbeigi et al. 2011). Calatayud and Rambold (1998) indicated that the presence of "two types of ascomata" represent different stages of ontogeny. However, there was no molecular evidence that could clarify the species-level phylogenetic relationships within *Immersaria*. In the two-loci phylogenetic tree of Buschbom and Mueller (2004), the lecideine species *Immersaria usbekica* (Hertel) M. Barbero, Nav.-Ros. & Cl. Roux was related to *Lecidea tessellata* Flörke. However, because only two loci of one lecideine species were included, this tree was insufficient to clarify the relationship of the lecanorine apotheciate species in *Immersaria*.

In this study, a phylogenetic tree of Lecideaceae, based on five loci, is established in order to verify the monophyly of *Immersaria*. The results show that *Immersaria* is split into two clades. One clade includes all the lecideine apotheciate species, which is sister to *Lecidea tessellata*, *L. auriculata* Th. Fr., *Cyclohymenia epilithica* McCune & M.J. Curtis and the *Porpidia albocaerulescens* group and the *Porpidia speirea* group. The second clade contains all the lecanorine apotheciate species and is closely related to the rest of the lecanorine apotheciate genera within this family: *Bellemerea* and *Koerberiella*. Therefore, the genus concept of *Immersaria* is revised, retaining only the species with lecideine apothecia. The lecanorine species of *Immersaria* are excluded and proposed as a new genus, *Lecaimmeria* C.M. Xie, Lu L. Zhang & Li S. Wang. Furthermore, four

new species for *Immersaria* and seven new species and three new combinations for the new genus *Lecaimmeria* are proposed, based on the four-loci phylogenetic trees. Keys to *Immersaria* and the new genus are provided below.

Methods

Morphological analysis

All the materials for this study were collected in mainland China, mostly from the Qinghai-Tibetan Plateau, during the authors' participation in The Second Tibetan Plateau Scientific Expedition and Research Program. These specimens were stored in the Herbarium of the Kunming Institute of Botany, Chinese Academy of Sciences (KUN) and the Lichen Section of the Botanical Herbarium, Shandong Normal University (SDNU). Type specimens were loaned from the University of Helsinki (H) and Universität Wien (WU). High-resolution photographs of type specimens were provided by the curators of H or obtained from the website Global Plants (https://plants.jstor.org/). Morphological descriptions were made from under a dissecting microscope COIX. Anatomical descriptions were based on observations made from hand-cut sections, mounted in water and using a NIKON microscope. Usually, twenty ascospores were measured and the values of measurement means smallest measured-largest measured, with outlying values in brackets. Photographs were captured with a NIKON Eclipse 50i microscope, equipped with a NIKON digital camera (DSFi2 high-definition colour camera head, NIKON, Japan). The specimens were tested with a 10% aqueous solution of potassium hydroxide (K), a solution of aqueous sodium hypochlorite (C) and 3% Lugol's iodine (I) in the medulla and the surface of the thallus. Secondary metabolites of all the specimens were examined by thin-layer chromatography (TLC) methods, using Solvents A, B and C, as described by Orange et al. (2001).

Phylogenetic analysis

Molecular analysis was carried out on the selected specimens. Genomic DNA was extracted from dry or fresh specimens using a DNAsecure Plant Kit (Tiangen), following the manufacturer's instructions. Five gene loci were amplified by using the following primers: ITS1F (Larena et al. 1999), ITS4 (White et al. 1990), LR0R (Rehner and Samuels 1994), LR5 (Vilgalys and Hester 1990), gRPB1a (Stiller and Hall 1997), fRPB1c (Matheny et al. 2002), RPB2–6f, RPB2–7cr (Liu et al. 1999), mrSSU1 and mrSSU3R (Zoller et al. 1999). The 25 μl PCR mixture consisted of 2 μl DNA, 1 μl of each primer, 12.5 μl 2 × Taq PCR MasterMix (Aidlab) (Taq DNA Polymerase [0.1 unit/ml]; 4 mM $MgCl_2$; and 0.4 mM dNTPs) and 8.5 μl ddH_2O. Conditions for PCR of nrITS, nrLSU and mtSSU were set for an initial denaturation at 94 °C for 10 min, followed by 34 cycles of denaturation at 95 °C for 45 s, annealing at 50 °C for 45 s, extension at 72 °C for 90 s and a final extension at 72 °C for 10 min. For RPB1 and

RPB2, the parameters were set to an initial denaturation at 94 °C for 10 min, followed by 34 cycles of denaturation at 95 °C for 45 s, annealing at 52 °C for 50 s, extension at 72 °C for 60 s and a final extension at 72 °C for 5 min. The PCR products were sequenced using Sanger technology by the company of Tsingke Biological Technology (Beijing).

The raw sequences were assembled and edited using SeqMan v.7.0 (DNAstar packages). Sequences extracted from new materials with each gene locus were aligned with additional sequences that were available from GenBank (Suppl. material 1: Table S1), by using MEGA v.10.0 and an online version of MAFFT v.7.0 to generate nrITS-nrLSU-RPB1-RPB2-mtSSU or nrITS-nrLSU-RPB1-RPB2 matrices. The five or four gene matrices were combined by SequenceMatrix v.1.7.8. and the concatenated alignments were estimated by PartitionFinder 2 (Lanfear et al. 2017), based on the Bayesian Information Criterion (BIC), to find the most appropriate nucleotide substitution model for each of the five loci.

Phylogenetic relationships were inferred using Bayesian Inference (BI) and Maximum Likelihood (ML). ML analyses were performed with RAxMLHPC using the general time reversible model of nucleotide substitution with the gamma model of rate heterogeneity (GTRGAMMA or GTRCAT). The analyses were run with a rapid bootstrap analysis using 1000 replicates with data partitioned. The Bayesian method was performed with MrBayes v.3.1.2 (Huelsenbeck and Ronquist 2001). Four Markov chains were run with 2 million generations for each dataset and trees were sampled every 100 generations. It was ensured that the average standard deviation of split frequencies was lower than 0.01. Posterior probabilities above 0.9 and bootstrap support above 70% were considered significant supporting values. All the trees were visualised with FigTree v. 1.4.0 (Rambaut 2012).

Results

A total of 172 sequences of the nrITS, nrLSU, RPB1, RPB2, and mtSSU were generated from 61 specimens representing 57 species. Although the five-loci tree only poorly resolved the hierarchy of genera within the family Lecideaceae and the split between the lecanorine and lecideine genera of Lecideaceae was without robust support, nonetheless the results revealed that the genus *Immersaria* was not a monophyletic lineage. Rather, it was divided into two distant and well-supported lineages: clade 1 which contained the lecideine apotheciate species and clade 2 which contained the lecanorine apotheciate species (Fig. 1).

Clade 1, together with *Amygdalaria* Norman, *Cyclohymenia* McCune & M.J. Curtis, *Lecidea* s str. and *Porpidia* Körb. (Fig. 1) formed a well-supported clade (93%

MLBS and 0.99 PP), all of which have lecideine apothecia. *Amygdalaria*, *Porpidia* and *Lecidea* s str. were nested together, which was consistent with the results of previous research (Buschbom and Mueller 2004; Fryday et al. 2014). However, the relationships between these genera still need further research. There was a high level of support for a monophyletic lineage of lecideine apotheciate species of *Immersaria*, with these being

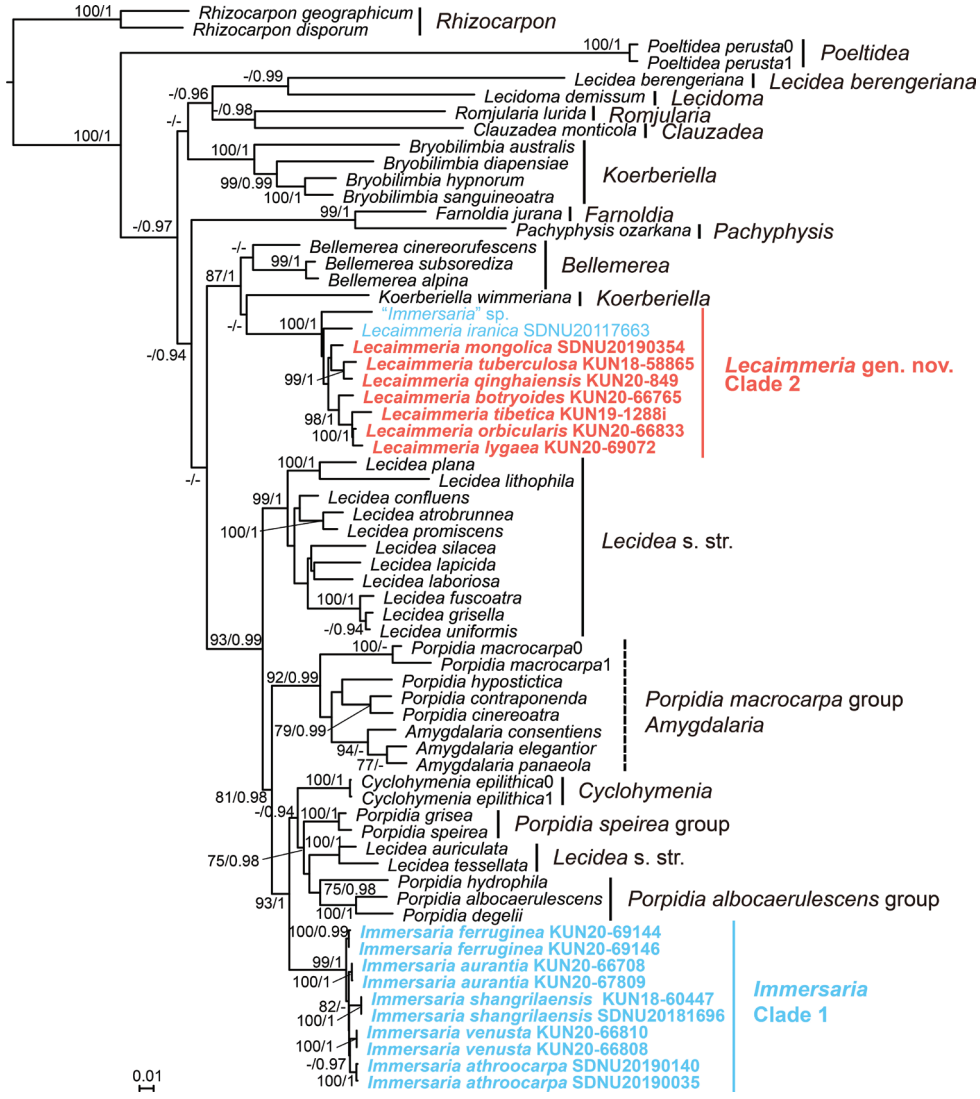

Figure 1. Phylogenetic tree constructed from Maximum Likelihood analyses in Lecideaceae, based on the concatenated nrITS-nrLSU-RPB1-RPB2-mtSSU dataset. Maximum Likelihood bootstrap probabilities above 70% (left) and Bayesian Inference posterior probabilities above 0.9 (right) are given at the nodes.

sister to the *Lecidea tessellata*, *L. auriculata*, *Cyclohymenia*, the *Porpidia albocaerulescens* group and the *Porpidia speirea* group. The type species of *Immersaria* (*I. athroocarpa*) was included in the lineage. Thus, only those *Immersaria* species with lecideine apothecia belong to *Immersaria* s. str. This revised concept of the genus *Immersaria* is as follows: a glossy surface of thallus with an epinecral layer, immersed lecideine apothecia with a reduced margin and *Porpidia*-type asci with halonate ascospores.

There was also a high level of support for clade 2 as a monophyletic lineage (100% MLBS and 1.00 PP), which was clustered with other genera of *Lecideales* with lecanorine apothecia: *Bellemerea* and *Koerberiella* (Fig. 1). *Bellemerea* could be distinguished from Clade 2 by its amyloid ascospores and *Koerberiella* by its adnate apothecia. Although the topology of clade 2 for *Bellemerea* and *Koerberiella* is not robust, there are conspicuous differences in their morphology and significant differences between the bases in their nucleotide sequences. Since clade 2 is monophyletic with strong support, a new genus, *Lecaimmeria*, is proposed to accommodate clade 2. The new genus has immersed lecanorine apothecia with a white margin and a distinct plectenchyma developed on top of the orange epihymenium.

Two additional phylogenetic trees were constructed, based on four loci (nrITS, nrLSU, RPB1, and RPB2), in order to assess the phylogenetic position of species within *Immersaria* and *Lecaimmeria*, respectively. The phylogenetic tree of *Immersaria* was comprised of one highly supported clade with five separate lineages, based on 105 sequences from 37 specimens (Fig. 2). All the species with brown, orange, irregular or aggregate thalli formed respective monophyletic lineages. *Immersaria shangrilaensis* C.M. Xie & Lu L. Zhang formed a well-supported clade and the aggregate areolae clearly distinguished *I. shangrilaensis* from other species. *Immersaria ferruginea* C.M. Xie & Li S. Wang also formed a well-supported clade and differed from other species by its greyish-brown thallus. It seems that *Immersaria shangrilaensis* is sister to *I. ferruginea*, but the nodes were without support. In addition, the morphology is distinct between *Immersaria shangrilaensis* and *I. ferruginea*. The robust lineage *Immersaria aurantia* C.M. Xie & Li S. Wang was distinguished by its irregular, conspicuously orange thallus and green epihymenium. *Immersaria athroocarpa* was sister to *I. venusta* C.M. Xie & Xin Y. Wang, but differed in its convex, polygon areolae and densely crowded apothecia.

The phylogenetic tree of *Lecaimmeria* was comprised of one well-supported clade with nine separate lineages, based on 140 sequences from 61 specimens (Fig. 3). "*Immersaria*" sp. and *Lecaimmeria iranica* (Valadb., Sipman & Rambold) C.M. Xie comprised the basal group. "*Immersaria*" sp. has only been recorded from Macedonia and *Lecaimmeria iranica* has been recorded from Inner Mongolia in China and from Iran. *Lecaimmeria tuberculosa* C.M. Xie & Xin Y. Wang was sister to *L. qinghaiensis* C.M. Xie & Li S. Wang, but conspicuously differed in its tuberculiform conidiomata. *Lecaimmeria mongolica* C.M. Xie & Lu L. Zhang formed a well-supported monophyletic lineage and its population was mainly recognised by its orange, irregular areolae and gyrophoric acid content. *Lecaimmeria botryoides* C.M. Xie & Li S. Wang formed a highly supported sister group to *L. orbicularis* C.M. Xie & Lu L. Zhang, *L. lygaea* C.M. Xie & Lu L. Zhang and *L. tibetica* C.M. Xie & Xin Y. Wang, but differed in its crowded apothecia. *Lecaimmeria orbicularis* formed a highly supported sister group to *L. lygaea* and *L. tibetica*, but differed in its round apothecia and the white margin of the apothecia. *Lecaimmeria lygaea* was seemingly sister to *L. tibetica* and differed in its areolae having a black margin and with a well-developed prothallus between areolae.

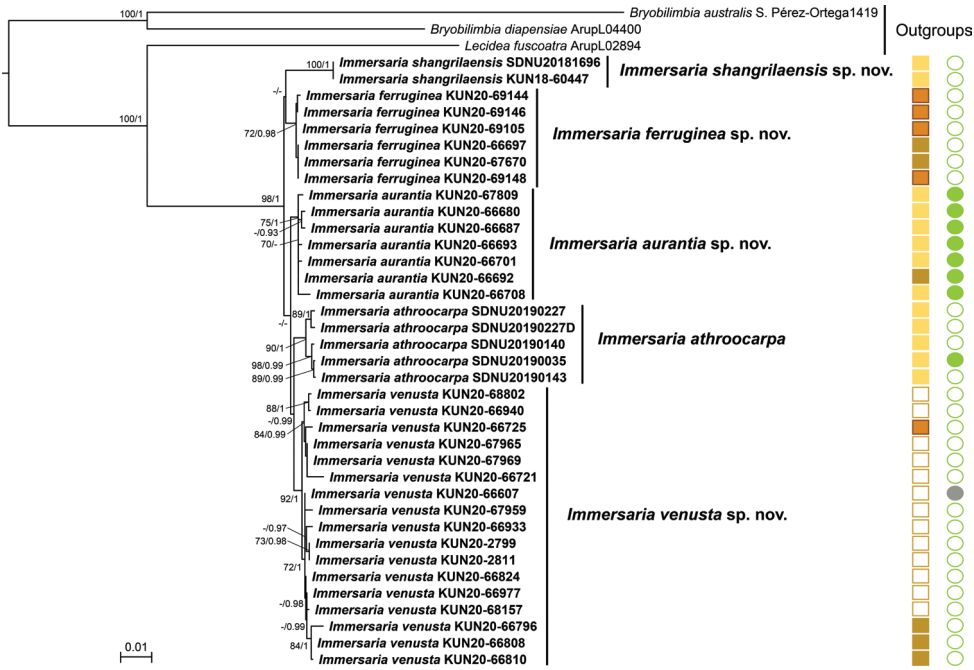

Figure 2. Phylogenetic tree constructed from Maximum Likelihood analyses in *Immersaria,* based on the concatenated nrITS-nrLSU-RPB1-RPB2 dataset. Maximum Likelihood bootstrap probabilities above 70% (left) and Bayesian Inference posterior probabilities above 0.9 (right) are given at the nodes. Solid brown rectangle: thallus brown; solid orange rectangle: thallus yellow brown to orange brown; solid red rectangle: thallus rusty; hollow brown rectangle: thallus pale yellow brown. Solid green circle: green epihymenium; solid grey circle: without apothecia; hollow green circular: brown epihymenium.

Discussion

Revised boundaries of *Immersaria*

Formerly, the boundaries for *Immersaria* species were: lecanorine or lecideine type of immersed apothecia, production of confluentic acid and gyrophoric acid and ostiole or stellate shapes of conidiomata. However, these characters were not good characters by which to distinguish this genus. The lecanorine species *Immersaria cupreoatra* was previously included in *Bellemerea*. Based on many specimens from China, it was also discovered that the ostiole or stellate shapes of conidiomata appeared in different stages of ontogeny. The main substances produced in the genus are confluentic acid and gyrophoric acid; confluentic acid only occurs in lecideine species, whereas gyrophoric acid appears in lecanorine species, with the exception of one lecideine species *Immersaria usbekica.* Furthermore, these characters, the types of apothecia and the shapes of conidiomata could not be applied as proper delimitations to classify species within *Immersaria*, neither were they supported by the phylogeny.

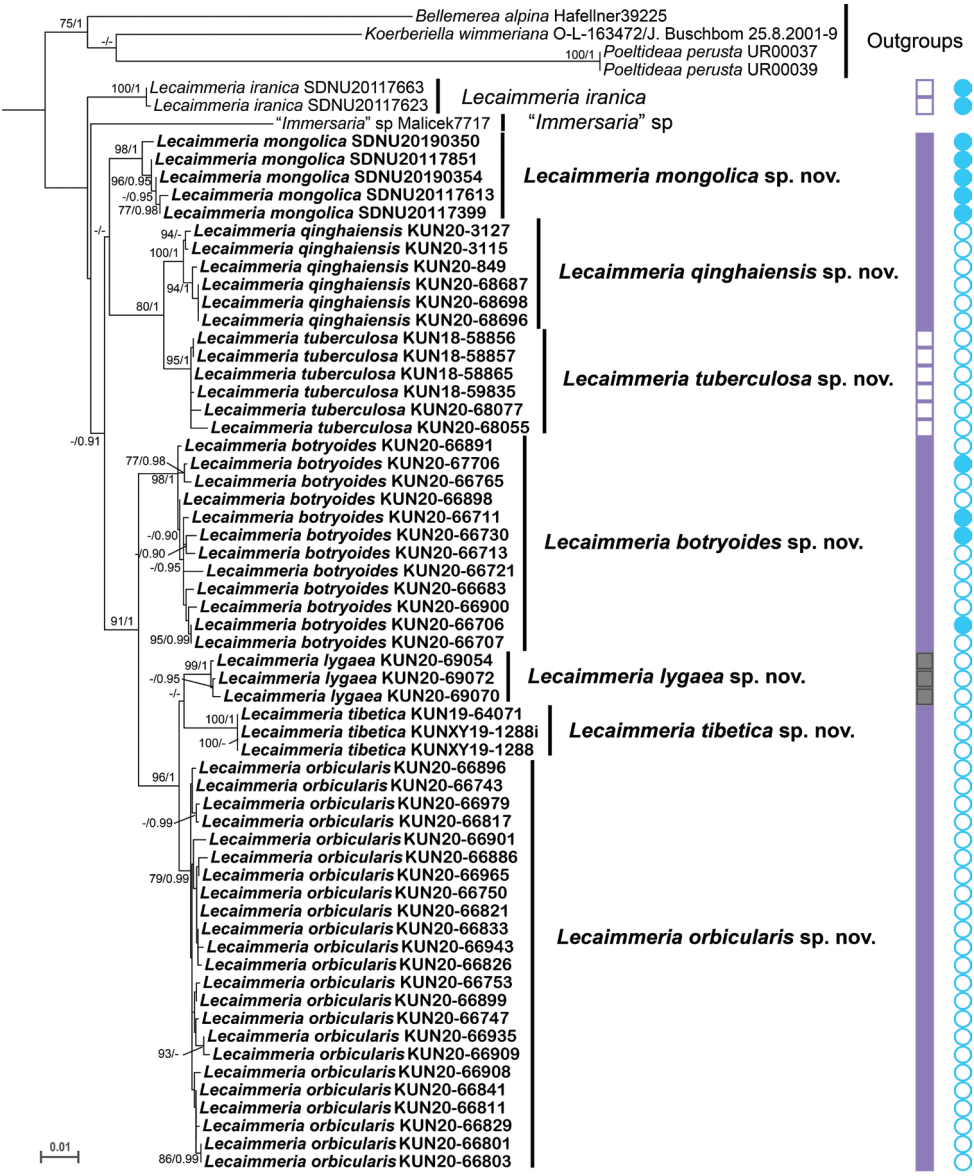

Figure 3. Phylogenetic tree constructed from Maximum Likelihood analyses in *Lecaimmeria,* based on the concatenated nrITS-nrLSU-RPB1-RPB2 dataset. Maximum Likelihood bootstrap probabilities above 70% (left) and Bayesian Inference posterior probabilities above 0.9 (right) are given at the nodes. Solid purple rectangle: areolae margin white; solid grey rectangle: areolae margin black; hollow purple rectangle: areolae margin jade green pigmented. Solid blue circle gyrophoric acid; hollow blue circle: none.

The five-loci based analysis (Fig. 1) was incompatible with previous circumscriptions of the genus *Immersaria*, the members of which in this study are defined by their lecideine immersed apothecia, brown areolae with an epinecral layer and brown/green epihymenium without a plectenchyma. Consequently, a new genus, *Lecaimmeria*,

is established to accommodate the excluded lecanorine species. The new taxonomic system, proposed here, revised the classification boundaries between *Immersaria* and *Lecaimmeria*, but it may still be difficult to distinguish between them in cases when apothecia are absent. In this case, they could be distinguished by the substances produced or by molecular methods.

Diagnostic traits within species of *Immersaria* and *Lecaimmeria*

Species of *Immersaria* could be identified by their different thallus colours (indicated in Fig. 2). *Immersaria ferruginea* has a conspicuously greyish-brown thallus, whereas *I. athroocarpa*, *I. aurantia*, *I. shangrilaensis* and *I. venusta* have a reddish-brown thallus. *Immersaria athroocarpa* (indicated in Fig. 2) is the species that mostly has a green epihymenium, whereas the other species mostly have a brown epihymenium. Almost all these species contain confluentic acid, which is often accompanied by 2'-O-methylmicrophyllinic acid. Planaic acid, which is newly reported from this genus, is only presented in specimens of *Immersaria aurantia*, *I. shangrilaensis* and *I. venusta*. All the characters discussed above were supported by the phylogeny, thus could be used as key characters to differentiate species in *Immersaria*.

Species of the new genus *Lecaimmeria* could be delimited by the colours of their areolae and margins, the existence of an apothecial margin and usually by the lack of substances. The margin of areolae (indicated in Fig. 3) was usually white, but rarely black or jade green. *Lecaimmeria lygaea* could be easily distinguished by the black margin of the areolae. The jade green margin occurs in *Lecaimmeria tuberculosa*, which grows on Qilian jade. The areolae margin of *Lecaimmeria qinghaiensis* is white, but is occasionally pigmented with very slightly green colour. The margin of the apothecia is absent in *Lecaimmeria tuberculosa* and *L. iranica*, whereas the apothecia of the other species have white margins. Most species of *Lecaimmeria* lack secondary metabolites, while gyrophoric acid was detected only in *Lecaimmeria botryoides*, *L. iranica* and *L. mongolica* (indicated in Fig. 3). In addition, an orange thallus appeared only in *Lecaimmeria mongolica* and *L. tibetica*, whereas the remaining species were brownish.

Taxonomy

***Immersaria* Rambold & Pietschm., Bibliotheca Lichenologica 34: 239 (1989).**

Type species. *Immersaria athroocarpa* (Ach.) Rambold & Pietschm., in Rambold, Biblioth. Lichenol. 34: 240 (1989).

Description. Thallus crustose, yellow-brown, red-brown, orange-brown or brown, sometimes rust coloured, continuous; areolae irregular or tending to rectangular, with a glossy surface (*atrobrunnea*-type) caused by a layer of dead, colourless cells above the upper cortex, areolae sometimes aggregate with black

prothallus and forming larger areolae; margin pruinose; prothallus distinct at the margin of thallus or absent. Upper cortex orange pigmented; epinecral layer colourless; algal layer continuous; medulla filled with grey granules. Apothecia lecideine, immersed, sometimes aggregate, round or irregular; disc black, flat, less concave, sometimes slightly raised, often poorly developed in section, pruinose or not; margin reduced. Exciple almost absent, sometimes developed, brown. Hymenium colourless; paraphyses simple, rarely branched, anastomosing or not; epihymenium brown, green or brown green, without plectenchyma; subhymenium colourless, sometimes pale brown; hypothecium pale brown to brown. Asci *Porpidia*-type, cylindrical, eight-spored; ascospores ellipsoid, halonate, non-amyloid. Conidiomata present or not, immersed, linear or stellate, black, margin pruinose; conidia bacilliform.

Chemistry. Thallus K–, C–. Medulla I+ violet. Confluentic acid, often accompanied with 2'-O-methylmicophyllinic acid, planaic acid or no substances detected by TLC. The compound planaic acid is newly reported in this genus.

Ecology and distribution. In China, growing on bare rock, sandstone or granite, from elevations of 3800 to 4500 m in the alpine zone of west China and elevations of 1200 to 1900 m in the steppe of north China. Worldwide distribution.

Notes. Species with lecanorine apothecia were previously included in *Immersaria* (Calatayud and Rambold 1998; Valadbeigi et al. 2011), but the five-loci phylogenetic analysis excluded these species from *Immersaria.* This exclusion entails a restricted concept of the genus. *Immersaria* is now defined by its orange-brown, yellow-brown, sometimes rusty coloured thallus, the amyloid medulla, the glossy surface of areolae with a pruinose margin, the black immersed lecideine apothecia with a reduced proper margin, the brown epihymenium and the *Porpidia*-type asci with eight halonate and non-amyloid ascospores. The members of this genus occur in alpine habitats.

Species of *Sporastatia* A. Massal. might be misidentified as members of *Immersaria* because of field observations of their glossy areolae and the immersed lecideine apothecia. However, they are characterised by multi-spored asci and their yellow-brown thallus. Additionally, *Miriquidica* Hertel & Rambold resembles *Immersaria* by its glossy areolae and the lecideine apothecia, but differs in its black brown thallus, its *Lecanora*-type asci with non-halonate ascospores and often containing miriquidic acid. The immersed apothecia of *Immersaria* may resemble *Aspicilia* A. Massal. and *Acarospora* A. Massal., but *Aspicilia* has a white or grey thallus, the *Aspicilia*-type asci with non-halonate ascospores; *Acarospora* has multi-spored asci.

Although four known species, *Immersaria carbonoidea* (J.W. Thomson) Esnault & Cl. Roux, *I. fuliginosa* Fryday, *I. olivacea* Calat. & Rambold and *I. usbekica*, currently lack molecular data, they are temporarily left in *Immersaria* due to their morphology which corresponds to that of *Immersaria.* Our morphological comparisons were based on high-resolution photographs of type materials and the original descriptions.

***Immersaria athroocarpa* (Ach.) Rambold & Pietschm., in Rambold, Biblioth. Lichenol. 34: 240 (1989).**
Figure 4a–e

Type. Sweden [no locality, no date, no collector], H9508237 (H-Ach-lectotype!–designated in Hertel 1977). High-resolution photographs seen.

Description. Thallus areolate, yellow-brown, orange-brown, continuous; areolae 0.2–1.0 mm across, often convex, regular polygons, tends to be squamalose at the margin, epruinose; margin pruinose; prothallus black, not distinct, sometimes absent. Upper cortex ca. 32.0 μm thick, yellow-brown; epinecral layer ca. 7.0 μm thick; algal layer ca. 82.0 μm thick, cells 8.0–10.0 × 7.5 μm in diam., ellipsoid. Apothecia frequent, densely crowded, immersed, 0.3–1.3 mm in diam.; disc black, rare pruinose, flat, epruinose; margin reduced. Exciple sometimes developed, 25.0–30.0 μm wide, brown. Hymenium 100–115 μm thick, colourless; paraphyses 1.0–2.0 μm wide, branched, not anastomosing; epihymenium 20.0–25.0 μm thick, brown, rarely green; subhymenium ca. 90.0 μm thick, colourless; hypothecium pale brown to brown. Asci *Porpidia*-type, cylindrical, eight-spored; ascospores 17.5–20.0 × 10.0 μm, ellipsoid, halonate. Conidiomata immersed, stellate, black, margin pruinose; conidia 7.5–10.0 × 1.0 μm in diam., bacilliform.

Chemistry. Thallus K–, C–. Medulla I+ violet. Chemotype I: Confluentic acid. Chemotype II: Unknown substance.

Ecology and distribution. In China, growing on granite in arid and semi-arid steppe habitats at elevations of 1200–1950 m. Worldwide distribution. This species is known from Inner Mongolia and Mt. Changbai (Hertel and Zhao 1982) in China.

Notes. The lectotype grows on siliceous rock and contains several intact apothecia. The materials from Inner Mongolia are identical with the lectotype, based on comparisons with high-resolution photographs and the description given by Hertel (1977). It is, therefore, treated as *Immersaria athroocarpa* at present. Some Inner Mongolian materials contain an unknown substance, but form a well-supported clade with other materials. *Immersaria athroocarpa* is characterised by the convex, yellow-brown areolae and the large sizes of ascospores. In this genus, only this species has ascospores up to 20.0 μm long.

Immersaria usbekica is similar to *I. athroocarpa* in its brown thallus and dense apothecia, but differs in its flat areolae, the brown epihymenium and the presence of confluentic acid and gyrophoric acid. By comparison with high-resolution photographs and the original descriptions (Hertel 1977) of *Immersaria usbekica*, we discovered that previous reports of this species from China (Zhang et al. 2015) were due to misidentification. It is known from Algeria, Iran, Spain, and the USSR (Barbero et al. 1990).

Specimens examined (SDNU). China. Inner Mongolia: Chifeng City, Balin Youqi, Hongshilazi, 1403.2 m elev., 44°13'N, 118°44'E, on rock, 2019, Ling Hu et al. SDNU20190035; Rongshen, Wangfengou, 1217.4 m elev., 44°16'N, 118°22'E, Ling Hu et al. SDNU20190140, SDNU20190143; Erlinba, 1915.2 m elev., 44°26'N, 118°41'E, Ling Hu et al. SDNU20190227.

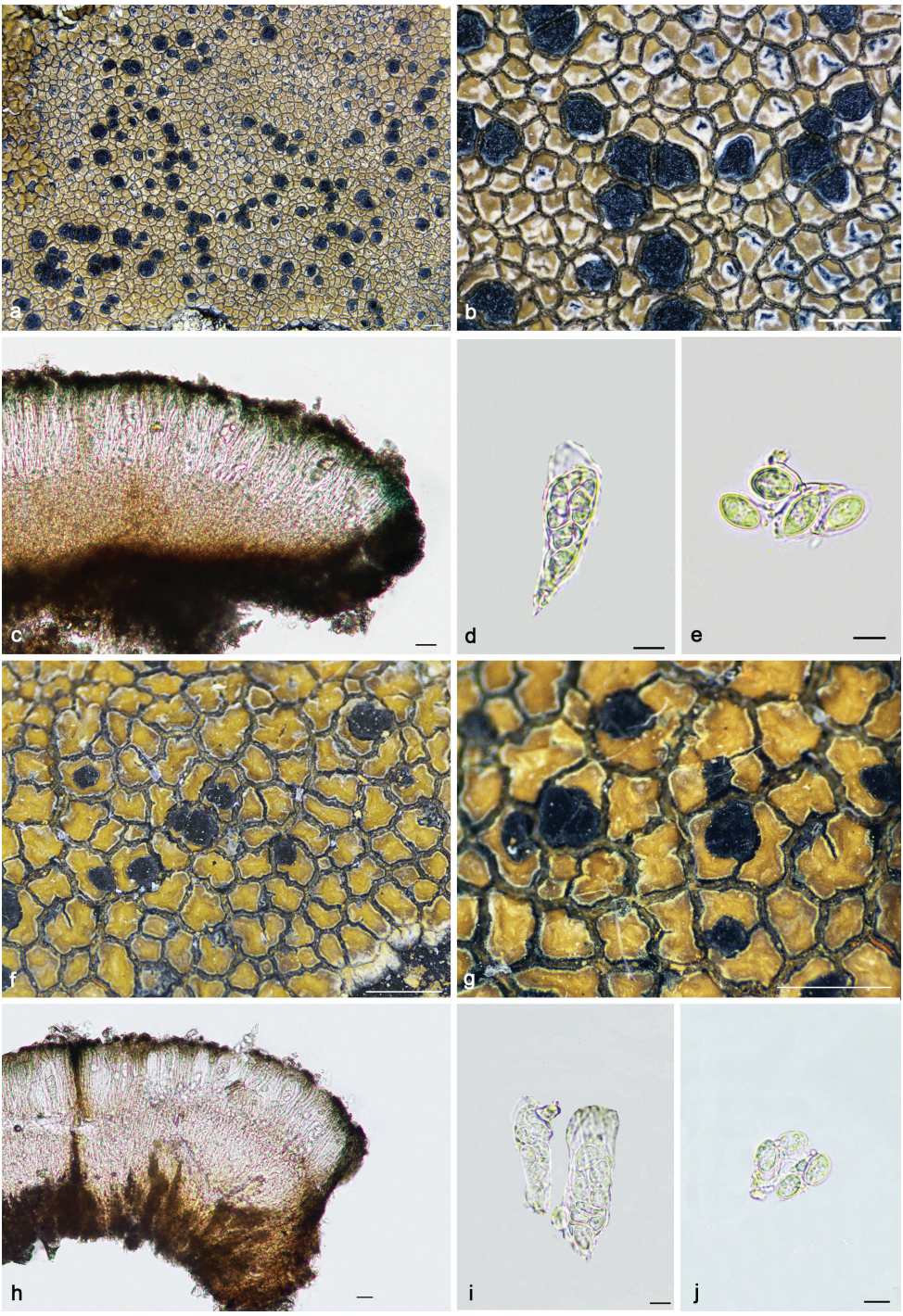

Figure 4. *Immersaria athroocarpa* (**a–e** SDNU20190227): **a–b** thallus **c** apothecial anatomy **d** ascus **e** ascospores. *I. aurantia* (**f–j** KUN XY19–1290): **f–g** thallus **h** apothecial anatomy **i** ascus **j** ascospores. Scale bars: 1 mm (**a–b, f–g**); 20 μm (**c, h**); 10 μm (**d–e, i–j**).

***Immersaria aurantia* C.M. Xie & Li S. Wang, sp. nov.**
MycoBank No: 839738
Figure 4f–j

Etymology. The name "aurantia" refers to the orange thallus.

Type. China. Tibet: Sajia Co., Mula Village, 4752 m elev., 28°40'N, 88°45'E, on rock, 28 Jun 2019, Xin-Yu Wang et al. XY19–1814 (KUN-holotype).

Description. Thallus areolate, orange, dark orange, pale orange to pale red-brown, continuous; areolae 0.7–1.3 mm across, flat, epruinose, irregular; margin thin pruinose; prothallus not seen. Upper cortex 25.0–45.0 μm thick, orange; epinecral layer (12.0–) 37.0–63.0 μm thick, uneven; algal layer 50.0–93.0 μm thick, cells 5.0–15.0 × 5.0–10.0 μm in diam., round to ellipsoid. Apothecia frequent, scattered, immersed or isolated from areolae, 0.3–1.3 mm in diam.; disc black, flat or concave, sometimes pruinose; margin reduced. Exciple sometimes developed, ca. 30.0 μm wide, brown. Hymenium 55.0–83.0 μm thick, colourless; paraphyses 2.0–3.0 μm wide, only branched and anastomosing at apex; epihymenium ca. 20.0 μm thick, green or green-brown; subhymenium colourless, not distinct or absent; hypothecium brown. Asci *Porpidia*-type, cylindrical, eight-spored; ascospores 8.0–15.0 × 5.0–7.5 μm in diam., ellipsoid, halonate. Conidiomata rare, immersed, oblate, black, margin white; conidia 7.5 × 1.0 μm, bacilliform.

Chemistry. Thallus K–, C–. Medulla I + violet. Chemotype I: Confluentic acid, often accompanied with 2'-O-methylmicrophyllinic acid. Chemotype II: Planaic acid. Chemotype III: none (rare).

Ecology and distribution. In China, growing on rock at elevations of 3900–4300 m in the alpine zone. This species is known from Qinghai, Sichuan Province and Tibet of China.

Notes. *Immersaria aurantia* is characterised by its distinct orange, irregular areolae and the mostly green epihymenium. *Immersaria athroocarpa* and *I. venusta* are similar to *I. aurantia*, but *I. athroocarpa* differs in the convex, regularly polygonal areolae and the more crowded apothecia; *I. venusta* differs in having yellow-brown, often rusty, cracked areolae and flat apothecia. Additionally, confluentic acid and planiaic acid do not appear simultaneously in *Immersaria aurantia*, whereas *I. venusta* always contains both compounds.

Specimens examined (KUN). China. Qinghai Province: Banma Co., 3933 m elev., 32°40'N, 100°48'E, on rock, 2020, Li-Song Wang et al. 20–66886, 3932 m elev., Li-Song Wang et al. 20–66897; Jiuzhi Co., Baiyu Village, 4285 m elev., 33°14'N, 100°58'E, Li-Song Wang et al. 20–67809. Sichuan Province: Rangtang Co., Mt. Haizi, 4223 m elev., 32°20'N, 101°25'E, on rock, 2020, Li-Song Wang et al. 20–66701, 4229 m elev., Li-Song Wang et al. 20–66693, 4217 m elev., Li-Song Wang et al. 20–66680, 4221 m elev., Li-Song Wang et al. 20–66692. Tibet: Changdu City, Mangkang Co., Luoni Village, 4145 m elev., 29°56'N, 98°33'E, on rock, 2020, Li-Song Wang et al. 20–69091, 4138 m elev., Li-Song Wang et al. 20–69091, 20–69094; Gatuo Town, 29°39'N, 98°35'E, 3831 m elev., Li-Song Wang et al. 20–69114, 3850 m elev.,

Li-Song Wang et al. 20–69122; Gongga Co., Jiangtang Town, 29°12'N, 90°38'E, 2019.7.23, 4560 m elev., Xin-Yu Wang et al. XY19–1287, 4556 m elev., XY19–1290; Sajia Co., Mula Village, 28°40'N, 88°45'E, 2019.7.28, 4752 m elev., Xin-Yu Wang et al. XY19–1814; Angren Co., Kerangla, 29°19'N, 87°01'E, 4530 m elev., Li-Song Wang et al. 19–63635.

Immersaria ferruginea **C.M. Xie & Li S. Wang, sp. nov.**
MycoBank No: 839739
Figure 5a–c

Etymology. The name "ferruginea" refers to the rusty brown colour of the thallus.

Type. China. Tibet: Changdu City, Mangkang Co., Quzika Village, 4093 m elev., 29°15'N, 98°40'E, on rock, 25 Sept 2020, Li-Song Wang et al. 20–69144 (KUN-holotype).

Description. Thallus areolate, greyish-brown, continuous; areolae 0.5–1.3 mm across, flat, less often convex, rectangular to polygonal, epruinose; margin pruinose; prothallus black, not distinct. Upper cortex 50.0–68.0 μm thick, brown; epinecral layer 17.0–40.0 μm thick; algal layer 75.0–78.0 μm thick, cells (4.0–) 7.0–13.0 μm diam., round. Apothecia frequent, densely crowded, immersed, 0.7–1.3 mm in diam.; disc black, flat, pruinose; margin pruinose, slightly raised. Exciple sometimes developed, 25.0–28.0 μm wide, brown. Hymenium 57.0–100.0 μm thick, colourless; paraphyses 1.0–3.0 μm wide, not branched, anastomosing; epihymenium 15.0–33.0 μm thick, brown; subhymenium 25.0–63.0 μm thick, colourless to pale brown, rusty or dark pink; hypothecium pale brown. Asci *Porpidia*-type, cylindrical; ascospores rare, 7.5–10.0 × 5.0 μm in diam., ellipsoid, halonate. Conidiomata not seen.

Chemistry. Thallus K–, C–. Medulla I+ violet. Confluentic acid, often accompanied with 2'-O-methylmicrophyllinic acid.

Ecology and distribution. In China, growing on quartz sandstone or granite at elevations of 3800–4300 m in the alpine zone. This species is known from Sichuan Province and Tibet of China.

Notes. *Immersaria ferruginea* is characterised by its brown, rusty thallus, its densely crowded apothecia and its brown epihymenium. The morphology of *Immersaria ferruginea* resembles *I. carbonoidea*, but the latter differs in its dark black-brown thallus containing norstictic acid and black-brown hypothecium.

Specimens examined (KUN). China. Sichuan Province: Rangtang Co., Mt. Haizi, 4227 m elev., 32°20'N, 101°25'E, on rock, 2020, Li-Song Wang et al. 20–66697, 4221 m elev., Li-Song Wang et al. 20–67670. Tibet: Changdu City, Mangkang Co., Quzika Village, 4093 m elev., 29°15'N, 98°40'E, Li-Song Wang et al. 20–69144, 4101, Li-Song Wang et al. 20–69146, 4122 m elev., Li-Song Wang et al. 20–69148; Gatuo Town, 3848 m elev., 29°39'N, 98°35'E, Li-Song Wang et al. 20–69105.

***Immersaria shangrilaensis* C.M. Xie & Lu L. Zhang, sp. nov.**
MycoBank No: 839741
Figure 5d–f

Etymology. The name "shangrilaensis" refers to the location at which the holotype was collected: "Shangri-La", a county of Yunnan Province in China.

Type. China. Yunnan Province: Shangri-La County., Mt. Hong Shan, 4363 m elev., 28°7'N, 99°54'E, on rock, 18 Aug 2018, Li-Song Wang et al. 18–60447 (KUN-holotype).

Description. Thallus areolate, yellow-brown, orange-brown, often appears as greyish-brown, generally heavily pruinose, continuous, 5.7–10.0 cm across; areolae aggregated by 4–14 small areolae (often surrounded by black prothallus), small areolae up to 0.1 mm across, concave or flat, irregular, pruinose; margin pruinose; prothallus black, distinct. Upper cortex 32.0–50.0 μm thick, yellow-brown granules pigmented; epinecral layer 15.0–20.0 μm thick; algal layer 47.5–65.0 μm thick, cells 7.5–8.0 × 5.0 μm in diam., ellipsoid. Apothecia frequent, crowded, immersed or isolated from areolae, 0.3–0.8 mm in diam.; disc black, concave to flat, aggregated, cracked once mature, thin pruinose; margin reduced, slightly raised. Exciple almost absent. Hymenium 100.0–138.0 μm thick, colourless; paraphyses ca. 2.5 μm wide, branched, anastomosing or not; epihymenium ca. 15.0 μm thick, brown; subhymenium ca. 55.0 μm thick, colourless; hypothecium pale brown to brown. Asci *Porpidia*-type, cylindrical, eight-spored; ascospores 7.0–9.0 × 3.0–4.0 μm, ellipsoid, halonate (sometimes not distinct). Conidiomata immersed, oblate, black, margin heavily pruinose; conidia 7.5 × 1.0 μm, bacilliform.

Chemistry. Thallus K–, C–. Medulla I+ violet. Confluentic acid, planaic acid and/or 2'-O-methylmicophyllinic acid.

Ecology and distribution. In China, growing on granite at elevations of 4300–4500 m in the alpine zone. This species is known from Yunnan Province of China.

Notes. The materials of *Immersaria athroocarpa* from the Shangri-La County of Yunnan Province are morphologically identical with the specimen Hertel (1977) reported from the same locality, but differ from the lectotype in its aggregate areolae, the aggregate apothecia and the smaller size of ascospores (7.0–9.0 × 3.0–4.0 μm). Based on the phenotypic and phylogenetic results, the material from Shangri-La is treated as a new species, *Immersaria shangrilaensis*. It is characterised by its large thallus, up to 10.0 cm in diam., the aggregate areolae and apothecia and the small size of ascospores.

Specimens examined. China. Yunnan Province: Shangri-La County, 4350–4500 m elev., on rock, 1915, Handel-Mazzetti no. 6945 = WU-Lichenes0037752 (WU); Mt. Hong Shan, 4363 m elev., 28°7'N, 99°54'E, on rock, 2018, Li-Song Wang et al. 18–60430 (KUN), Li-Song Wang et al. 18–60447 (KUN) 4503.1 m elev., Chun-Xiao Wang et al. SDNU20181696 (SDNU), 4361.9 m elev., Chun-Xiao Wang et al. SDNU20181675 (SDNU); Luquan Co., Mt. Jiaozixueshan, 3800 m elev., 2008, Hai-Ying Wang SDNU20082253 (SDNU); Lijiang City, Mt. Laojun, 3981 m elev., 26°37'N, 99°43'E, 2018, Li-Song Wang et al. 18–60555, 18–60602 (KUN).

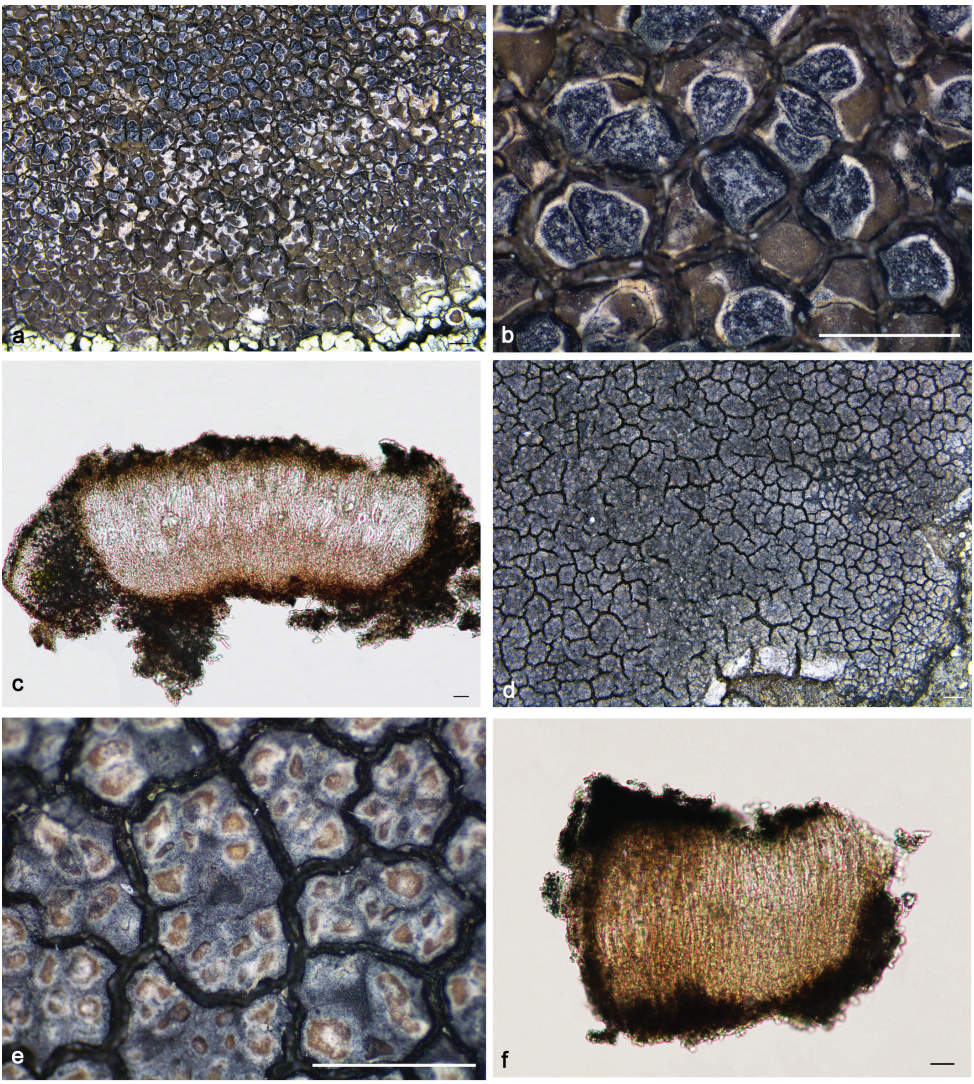

Figure 5. *Immersaria ferruginea* (**a–c** KUN 20–69144): **a–b** thallus **c** apothecial anatomy. *I. shangrilaensis* (**d–f** KUN 18–60430): **d–e** thallus **f** apothecial anatomy. Scale bars: 1 mm (**a–b, d–e**); 20 μm (**c, f**).

Immersaria venusta **C.M. Xie & Xin Y. Wang, sp. nov.**
MycoBank No: 839742
Figure 6a–d

Etymology. The name "venusta" refers to the beautiful appearance of the thallus.

Type. China. Qinghai Province: Maqing Co., Xueshan Village, 4187 m elev., 34°37'N, 99°42'E, on rock, 11 Sept 2020, Li-Song Wang et al. 20–67969 (KUN-holotype).

Description. Thallus areolate, brown, orange-brown, more or less rusty, continuous; areolae 0.5–1.3 mm across, flat or slightly convex, irregular, tending to rectangular, often cracked, sometimes pruinose; margin pruinose; prothallus not seen. Upper cortex ca. 38.0 μm thick, yellow brown granules pigmented; epinecral layer ca. 12.0 μm thick; algal layer ca. 128.0 μm thick, cells 5.0–10.0 × 5.0–7.5 μm in diam., round to ellipsoid. Apothecia frequent, crowded, immersed or isolated from areolae, 0.6–1.0 mm in diam.; disc black, flat, epruinose; margin reduced, sometimes developed. Exciple sometimes developed, ca. 35.0 μm wide, brown. Hymenium 92.0–113.0 μm thick, colourless; paraphyses ca. 2.0 μm wide, anastomosing; epihymenium 27.5–30.0 μm thick, brown; subhymenium ca. 62.0 μm thick, colourless; hypothecium brown. Asci *Porpidia*-type, cylindrical, eight-spored; ascospores 10.0–12.5 × 5.0–7.5 μm, ellipsoid, halonate. Conidiomata immersed, linear, black, margin pruinose; conidia not seen.

Chemistry. Thallus K–, C–. Medulla I+ violet. Chemotype I: Confluentic acid, often accompanied with 2'-O-methylmicrophyllinic acid. Chemotype II: Planaic acid. Chemotype III: none (rare).

Ecology and distribution. In China, growing on quartz sandstone or granite at elevations of 3900–4300 m in the alpine zone. This species is known from Qinghai Province of China.

Notes. *Immersaria venusta* is characterised by its yellow-brown, cracked areolae, its flat apothecia and brown epihymenium. It resembles *Immersaria shangrilaensis* by its cracked areolae, but its areolae have the tendency to split into several patches, but not aggregate like those of *I. shangrilaensis. Immersaria athroocarpa* is similar to *I. venusta* in the brown appearance of its thallus and in forming a sister group in the phylogenetic tree, but it differs in its yellow brown thallus, convex areolae, densely crowded apothecia and larger ascospores (17.5–20.0 × 10.0 μm). *Immersaria venusta* is also similar to *I. aurantia* (see notes for *I. aurantia*). The brown thallus of *Immersaria venusta* possibly resembles that of *I. olivacea*, but the latter differs in its simple or one-septate ascospores, pyriform conidia and dark bluish-green epihymenium.

Specimens examined (KUN). China. Qinghai Province: Maqing Co., Xueshan Village, 4187 m elev., 34°37'N, 99°42'E, on rock, 2020, Li-Song Wang et al. 20–67969, 20–67965; Banma Co., Yaertang Village, 3930 m elev., 32°42'N, 100°42'E, Li-Song Wang et al. 20–66940. Sichuan Province: Shiqu Co., Xinrong Village, 4043 m elev., 32°59'N, 98°19'E, on rock, 2020, Li-Song Wang et al. 20–68802; Rangtang Co., Mt. Haizi, 4246 m elev., 32°21'N, 101°24'E, Li-Song Wang et al. 20–66721, 20–66725.

Selected additional comparative material was examined.

Bellemerea alpina (Sommerf.) Clauzade & Cl. Roux Russia, Lps. Petsamo, Pummangin vuonon N-puoli, 1938, Räsänen, V., H9503269 (H); Lps. Petsamo, inter Vaitolahti et Kervanto, 1938, Räsänen, V., H9503270 (H).

Bellemerea cinereorufescens (Ach.) Clauzade & Cl. Roux Finland, Ob. Simo. Anteroinen. Rantakivellä, 1920, Räsänen, V., H9503267 (H); Le. Enontekiö, Kirkonkylä, 1925, Kari, L.E., H9503268 (H).

High-resolution photographs seen.

Immersaria carbonoidea (J.W. Thomson) Esnault & Cl. Roux USA, Alaska, along the Pitmegea River, 15 miles upstream from Cape Sabine, 1958, Thomson, J.W., M0082171 (M-isotype!), G00126754 (G-isotype!).

Immersaria olivacea Calat. & Rambold Spain, Espana, Castelló: Benicàssim, Parreta Alta, 390 m elev., 1993, Calatayud, V., M0101779 (M-isotype!).

Immersaria usbekica (Hertel) M. Barbero, Nav.-Ros. & Cl. Roux Algeria Algerie-Atlas Tellieu, Larba, Piste de Bougara á Tablat au S-E de l'arboretum de Meindja, 1985, Esnault, J., M0101787 (M-paratype!).

Lecaimmeria C.M. Xie, Lu L. Zhang & Li S. Wang, gen. nov.

MycoBank No: 839743

Etymology. The name "*Lecaimmeria*" refers to the immersed lecanorine apothecia of all known species.

Type species. *Lecaimmeria orbicularis* C.M. Xie & Lu L. Zhang, sp. nov.

Description. Thallus crustose, red-brown, orange-brown or dark brown, continuous or not; areolae irregular or tending to rectangular, with a glossy surface (*atrobrunnea*-type) caused by a layer of dead, colourless cells above the upper cortex; margin white or black; prothallus distinct at the margin of thallus or absent, sometimes developed between areolae. Upper cortex orange; epinecral layer colourless; algal layer continuous; medulla filled with grey granules. Apothecia lecanorine, immersed, round or irregular; disc red-brown, dark red-brown or dark orange-brown, flat or concave; margin present or absent, black or white, rarely green, pruinose or not. Exciple reduced, tissue at the lateral sides of the hymenium corresponding to the upper cortex and the algal layer of the vegetative areolae and to hypothecial hyphal cells when apothecia reach the margin of the areole (indicated in Figs. 7c, g, 8c, 9c, h, 10c, h). Hymenium colourless; paraphyses simple, rarely branched, anastomosing or not; epihymeinum orange, orange-brown, rarely brown, with a plectenchyma. Asci *Porpidia*-type (indicated in Fig 9d), cylindrical, eight-spored; ascospores ellipsoid, halonate, non-amyloid. Conidiomata present or absent, immersed, rarely convex, linear or stellate, rarely tuberculiform; conidia bacilliform.

Chemistry. Thallus K–, C+/–. Medulla I+ violet. Gyrophoric acid, 4-O-demethyl-planaic acid or no substances detected by TLC.

Ecology and distribution. In China, growing on rock, sandstone, granite or Qilian jade (rare), from elevations of 3100 to 4800 m in the alpine zone of west China and from 1200 to 1900 m in the steppe of north China. This genus is known from China, Europe, Iran, Mongolia, Romania, Russia, and USA.

Notes. The five-loci phylogenetic analysis showed that the species with lecanorine apothecia formed a novel lineage and should be excluded from *Immersaria*; thus, they are here treated as a new genus *Lecaimmeria*. *Lecaimmeria* is distinguished from related genera by its glossy surface, orange or red-brown areolae with margins, the amyloid

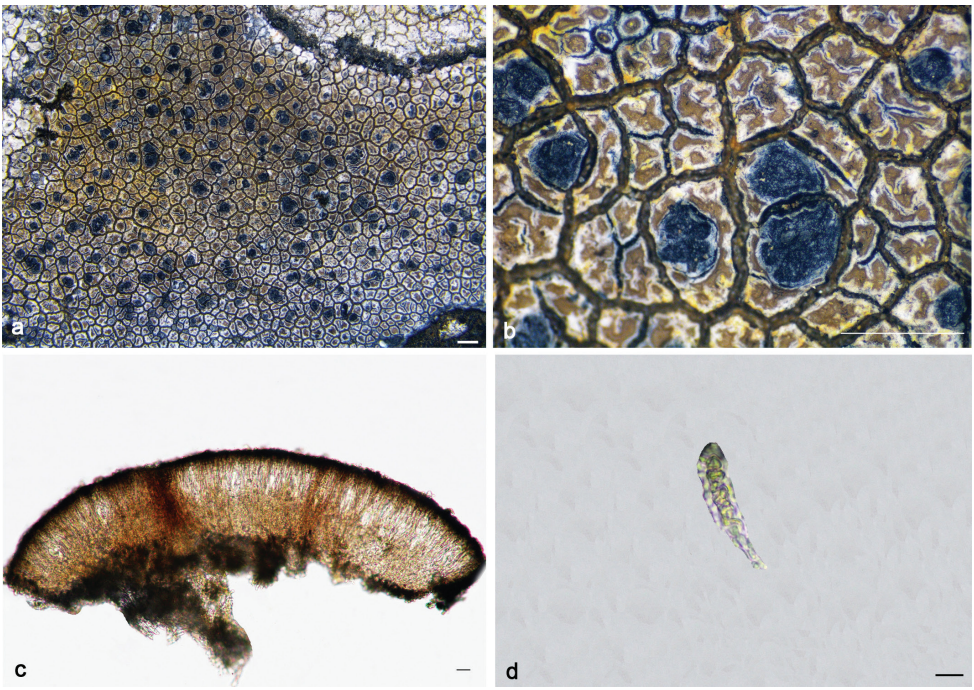

Figure 6. *Immersaria venusta* (**a–d** KUN 20–66725): **a–b** thallus **c** apothecial anatomy **d** ascus. Scale bars: 1 mm (**a–b**); 20 μm (**c**); 10 μm (**d**).

medulla, the red-brown immersed lecanorine apothecia, the orange epihymenium with a plectenchyma and the *Porpidia*-type asci with eight halonate and non-amyloid ascospores. In China, the genus is distributed in alpine areas, high altitude desert-steppe areas or high latitude steppe. Almost all the species of *Lecaimmeria* grow on granite or sandstone, with the exception of one species, *L. tuberculosa*, which grows on jade. Interestingly, the margin of conidiomata and areolae of *Lecaimmeria tuberculosa* appear with heavily jade-green pruinose.

The immersed apothecia and brown thallus of *Lecaimmeria* often resemble those of *Immersaria*, but *Lecaimmeria* differs in its red-brown lecanorine apothecia, often with a white margin, their orange epihymenium with a plectenchyma and the thallus containing gyrophoric acid. This genus might be confused with *Bellemerea* by its lecanorine apothecia and the *Porpidia*-type asci with halonate ascospores, but the latter genus differs in its amyloid ascospores.

Three species, previously included in *Immersaria*, *I. cupreoatra*, *I. iranica* and *I. mehadiana*, have lecanorine apothecia, but two of these, *I. cupreoatra* and *I. mehadiana*, currently lack molecular sequences. We suggest that these three species should be transferred to *Lecaimmeria*, based on the following factors. Their morphology is consistent with *Lecaimmeria* according to molecular results and comparisons with type specimens, high-resolution photographs of the type materials and the original descriptions. One unknown "*Immersaria*" species from Macedonia is sister to *Lecaimmeria iranica* in

the phylogenetic tree (Fig. 3), but comparison with high-resolution photograph and previous records (Malíček and Mayrhofer 2017) show that it differs in its black margin of areolae and absence of gyrophoric acid. This unknown species with lecanorine apothecia is possibly a member of *Lecaimmeria*, but descriptions are lacking and the specimens were not seen. Thus, this species is temporarily retained in *Immersaria*.

Lecaimmeria botryoides **C.M. Xie & Li S. Wang, sp. nov.**
MycoBank No: 839744
Figure 7a–d

Etymology. The name "botryoides" refers to the crowded apothecia while immature.

Type. China. Sichuan Province: Aba City, Rangtang County, Haizi Mt., 4225 m elev., 32°21'N, 101°24'E, on rock, 6 Sept 2020, Li-Song Wang et al. 20–66730 (KUN-holotype).

Description. Thallus areolate, red-brown, discontinuous; areolae 0.2–1.0 mm across, flat, slightly concave or convex, pruinose, polygonal, tending to be rectangular, margins heavily pruinose. Prothallus black, distinct in the margin of thallus. Upper cortex 20.0–25.0 μm thick, brown; epinecral layer 22.0–48.0 μm thick; algal layer ca. 37.0 μm thick, cells 7.5–10.0 μm diam., round. Apothecia frequent, irregular, densely crowded while immature (3–6/areolae), aggregate once mature, immersed, 0.2–1.3 mm in diam.; disc red-brown, flat, or concave, epruinose; margin pruinose, slightly raised. Hymenium 67.0–100.0 (–155.0) μm thick, colourless; paraphyses ca. 2.0 μm wide, simple, only branched at the top, not anastomosing; epihymenium 25.0–30.0 μm thick, orange; plectenchyma 2.0–8.0 μm thick; subhymenium 17.0–38.0 μm thick, colourless; hypothecium pale brown to brown. Asci *Porpidia*-type, cylindrical, eight-spored; ascospores 7.5–8.0 × 4.0–6.0 μm in diam., ellipsoid, halonate. Conidiomata not seen; conidia not seen.

Chemistry. Thallus K–, C+/–. Medulla I+ violet. Chemotype I: Gyrophoric acid. Chemotype II: none.

Ecology and distribution. In China, growing on rock at elevations of 3100–4300 m in the alpine zone. This species is known from Qinghai and Sichuan Provinces of China.

Notes. *Lecaimmeria botryoides* is characterised by its discontinuous thallus, densely crowded apothecia while immature and the orange epihymenium. *Lecaimmeria orbicularis* is similar to *L. botryoides* in its red-brown thallus, but differs in its round, flat apothecia and continuous thallus. The red-brown thallus of *Lecaimmeria botryoides* resembles *L. cupreoatra*, but the latter differs in the black margin of its apothecia and its distinct black prothallus between areolae.

Specimens examined (KUN). China. Qinghai Province: Banma Co., 3958 m elev., 32°40'N, 100°48'E, on rock, 2020, Li-Song Wang et al. 20–66900, 3932 m elev., Li-Song Wang et al. 20–66898, 3935 m elev., Li-Song Wang et al. 20–66891, 3178 m elev., Li-Song Wang et al. 20–66765. Sichuan Province: Rangtang Co., Mt. Haizi,

4256 m elev., 32°21'N, 101°24'E, on rock, 2020, Li-Song Wang et al. 20–66721, 4300 m elev., Li-Song Wang et al. 20–67706, 4276 m elev., Li-Song Wang et al. 20–66706, 4255 m elev., Li-Song Wang et al. 20–66707, 4274 m elev., Li-Song Wang et al. 20–66713, 4274 m elev., Li-Song Wang et al. 20–66711, 20–66705, 4225 m elev., Li-Song Wang et al. 20–66730, 4220 m elev., 32°20'N, 101°25'E, Li-Song Wang et al. 20–66683.

***Lecaimmeria cupreoatra* (Nyl.) C.M. Xie, comb. nov.**
MycoBank No: 839745

Basionyms. *Lecanora cupreoatra* Nyl., Lichens Lapponiae orientalis: 181 (1866).

Type. Russia. "Medvæschiigora, ad Onegam", 13 June 1863, Th. Simming, H9508237 (H-lectotype!).

Description. Nylander (1866) and Clauzade and Roux (1985).

Notes. The lectotype grows on siliceous rock and contains several intact apothecia. As "*Immersaria*" *cupreoatra* has lecanorine apothecia and is related to *I. lygeae* in our phylogeny, it is, therefore, transferred to *Lecaimmeria*. This species has not been correctly recorded in China (see notes for *Lecaimmeria mongolica*). The species is known from Europe, Mongolia, Russia, and USA (Calatayud and Rambold 1998).

Specimens examined (H). Russia. Kl. Kurkijoki, Kuuppala, Himohirsi, 12 May 1934, Räsänen, V., H9503417, H9510194.

***Lecaimmeria iranica* (Valadb., Sipman & Rambold) C.M. Xie, comb. nov.**
MycoBank No: 839746

Basionyms. *Immersaria iranica* Valadb., Sipman & Rambold, Lichenologist 43(3): 204 (2011).

Type. Iran. Mazandaran, Haraz Road, 20 km to Aamol, 36°17'N, 52°21'E, on calcareous rock, 1475 m, 7 Apr 2006, T. Valadbeigi 9008 (TARI-holotype; B, hb. Valadbeigi-isotype). Not seen.

Description. Valadbeigi et al. (2011).

Notes. "*Immersaria*" *iranica* has lecanorine apothecia, a distinct epinecral layer and halonate ascospores (Valadbeigi et al. 2011). The materials from China are in accordance with the materials of Iran, based on comparisons with the original descriptions and the photographs given by Valadbeigi et al. (2011). The characters of this species are consistent with the new genus and the phylogenetic results showed that it was clustered with species of *Lecaimmeria*. Therefore, it was transferred to *Lecaimmeria*. This species is currently known from Iran and China.

Specimens examined (SDNU). China. Xinjiang: Urumqi, Mt. Tianshan-glacier No.1, alt. 3800 m, on rock, 2011, Z.L. Huang SDNU20126106, SDNU20129049.

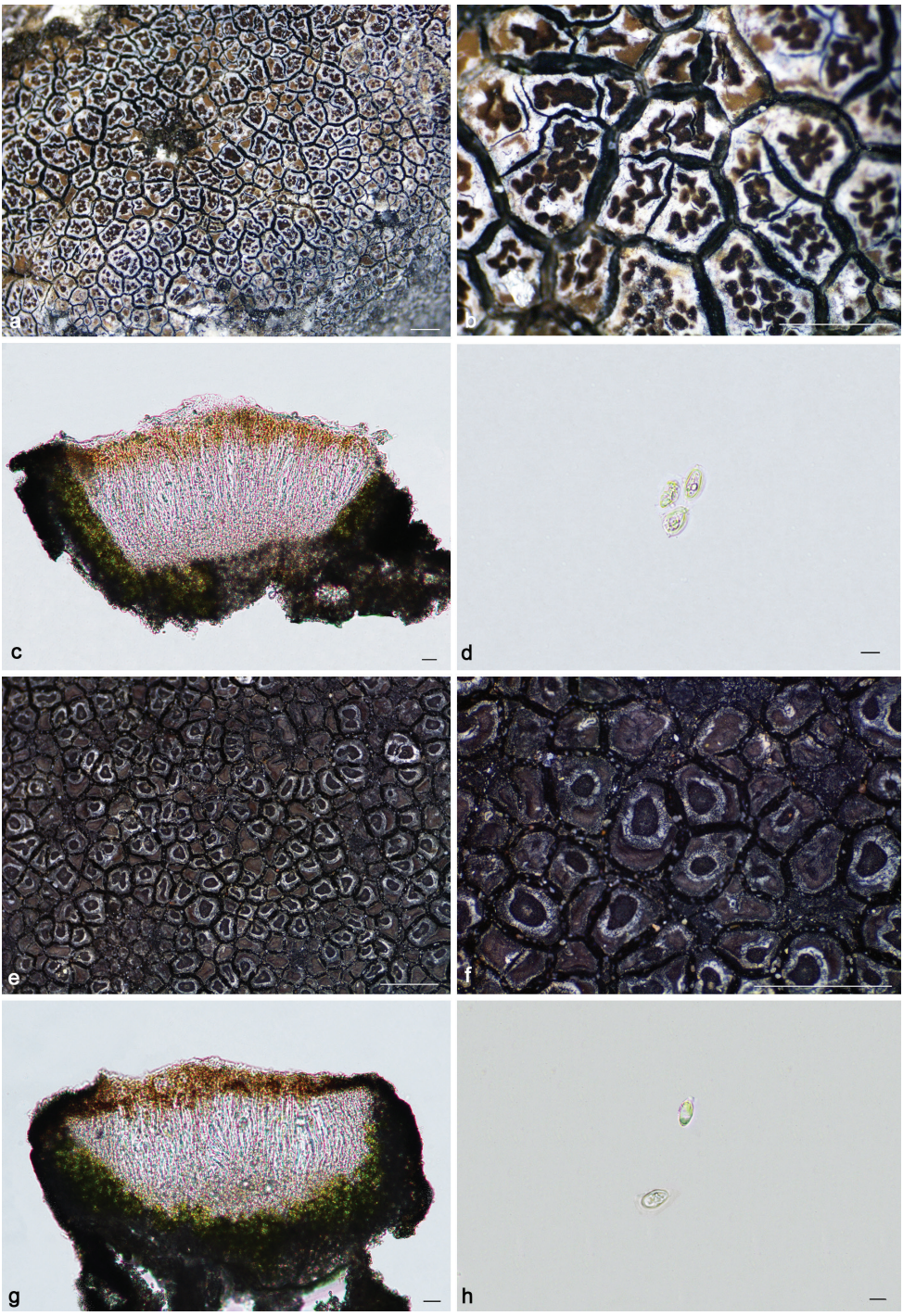

Figure 7. *Lecaimmeria botryoides* (**a–d** KUN 20–66730): **a–b** thallus **c** apothecial anatomy. *L. lyagea* (**e–h** KUN 20–69070): **e–f** thallus **g** apothecial anatomy **h** scospores. Scale bars: 1 mm (**a–b, e–f**); 20 μm (**c, g**); 10 μm (**d, h**).

Lecaimmeria lygaea **C.M. Xie & Lu L. Zhang, sp. nov.**
MycoBank No: 839747
Figure 7e–h

Etymology. The name "lygaea" refers to the dark appearance of the thallus.

Type. China. Tibet: Changdu City, Mangkang County, Luoni Village, 4127 m elev., 29°56'N, 98°33'E, on rock, 24 Sept 2020, Li-Song Wang et al. 20–69072 (KUN-holotype).

Description. Thallus areolate, dark red-brown, dark brown, continuous; areolae 0.5–1.0 mm across, flat, epruinose, irregular pentagonal, sometimes rectangular, fissures between areolae often filled with black prothallus; margin black, thinly pruinose; prothallus black, developed between areolae, also distinct in the margin. Upper cortex ca. 20.0 μm thick, orange-brown; epinecral layer ca. 15.0 μm thick; algal layer ca. 50.0 μm thick, cells 7.0–13.0 μm in diam., round. Apothecia frequent, round, crowded, immersed, 0.2–0.8 mm in diam.; disc red-brown, flat, or concave, epruinose; margin black, moderately thick, pruinose, raised. Hymenium 75.0–93.0 μm thick, colourless; paraphyses ca. 2.0 μm wide, simple, unbranched, not anastomosing; epihymenium 25.0–38.0 μm thick, orange brown; plectenchyma ca. 7.0 μm thick; subhymenium 20.0–25.0 μm thick, colourless; hypothecium brown Asci *Porpidia*-type, cylindrical, eight-spored; ascospores 12.5–20.0 × 5.0–7.5 μm in diam., ellipsoid, halonate. Conidiomata immersed, stellate, black, margin pruinose; conidia 5.0 × 1.0 μm, bacilliform.

Chemistry. Thallus K–, C–. Medulla I+ violet. Unknown fatty acid by TLC.

Ecology and distribution. In China, growing on sandstone at elevations of 4000–4200 m in the alpine zone. This species is known from the Tibet Region of China.

Notes. *Lecaimmeria lygaea* is characterised by its dark brown thallus, black margin of its areolae, black prothallus which fills the fissures between areolae, dark orange apothecia and its orange brown epihymenium. *Lecaimmeria cupreoatra* and *L. mehadiana* are similar to *L. lygaea*, but *L. cupreoatra* has a discontinuous thallus, with each areola surrounded by black prothallus, dark red-brown to black-brown apothecia without a margin. *Lecaimmeria mehadiana* has areolae with a white margin, black-brown apothecia, brown epihymenium and contains 4-O-demethylplanaic acid. The phylogenetic results show that *Lecaimmeria tibetica* is the sister species to *L. lygaea.* They are similar in chemistry, but differ in its orange-brown thallus and dark orange brown apothecia.

Specimens examined (KUN). China. Tibet: Changdu City, Mangkang Co., Luoni Village, 4099 m elev., 29°56'N, 98°33'E, on rock, 2020, Li-Song Wang et al. 20–69054, 4131 m elev., Li-Song Wang et al. 20–69070, 4127 m elev., Li-Song Wang et al. 20–69072, 4095 m elev., Li-Song Wang et al.20–69053.

***Lecaimmeria mehadiana* (Calatayud & Rambold) C.M. Xie, comb. nov.**
MycoBank No: 839748

Basionyms. *Immersaria mehadiana* Calat & Rambold, Lichenologist 30(3): 233 (1998).

Type. Romania. Caras-Severin Comitat, Mehadía, Strájot Mtn., on rock, 1994, Rambold, G.W., M0101781 (M-holotype!), M0101780, M0101782, M0101783 (M-isotype!). High-resolution photographs seen.

Description. Calatayud and Rambold (1998).

Notes. As "*Immersaria*" *mehadiana* has lecanorine apothecia and resembles *L. lygaea* and *L. cupreoatra*, having a dark brown thallus, it is, therefore, transferred to *Lecaimmeria*. This species is characterised by its greyish prothallus, dark brown apothecia and the brown epihymenium. It is only known from Romania (Calatayud and Rambold 1998).

***Lecaimmeria mongolica* C.M. Xie & Lu L. Zhang, sp. nov.**
MycoBank No: 839749
Figure 8a–d

Etymology. The name "mongolica" refers to the collection of the holotype within Inner Mongolia, an autonomous region of China.

Type. China. Inner Mongolia: Chifeng City, Balinyouqi, Han Mountain, 1445m elev., 44°11'N, 118°44'E, on rock, 22 Jul 2019, Zun-Tian Zhao et al. SDNU20190354 (SDNU-holotype).

Description. Thallus areolate, orange, continuous; areolae 0.4–0.8 mm across, epruinose, neatly arranged, irregular, tending to be rectangular, margin pruinose; prothallus black, not distinct. Upper cortex ca. 20.0 μm thick, brown; epinecral layer 5.0–8.0 μm thick; algal layer ca. 87.0 μm thick, cells 7.5–12.5 μm diam., round. Apothecia frequent, crowded, immersed or isolated from areolae, 0.2–0.8 mm in diam.; disc red-brown, flat, slightly convex, epruinose; margin pruinose. Hymenium 62.0–83.0 μm thick, colourless; paraphyses ca. 2.0 μm wide, unbranched, not anastomosing; epihymenium ca. 42.0 μm thick, orange; plectenchyma 5.0–10.0 μm thick; subhymenium 30.0–38.0 μm thick, colourless; hypothecium brown. Asci *Porpidia*-type, cylindrical, eight-spored; ascospores 10.0–17.5 × 6.0–7.5 μm in diam., ellipsoid, halonate. Conidiomata immersed, oblate, rare ellipsoid, black, margin pruinose; conidia 5.0 × 1.0 μm, bacilliform.

Chemistry. Thallus K–, C+. Medulla I+ violet. Gyrophoric acid.

Ecology and distribution. In China, growing on granite at elevations of 1400–2000 m in steppe or mountains. This species is known from Inner Mongolia of China.

Notes. This species was once reported as "*Immersaria*" *cupreoatra* from China (Zhang et al. 2015), but after comparing our collections with the type material, this was found to be a misclassification. Additionally, the phylogenetic results showed that these collections formed a well-supported lineage belonging to *Lecaimmeria*. Therefore, it is here treated as a new species, *Lecaimmeria mongolica*, characterised by its orange-brown thallus, red-brown apothecia with a distinct white margin and the thallus containing

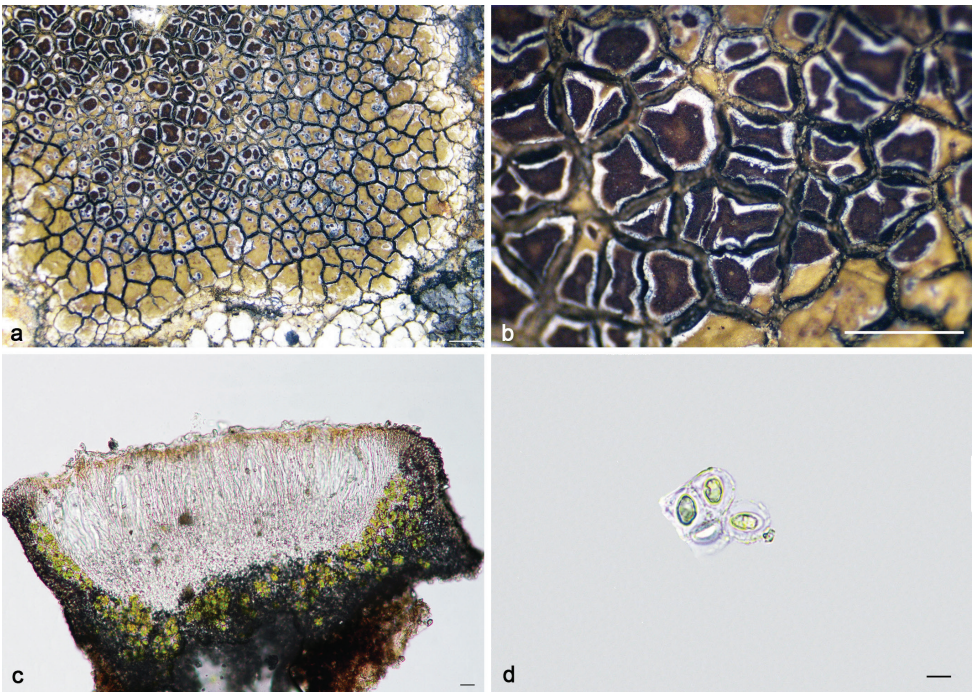

Figure 8. *Lecaimmeria mongolica* (**a–d** SDNU20190354): **a–b** thallus **c** apothecial anatomy **d** ascospores. Scale bars: 1 mm (**a–b**); 20 µm (**c**); 10 µm (**d**).

gyrophoric acid. *Lecaimmeria cupreoatra* resembles *L. mongolica* by containing gyrophoric acid, but it differs in its dark black brown thallus and the black margin of its apothecia. *Lecaimmeria tibetica* is similar to *L. mongolica* in its orange thallus, but differs in its smaller, dark orange apothecia and that no substance can be detected by TLC.

Specimens examined (SDNU). China. Inner Mongolia: Chifeng City, Balin Youqi, Mt. Qingyangcheng, 1445 m elev., 43°35'N, 117°30'E, on rock, 2019, Zun-Tian Zhao et al. SDNU20190350; Han Shan, 1563 m elev., 44°11'N, 118°44'E, on rock, Zun-Tian Zhao et al. SDNU20190354; A'ershan City, Mt. Jiguan, 1500 m elev., on rock, 2011, Yu-Liang Cheng SDNU20124912, 1400 m elev., Dai-Feng Jiang SDNU20124859; Ke Qi, Huanggangliang, 2000 m elev., on rock, Pan-Meng Wang SDNU20117613, Xing-Ran Kou SDNU20117399.

***Lecaimmeria orbicularis* C.M. Xie & Lu L. Zhang, sp. nov.**
MycoBank No: 839750
Figure 9a–e

Etymology. The name "orbicularis" refers to the round shape of the apothecia.

Type. China. Sichuan Province: Rangtang Co., Gangmuda Village, 3800 m elev., 32°18'N, 101°3'E, on rock, 7 Sept 2020, Li-Song Wang et al. 20–66753 (KUN-holotype).

Description. Thallus areolate, red-brown, rarely orange-brown, continuous; areolae 0.2–1.0 mm across, flat, occasionally wrinkled, tending to rectangular, fissures between areolae often filled with black prothallus, margin pruinose; prothallus black, developed between areolae, also distinct in the margin. Upper cortex 42.0–58.0 μm thick, brown; epinecral layer 5.0–20.0 μm thick; algal layer 70.0–113.0 μm thick, cells 10.0–15.0 × 7.5–10.0 μm in diam., ellipsoid to round. Apothecia frequent, scattered, immersed or isolated from areolae, 0.5–1.3 mm in diam.; disc red-brown, flat, round, epruinose; margin white, slightly raised. Hymenium 75.0–113.0 μm thick, colourless; paraphyses ca. 2.0 μm wide, simple, unbranched, not anastomosing; epihymenium 17.5–30.0 μm thick, orange; plectenchyma 5.0–15.0 μm thick; subhymenium 30.0–63.0 μm thick, colourless; hypothecium brown. Asci *Porpidia*-type, cylindrical, eight-spored; ascospores 12.5–15.0 × 5.0–6.0 μm, ellipsoid, halonate. Conidiomata not seen.

Chemistry. Thallus K–, C–. Medulla I+ violet. None.

Ecology and distribution. In China, growing on granite or sandstone at elevations of 3700–4200 m in the alpine zone. This species is known from Qinghai and Sichuan Provinces of China.

Notes. *Lecaimmeria orbicularis* is characterised by its orange brown thallus, neatly arranged areolae and round, flat apothecia. *Lecaimmeria botryoides* is similar to *L. orbicularis* (see notes for *L. botryoides*). *Lecaimmeria mongolica* might be confused with *L. orbicularis* due to its large apothecia with a white margin, but differs in its red-brown thallus and distribution in steppes. The red-brown thallus of *Lecaimmeria cupreoatra* resembles that of *L. orbicularis*, but differs in the black margin of its apothecia and its distinct black prothallus between areolae.

Specimens examined (KUN). China. Qinghai Province: Jiuzhi Co., Nianbaoyuze, 4200 m elev., 33°14'N, 100°58'E, on rock, 2020, Li-Song Wang et al. 20–66811, 20–66829, 20–66801, 20–66826A, 20–66821, 20–66805, 20–66833, 20–66817, 20–66841; Banma Co., Nianbaoyuze, 3930 m elev., 32°40'N, 100°48'E, Li-Song Wang et al. 20–66909, 20–66908, 20–66896, 20–66886B, 20–66899, 20–66935, 20–66943; Zhiqingsongduo Town, 3712 m elev., 33°24'N, 101°25'E, Li-Song Wang et al. 20–66965; Suohurima Village, 4029 m elev., 33°23'N, 100°57'E, Li-Song Wang et al. 20–66979. Sichuan Province: Rangtang Co., Gangmuda Village, 3800 m elev., 32°18'N, 101°3'E, on rock, 2020, Li-Song Wang et al. 20–66753, 20–66750, 3793 m elev., Li-Song Wang et al. 20–66747, Shangrangtang Village, 3730 m elev., 32°16'N, 101°21'E, Li-Song Wang et al. 20–66743.

***Lecaimmeria qinghaiensis* C.M. Xie & Li S. Wang, sp. nov.**

MycoBank No: 839751

Figure 9f–i

Etymology. The name "qinghaiensis" refers to the location in which the holotype was collected, in "Qinghai", a province of China.

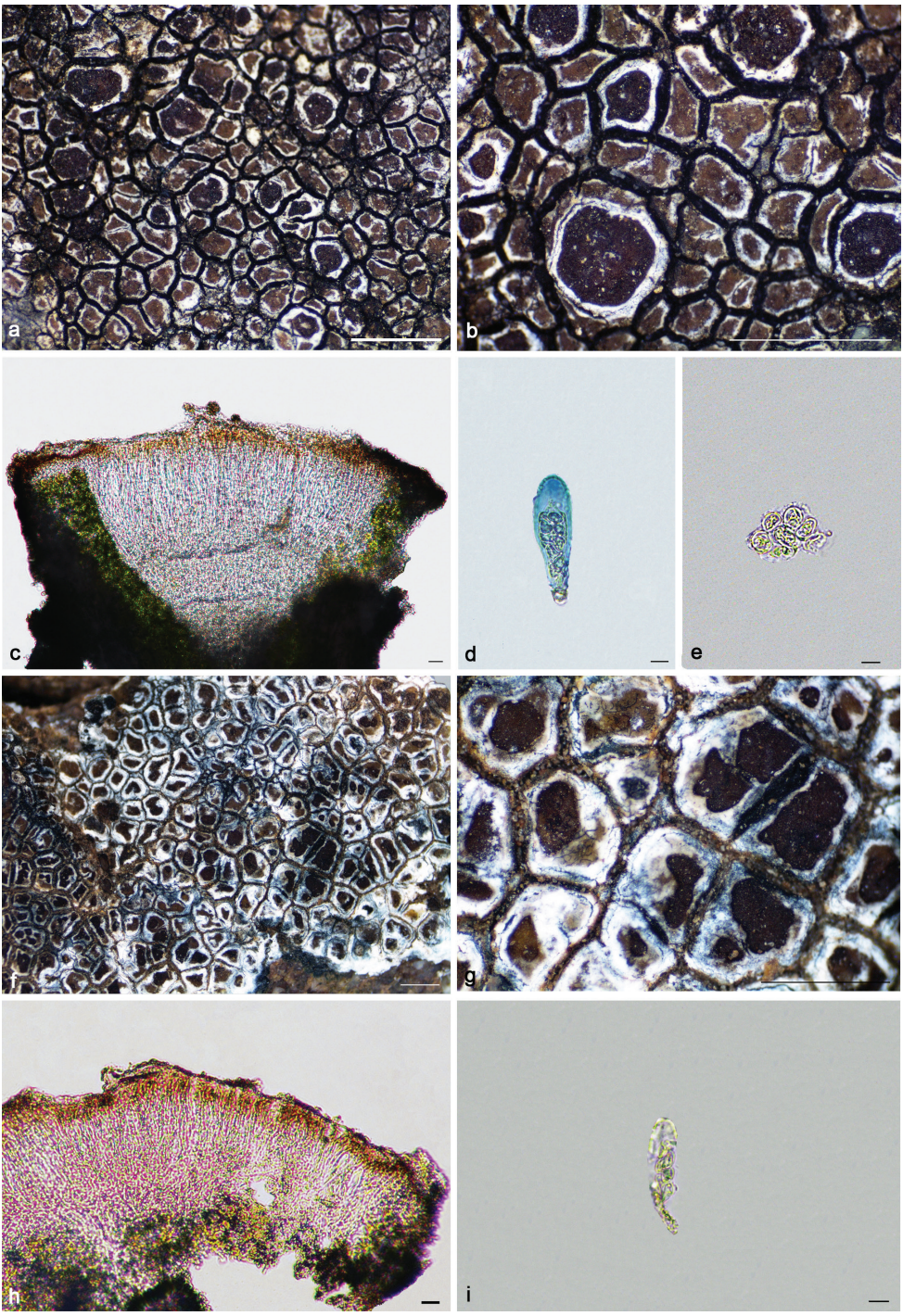

Figure 9. *Lecaimmeria orbicularis* (**a–e** KUN 20–66753): **a–b** thallus **c** apothecial anatomy **d** ascus (Lugol's iodine) **e** ascospores. *L. qinghaiensis* (**f–i** KUN 20–68696): **f–g** thallus **h** apothecial anatomy **i** ascus. Scale bars: 1 mm (**a–b, f–g**); 20 µm (**c, h**); 10 µm (**d, e, i**).

Type. China. Qinghai Province: Yushu City, Zaduo County, Sahuteng Town, 4634 m elev., 32°55'N, 95°46'E, on rock, 20 Sept 2020, Li-Song Wang et al. 20–68698 (KUN-holotype).

Description. Thallus areolate, yellow-brown, rusty, continuous; areolae 0.5–1.5 mm across, flat, epruinose; margin pruinose, occasionally green pigmented; prothallus black, distinct at the margin. Upper cortex 27.0–38.0 μm thick, brown; epinecral layer 12.0–20.0 μm thick; algal layer 57.0–93.0 μm thick, cells 7.5–12.5 × 5.0–12.5 μm in diam., ellipsoid to round. Apothecia frequent, immersed or isolated from areolae, round or somewhat irregular while immature, ellipsoid and tending to be rectangular or occupying the whole areolae once mature, 0.2–1.3 mm in diam.; disc brown, dark red-brown, flat, occasionally with a fissure when mature, epruinose; margin white, slightly raised. Hymenium 52.0–63.0 μm thick, colourless; paraphyses 2.0–3.0 μm wide, unbranched, not anastomosing; epihymenium 25.0–30.0 μm thick, dark orange-brown; plectenchyma 7.0–18.0 μm thick; subhymenium 50.0–63.0 μm thick, colourless; hypothecium brown. Asci *Porpidia*-type, cylindrical, eight-spored; ascospores 8.0–15.0 × 5.0–7.5 μm in diam., ellipsoid, not distinctly halonate. Conidiomata rare, immersed, flat, slightly convex, liner, stellate, graphidoid once mature, black, margin pruinose; conidia not seen.

Chemistry. Thallus K–, C–. Medulla I+ violet. None.

Ecology and distribution. In China, growing on rock at elevations of 4600–4900 m in the alpine zone. This species is known from Qinghai Province of China.

Notes. *Lecaimmeria qinghaiensis* is characterised by the yellow-brown, rusty thallus, the red-brown apothecia often occupying the whole areolae at maturity and the dark orange-brown epihymenium. The phylogenetic results showed that *Lecaimmeria tuberculosa* is the sister species to *L. qinghaiensis* which is similar in the appearance of the thallus, but differs in the brown, never rusty thallus, the red-brown apothecia and the green, tuberculiform conidiomata. The red-brown apothecia of *Lecaimmeria qinghaiensis* resembles *L. iranica*, but differs in the rusty thallus and the white margin of the apothecia.

Specimens examined (KUN). China. Qinghai Province: Zaduo Co., Sahuteng Town, 4634 m elev., 32°55'N, 95°46'E, on rock, 2020, Li-Song Wang et al. 20–68698, 4637 m elev., Li-Song Wang et al. 20–68687, 4622 m elev., Li-Song Wang et al. 20–68696; 4790 m elev., 33°31'N, 95°8'E, Xin-Yu Wang et al. 20–3115, 4791 m elev., Xin-Yu Wang et al. 20–3127; Zaqing Village, 4815 m elev., Xin-Yu Wang et al. 20–849.

***Lecaimmeria tibetica* C.M. Xie & Xin Y. Wang, sp. nov.**

MycoBank No: 839752

Figure 10a–e

Etymology. The name "tibetica" refers to the location from which the holotype was collected: "Tibet", an autonomous region of China.

Type. China. Tibet: Gongga Co., Jiangtang Town, 4557 m elev., 29°12'N, 90°38'E, on rock, 9 Sept 2019, Xin-Yu Wang et al. XY19–1291 (KUN-holotype).

Description. Thallus areolate, orange-brown, epruinose; areolae 0.3–0.5 mm across, irregular, upper surface uneven, margin lacking, pruinose; prothallus black, distinct at the margin. Upper cortex 17.0–33.0 µm thick, brown; epinecral layer 10.0–20.0 µm thick; algal layer ca. 75.0 µm thick, cells 7.0–10.0 diam., round. Apothecia rare, immersed or isolated from areolae, 0.2–0.5 mm in diam.; disc dark orange-brown, epruinose, flat, slightly convex; margin pruinose. Hymenium 105.0–138.0 µm thick, colourless; paraphyses ca. 2.0 µm wide, unbranched, not anastomosing; epihymenium ca. 25.0 µm thick, orange; plectenchyma ca. 12.0 µm thick; subhymenium almost absent, colourless; hypothecium brown. Asci *Porpidia*-type, cylindrical, eight-spored; ascospores 12.5–15.0 × 5.0–6.0 µm, ellipsoid, halonate. Conidiomata immersed, oblate, black, margin pruinose; conidia 5.0 × 1.5–2.0 µm in diam., bacilliform.

Chemistry. Thallus K–, C–. Medulla I+ violet. None.

Ecology and distribution. In China, growing on quartz sandstone at elevations of 4300–4600 m in the alpine zone. This species is known from Tibet, China.

Notes. *Lecaimmeria tibetica* is characterised by the orange-brown thallus, the black pigmentation of the areolae margin and the dark orange-brown and small size of the apothecia. *Lecaimmeria tibetica* is similar to *L. mongolica* (see notes for *L. mongolica*). The red-brown apothecia of *Lecaimmeria cupreoatra* resembles *L. tibetica*, but that species differs in its dark red-brown thallus and the presence of gyrophoric acid.

Specimens examined (KUN). China. Tibet: Gongga Co., Jiangtang Town, 4583 m elev., 29°12'N, 90°38'E, on rock, 2019, Xin-Yu Wang et al. XY19–1288, 4557 m elev., XY19–1291, 4560 m elev., XY19–1280; Dingri Co., Zhaguozhong, 4310 m elev., 28°35'N, 86°53'E, Li-Song Wang et al. 19–64071.

Lecaimmeria tuberculosa **C.M. Xie & Xin Y. Wang, sp. nov.**
MycoBank No: 839754
Figure 10f–i

Etymology. The name "tuberculosa" refers to the tuberculiform conidiomata.

Type. China. Gansu Province: Zhangye City, Sunan Co., Along the way from Sunan to Qilian, 3928 m elev., 38°37'N, 99°28'E, on rock, 30 May 2018, Li-Song Wang et al. 18–58865 (KUN-holotype).

Description. Thallus areolate, red-brown, continuous; areolae 0.5–1.3 mm across, slightly convex, epruinose; margin pruinose, often jade-green pigmented; prothallus not distinct. Upper cortex ca. 27.0 µm thick, orange; epinecral layer up to 28.0 µm thick, uneven, sometimes absent; algal layer ca. 50.0 µm thick, cells 6.0–10.0 µm diam., round. Apothecia frequent, scattered, immersed, 0.3–0.6 mm in diam.; disc red-brown, concave, epruinose; margin absent. Hymenium 55.0–83.0 µm thick, colourless; paraphyses ca. 2.0 µm wide, unbranched, not anastomosing; epihymenium 15.0–30.0 µm thick, orange; plectenchyma ca. 5.0 µm thick, discontinuous; subhymenium ca. 38.0 µm thick, colourless; hypothecium brown. Asci *Porpidia*-type, cylindrical, eight-spored; ascospores 6.0–12.5 × 3.0–5.0 µm in diam., ellipsoid, halonate.

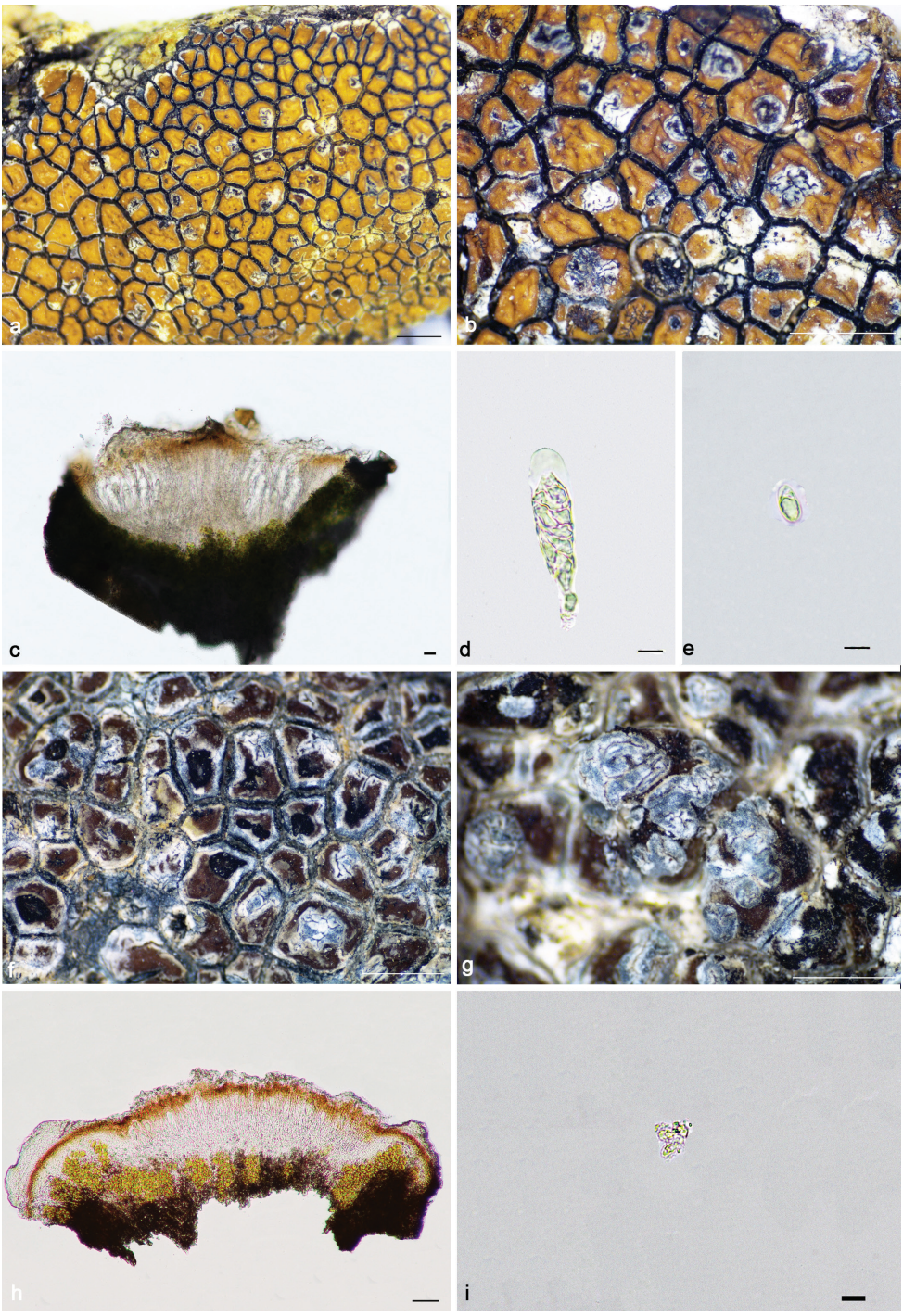

Figure 10. *Lecaimmeria tibetica* (**a–e** KUN XY19–1288): **a–b** thallus **c** apothecial anatomy **d** ascus **e** ascospore. *L. tuberculosa* (**f–i** KUN 18–58864): **f** thallus **g** conidiomata **h** apothecial anatomy **i** ascospores. Scale bars: 1 mm (**a–b, f–g**); 20 μm (**c**); 50 μm (**h**); 10 μm (**d, e, i**).

Conidiomata stellate, strongly convex, rarely immersed, forming tuberculiform, black, margin pruinose, jade-green pigmented; conidia 3.0–4.5 × 1.0 μm in diam., oblong to bacilliform.

Chemistry. Thallus K–, C–. Medulla I+ violet. No substances by TLC.

Ecology and distribution. In China, growing on the Qilian jade or sandstone at elevations of 3900–4200 m in the alpine zone. This species is known from Qinghai Province and Gansu Province of China.

Notes. *Lecaimmeria tuberculosa* is characterised by its red-brown thallus, the jade-green pruinose colour at the margin of its areolae, its red-brown, concave apothecia without a proper margin and tuberculiform conidiomata. *Lecaimmeria qinghaiensis* is similar to *L. tuberculosa* (see notes for *L. qinghaiensis*). *Lecaimmeria tuberculosa* usually grows on jade and, interestingly, the margin of the conidiomata and areolae of the species are heavily jade-green pigmented. *Lecaimmeria iranica* resembles *L. tuberculosa* by the absence of an apothecial margin, but differs in its immersed conidiomata and the white margin of its areolae.

Specimens examined (KUN). China. Qinghai Province: Gande Co., Qingzhen Village, 4124 m elev., 34°11'N, 100°12'E, on rock, 2020, Li-Song Wang et al. 20–68077, 4145 m elev., Li-Song Wang et al. 20–68055. Gansu Province: Zhangye City, Sunan Co., along the way from Sunan to Qilian, 3928 m elev., 38°37'N, 99°28'E, on rock, 2018, Li-Song Wang et al. 18–58856, 18–58857, 18–58865, 18–59835.

Key to species of *Immersaria* in China

1 Thallus greyish-brown; apothecia crowded ..... ***I. ferruginea***
– Thallus reddish-brown; apothecia rarely crowded **2**
2 Thallus orange; areolae irregular ..... ***I. aurantia***
– Thallus not orange; areolae irregular, polygonal or rectangular **3**
3 Thallus large, 6–10 cm across; areolae aggregated by several smaller areolae and black prothallus ..... ***I. shangrilaensis***
– Thallus smaller, 2–5 cm across; areolae not aggregated **4**
4 Thallus areolae convex, not rusty, not cracked; ascospores over 15 μm long .. .. ***I. athroocarpa***
– Thallus areolae flat, often rusty, cracked; ascospores never over 15 μm long .. .. ***I. venusta***

Key to species of *Lecaimmeria* in China

1 Prothallus distinct and filling the fissures between areolae ..... ***L. lygaea***
– Prothallus only distinct at the margin **2**
2 Thallus orange **3**
– Thallus reddish-brown **4**
3 Apothecia red-brown; containing gyrophoric acid ..... ***L. mongolica***
– Apothecia dark orange; no substance detected by TLC ..... ***L. tibetica***

4 Apothecia margin absent **5**
– Apothecia margin present **6**
5 Areolae margin white; epihymenium brown; pycindia immersed, linear or stellate ..... ***L. iranica***
– Areolae margin green; epihymenium orange; pycindia convex, tuberculiform ..... ***L. tuberculosa***
6 Thallus rusty; apothecia occupy the whole areolae ..... ***L. qinghaiensis***
– Thallus not rusty; apothecia do not occupy the areolae **7**
7 Apothecia irregular, crowded while immature, aggregate when mature ..... ***L. botryoides***
– Apothecia round, rarely crowded, not aggregate ..... ***L. orbicularis***

Acknowledgements

We are very grateful to Dr. Saara Velmala and Dr. Leena Myllys from the University of Helsinki (H) and Dr. Water Till from the Universität Wien (WU) for the loan of type materials, to Dr. Fiona Ruth Worthy, a post-doctoral researcher from Kunming Institute of Botany, Centre for Mountain Ecosystem Studies, for carefully correcting our English and to Dr. Einar Timdal (Natural History Museum, Norway) and Dr. Alan Fryday (Michigan State University) for the very careful review and the useful comments on the manuscript. This study was supported by the National Natural Science Foundation of China (31750001, 31970022, 32170002), the Second Tibetan Plateau Scientific Expedition and Research Program (STEP) (2019QZKK0503), the Youth Innovation Promotion Association CAS (2020388) and the State Key Laboratory of Phytochemistry and Plant Resources in West China (P2020-KF08).

References

Barbero M, Navarro-Rosinés P, Roux C (1990) *Immersaria usbekica* (Hertel) Barbero, Nav.-Ros. et Roux comb. nov.[= *Amygdalaria tellensis* Esnault et Roux] nove trovita en Europo. Bulletin de la Société Linéenne de Provence 41: 139–142.

Buschbom J, Mueller G (2004) Resolving evolutionary relationships in the lichen-forming genus *Porpidia* and related allies (Porpidiaceae, Ascomycota). Molecular Phylogenetics and Evolution 32: 66–82. https://doi.org/10.1016/j.ympev.2003.11.012

Calatayud V, Rambold G (1998) Two new species of the lichen genus *Immersaria* (Porpidiaceae). Lichenologist 30: 231–244. https://doi.org/10.1006/lich.1997.0133

Clauzade G, Roux C (1984) Les genres Aspicilia Massal. et Bellemerea Hafellner & Roux. Bulletin de la Société Botanique du Centre-Ouest 15: 127–141.

Fryday AM, Hertel H (2014) A contribution to the family Lecideaceae s. lat. (Lecanoromycetidae inc. sed., lichenized Ascomycota) in the southern subpolar region; including eight new species and some revised generic circumscriptions. Lichenologist 46(3): 389–412. https://doi.org/10.1017/S0024282913000704

Fryday AM, Printzen C, Ekman S (2014) *Bryobilimbia*, a new generic name for *Lecidea hypnorum* and closely related species. Lichenologist 46(1): 25–37. https://doi.org/10.1017/S0024282913000625

Hertel H, Zhao CF (1982) Lichens from Changbai Shan-some additions to the lichen flora of northeast China. Lichenologist 14: 139–152. https://doi.org/10.1017/S0024282982000280

Hertel H (1977) Gesteinsbewohnende Arten der Sammelgattung *Lecidea* (Lichenes) aus Zentral-, Ost- und Sudasien. Khumbu Himal, Ergebnisse des Forschungsunternehmens Nepal Himalaya 6: 145–458.

Huelsenbeck JP, Ronquist F (2001) MRBAYES: Bayesian inference of phylogenetic trees. Bioinformatics 17: 754–755. https://doi.org/10.1093/bioinformatics/17.8.754

Lanfear R, Frandsen PB, Wright AM, Senfeld T, Calcott B (2017) PartitionFinder 2: new methods for selecting partitioned models of evolution for molecular and morphological phylogenetic analyses. Molecular Biology and Evolution 34(3): 772–773. https://doi.org/10.1093/molbev/msw260

Larena I, Salazar O, Gonzalez V, Julian MC, Rubio V (1999) Design of a primer for ribosomal DNA internal transcribed spacer with enhanced specificity for ascomycetes. Journal of Biotechnology 75(2–3): 187–194. https://doi.org/10.1016/S0168-1656(99)00154-6

Liu YJ, Whelen S, Hall BD (1999) Phylogenetic relationships among ascomycetes: evidence from an RNA polymerase II subunit. Molecular Biology and Evolution 16(12): 1799–1808. https://doi.org/10.1093/oxfordjournals.molbev.a026092

Lücking R, Hodkinson BP, Leavitt SD (2017) The 2016 classification of lichenized fungi in the Ascomycota and Basidiomycota-approaching one thousand genera. Bryologist 119: 361–416. https://doi.org/10.1639/0007-2745-119.4.361

Malíček J, Mayrhofer H (2017) Additions to the lichen diversity of Macedonia (FYROM) [Ergänzungen zur Flechtendiversität von Makedonien (FYROM)]. Herzogia 30(2): 431–444. https://doi.org/10.13158/heia.30.2.2017.431

Matheny PB, Liu YJ, Ammirati JF, Hall BD (2002) Using RPB1 sequences to improve phylogenetic inference among mushrooms (Inocybe, Agaricales). American Journal of Botany 89: 688–698. https://doi.org/10.3732/ajb.89.4.688

McCune B, Curtis MJ, Di Meglio J (2017) New taxa and a case of ephemeral spore production in Lecideaceae from western North America. Bryologist 120(2): 115–124. https://doi.org/10.1639/0007-2745-120.2.115

Nylander W (1866) Lichenes Lapponiae orientalis. Notiser ur Sällskapets pro Fauna et Flora Fennica Förhandlingar 8: 101–192.

Orange A, James PW, White FJ (2010) Microchemical methods for the identification of lichens (2nd edn.). British Lichen Society, London, 101 pp.

Rambaut A (2012) FigTree, v. 1.4.0. Institute of Evolutionary Biology, University of Edinburgh.

Rambold GA (1989) A monograph of the Saxicolous Lecideoid Lichens of Australia (excl. Tasmania). Bibliotheca Lichenologica 34: 239–240.

Rehner SA, Samuels GJ (1994) Taxonomy and phylogeny of *Gliocladium* analysed from nuclear large subunit ribosomal DNA sequences. Mycological Research 98: 625–634. https://doi.org/10.1016/S0953-7562(09)80409-7

Stiller JW, Hall BD (1997) The origin of red algae: Implications for plastid evolution. PNAS 94: 4520–4525. https://doi.org/10.1073/pnas.94.9.4520

Valadbeigi T, Sipman H, Rambold G (2011) The genus *Immersaria* (Lecideaceae) in Iran, including *I. iranica* sp. nov. Lichenologist 43(3): 203–208. https://doi.org/10.1017/S0024282911000077

Vilgalys R, Hester M (1990) Rapid genetic identification and mapping of enzymatically amplified ribosomal DNA from several *Cryptococcus* species. Journal of Bacteriology 172: 4239–4246. https://doi.org/10.1128/jb.172.8.4238-4246.1990

White T, Bruns T, Lee S, Taylor F, White TJ, Lee SH, Taylor L, Shawetaylor J (1990) Amplification and direct sequencing of fungal ribosomal RNA genes for phylogenetics. In: Innis M, Gel-fand J, Sainsky J, et al. (Eds) PCR Protocols: A Guide to Methods and Applications. Academic Press, San Diego, 315–322. https://doi.org/10.1016/B978-0-12-372180-8.50042-1

Zhang LL, Hu L, Zhao XX, Zhao ZT (2015) New records of *Clauzadea* and *Immersaria* from China. Mycotaxon, Ithaca NY, 130 (3): 899–905. https://doi.org/10.5248/130.899

Zoller S, Scheidegger C, Sperisen C (1999) PCR primers for the amplification of mitochondrial small subunit ribosomal DNA of lichen-forming ascomycetes. Lichenologist 31(5): 511–516. https://doi.org/10.1006/lich.1999.0220

Supplementary material 1

Table S1

Authors: Cong-Miao Xie, Li-Song Wang, Zun-Tian Zhao, Yan-Yun Zhang, Xin-Yu Wang, Lu-Lu Zhang

Data type: docx. file

Explanation note: A list of specimens and GenBank accession number of sequences used in this study. The new sequences generated are in bold.

Link: https://doi.org/10.3897/mycokeys.87.72614.suppl1

MycoKeys 87: 133–157 (2022)
doi: 10.3897/mycokeys.87.76085
https://mycokeys.pensoft.net

RESEARCH ARTICLE

A peer-reviewed open-access journal
MycoKeys
Launched to accelerate biodiversity research

Five new species of *Trichoderma* from moist soils in China

Guang-Zhi Zhang[1], He-Tong Yang[1], Xin-Jian Zhang[1], Fang-Yuan Zhou[1], Xiao-Qing Wu[1], Xue-Ying Xie[1], Xiao-Yan Zhao[1], Hong-Zi Zhou[1]

1 *Qilu University of Technology (Shandong Academy of Sciences), Ecology Institute, Shandong Provincial Key Laboratory for Applied Microbiology, Jinan 250103, China*

Corresponding author: Xin-Jian Zhang (zhangxj@sdas.org)

Academic editor: Rungtiwa Phookamsak | Received 4 October 2021 | Accepted 20 January 2022 | Published 17 February 2022

Citation: Zhang G-Z, Yang H-T, Zhang X-J, Zhou F-Y, Wu X-Q, Xie X-Y, Zhao X-Y, Zhou H-Z (2022) Five new species of *Trichoderma* from moist soils in China. MycoKeys 87: 133–157. https://doi.org/10.3897/mycokeys.87.76085

Abstract

Trichoderma isolates were collected from moist soils near a water source in different areas of China. ITS sequences were submitted to MIST (Multiloci Identification System for *Trichoderma*) and meets the *Trichoderma* [ITS_{76}] standard. Combined analyses of phylogenetic analyses of both phylograms (*tef1-α* and *rpb2*) and morphological characteristics, revealed five new species of *Trichoderma*, namely *Trichoderma hailarense*, *T. macrofasciculatum*, *T. nordicum*, *T. shangrilaense* and *T. vadicola*. Phylogenetic analyses showed *T. macrofasciculatum* and *T. shangrilaense* belong to the Polysporum clade, *T. hailarense*, while *T. nordicum* and *T. vadicola* belong to the Viride clade. Each new taxon formed a distinct clade in phylogenetic analysis and have unique sequences of *tef1-α* and *rpb2* that meet the *Trichoderma* new species standard. The conidiation of *T. macrofasciculatum* typically appeared in white pustules in concentric rings on PDA or MEA and its conidia had one or few distinctly verrucose. Conidiophores of *T. shangrilaense* are short and rarely branched, phialides usually curved and irregularly disposed. The aerial mycelium of *T. hailarense* and *T. vadicola* formed strands to floccose mat, conidiation tardy and scattered in tufts, conidiophores repeatedly rebranching in dendriform structure. The phialides of *T. nordicum* lageniform are curved on PDA and its conidia are globose to obovoidal and large.

Keywords

Hypocreales, phylogenetic analysis, soil fungi, Sordariomycetes, taxonomy

Introduction

The genus *Trichoderma* belongs to one of the most useful groups of microbes to have had an impact on human welfare in recent times. They are most widely used as biofungicides and plant growth modifiers and are sources of enzymes of industrial utility, including those used in the biofuels industry (Mukherjee et al. 2013). Some *Trichoderma* species have great potential applications to remediate soil and water pollution (Tripathi et al. 2013). *Trichoderma* is a hyperdiverse fungal genus (Jaklitsch and Voglmayr 2015). Formerly the species-level identification of *Trichoderma* was performed, based on their morphological characteristics (Gams and Bissett 1998) and is becoming more and more difficult because there are only a few relatively invariable morphological characteristics, leading to overlap amongst species (Samuels 2006).

DNA sequence analysis was introduced and provided more reliable identification of *Trichoderma* species (Druzhinina et al. 2006; Samuels 2006; Samuels et al. 2006). Given their low sequence variability or missing adequate sequence data, ITS, *cal1* and *chi18-5* are rarely used for new *Trichoderma* species identifications (Bissett et al. 2015; Cai and Druzhinina 2021). *Tef1-α* and *rpb2* facilitate reliable species identifications through phylogenetic analyses (Bissett et al. 2015; Jaklitsch and Voglmayr 2015; Cai and Druzhinina 2021) and have been used in the phylogenetic analysis and identification of new *Trichoderma* species in recent years. This has resulted in the exponential expansion of *Trichoderma* taxonomy, with up to 20 new species recognised per year (Cai and Druzhinina 2021). As of July 2021, a total of 405 species has been reported and recognised (Bustamante et al. 2021; Cai and Druzhinina 2021; Rodríguez et al. 2021; Zheng et al. 2021). The new molecular identification protocol provides a standard for the molecular identification of *Trichoderma* (Cai and Druzhinina 2021; www.trichoderma.info). According to this protocol, the new species should meet the *Trichoderma* [ITS_{76}] standard and has unique sequences of *rpb2* or *tef1* (does not meet the $sp\exists!(rpb2_{99} \cong tef1_{97})$ standard for known species).

Trichoderma species are cosmopolitan and prevalent components of different ecosystems in a wide range of climatic zones (Kubicek et al. 2008). They are mainly found in natural soils and decaying wood and plant material (Kredics et al. 2014). Many new *Trichoderma* species were first discovered in China, with up to 115 new *Trichoderma* species being reported since 2016 (Zhu and Zhuang 2015a, b, 2018; Chen and Zhuang 2016, 2017a, b, c, d; Qin and Zhuang 2016a, b, c, 2017; Sun et al. 2016; Zeng and Zhuang 2017, 2019; Zhang and Zhuang 2017, 2018, 2019; Li et al. 2018; Qiao et al. 2018; Zhao et al. 2018; Ding et al. 2020; Gu et al. 2020; Liu et al. 2020; Zheng et al. 2021). Amongst these 115 species, 75 were isolated from soils, 36 were collected from the plant branch or rotten twigs, while the other four species were collected from mushroom, pollen or rotten fruit.

Trichoderma has been segregated into many clades (Bissett 1991; Atanasova et al. 2013). The Polysporum clade (formerly section Pachybasium) was first defined by Bissett (1991), including 20 species. However, molecular phylogeny has shown that it is paraphyletic (Kindermann et al. 1998; Kullnig-Gradinger et al. 2002) and the species composition was subdivided subsequently into five unrelated clades, such as Ceram-

ica, Chlorospora, Harzianum, Semiorbis, Strictipilosa or Stromaticum (Chaverri and Samuels 2003; Jaklitsch 2009; Jaklitsch 2011). *Trichoderma hamatum* and some other species were found to belong to the section Trichoderma. The removal of *T. hamatum* determined that Bissett's sectional name could not be used anymore. Lu et al. (2004) refined the clade containing the remaining species around *T. polysporum/Hypocrea pachybasioides* and it was named the *Pachybasium* core group by Jaklitsch (2011), which includes 13 species. In subsequent years, several new species were added to this clade, increasing the number of *Trichoderma* species to 21 species (Jaklitsch and Voglmayr 2015; Zhu and Zhuang 2015; Qin and Zhuang 2016c; Chen and Zhuang 2017b).

The Virde clade is basically in accordance with Bissett's (1991) concept, but later, some other species have been added constantly. As of 2015, this large clade has 72 species to be confirmed and described, amongst which 55 species have been well located in the six subclades (Hamatum/Asperellum, Koningii, Neorufum, Rogersonii, Viride and Viridescens) and 17 species have not been located in the unnamed branches (Park et al. 2014; Bissett et al. 2015; Jaklitsch and Voglmayr 2015). In subsequent years, 25 new species were added to this clade, increasing the number of *Trichoderma* species to 97 (Montoya et al. 2016; Qin and Zhuang 2016a; Chen and Zhuang 2017c; Zeng et al. 2017; Zhang and Zhuang 2017; du Plessis et al. 2018; Qiao et al. 2018; Zhang and Zhuang 2018; Crous et al. 2019; Ding et al. 2020; Tomah et al. 2020). Cai and Druzhinina (2021) reconstructed the core topology of the phylogram, based on the Maximum Likelihood (ML) phylogeny of the 361 *rpb2*-barcoded *Trichoderma* species and 361 species have been located in the eight main clades (numerically named 1–8). All *Trichoderma* species in the adjacent Polysporum and Viride clades were remerged into the 5th clade, which also included several *Trichoderma* species from the *Harzianum* and *lone lineage* clades (Jaklitsch and Voglmayr 2015; Sun et al. 2016; Zhang and Zhuang 2017).

The present study performed the phylogenetic analysis of the five new species of *Trichoderma* to establish their new status. Five new species were collected from moist soils near water in different areas of China. *Tef1-α* and *rpb2* sequences were used for the phylogenetic reconstruction of the five new species in the present study and meet the *Trichoderma* new species standard (Cai and Druzhinina 2021).

Materials and methods

Isolates and specimens

Specimens were collected from Sichuan, Yunnan, Beijing, Shandong and Inner Mongolia. *Trichoderma* strains were isolated from soils on *Trichoderma* Selective Medium (K_2HPO_4 0.90 g; $MgSO_4{\cdot}7H_2O$ 0.20 g; NH_4NO_3 1.0 g; KCl 0.15 g; glucose 3.0 g; Rose Bengal 0.15 g; Agar 15.0 g; distilled water 1.0 litre. Post autoclaving, chloromycetin (0.25 g), streptomycin (0.03 g) and pentachloronitrobenzene (0.2 g) were added) (Martin 1950). Ex-type living cultures of new species were deposited in the Agricultural Culture Collection of China (ACCC) (Institute of Agricultural Resources and Regional Planning, Chinese Academy of Agricultural Sciences, Beijing, China).

Morphological characterisations

Morphological observation of the colonies and conidium-bearing structures was based on isolates grown on PDA (potato dextrose agar, Difco), CMD (Difco cornmeal agar + 2% w/v dextrose), MEA (malt extract agar, Difco) and Nirenberg's SNA medium (Nirenberg 1976) for 2 weeks in an incubator at 25 °C with alternating 12 h/12 h fluorescent light/darkness. Microscopic observations were conducted with an Olympus BX53 microscope and a MicroPublisher 5.0 RTV digital camera (Olympus Corp., Tokyo, Japan). Continuous characters, such as length and width, were measured with the CellSens Standard Image software (Olympus Corp., Tokyo, Japan). Continuous measurements were based on 10–30 measured units and were reported as the extremes (maximum and minimum) in brackets separated by the mean plus and minus one standard deviation. Colour standards were from Kornerup and Wanscher (1978). Growth-rate trials were performed on 9 cm Petri dishes with 20 ml of CMD, PDA, MEA and SNA at 15 °C, 20 °C, 25 °C, 30 °C, and 35 °C. Petri dishes were incubated in darkness up to 1 week or until the colony covered the agar surface. Colony radii were measured daily. Trials were replicated three times.

DNA extraction, polymerase chain reaction (PCR) and sequencing

Strains were grown in 9 cm-diameter Petri dishes containing PDA (potato dextrose agar, Difco). Cultures were incubated at 25 °C for ca. 3–5 days. Genomic DNA was extracted from the mycelial mat harvested from the surface of the broth with the Fungal Genomic DNA Extraction Kit (Aidlab Biotechnologies Co. Ltd., Beijing, China). The amplification of ITS was performed using the primer pair ITS5 and ITS4 (White et al. 1990), for *tef1*-α, primer pair EF1-728F (Carbone and Kohn 1999) and tef1-ALLErev (Jaklitsch et al. 2005) was used and, for *rpb2*, primer pair frpb2-5f and frpb2-7cr (Liu et al. 1999) was used. PCR amplification of each gene was performed as described by Park et al. (2014) and Chaverri et al. (2011). PCR products were purified and sequenced by ABI3730 Gene Analyzer at Sangon (Sangon Biotech (Shanghai) Co., Ltd.).

Molecular identification and phylogenetic analyses

We followed the molecular identification protocol for a single *Trichoderma* isolate (Cai and Druzhinina 2021; www.trichoderma.info) and estimated the pairwise similarity between the ITS sequence of the query strain and the sequences that are given in the ITS56 datasets (Cai and Druzhinina 2021). *Tef1*-α and *rpb2* sequences were subjected to Multiloci Identification System for *Trichoderma* (MMIT) (mmit.china-cctc.org) (Dou et al. 2020) and NCBI nucleotide BLAST (https://blast.ncbi.nlm.nih.gov/Blast.cgi) to detect the most closely related species. A sufficient number of representative sequences (n > 6) of *Trichoderma* species (Bissett et al. 2015; Cai and Druzhinina 2021) that are closely related to the new species were chosen for phylogenetic analyses. *Protocrea illinoensis* and *Protocrea farinose* were selected as outgroups.

Sequences were aligned with ClustalW (Thompson et al. 1994) and adjusted manually. Gaps were treated as missing data. Phylogenetic analyses were performed with *tef1*-α or *rpb2* with MEGA-X software (Kumar et al. 2018). Model testing was used to find the best DNA model for ML analyses. The stability of clades was evaluated by bootstrap tests with 1000 replications. Bootstrap values above 50% were indicated on the corresponding branches. Maximum Parsimony (MP) analyses were performed with MEGA-X software (Kumar et al. 2018) using 1000 replicates of heuristic search with the random addition of sequences and tree bisection reconnection as the MP search method. All molecular characters were weighted equally and gaps were treated as missing data. Bootstrap proportions were calculated from 1000 replicates, each with 10 replicates of random addition of taxa.

Results

Molecular identification and sequence analyses

We estimated the pairwise similarity between the ITS sequence of the query strain and the sequences that are given in the ITS56 datasets. All the query strain belongs to the genus *Trichoderma* spp. with similarity value > 81% compared to the sequences in the datasets. The query strain has unique sequences of *tef1*-α and *rpb2* (does not meet the $sp\exists!(rpb2_{99} \cong tef1_{97})$ standard for known *Trichoderma* species).

Tef1-α or *rpb2* sequences of new taxon were subjected to MMIT and NCBI nucleotide BLAST and 34 representative sequences of *Trichoderma* species (all the species with similarity *rpb2* and *tef1*-α ≥ 92% in the Viride clade) that are closely related to the new species, were chosen for phylogenetic analyses of *T. hailarense*, *T. nordicum* and *T. vadicola*. The accession numbers for the sequences are provided in Table 1. Model testing suggested using the Hasegawa-Kishino-Yano model (HKY; Hasegawa 1985) with gamma distributed with invariant sites (HKY+G+I) for ML analyses of *tef1*-α and the Tamura-Nei model (TN93; Tamura 1993) with gamma distributed substitution rates (TN93+G) for *rpb2*. The phylogenetic trees from *rpb2* or *tef1*-α analyses are shown in Figs 1 and 2, respectively. Sequence alignments and the trees obtained were deposited in TreeBASE (http://purl.org/phylo/treebase/phylows/study/TB2:S29166). Twenty representative sequences of closely-related *Trichoderma* species (all the *Trichoderma* species in the Polysporum clade) were chosen for phylogenetic analyses of *T. macrofasciculatum* and *T. shangrilaense* (Table 1). Model testing suggested using the Hasegawa-Kishino-Yano model (HKY; Hasegawa 1985) with gamma distributed substitution rates (HKY+G) for ML analyses of *tef1*-α and the Kimura 2-parameter (K2; Kimura 1980) with gamma distributed substitution rates (K2+G) for *rpb2*. The phylogenetic trees from *rpb2* or *tef1*-α analyses are shown in Figs 3 and 4, respectively. Sequence alignments and the trees obtained were deposited in TreeBASE (http://purl.org/phylo/treebase/phylows/study/TB2:S29166).

Table 1. Strain numbers and GenBank accession numbers of sequences used for phylogenetic analyses.

Species	Clade	Strain	GenBank accession numbers		
			ITS	*tef1-α*	*rpb2*
T. adaptatum	Viride	HMAS 248800	–	KX428024	KX428042
T. albofulvopsis	Viride	HMAS 273760	–	KU529127	KU529138
T. alutaceum	Polysporum	CBS 120535	FJ860725	FJ179567	FJ179600
T. appalachiense	Viride	GJS 97-243	DQ315419	DQ307503	DQ307503
T. atlanticum	Polysporum	CBS 120632	FJ860781	FJ860649	FJ860546
T. atroviride	Viride	CBS 119499	FJ860726	FJ860611	FJ860518
T. bavaricum	Polysporum	CBS 120538	FJ860737	FJ860621	FJ860527
T. beijingense	Viride	HMAS 248804	–	KX428025	KX428043
T. bifurcatum	Viride	HMAS 248795	–	KX428018	KX428036
T. caerulescens	Viride	S195	JN715589	JN715621	JN715604
T. composticola	Viride	S590=CBS 133497	–	KC285631	KC285754
T. europaeum	Polysporum	S611	–	KJ665489	KJ665268
T. foliicola	Polysporum	Hypo 645	JQ685871	JQ685862	JQ685876
T. gamsii	Viride	S488	–	JN715613	KJ665270
T. hailarense	**Viride**	**WT17901*= ACCC 39711**	**MH287485**	**MH287505**	**MH287506**
T. hailarense	**Viride**	**WT17803**	**MH606226**	**MH606229**	**MH606232**
T. hispanicum	Viride	S453=CBS 130540	JN715595	JN715659	JN715600
T. istrianum	Viride	S123	–	KJ665521	KJ665280
T. laevisporum	Viride	HMAS 273756	–	KU529128	KU529139
T. lacuwombatense	Polysporum	GJS 99-198	–	KJ665547	KJ665286
T. leucopus	Polysporum	CBS 122499	FJ860764	FJ179571	FJ179605
T. luteffusum	Polysporum	CBS 120537	FJ860773	FJ860645	FJ860543
T. macrofasciculatum	**Polysporum**	**WT37805* = ACCC 39712**	**MH287487**	**MH287509**	**MH287493**
T. macrofasciculatum	**Polysporum**	**WT37810**	**MH287488**	**MH287510**	**MH287494**
T. mediterraneum	Polysporum	S190	–	KJ665568	KJ665296
T. minutisporum	Polysporum	GJS 90-82	–	KJ665618	KJ665316
T. neokoningii	Viride	CBS 120070=GJS 04-216	DQ841734	KJ665620	KJ665318
T. nordicum	**Viride**	**WT13001* =ACCC 39713**	**MH287483**	**MH287501**	**MH287502**
T. nordicum	**Viride**	**WT61001**	**MH287484**	**MH287503**	**MH287504**
T. nybergianum	Polysporum	CBS 122500	FJ860791	FJ179575	FJ179611
T. ochroleucum	Viride	CBS 119502	FJ860793	FJ860659	FJ860556
T. olivascens	Viride	S475=CBS 132574	–	KC285624	KC285752
T. pachypallidum	Polysporum	CBS 122126	FJ860798	FJ860662	JQ685879
T. palidulum	Viride	HMAS 275665	–	MG383493	MG383487
T. paratroviride	Viride	CBS136489	–	KJ665627	KJ665321
T. paraviridescens	Viride	CBS 119321	DQ677651	DQ672610	KC285763
T. parapiluliferum	Polysporum	CBS 120921	FJ860799	FJ179578	FJ179614
T. piluliferum	Polysporum	CBS 120927	FJ860810	FJ860674	FJ179615
T. placentula	Polysporum	CBS 120924	–	FJ179580	FJ179616
T. polysporum	Polysporum	CPK 3131	–	FJ860661	FJ860558
T. pruinosum	Polysporum	HMAS 247217	–	MF371227	MF371212
T. samuelsii	Viride	S5=CBS 130537	JN715593	JN715651	JN715599
T. sempervirentis	Viride	S599=CBS 133498	–	KC285632	KC285755
T. seppoi	Polysporum	CBS 122498	–	FJ179581	FJ179617
T. shangrilaense	**Polysporum**	**WT34004*= ACCC 39714**	**MH287489**	**MH287495**	**MH287496**
T. shangrilaense	**Polysporum**	**WT40502**	**MH606224**	**MH606227**	**MH606230**
T. shaoguanicum	Viride	HMAS 248809	–	KX428031	KX428049
T. sinoluteum	Polysporum	HMAS 252868	–	KJ634777	KJ634744
T. speciosum	Viride	CGMCC 3.19079	MH113929	MH183184	MH155270
T. sphaerosporum	Viride	HMAS 273763	–	KU529134	KU529145
T. subviride	Viride	HMAS 273761	–	KU529131	KU529142
T. tardum	Viride	HMAS 248798	–	KX428020	KX428038
T. trixiae	Viride	ATCC 32630	DQ315445	DQ307526	KC285770

Species	Clade	Strain	GenBank accession numbers		
			ITS	*tef1-α*	*rpb2*
T. vadicola	**Viride**	**WT10708*= ACCC 39716**	**MH287491**	**MH287499**	**MH287511**
T. vadicola	**Viride**	**WT32801**	**MH606225**	**MH606228**	**MH606231**
T. valdunense	Viride	CBS 120923	FJ860863	FJ860717	FJ860605
T. vinosum	Viride	GJS 99-158=CBS 119087	AY380904	AY376047	KC285779
T. viridarium	Viride	S136=CBS 132568	–	KC285658	KC285760
T. viride	Viride	CBS 119327	DQ677655	DQ672617	EU711362
T. viridescens	Viride	S452=CBS 132573	–	KC285646	KC285758
T. viridialbum	Viride	S250=CBS 133495	–	KC285706	KC285774
T. virilente	Viride	S281=CBS 132569	–	KC285692	KC285767
T. vulgatum	Viride	HMAS 248796	–	KX428019	KX428037
Protocrea illinoensis	Outgroup	TFC 96-98	EU703930	EU703905	EU703952
Protocrea farinosa	Outgroup	CPK 3144	EU703917	EU703894	EU703938

Newly-sequenced material is indicated in bold type.

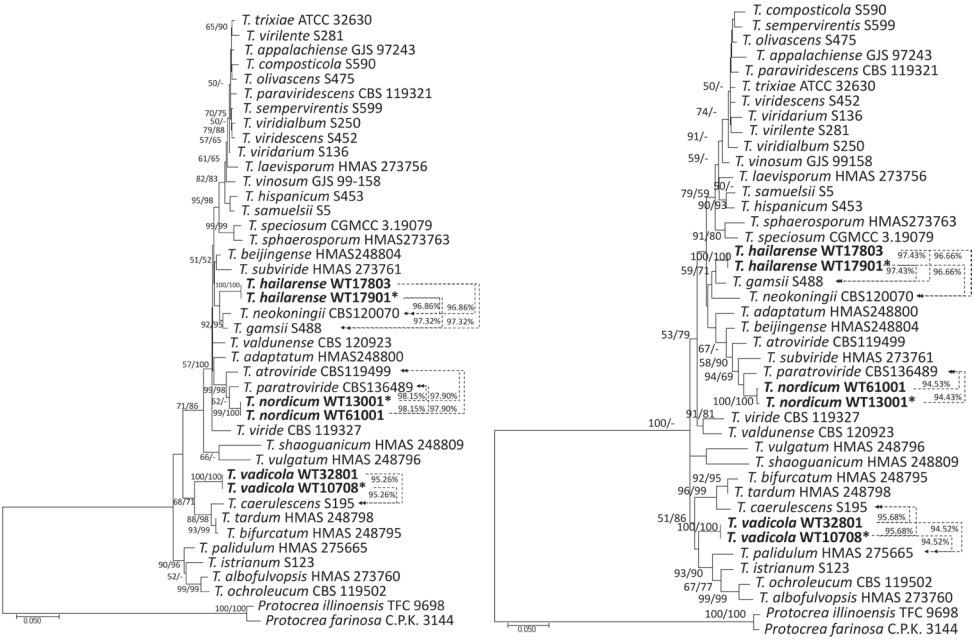

Figure 1. Phylogenetic tree, based on the Maximum Likelihood analysis of the *rpb2* (left; InL = -5930.92) and *tef1-α* (right; InL = -7681.95) dataset. Bootstrap values of Maximum Likelihood (left) and Maximum Parsimony (right) above 50% are indicated at the nodes. The tree is rooted with *Protocrea illinoensis* TFC 9698 and *P. farinose* CPK 3144. New species proposed here are indicated in bold. The type strains are indicated with an asterisk (*) after the strain number. Results of the pairwise sequence similarity are illustrated on the dashed lines between the query strain and its closely-related species (arrows point to the reference strains).

The MP analyses using *tef1-α* and *rpb2* (Fig. 1) resulted in topologically similar trees with minor differences. Each new taxon of *Trichoderma* formed a distinct clade and meets the *Trichoderma* new species standard (does not meet the $sp\exists!(rpb2_{99} \cong tef1_{97})$ standard for known *Trichoderma* species) (Cai and Druzhinina 2021). The similarity value between the new species and the reference strain is shown in the number on the right side of the phylogenetic trees.

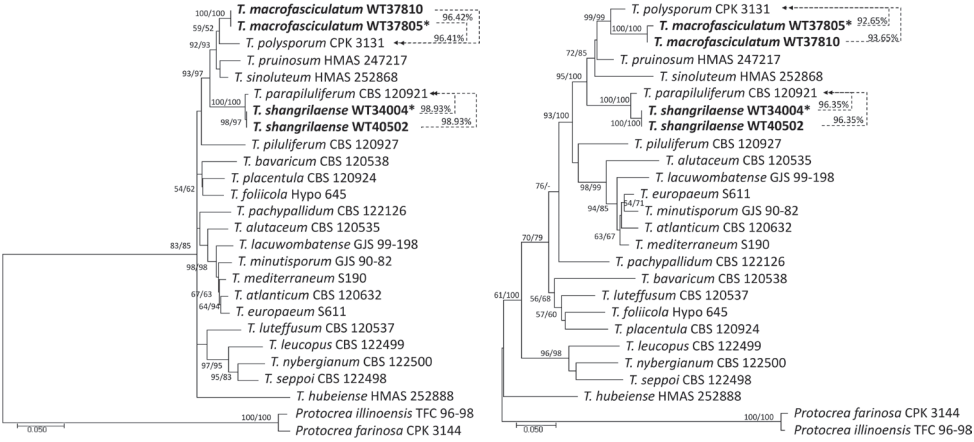

Figure 2. Phylogenetic tree based on the Maximum Likelihood analysis of the *rpb2* (left; InL = -5912.02) and *tef1*-α (right; InL = -9060.53) dataset. Maximum Likelihood bootstrap values (left) and MPBP (right) above 50% are indicated at the nodes. The tree is rooted with *Protocrea illinoensis* TFC 9698 and *P. farinose* CPK 3144. New species proposed here are indicated in bold. The type strains are indicated with an asterisk (*) after the strain number. Results of the pairwise sequence similarity are illustrated on the dashed lines between the query strain and its closely-related species (arrows point to the reference strains).

Trichoderma hailarense clearly separated from *T. gamsii* S488 (with similarity *rpb2* = 97.32% and *tef1*-α = 97.43%) and *T. neokoningii* CBS120070 (with similarity *rpb2* = 96.86% and *tef1*-α = 96.66%). *Trichoderma nordicum* was associated, but clearly separated from *T. paratroviride* CBS136489 with similarity *rpb2* = 98.15% and *tef1* = 94.43%. *Trichoderma vadicola* was associated, but clearly separated from *T. caerulescens* S195 (with similarity 95.26%), *T. tardum* HMAS 248798 (with similarity 95.57%) and *T. bifurcatum* S195 (with similarity 95.76%) in the phylogenetic tree of the *rpb2*. However, there were differences in the phylogenetic tree of the *tef1*-α; *T. vadicola* was associated and separated from *T. palidulum* HMAS 275665 (with similarity 94.52%), *T. istrianum* S123 (with similarity 96.14%), *T. ochroleucum* CBS 119502 (with similarity 93.49%) and *T. albofulvopsis* HMAS 273760 (with similarity 93.16%) (Fig. 1). The strains of *T. macrofasciculatum* were associated, but clearly separated from *T. polysporum* C.P.K. 3131 with similarity *rpb2* = 96.41% and *tef1*-α = 92.81%; *T. shangrilaense* was closely related and separated from *T. parapiluliferum* CBS 120927 with similarity *rpb2* = 98.93% and *tef1*-α = 96.35% (Fig. 2).

Taxonomy

***Trichoderma hailarense* G.Z. Zhang, sp. nov.**
MycoBank no: MB 821318
Fig. 3

Etymology. The specific epithet "*hailarense*" refers to the locality, the Hailar River Basin in Inner Mongolia of China where the holotype was found.

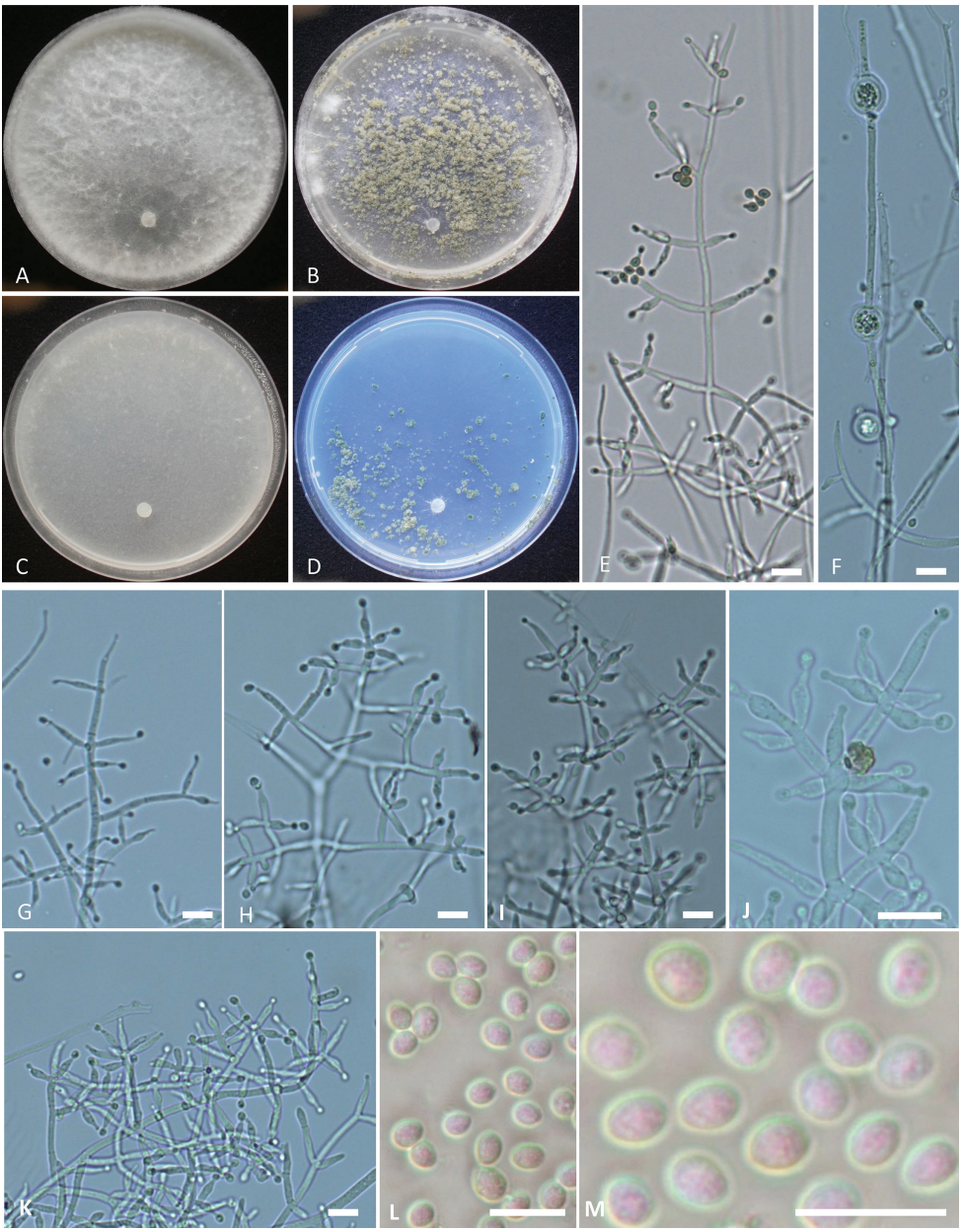

Figure 3. *Trichoderma hailarense* **A–D** cultures on different media incubated at 25 °C for 14 days (**A** on PDA **B** on MEA **C** on CMD **D** on SNA) **E, G–K** conidiophores and phialides **F** chlamydospores **L, M** conidia. Notes: **E** on MEA **F–M** on PDA **A–M** from WT17901. Scale bars: 10 μm (**E–J**).

Typification. China. Inner Mongolia, Hailar River Basin, 618 m (altitude), isolated from soil, 17 September 2016, G.Z. *Zhang* (Holotype WT 17901).

Diagnosis. Phylogenetically, *Trichoderma hailarense* formed a distinct clade and is related to *T. gamsii* and *T. neokoningii* (Fig. 1). The sequence similarity of *rpb2*

with *T. gamsii* S488 and *T. neokoningii* CBS120070 was 97.32% and 96.86%, respectively and the sequence similarity of *tef1*-α with *T. gamsii* S488 and *T. neokoningii* CBS120070 was 97.43% and 96.66%, respectively. Colonies of *T. hailarense* did not form conidia on PDA and conidia of *T. hailarense* on other media were obovoid, delicately roughened and easily distinguished from those of *T. gamsii* and *T. neokoningii*.

Teleomorph. Unknown.

Growth optimal at 30 °C, slow at 35 °C on all media. Colony radius after 72 h at 30 °C 53–56 mm on PDA, 54–56 mm on CMD, 33–37 mm on MEA and 33–36 mm on SNA. Colony radius after 72 h at 35 °C 13–15 mm on PDA, 10–14 mm on CMD, 9–12 mm on MEA and 10–12 mm on SNA. Aerial mycelia abundant, arachnoid on PDA after 72 h at 25 °C under 12 h photoperiod. Conidiation started around the inoculation point after 7 days on PDA, with relatively few or small conidia. Diffusing pigment or distinctive odour absent. Conidiation started around the inoculation point after 7 days on MEA, forming a few large pustules, cream yellow. On SNA, aerial mycelia were few, forming a few large pustules around the inoculation point in age, cream-yellow. Conidiophores and branches narrow and flexuous, tending to be regularly verticillate, forming a pyramidal structure, with each branch terminating in a cruciate whorl of up to five phialides. Phialides, lageniform, (8.0–)9.4–13.1(–15.5) × (2.5–)3.0–3.5(–3.6) µm (mean = 11.2 × 3.3 µm), base 1.8–2.5 µm (mean = 2.1 µm); phialide length/width ratio (2.33–)2.7–4.4(–5.9) (mean = 3.4). Conidia obovoid, (4.2–)4.3–4.7(–4.9) × (3.4–)3.6–3.9(–4.1) µm (mean = 4.5 × 3.7 µm), length/width ratio 1.1–1.4 (mean = 1.2), delicately roughened. Chlamydospores: (7.0–)7.5–8.2(–8.5) × (6.5–)7.0–7.5(–8.3) µm.

Distribution. China. Inner Mongolia.

Additional specimen examined. China. Inner Mongolia, Hulun Buir, 610 m (altitude), isolated from soil, 17 September 2016, *J.D. Hu* (WT17905).

Notes. Phylogenetically *Trichoderma hailarense* is related to *T. gamsii* and *T. neokoningii* (Fig. 1) and does not meet the $sp\exists!(rpb2_{99} \cong tef1_{97})$ standard for *T. gamsii* or *T. neokoningii*. Morphologically, colonies of *T. gamsii* and *T. neokoningii* on PDA formed conidia sporadically or in hemispherical pustules and conidia of *T. gamsii* and *T. neokoningii* were ellipsoidal to oblong, smooth-walled (Jaklitsch et al. 2006). However, colonies of *T. hailarense* did not form conidia on PDA and conidia of *T. hailarense* on other media were obovoid, delicately roughened and easily distinguished from those of *T. gamsii* and *T. neokoningii*.

***Trichoderma macrofasciculatum* G.Z. Zhang, sp. nov.**

MycoBank no: MB 821299

Fig. 4

Etymology. The specific epithet "*macrofasciculatum*" refers to the morphological feature of the conidiation, conidiophores aggregated into large fascicles in concentric rings.

Typification. China, Sichuan, Nine-Village Valley, 2405 m (altitude), isolated from soil, 24 September 2016, G.Z. *Zhang* (Holotype WT 37805).

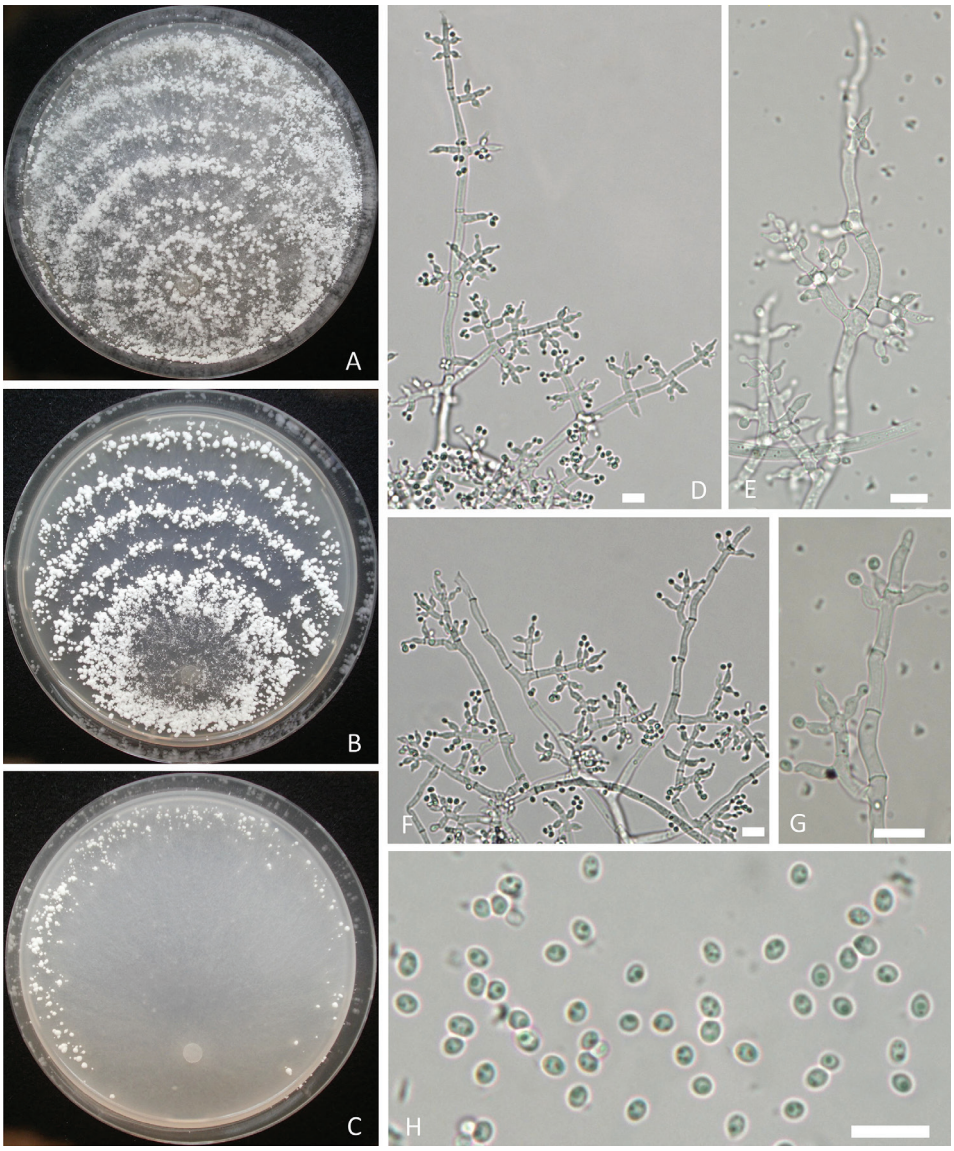

Figure 4. *Trichoderma macrofasciculatum* **A–C** cultures on different media incubated at 25 °C for 7 days (**A** on PDA **B** on MEA **C** on CM) **D–G** conidiophores and phialides **H** conidia with guttules. Notes: **A, D, E** from WT37810 **B, C, F, G** from WT37805. Scale bars: 10 μm (**D–H**).

Diagnosis. Phylogenetically, *Trichoderma macrofasciculatum* WT37805 and WT37810 formed a distinct clade and is related to *T. polysporum* C.P.K. 3131 in the Polysporum clade, but the similarities of *rpb2* and *tef1*-α between these two species were only 96.41% and 92.81%, respectively. *Trichoderma macrofasciculatum* cannot grow at 35 °C as *T. polysporum* and the former formed large and white pustules in concentric rings at 25 °C, elongations were rarely observed and conidia had few guttules, which are distinct from *T. polysporum*.

Teleomorph. Unknown.

Growth optimum at 20 °C, slow or limited at 30 °C, absent at 35 °C. Colony radius after 72 h at 25 °C 21–24 mm on PDA, 23–27 mm on CMD, 17–20 mm on MEA and 12–16 mm on SNA. Aerial mycelia abundant on PDA and MEA after incubation for 72 h at 25 °C under a 12 h photoperiod. Conidiation typically in pustules in concentric rings on PDA, solitary or aggregated, producing a farinose to granular mat. Diameter of pustules up to 2.2 mm, pompon-like, white. Diffusing pigment and distinct odour absent. Conidiation on MEA typically in pustules in concentric rings, pompon-like as on PDA. On CMD, aerial mycelia sparsely developed. Conidiation aggregated in sporadic pustules near the colony margin, white. On SNA, aerial mycelia few and conidiation not observed. Conidiophores and branches irregularly branched in a dendriform structure, with each branch terminating in a cruciate whorl of up to five phialides. Hyphal septa clearly visible. Phialides flask-shaped, often curved, (4.9–)5.6–7.8(–8.8) × (2.8–)3.0–3.2(–3.4) μm (mean = 6.7 × 3.1 μm), 1.8–2.6 μm (mean = 2.2 μm) near the base; phialide length/width ratio (1.5–)1.8–2.4(–2.8) (mean = 2.1). Conidia subglobose to ellipsoid, hyaline, smooth, with one or few distinctly verrucose, (2.6–)2.8–3.3(–3.6) × (2.4–)2.5–2.7(–2.9) μm (mean = 3.0 × 2.6 μm), length/width ratio 1.0–1.3 (mean = 1.2). Chlamydospores not observed.

Distribution. China, Sichuan Province.

Additional material examined. China, Sichuan, Nine-Village Valley, 2405 m (altitude), isolated from soil, 24 September 2016, G.Z. *Zhang* (WT 37810).

Notes. Phylogenetically *Trichoderma macrofasciculatum* WT 37805 is related to *T. polysporum* C.P.K. 3131 in the Polysporum clade (Fig. 1), but the similarities of *rpb2* and *tef1*-α between these two species were only 96.41% and 92.81% respectively, with 94 and 41 bp differences amongst 1311 and 1152 bp. *Trichoderma macrofasciculatum* cannot grow at 35 °C as *T. polysporum* and the former formed large and white pustules in concentric rings at 25 °C, elongations were rarely observed and conidia had few guttules, which are distinct from *T. polysporum* (Lu et al. 2004).

***Trichoderma nordicum* G.Z. Zhang, sp. nov.**

MycoBank no: MB 8212301

Fig. 5

Etymology. "nord" means found in the north of China.

Holotype. China, Beijing, Yu-yuan-tan Park, 43 m (altitude), isolated from soil, 27 October 2016, G.Z. Zhang (Holotype WT 13001), ex-type culture ACCC 39713.

Diagnosis. Phylogenetically *Trichoderma nordicum* is related to *T. paratroviride*, but the sequence similarities of *rpb2* and *tef1*-α were 98.15% and 94.43%, respectively. That does not meet the $sp\exists!(rpb2_{99} \cong tef1_{97})$ standard for *T. paratroviride* or other known *Trichoderma* species. Morphologically, conidiophores of *T. paratroviride* consisting of a main axis and often distantly-spaced side branches, not re-branching. Conidiophores of *T. nordicum* are branched in a more complex manner; conidia are larger than those of *T. paratroviride*.

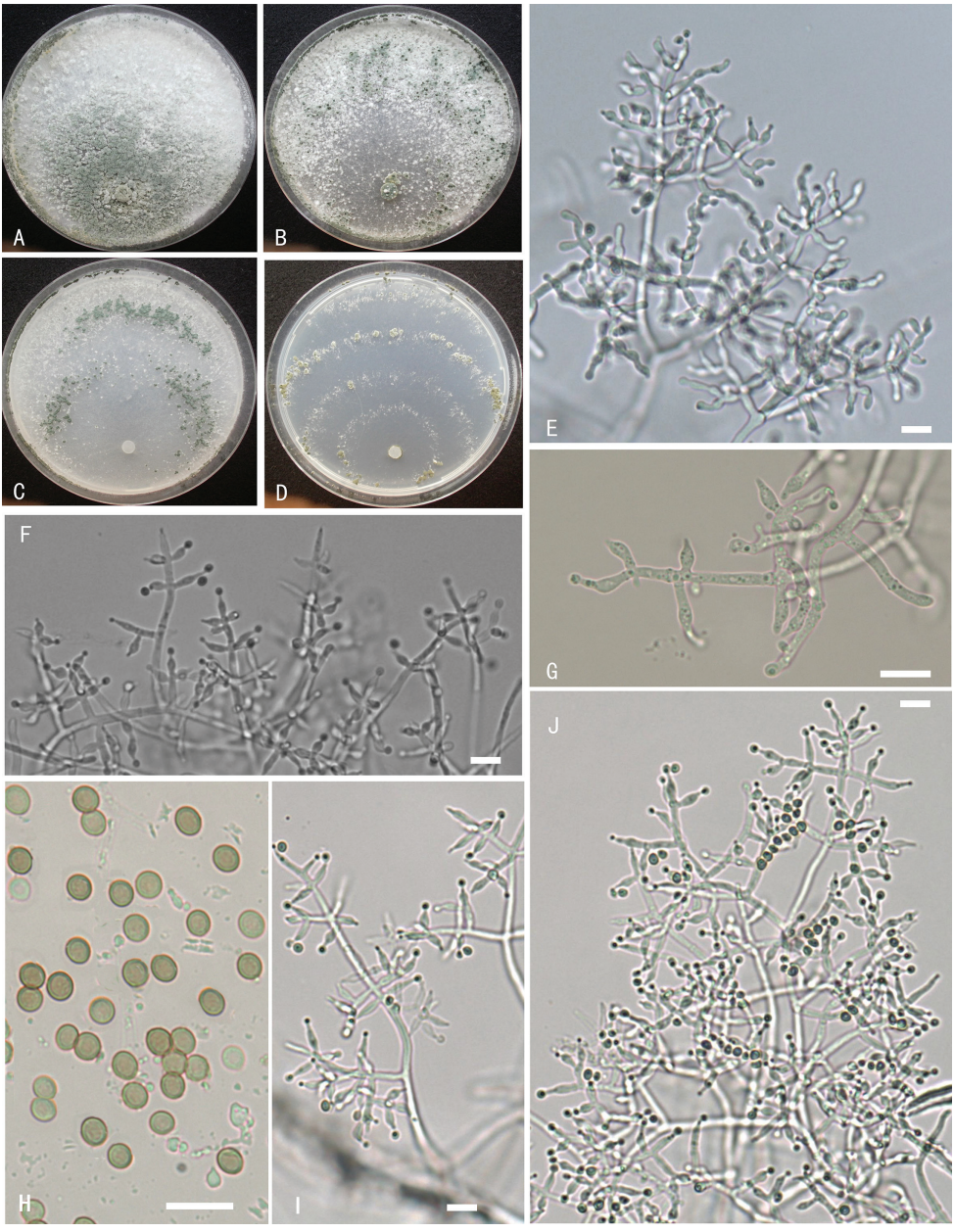

Figure 5. *Trichoderma nordicum* **A–D** cultures on different media at 25 °C after 10 days (**A** on PDA **B** on MEA **C** on CMD **D** on SNA) **E–G, I, J** conidiophores and phialides **H** conidia. Notes: **E** on PDA **F–J** on MEA **A–D** from WT13001 **E–J** from WT61001. Scale bars: 10 µm (**E–J**).

Teleomorph. Unknown.

Growth optimal at 25 °C, slow or limited at 30 °C, absent at 35 °C. Colonies grew fast on PDA, CMD and MEA and slow on SNA. Colony radius after 72 h at 25 °C 67–71 mm on PDA, 68–71 mm on CMD, 51–55 mm on MEA and 21–24 mm on

SNA. Aerial mycelia sparse on PDA after 72 h at 25 °C under 12 h photoperiod and conidiation developed within 48 h beginning at the inoculation point and progressed around, grey-white at first and slowly turning green. Diffusing pigment or distinctive odour absent. Aerial mycelia sparse and flocculence on MEA after 72 h at 20 °C under 12 h photoperiod. Conidia developed within 48 h beginning near the colony margin on MEA, grey-white at first and slowly turning green, transparent liquid secreted. Aerial mycelia few on SNA and CMD after 72 h at 25 °C, conidia formed around the inoculation point and in distinct concentric rings after 96 h under 12 h photoperiod on SNA and CMD, diffusing pigment not produced. Conidiophores and branches narrow and flexuous, tending to be regularly verticillate forming a pyramidal structure, each branch terminating in a cruciate whorl of up to five phialides. Phialides, lageniform, (6.2–)7.2–10.3(–12.9) × (2.6–)2.9–3.2(–3.4) μm (mean = 8.8 × 3.1 μm), 1.6–2.3 μm (mean = 1.9 μm) near the base; phialide length/width ratio (2.1–)2.4–3.4(–4.3) (mean = 2.9). On PDA, phialides curved, distinguished from those on other media. Conidia, globose to obovoidal, (4.1–)4.4–4.8(–5.0) × (4.0–)4.1–4.4(–4.6) μm (mean = 4.6 × 4.3 μm), length/width ratio 1.0–1.2 (mean = 1.1). Chlamydospores sometimes present, (8.7–)9.8 × 10.4(–12.5) μm.

Distribution. China, Beijing and Hebei.

Additional specimen examined. China. Hebei, Bai-yang Lake, 19 m (altitude), isolated from soil, 15 September 2016, *J.S. Li* (WT 61001).

Notes. Phylogenetically, *Trichoderma nordicum* is related to *T. paratroviride* (Fig. 1), but the sequence similarities of *rpb2* and *tef1*-α were 98.15% and 94.43%, respectively. That does not meet the $sp\exists!(rpb2_{99} \cong tef1_{97})$ standard for *T. paratroviride* or other known *Trichoderma* species. Morphologically, conidiophores of *T. paratroviride* consist of a main axis and often distantly-spaced side branches, not re-branching. Conidiophores of *T. nordicum* are branched in a more complex manner; conidia are larger than those of *T. paratroviride* (Jaklitsch and Voglmayr 2015).

Trichoderma shangrilaense G.Z. Zhang, sp. nov.

MycoBank no: MB 821300
Fig. 6

Etymology. "*shangrilaense*" was originally found at Shangrila in Yunnan Province of China.

Typification. China. Yunnan, Pudacuo National Park, 3611 m (altitude), isolated from soil, 21 June 2016, G.Z. Zhang (Holotype WT 34004), Ex-type culture ACCC 39714.

Diagnosis. Phylogenetically, *Trichoderma shangrilaense* is related to *T. parapiluliferum* (CBS 120921) (Fig. 1), but the sequence similarity of *rpb2* between these two species was 98.93% and the sequence similarity of *tef1*-α was 96.35%. That does not meet the $sp\exists!(rpb2_{99} \cong tef1_{97})$ standard for *T. parapiluliferum* or other known *Trichoderma* species. Conidiophore main axis of *T. shangrilaense* fertile to apex, conidia obovoid to ellipsoid, easily distinguished from that of *T. parapiluliferum*.

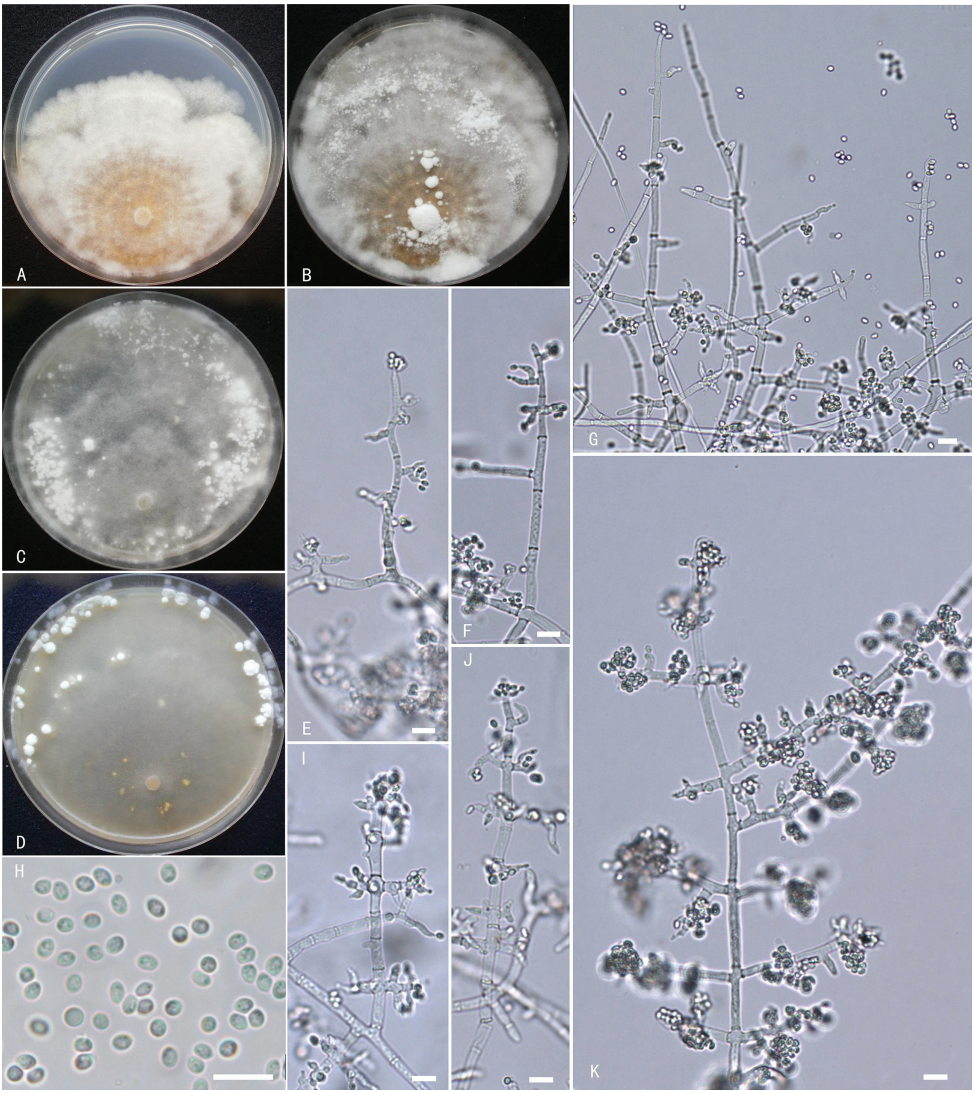

Figure 6. *Trichoderma shangrilaense* **A–D** cultures (**A** on PDA, 25 °C, 10 days **B** on PDA, 25 °C, 21 days **C** on MEA, 25 °C, 21 days **D** on CMD, 25 °C, 21 days) **E–G, I–K** conidiophores and phialides **H** conidia **A–K** from WT34004. Scale bars: 10 µm (**E–K**).

Teleomorph. Unknown.

Growth optimal at 20 °C, slow, limited at 25 °C and absent at 30 °C or 35 °C. Colony radius after 72 h at 20 °C 19–21 mm on PDA, 23–24 mm on CMD, 19–21 mm on MEA and 8–11 mm on SNA. Aerial mycelia abundant, compact on PDA after 7 days at 20 °C under 12 h photoperiod, conidiation not easily formed and a yellow diffusing pigment developed near the inoculation point; conidiation formed unequal in size, white pustules after 14 days. Conidiophores and branches narrow and

flexuous, forming a dendriform structure and irregularly branched, not rebranched, main axis to 4.3–5.0 µm wide, fertile to apex. Phialides, flask-shaped, often curved, (4.5–)5.7–9.0(–11.1) × (2.9–)3.2–3.5(–4.1) µm (mean = 7.4 × 3.4 µm), 1.6–3.4 µm wide (mean = 2.6 µm) near the base; phialide length/width ratio (1.5–)2.0–2.6(–3.0) (mean = 2.3). Conidia, obovoid to ellipsoidal, smooth, (3.3–)3.5–4.0(–4.4) × (2.8–)3.0–3.3(–3.5) µm (mean = 3.8 × 3.19 µm), length/width ratio 1.1–1.4 (mean = 1.2). Chlamydospores not observed.

Colony radius 28–33 mm, aerial mycelia abundant and floccose after 7 days at 20 °C under 12 h photoperiod. Conidiation slowly developing on MEA. After about 14 days, pompon-like, white fascicles developed. No diffusing pigment observed. On CMD after 7 days at 20 °C under 12 h photoperiod, colony radius 28–33 mm, aerial mycelia few. Conidiation formed flat or cushion-shaped pustules near the colony margin after 21 days and a yellow diffusing pigment developed near the inoculation point. On SNA after 7 days at 20 °C under 12 h photoperiod, colony mycelia sparse and no conidiation formed. After 10 days, pustules scattered around the periphery of the colony. Diffusing pigment not developed.

Distribution. China. Yunnan and Sichuan.

Additional specimen examined. China. Sichuan, Huanglong Nature Reserve, 3561 m (altitude), isolated from soil, 25 September 2016, *Z. Li* (WT 34012).

Notes. Phylogenetically, *Trichoderma shangrilaense* is related to *T. parapiluliferum* (CBS 120921) (Fig. 1), but the sequence similarity of *rpb2* between these two species was 98.93% and the sequence similarity of *tef1-α* was 96.35%. The sequence similarity of *tef1-α* with the ex-type culture G.J.S. 91-60 (GenBank accession no. AY937444) was only 92%. Optimum temperature for growth of *T. shangrilaense* was 20 °C, no growth occurred at 30 °C as in *T. parapiluliferum* and conidiation structures consist of flat or cushion-shaped pustules, formed near the colony margin on MEA, SNA and CMD. Conidiophore main axis of *Trichoderma parapiluliferum* has conspicuous spiral sterile apical elongations, conidia ellipsoidal to oblong (Lu et al. 2004). Conidiophore main axis of *T. shangrilaense* fertile to apex, conidia obovoid to ellipsoid, easily distinguished from that of *T. parapiluliferum*.

Trichoderma vadicola G.Z. Zhang, sp. nov.

MycoBank no: MB 821316
Fig. 7

Etymology. The specific epithet "*vadicola*", from the noun "vadum", reflects the ecological environment and means that the species inhabits shallow water.

Typification. China. Shandong, 2 m (altitude), isolated from soil, 13 August 2016, G.Z. Zhang (Holotype WT 10708), Ex-type culture ACCC 39716.

Diagnosis. Phylogenetically, *Trichoderma vadicola* is related to *T. caerulescens* in the Viride clade (Fig. 1), but the sequence similarity of *tef1-α* and *rpb2* between these species was all 95%. Morphologically, colonies of *T. vadicola* and *T. caerulescens* on PDA

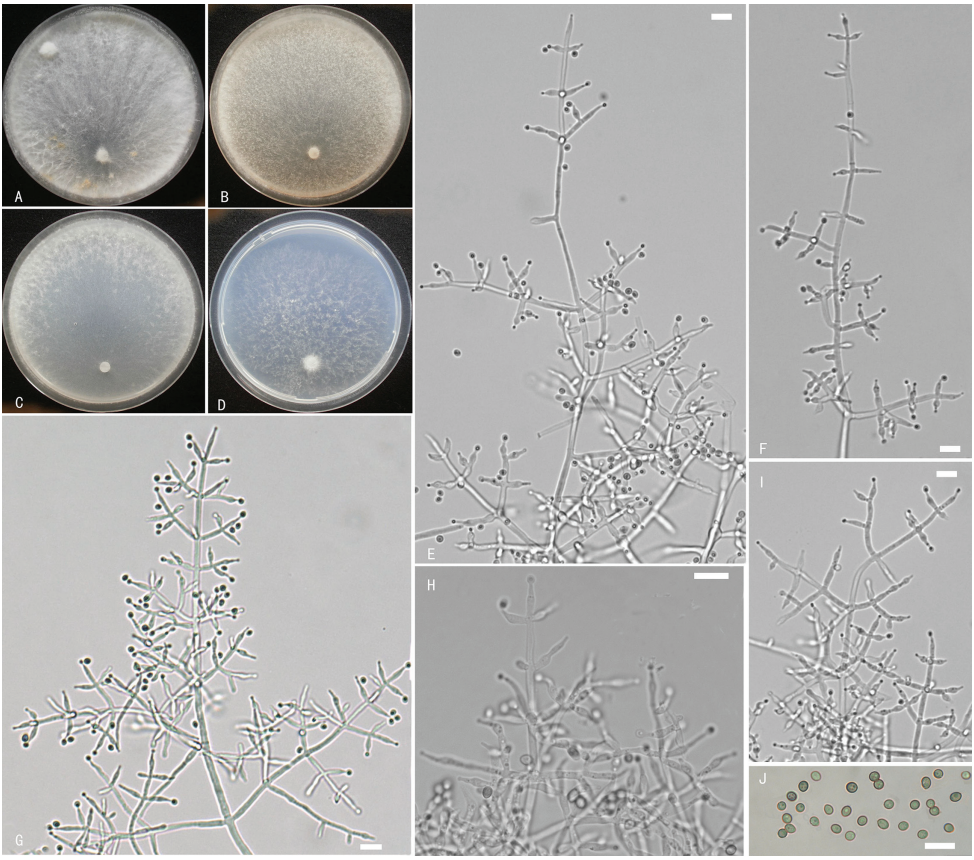

Figure 7. *Trichoderma vadicola* **A–D** cultures on different media at 25 °C (**A** on PDA after10 days **B** on MEA, after 7 days **C** on CMD after 7 days **D** on SNA after 7 days) **E–I** conidiophores and phialides **J** conidia. Notes: **E, F, H–J** on MEA **G** on SNA **A–J** from WT10708. Scale bars: 10 μm (**E–J**).

have similar features, such as abundant aerial hyphae, forming strands and a whitish hairy or floccose mat. However, the former *Trichoderma vadicola* formed no or relatively few conidia and the latter forming greyish-bluish patches around the plug. On CMD, *T. caerulescens* peculiar greyish-blue pigment formed after 1–2 months and conidiophores simply or slightly branched; the former had no observed diffusing pigment and conidiophores branched in a complex manner in pyramidal structure or tree-like.

Teleomorph. Unknown.

Growth optimal at 25 °C, no grow at 35 °C on all media. Colony radius after 72 h at 25 °C 25–29 mm on PDA, 24–27 mm on CMD, 23–26 mm on MEA and 22–26 mm on SNA. Aerial mycelia abundant on PDA after 72 h at 25 °C under 12 h photoperiod, forming strands and floccose mat. Conidiation not formed or relatively few. No diffusing pigment or distinctive odour was produced. On MEA after 72 h at 25 °C under 12 h photoperiod, aerial mycelia abundant, floccose. After 7 days, mycelia covered the plate and conidia appeared, effuse, granuliform. On CMD after 72 h

at 25 °C under 12 h photoperiod, aerial mycelia not observed. After 7 days, mycelia covered the plate and conidia developed near the colony margin. On SNA after 72 h at 25 °C under 12 h photoperiod, aerial mycelia not observed. After 7 days, mycelia covered the plate, aerial mycelia floccose and conidia formed, effuse. Conidiophores and branches regularly verticillate, formed a pyramidal structure, each branch terminating in a cruciate whorl of 3–5 phialides. Phialides lageniform, (8.3–)9.9–12.3(–15.1) × (2.0–)2.6–3.2(–3.4) µm (mean = 11.1 × 2.9 µm), 1.1–2.9 µm wide (mean = 1.9 µm) near the base; phialide length/width ratio (2.7–)3.2–4.6(–6.6) (mean = 3.9). Conidia subglobose or obovoidal, (3.5–)3.7–4.3(–4.8) × (3.2–)3.4–3.6(–3.8) µm (mean = 4.0 × 3.5 µm), length/width ratio 1.0–1.3 (mean = 1.1). Chlamydospores not observed.

Distribution. China. Shandong and Yunnan Provinces.

Additional specimen examined. China. Yunnan, Shangri-La, Pudacuo National Park, 3551 m (altitude), isolated from soil, 21 September 2016, H.T. Yang (WT 10713).

Notes. Phylogenetically, *Trichoderma vadicola* is related to *T. caerulescens* in the Viride clade (Fig. 1), but the sequence similarity of *tef1-α* and *rpb2* between these species was all 95%, with 62 and 60 bp differences amongst 1218 and 1130 bp, respectively. Morphologically, colonies of *T. vadicola* and *T. caerulescens* on PDA have similar features, such as abundant aerial hyphae, forming strands and a whitish hairy or floccose mat. However, the former *Trichoderma vadicola* formed no or relatively few conidia, with the latter forming greyish-bluish patches around the plug. On CMD, *T. caerulescens* formed peculiar greyish-blue pigment after 1–2 months and conidiophores simply or slightly branched (Jaklitsch et al. 2012); the former had no observed diffusing pigment and conidiophores branched in a complex manner in pyramidal structure or tree-like.

Discussion

In this paper, five new species of *Trichoderma* were described from wetland soils. An ML tree was reconstructed, based on individual *tef1-α* and *rpb2*, to explore the taxonomic positions of the new species. Our phylogenetic analyses showed that the five new *Trichoderma* species belong to the Polysporum clade or the Virde clade. *Trichoderma macrofasciculatum* and *T. shangrilaense* belong to the Polysporum clade (as *Pachybasium* core group; Jaklitsch 2011) (Fig. 2). Here, we added two new species, *T. macrofasciculatum* and *T. shangrilaense*, which are close to *T. polysporum* and *T. parapiluliferum*. Morphologically, species in this clade are heterogeneous, comprising teleomorphs with upright, stipitate or small pulvinate stromata. The teleomorphs of *T. macrofasciculatum* and *T. shangrilaense* have not been found at present, but their asexual characteristics, such as conidiation in white pustules, resemble other species in this clade.

Trichoderma nordicum, *T. vadicola*, and *T. hailarense* belong to the Viride clade (formerly section *Trichoderma*) (Fig. 1). Here, we added three new species, *T. hailarense T. nordicum* and *T. vadicola*, which are all located in the unnamed branches and close

to *T. gamsii*/*T. neokoningii*, *T. paratroviride* and *T. caerulescens*, respectively. Phenotypically, phialides of three new species are lageniform and have green conidia, which is consistent with the characteristics of *Trichoderma* species in the Viride clade. Only *T. hailarense* has coarsely warted conidia, two other species being smooth-walled.

At present, the identification of *Trichoderma* species is mainly based on phylogenetic analysis and morphological characteristics. The new species hypothesis needs to be supported by the topology of both phylograms (*rpb2* and *tef1-α*). However, there are no numerical standards of the similarity threshold at the level which is sufficient for identification for most of the existing species (Cai and Druzhinina 2021) and this has led to many inaccuracies in the original identification of *Trichoderma*. In the phylogenetic tree constructed in this paper, some *Trichoderma* species combinations showed low bootstrap values (Figs 1 and 2) and have high similarity, which meet the $sp\exists!(rpb2_{99} \cong tef1_{97})$ standard developed by Cai and Druzhinina (2021). They may be identified as the same *Trichoderma* species: for example, *T. viridialbum*, *T. viridarium* and *T. sempervirentis*, which belong to the *Trichoderma viridescens* complex (Jaklitsch et al. 2013), may still be identified as *T. viridescens*. *T. paraviridescens*, *T. trixiae* and *T. appalachiense* may be identified as the same *Trichoderma* species.

Trichoderma species cannot be identified by phylogenetic analysis without considering the sequence similarity values. Therefore, Cai and Druzhinina (2021) developed a protocol for molecular identification of *Trichoderma* that requires analysis of the three DNA barcodes (ITS, *tef1-α* and *rpb2*). Molecular identification of *Trichoderma* species can be achieved, based on the analysis of sequence similarities between the query strain and the reference strains that are analysed for *tef1-α* (≥ 97%) and *rpb2* (≥ 99%). If this condition is not met, the query strain may be a new species of *Trichoderma* and the new species hypothesis can be made, based on sequence similarities and phylogenetic concordance, i.e. analysis of single loci tree topologies for *tef1-α* and *rpb2* and must be verified, based on morphology. In the identification process of the new species, we made full reference to this protocol and there were sufficient differences in sequence similarity between the newly-identified species and the reference species, as well as significant differences in morphological characteristics. According to Jaklitsch et al. (2013), the morphology of *T. viridialbum*, *T. viridarium* and *T. sempervirentis* (meeting the $sp\exists!(rpb2_{99} \cong tef1_{97})$ standard) shows a high degree of similarity and should still be identified as *T. viridescens*. This also fully verified that the identification protocol developed by Cai and Druzhinina (2021) is helpful to ensure the accuracy of *Trichoderma* species identification, which is worth promoting and applying, especially for the identification of *Trichoderma* species.

Acknowledgements

The authors sincerely thank Jin Dong Hu, Zhe Li and Ji Shun Li for providing the soil specimens. The authors are grateful to Konstanze Bensch for advising on the Latin names. This work was financed by the Shandong Key Research and Development

Project (2014GSF121028; 2019GSF107086), Shandong Major Science and Technology innovation project (2019JZZY020610) and National Natural Science Foundation of China (Project no. 31700426; 31901928).

References

Atanasova L, Druzhinina IS, Jaklitsch WM (2013) Two hundred *Trichoderma* species recognized on the basis of molecular phylogeny. In: Mukherjee PK, Horwitz BA, Singh US, Mukherjee M, Schmoll M (Eds) *Trichoderma*: biology and applications. CAB International, Croydon, 10–42. https://doi.org/10.1079/9781780642475.0010

Bissett J (1991) A revision of the genus *Trichoderma* III. Infrageneric classification. Canadian Journal of Botany-revue Canadienne de botanique 69: 2372–2417. https://doi.org/10.1139/b91-297

Bissett J, Gams W, Jaklitsch W, Samuels GJ (2015) Accepted *Trichoderma* names in the year 2015. IMA Fungus 6(2): 263–295. https://doi.org/10.5598/imafungus.2015.06.02.02

Bustamante DE, Calderon MS, Leiva S, Mendoza JE, Arce M, Oliva M (2021) Three new species of *Trichoderma* in the Harzianum and Longibrachiatum lineages from Peruvian cacao crop soils based on an integrative approach. Mycologia 113(5): 1056–1072. https://doi.org/10.1080/00275514.2021.1917243

Cai F, Druzhinina IS (2021) In honor of John Bissett: authoritative guidelines on molecular identification of *Trichoderma*. Fungal Diversity 107: 1–69. https://doi.org/10.1007/s13225-020-00464-4

Carbone I, Kohn LM (1999) A method for designing primer sets for speciation studies in filamentous ascomycetes. Mycologia 91(3): 553–556. https://doi.org/10.1080/00275514.1999.12061051

Chaverri P, Samuels GJ (2003) *Hypocrea*/*Trichoderma* (Ascomycota, Hypocreales, Hypocreaceae), Species with green ascospores. Studies in Mycology 48: 1–116.

Chaverri P, Gazis RO, Samuels GJ (2011) *Trichoderma amazonicum*, a new endophytic species on *Hevea brasiliensis* and *H. guianensis* from the Amazon Basin. Mycologia 103(1): 139–151. https://doi.org/10.3852/10-078

Chen K, Zhuang WY (2016) *Trichoderma shennongjianum* and *Trichoderma tibetense*, two new soil-inhabiting species in the Strictipile clade. Mycoscience 57(5): 311–319. https://doi.org/10.1016/j.myc.2016.04.005

Chen K, Zhuang WY (2017a) Three new soil-inhabiting species of *Trichoderma* in the Stromaticum clade with test of their antagonism to pathogens. Current Microbiology 74(9): 1049–1060. https://doi.org/10.1007/s00284-017-1282-2

Chen K, Zhuang WY (2017b) Seven new species of *Trichoderma* from soil in China. Mycosystema 36(11): 1441–1462.

Chen K, Zhuang WY (2017c) Seven soil-inhabiting new species of the genus *Trichoderma* in the Viride clade. Phytotaxa 312(1): 28–46. https://doi.org/10.11646/phytotaxa.312.1.2

Chen K, Zhuang WY (2017d) Discovery from a large-scaled survey of *Trichoderma* in soil of China. Scientific Reports 7(1): e9090. https://doi.org/10.1038/s41598-017-07807-3

Crous PW, Wingfield MJ, Lombard L, Roets F, Swart WJ, Alvarado P, Carnegie AJ, Moreno G, Luangsa-ard J, Thangavel R, Alexandrova AV, Baseia IG, Bellanger J-M, Bessette AE, Bessette AR, la Peña-Lastra SDe, García D, Gené J, Pham THG, Heykoop M, Malysheva E, Malysheva V, Martín MP, Morozova OV, Noisripoom W, Overton BE, Rea AE, Sewall BJ, Smith ME, Smyth CW, Tasanathai K, Visagie CM, Adamčík S, Alves A, Andrade JP, Aninat MJ, Araújo RVB, Bordallo JJ, Boufleur T, Baroncelli R, Barreto RW, Bolin J, Cabero J, Caboň M, Cafà G, Caffot MLH, Cai L, Carlavilla JR, Chávez R, de Castro RRL, Delgat L, Deschuyteneer D, Dios MM, Domínguez LS, Evans HC, Eyssartier G, Ferreira BW, Figueiredo CN, Liu F, Fournier J, Galli-Terasawa LV, Gil-Durán C, Glienke C, Gonçalves MFM, Gryta H, Guarro J, Himaman W, Hywel-Jones N, Iturrieta-González I, Ivanushkina NE, Jargeat P, Khalid AN, Khan J, Kiran M, Kiss L, Kochkina GA, Kolařík M, Kubátová A, Lodge DJ, Loizides M, Luque D, Manjón JL, Marbach PAS, Massola Jr NS, Mata M, Miller AN, Mongkolsamrit S, Moreau P-A, Morte A, Mujic A, Navarro-Ródenas A, Németh MZ, Nóbrega TF, Nováková A, Olariaga I, Ozerskaya SM, Palma MA, Petters-Vandresen DAL, Piontelli E, Popov ES, Rodríguez A, Requejo Ó, Rodrigues ACM, Rong IH, Roux J, Seifert KA, Silva BDB, Sklenář F, Smith JA, Sousa JO, Souza HG, De Souza JT, Švec K, Tanchaud P, Tanney JB, Terasawa F, Thanakitpipattana D, Torres-Garcia D, Vaca I, Vaghefi N, van Iperen AL, Vasilenko OV, Verbeken A, Yilmaz N, Zamora JC, Zapata M, Jurjević Ž, Groenewald JZ (2019) Fungal Planet description sheets: 951–1041. Persoonia 43: 223–425. https://doi.org/10.3767/persoonia.2019.43.06

Ding MY, Chen W, Ma XC, Lv BW, Jiang SQ, Yu YN, Rahimi MJ, Gao RW, Zhao Z, Cai D, Druzhinina IS (2020) Emerging salt marshes as a source of *Trichoderma arenarium* sp. nov. and other fungal bioeffectors for biosaline agriculture. Journal of Applied Microbiology 130: 179–195. https://doi.org/10.1111/jam.14751

Dodd SL, Lieckfeldt E, Samuels GJ (2003) *Hypocrea atroviridis* sp. nov., the teleomorph of *Trichoderma atroviride*. Mycologia 95(1): 27–40. https://doi.org/10.1080/15572536.2004.11833129

Dou K, Lu Z, Wu Q, Ni M, Yu C, Wang M, Li Y, Wang X, Xie H, Chen J, Zhang C (2020) MIST: a multilocus identification system for *Trichoderma*. Applied and Environmental Microbiology 86(18): e01532-20. https://doi.org/10.1128/AEM.01532-20

Druzhinina IS, Kopchinskiy AG, Kubicek CP (2006) The first 100 *Trichoderma* species characterized by molecular data. Mycoscience 47(2): 55–64. https://doi.org/10.1007/S10267-006-0279-7

du Plessis IL, Druzhinina IS, Atanasova L, Yarden O, Jacobs K (2018) The diversity of *Trichoderma* species from soil in South Africa with five new additions. Mycologia 110(3): 59–583. https://doi.org/10.1080/00275514.2018.1463059

Gams W, Bissett J (1998) Morphology and identification of *Trichoderma*. In: Kubicek CP, Harman GE (Eds) *Trichoderma* and *Gliocladium*. Vol. 1. Basic biology, taxonomy and genetics. Taylor and Francis Ltd., Lindon, 3–34.

Gu X, Wang R, Sun Q, Wu B, Sun JZ (2020) Four new species of *Trichoderma* in the Harzianum clade from northern China. MycoKeys 73: 109–132. https://doi.org/10.3897/mycokeys.73.51424

Hasegawa M, Kishino H, Yano T (1985) Dating the human-ape split by a molecular clock of mitochondrial DNA. Journal of Molecular Evolution 22(2): 160–174. https://doi.org/10.1007/BF02101694

Thompson JD, Higgins DG, Gibson TJ (1994) CLUSTAL W: improving the sensitivity of progressive multiple sequence alignment through sequence weighting, position-specific gap penalties and weight matrix choice. Nucleic Acids Research 22(22): 4673–4680. https://doi.org/10.1093/nar/22.22.4673

Jaklitsch WM, Komon M, Kubicek CP, Druzhinina IS (2005) *Hypocrea voglmayrii* sp. nov. from the Austrian Alps represents a new phylogenetic clade in *Hypocrea*/*Trichoderma*. Mycologia 97(6): 1365–1378. https://doi.org/10.3852/mycologia.97.6.1365

Jaklitsch WM, Komon M, Kubicek CP, Druzhinina IS (2006) *Hypocrea crystalligena* sp. nov., a common European species with a white-spored *Trichoderma* anamorph. Mycologia 98(3): 499–513. https://doi.org/10.3852/mycologia.98.3.499

Jaklitsch WM (2009) European species of *Hypocrea* Part I. The green-spored species. Studies in Mycology 63: 1–91. https://doi.org/10.3114/sim.2009.63.01

Jaklitsch WM (2011) European species of *Hypocrea* Part II: species with hyaline ascospores. Fungal Diversity 48(1): 1–250. https://doi.org/10.1007/s13225-011-0088-y

Jaklitsch WM, Stadler M, Voglmayr H (2012) Blue pigment in *Hypocrea caerulescens* sp. nov. and two additional new species in sect. Trichoderma. Mycologia 104: 925–941. https://doi.org/10.3852/11-327

Jaklitsch WM, Samuels GJ, Ismaiel A, Voglmayr H (2013) Disentangling the *Trichoderma viridescens* complex. Persoonia 31: 112–146. https://doi.org/10.3767/003158513X672234

Jaklitsch WM, Voglmayr H (2015) Biodiversity of *Trichoderma* (Hypocreaceae) in Southern Europe and Macaronesia. Studies in Mycology 80: 1–87. https://doi.org/10.1016/j.simyco.2014.11.001

Kimura M (1980) A simple method for estimating evolutionary rate of base substitutions through comparative studies of nucleotide sequences. Journal of Molecular Evolution 16(2): 111–120. https://doi.org/10.1007/BF01731581

Kindermann J, El-Ayouti Y, Samuels GJ, Kubicek CP (1998) Phylogeny of the genus *Trichoderma* based on sequence analysis of the internal transcribed spacer region 1 of the rDNA cluster. Fungal Genetics and Biology 24(3): 298–309. https://doi.org/10.1006/fgbi.1998.1049

Kornerup A, Wanscher JH (1978) Methuen Handbook of Colour, 3rd edn. Sankt Jørgen Tryk, Copenhagen.

Kredics L, Hatvani L, Naeimi S, Körmöczi P, Manczinger L, Vágvölgyi C, Druzhinina I (2014) Biodiversity of the genus *Hypocrea*/*Trichoderma* in different habitats. In: Gupta VK, Schmoll M, Herrera-Estrella M, Upadhyay RS, Druzhinina I, Tuohy MG (Eds) Biotechnology and biology of *Trichoderma*. Elsevier, Waltham, 3–18. https://doi.org/10.1016/B978-0-444-59576-8.00001-1

Kubicek CP, Komon-Zelazowska M, Druzhinina IS (2008) Fungal genus *Hypocrea*/*Trichoderma*: from barcodes to biodiversity. Journal of Zhejiang University Science B 9(10): 753–763. https://doi.org/10.1631/jzus.B0860015

Kullnig-Gradinger CM, Szakacs G, Kubicek CP (2002) Phylogeny and evolution of the fungal genus *Trichoderma*: a multigene approach. Mycological Research 106: 757–767. https://doi.org/10.1017/S0953756202006172

Kumar S, Stecher G, Li M, Knyaz C, Tamura K (2018) MEGA X: Molecular Evolutionary Genetics Analysis across computing platforms. Molecular Biology and Evolution 35(6): 1547–1549. https://doi.org/10.1093/molbev/msy096

Li J, Wu Y, Chen K, Wang Y, Hu J, Wei Y, Yang H (2018) *Trichoderma cyanodichotomus* sp. nov., a new soil-inhabiting species with a potential for biological control. Canadian Journal of Microbiology 64(12): 1020–1029. https://doi.org/10.1139/cjm-2018-0224

Liu YL, Whelen S, Hall BD (1999) Phylogenetic relationships among ascomycetes: evidence from an RNA polymerase II subunit. Molecular Biology and Evolution 16(12): 1799–1808. https://doi.org/10.1093/oxfordjournals.molbev.a026092

Liu SY, Yu Y, Zhang TY, Zhang MY, Zhang YX (2020) *Trichoderma panacis* sp. nov., an endophyte isolated from *Panax notoginseng*. International Journal of Systematic and Evolutionary Microbiology 70(5): 3162–3166. https://doi.org/10.1099/ijsem.0.004144

Lu B, Druzhinina IS, Fallah P, Chaverri P, Gradinger C, Kubicek CP, Samuels GJ (2004) *Hypocrea*/*Trichoderma* species with pachybasium-like conidiophores: sexual morphs for *T. minutisporum* and *T. polysporum* and their newly discovered relatives. Mycologia 96(2): 310–342. https://doi.org/10.1080/15572536.2005.11832980

Martin J (1950) Use of acid, rose bengal and streptomycin in the plate method for estimating soil fungi. Soil Science 69(3): 215–232. https://doi.org/10.1097/00010694-195003000-00006

Montoya QV, Meirelles LA, Chaverri P, Rodrigues A (2016) Unraveling *Trichoderma* species in the attine ant environment: description of three new taxa. Antonie van Leeuwenhoek 109(5): 633–651. https://doi.org/10.1007/s10482-016-0666-9

Mukherjee PK, Horwitz BA, Singh U, Mukherjee M, Schmoll M (2013) *Trichoderma* in agriculture, industry and medicine: an overview. In: Mukherjee PK, Horwitz BA, Singh US, Mukherjee M, Schmoll M (Eds) Trichoderma: biology and applications. CAB International, Croydon, 1–7. https://doi.org/10.1079/9781780642475.0001

Nirenberg HI (1976) Untersuchungen über die morphologische und biologische Differenzierung in der *Fusarium*-Sektion *Liseola*. Mitteilungen aus der Biologischen Bundesanstalt für Land-und Forstwirtschaft 169: 1–117.

Park MS, Oh SY, Cho HJ, Fong JJ, Cheon WJ, Lim YW (2014) *Trichoderma songyi* sp. nov., a new species associated with the pine mushroom (*Tricholoma matsutake*). Antonie van Leeuwenhoek 106(4): 593–603. https://doi.org/10.1007/s10482-014-0230-4 [Epub 2014 Jul 23]

Qiao M, Du X, Zhang Z, Xu JP, Yu ZF (2018) Three new species of soil-inhabiting *Trichoderma* from southwest China. MycoKeys 44: 63–80. https://doi.org/10.3897/mycokeys.44.30295

Qin WT, Zhuang WY (2016a) Seven wood-inhabiting new species of the genus *Trichoderma* (Fungi, Ascomycota) in Viride clade. Scientific Reports 6: e27074. https://doi.org/10.1038/srep27074

Qin WT, Zhuang WY (2016b) Four new species of *Trichoderma* with hyaline ascospores in the Brevicompactum and Longibrachiatum clades. Mycosystema 35(11): 1317–1336. https://doi.org/10.13346/j.mycosystema.160158

Qin WT, Zhuang WY (2016c) Two new hyaline-ascospored species of *Trichoderma* and their phylogenetic positions. Mycologia 108(1): 205–214. https://doi.org/10.3852/15-144

Qin WT, Zhuang WY (2017) Seven new species of *Trichoderma* (Hypocreales) in the Harzianum and Strictipile clades. Phytotaxa 305(3): 121–139. https://doi.org/10.11646/phytotaxa.305.3.1

Rodríguez María del CH, Evans HC, de Abreu LM, de Macedo DM, Ndacnou MK, Bekele KB, Barreto RW (2021) New species and records of *Trichoderma* isolated as mycoparasites

and endophytes from cultivated and wild coffee in Africa. Scientific Reports 11: e5671. https://doi.org/10.1038/s41598-021-84111-1

Samuels GJ (2006) *Trichoderma*: systematics, the sexual state, and ecology. Phytopathology 96: 195–206. https://doi.org/10.1094/PHYTO-96-0195

Samuels GJ, Dodd S, Lu BS, Petrini O, Schroers HJ, Druzhinina IS (2006) The *Trichoderma koningii* aggregate species. Studies in Mycology 56: 67–133. https://doi.org/10.3114/sim.2006.56.03

Sun J, Pei Y, Li E, Li W, Hyde KD, Yin WB, Liu X (2016) A new species of *Trichoderma hypoxylon* harbours abundant secondary metabolites. Scientific Reports 6: e37369. https://doi.org/10.1038/srep37369

Tamura K, Nei M (1993) Estimation of the number of nucleotide substitutions in the control region of mitochondrial DNA in humans and chimpanzees. Molecular Biology and Evolution 10(3): 512–526. https://doi.org/10.1093/oxfordjournals.molbev.a040023

Tomah AA, Alamer IS, Li B, Zhang JZ (2020) A new species of *Trichoderma* and gliotoxin role: A new observation in enhancing biocontrol potential of *T. virens* against *Phytophthora capsici* on chili pepper. Biological Control 145: 104261. https://doi.org/10.1016/j.biocontrol.2020.104261

Tripathi P, Singh PC, Mishra A, Chauhan PS, Dwivedi S, Bais RT, Tripathi RD (2013) *Trichoderma*: a potential bioremediator for environmental clean up. Clean Technologies and Environmental Policy 15(4): 541–550. https://doi.org/10.1007/s10098-012-0553-7

White TJ, Bruns T, Lee S, Taylor J (1990) Amplification and direct sequencing of fungal ribosomal RNA genes for phylogenetics. In: Innis MA, Gelfand DH, Sninsky JJ et al. (Eds) PCR protocols: a guide to methods and applications. Academic Press, San Diego, 315–322. https://doi.org/10.1016/B978-0-12-372180-8.50042-1

Zeng ZQ, Zhuang WY (2017) Phylogenetic position of *Pseudohypocrea* (Hypocreales). Mycoscience 58(4): 274–281. https://doi.org/10.1016/j.myc.2017.04.005

Zeng ZQ, Zhuang WY (2019) Two new species and a new Chinese record of Hypocreaceae as evidenced by morphological and molecular data. Mycobiology 47(3): 280–291. https://doi.org/10.1080/12298093.2019.1641062

Zhang YB, Zhuang WY (2017) Four new species of *Trichoderma* with hyaline ascospores from southwest China. Mycosphere 8(10): 1914–1929. https://doi.org/10.5943/mycosphere/8/10/14

Zhang YB, Zhuang WY (2018) New species of *Trichoderma* in the Harzianum, Longibrachiatum and Viride clades. Phytotaxa 379(2): 131–142. https://doi.org/10.11646/phytotaxa.379.2.1

Zhang YB, Zhuang WY (2019) *Trichoderma bomiense* and *T. viridicollare*, two new species forming separate terminal lineages among the green-ascospored clades of the genus. Mycosystema 38(1): 11–22. https://doi.org/10.13346/j.mycosystema.180304

Zheng H, Qiao M, Lv YF, Du X, Zhang KQ, Yu ZF (2021) New species of *Trichoderma* isolated as endophytes and saprobes from southwest China. Journal of Fungi 7(6): e467. https://doi.org/10.3390/jof7060467

Zhao YZ, Zhang ZF, Cai L, Peng WJ, Liu F (2018) Four new filamentous fungal species from newly-collected and hive-stored bee pollen. Mycosphere 9(6): 1089–1116. https://doi.org/10.5943/mycosphere/9/6/3

Zhu ZX, Zhuang WY (2015a) Three new species of *Trichoderma* with hyaline ascospores from China. Mycologia 107(2): 328–345. https://doi.org/10.3852/14-141

Zhu ZX, Zhuang WY (2015b) *Trichoderma* (*Hypocrea*) species with green ascospores from China. Persoonia 34: 113–129. https://doi.org/10.3767/003158515X686732

Zhu ZX, Zhuang WY (2018) A new species of the Longibrachiatum clade of *Trichoderma* (Hypocreaceae) from northeast China. Nova Hedwigia 106(3–4): 441–453. https://doi.org/10.1127/nova_hedwigia/2017/0444

Supplementary material 1

Five new species of *Trichoderma* from moist soils in China

Authors: Guang-Zhi Zhang, He-Tong Yang, Xin-Jian Zhang, Fang-Yuan Zhou, Xiao-Qing Wu, Xue-Ying Xie, Xiao-Yan Zhao, Hong-Zi Zhou

Data type: COL

Explanation note: *Trichoderma hailarense* G.Z. Zhang, sp. nov.; *Trichoderma macrofasciculatum* G.Z. Zhang, sp. nov.; *Trichoderma nordicum* G.Z. Zhang, sp. nov.; *Trichoderma shangrilaense* G.Z. Zhang, sp. nov.; *Trichoderma vadicola* G.Z. Zhang, sp. nov.

Link: https://doi.org/10.3897/mycokeys.87.76085.suppl1

MycoKeys 87: 159–182 (2022)
doi: 10.3897/mycokeys.87.71524
https://mycokeys.pensoft.net

RESEARCH ARTICLE

A peer-reviewed open-access journal
MycoKeys
Launched to accelerate biodiversity research

Two new *Rinodina* lichens from South Korea, with an updated key to the species of *Rinodina* in the far eastern Asia

Beeyoung Gun Lee[1], Jae-Seoun Hur[2]

1 *Baekdudaegan National Arboretum, Bonghwa, 36209, Republic of Korea* **2** *Korean Lichen Research Institute, Sunchon National University, Suncheon 57922, Republic of Korea*

Corresponding author: Beeyoung Gun Lee (gitanoblue@koagi.or.kr)

Academic editor: Garima Singh | Received 13 July 2021 | Accepted 24 December 2021 | Published 23 February 2022

Citation: Lee BG, Hur J-S (2022) Two new *Rinodina* lichens from South Korea, with an updated key to the species of *Rinodina* in the far eastern Asia. MycoKeys 87: 159–182. https://doi.org/10.3897/mycokeys.87.71524

Abstract

Rinodina salicis Lee & Hur and *Rinodina zeorina* Lee & Hur are described as new lichen-forming fungi from forested wetlands or a humid forest in South Korea. *Rinodina salicis* is distinguishable from *Rinodina excrescens* Vain., the most similar species, by its olive-gray thallus with smaller areoles without having blastidia, contiguous apothecia, non-pruinose discs, paler disc color, wider ascospores in the *Pachysporaria*-type II, and the absence of secondary metabolites. *Rinodina zeorina* differs from *Rinodina hypobadia* Sheard by areolate and brownish thallus, non-pruinose apothecia, colorless and wider parathecium, narrower paraphyses with non-pigmented and unswollen tips, longer and narrower ascospores with angular to globose lumina, and the absence of pannarin. Molecular analyses employing internal transcribed spacer (ITS) sequences strongly support the two new species to be unique in the genus *Rinodina*. An updated key is provided to assist in the identification of all 63 taxa in *Rinodina* of the far eastern Asia.

Keywords

Biodiversity, corticolous, phylogeny, Physciaceae, taxonomy

Introduction

Rinodina, the largest genus in the family Physciaceae, comprises about three hundred species worldwide (Sheard et al. 2017; Wijayawardene et al. 2020). Several infrageneric groups have been studied since Malme (1902) introduced the ascospore-type

concept for the groups in *Rinodina* (Poelt 1965; Grube and Arup 2001). Although the classification based on different ascospore types has been coarsely accepted, the variety of ascospores does not always correspond to the infrageneric classification. As the pattern of ascospore ontogeny is considered more important than the spore type itself, it is understood that the ascospore types should be respected in developmental stages of a spore (Giralt 1994; Grube and Arup 2001; Sheard 2010; Resl et al. 2016).

The *Rinodina* has been studied in Europe (Mayrhofer and Poelt 1979; Giralt et al. 1995; Giralt 2001; Mayrhofer and Moberg 2002), North America (Sheard and Mayrhofer 2002; Sheard 2004, 2010, 2018; Sheard et al. 2011, 2012; Lendemer et al. 2012, 2019; Morse and Sheard 2020), islands of South America (Bungartz et al. 2016), Australia to New Zealand (Mayrhofer 1983, 1984b; Kaschik 2006; Elix 2011; Elix et al. 2020), Asia to Russian Far East (Mayrhofer 1984a; Galanina et al. 2011; Lendemer et al. 2012; Sheard et al. 2017; Galanina et al. 2018; Galanina and Ezhkin 2019; Zheng and Ren 2020; Galanina et al. 2021; Kumar et al. 2021), and South Africa (Matzer and Mayrhofer 1996; Mayrhofer et al. 2014). Molecular works have been accomplished over the continents (Grube and Arup 2001; Wedin et al. 2002; Nadyeina et al. 2010; Resl et al. 2016).

Sheard et al. (2017) achieved the first and comprehensive study on the genus *Rinodina* of the far eastern Asia (Korea, Japan, and Russian Far East). Several studies announced further more species in the genus, such as *R. badiexcipula* Sheard, *R. convexula* H. Magn., *R. occulta* (Körb.) Sheard, *R. oxneriana* S.Y. Kondr., Lőkös & Hur and *R. tephraspis* (Tuck.) Herre from South Korea (Kondratyuk et al. 2016, 2017; Yakovchenko 2018; Kondratyuk et al. 2020) and *R. colobinoides* (Nyl.) Müll. Arg., *R. herrei* H. Magn., *R. laevigata* (Ach.) Malme, and *R. parasitica* H. Mayrhofer & Poelt from the Kuril Islands and the Magadan region, Russian Far East (Galanina and Ezhkin 2019; Galanina et al. 2021). Among them, *R. oxneriana* was discovered as a new species and other eight species were reported as new records to the far eastern Asia. The species of *Rinodina* in the far eastern Asia are mainly corticolous and the main genera of the substrate trees are *Quercus*, *Picea*, *Salix*, *Betula* and *Alnus* (Fig. 1) (Lendemer et al. 2012; Sheard et al. 2012; Joshi et al. 2013; Kondratyuk et al. 2013, 2016, 2017, 2020; Aptroot and Moon 2014; Sheard et al. 2017; Yakovchenko et al. 2018; Galanina and Ezhkin 2019; Gananina et al. 2021). Those main substrates vigorously grow in a humid forest, a valley or a wetland, and particularly the genera *Salix* and *Alnus* often inhabit the water. Inhabiting those tree barks, diverse *Rinodina* species are easily detected in shaded forests and forested wetlands in which are one of the representative lichens of the ecosystems.

This study describes two new lichen-forming fungi in the genus *Rinodina*. Field surveys for the lichen biodiversity in the forested wetlands of South Korea were carried out during the summer of 2020, and a couple of specimens of *Rinodina* were collected from barks of *Quercus* and *Salix*, the most common genera of the substrates for corticolous *Rinodina* species in the far eastern Asia, in a humid forest and a forested wetland on mountains (Fig. 2). The specimens were comprehensively analyzed in ecology, morphology, chemistry and molecular phylogeny and did not correspond to any

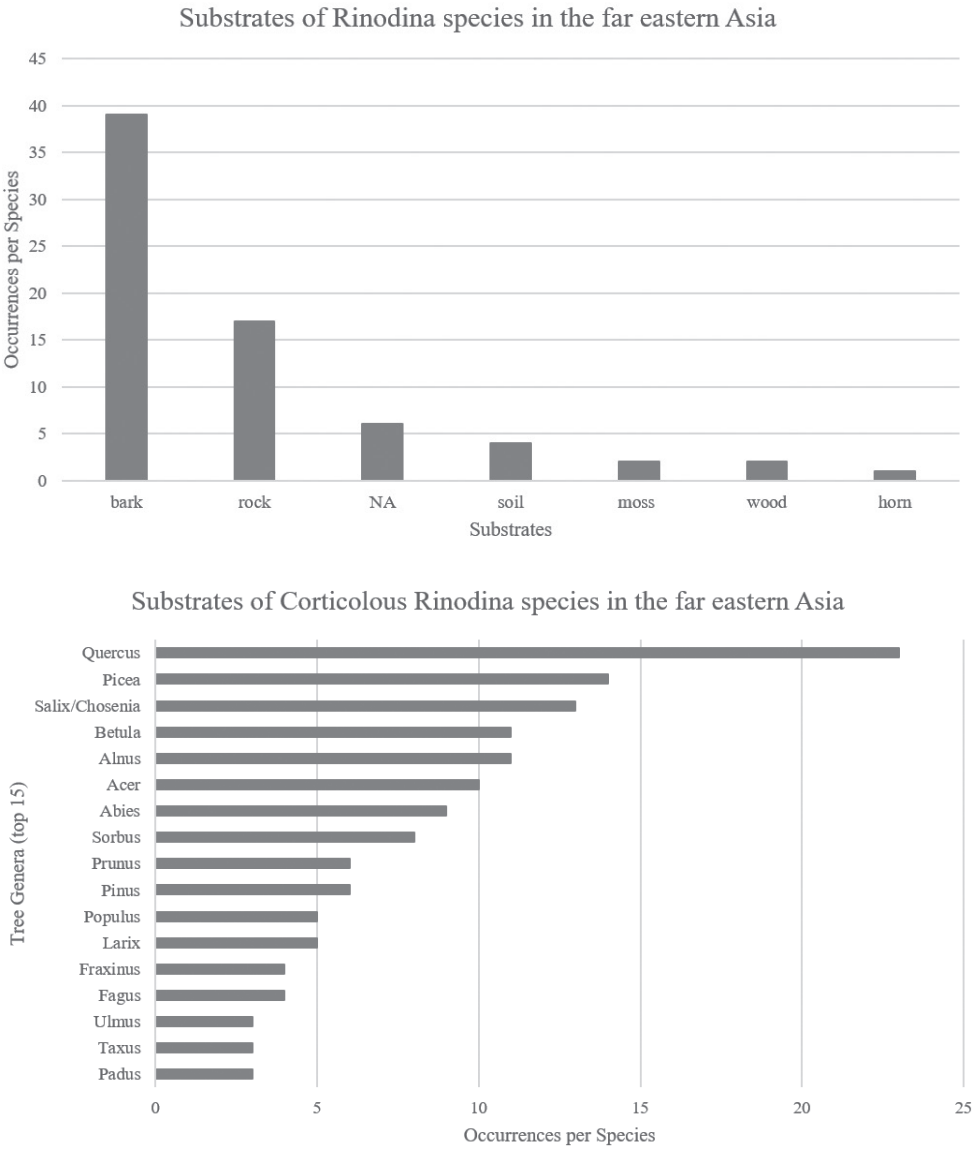

Figure 1. Substrates of *Rinodina* species in the far eastern Asia. *Rinodina* species of the far eastern Asia occur mainly on bark, and the genera *Quercus*, *Picea*, *Salix*, *Betula* and *Alnus* are the main substrates for corticolous *Rinodina* species of the far eastern Asia.

previously known species. We describe them as new species, *Rinodina salicis* and *R. zeorina*, and this discovery contributes to the taxonomy with overall 63 taxa in the genus *Rinodina* of the far eastern Asia. The type specimens are deposited in the herbarium of the Baekdudaegan National Arboretum (KBA, the herbarium acronym in the Index Herbariorum), South Korea.

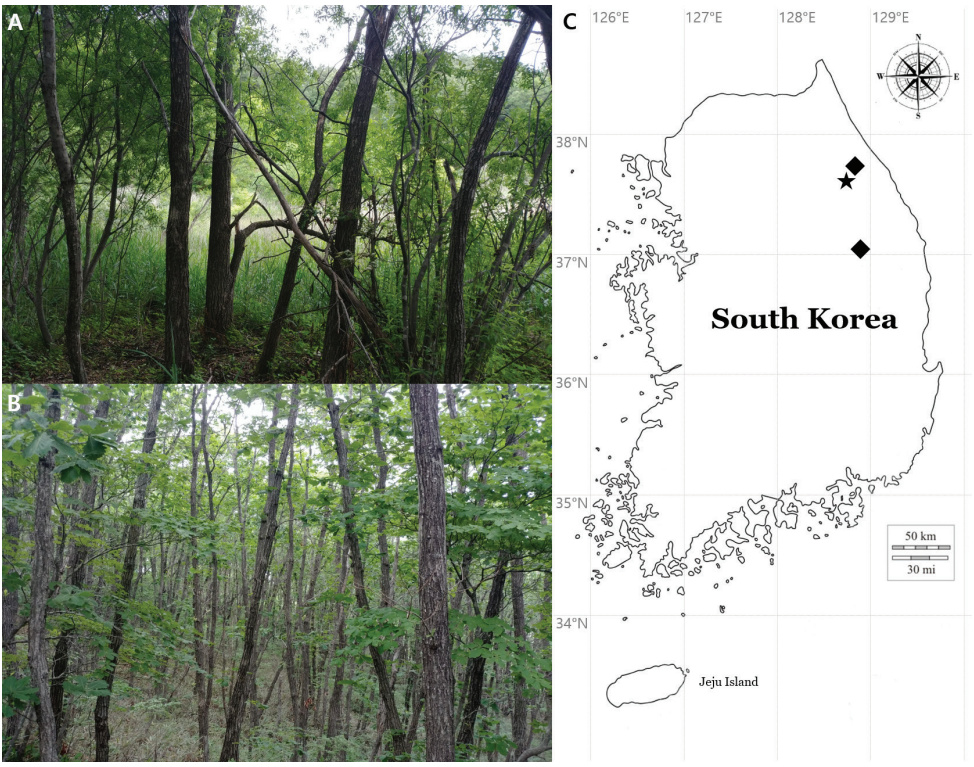

Figure 2. Specific collection sites for two new species **A** habitat/landscape for *R. salicis* **B** habitat/landscape for *R. zeorina* **C** location for *R. salicis* (a black star); locations for *R. zeorina* (two black diamonds).

Materials and methods

Morphological and chemical analyses

Hand sections were prepared manually with a razor blade under a stereomicroscope (Olympus optical SZ51; Olympus, Tokyo, Japan), scrutinized under a compound microscope (Nikon Eclipse E400; Nikon, Tokyo, Japan) and pictured using a software program (NIS-Elements D; Nikon, Tokyo, Japan) and a DS-Fi3 camera (Nikon, Tokyo, Japan) mounted on a Nikon Eclipse Ni-U microscope (Nikon, Tokyo, Japan). The ascospores were examined at 1000× magnification in water. The length and width of the ascospores were measured and the range of spore sizes was shown with average, standard deviation (SD), length-to-width ratio, and the number of measured spores. Thin-layer chromatography (TLC) was performed using solvent systems A and C according to standard methods (Orange et al. 2001).

Isolation, DNA extraction, amplification, and sequencing

Hand-cut sections of ten to twenty ascomata per collected specimen were prepared for DNA isolation and DNA was extracted with a NucleoSpin Plant II Kit in line with the manufacturer's instructions (Macherey-Nagel, Düren, Germany). PCR amplifications

for the internal transcribed spacer region (ITS1-5.8S-ITS2 rDNA) RNA genes were achieved using Bioneer's AccuPower PCR Premix (Bioneer, Daejeon, Korea) in 20-µl tubes with 16 µl of distilled water, 2 µl of DNA extracts and 2 µl of the primers ITS5 and ITS4 (White et al. 1990). The PCR thermal cycling parameters used were 95 °C (15 sec), followed by 35 cycles of 95 °C (45 sec), 54 °C (45 sec), and 72 °C (1 min), and a final extension at 72 °C (7 min) based on Ekman (2001). The annealing temperature was occasionally altered by ±1 degree in order to get a better result. PCR purification and DNA sequencing were accomplished by the genomic research company Macrogen (Seoul, Korea).

Phylogenetic analyses

All ITS sequences (Table 1) were aligned and edited manually using ClustalW in Bioedit V7.2.6.1 (Hall 1999). All missing and ambiguously aligned data and parsimony-uninformative positions were removed and only parsimony-informative regions were finally analyzed in MEGA X (Stecher et al. 2020). The final alignment comprised 974 bp in which 167 variable regions were detected. The phylogenetically informative regions were 523. Phylogenetic trees with bootstrap values were obtained in RAxML GUI 2.0 beta (Edler et al. 2019) using the maximum likelihood method with a rapid bootstrap with 1000 bootstrap replications and GTR GAMMA for the substitution matrix. The posterior probabilities were obtained in BEAST 2.6.4 (Bouckaert et al. 2019) using the GTR 121343 model, as the appropriate model of nucleotide substitution produced by the bayesian model averaging methods with bModelTest (Bouckaert and Drummond 2017), empirical base frequencies, gamma for the site heterogeneity model, four categories for gamma, and a 10,000,000 Markov chain Monte Carlo chain length with a 10,000-echo state screening and 1000 log parameters. Then, a consensus tree was constructed in TreeAnnotator 2.6.4 (Bouckaert et al. 2019) with no discard of burnin, no posterior probability limit, a maximum clade credibility tree for the target tree type, and median node heights. All trees were displayed in FigTree 1.4.2 (Rambaut 2014) and edited in Microsoft Paint. The bootstrapping and posterior probability analyses were repeated three times for the result consistency and no significant differences were shown for the tree shapes and branch values. The phylogenetic trees and DNA sequence alignments are deposited in TreeBASE under the study ID 28192. Overall analyses in the materials and methods were accomplished based on Lee and Hur (2020).

Results and discussion

Phylogenetic analyses

An independent phylogenetic tree for the genus *Rinodina* and related genera was produced from 67 sequences from GenBank and 11 newly generated sequences for the two new species and related species (Table 1). The two new species were positioned in the genus *Rinodina* in the ITS tree. The ITS tree describes that *R. salicis*, a new species, is com-

Table 1. Species list and DNA sequence information employed for phylogenetic analysis.

No.	Species	ID (ITS)	Voucher
1	*Amandinea lignicola*	JX878521	Tønsberg 36426 (BG)
2	*Amandinea punctata*	HQ650627	AFTOL-ID 1306
3	*Buellia badia*	MG250192	TS1767 (LCU)
4	*Buellia boseongensis*	MF399000	KoLRI 041680
5	*Buellia numerosa*	LC153799	CBM:Watanuki:L01034
6	*Rinodina afghanica*	MT260860	500103 (XJU-L)
7	*Rinodina alba*	GU553290	GZU 000272655
8	*Rinodina albana*	GU553297	GZU 000272651
9	*Rinodina anomala*	MN587028	Sipman 62934
10	*Rinodina archaea*	DQ849292	H. Mayrhofer 15752 (GZU)
11	*Rinodina atrocinerea*	AF540544	H. Mayrhofer 13.740 & U. Arup (GZU)
12	*Rinodina balanina*	KY266842	O-L-195705
13	*Rinodina bischoffii*	DQ849291	M. Lambauer 0031 (GZU)
14	*Rinodina cacaotina*	DQ849295	H. Mayrhofer 10770 (HO)
15	*Rinodina calcarea*	GU553292	GZU 000272654
16	*Rinodina cana*	MN587029	Sipman 63008
17	*Rinodina capensis*	DQ849296	W. Obermayer 09230 (GZU)
18	*Rinodina confragosa*	DQ849297	W. Obermayer 09091 (GZU)
19	*Rinodina confragosula*	DQ849298	M. Lambauer 0044 (GZU)
20	*Rinodina degeliana*	KX015681	Tønsberg 42631
21	*Rinodina destituta*	KT695382	BIOUG24047-H02
22	*Rinodina disjuncta*	MK812529	TRH-L-15387
23	*Rinodina efflorescens*	KX015683	Malicek 5462
24	*Rinodina exigua*	GU553294	GZU 000272652
25	*Rinodina gallowayi*	DQ849299	M. Lambauer 0125 (GZU)
26	*Rinodina gennarii*	AJ544187	B44435
27	*Rinodina glauca*	GU553295	GZU 000272662
28	*Rinodina herteliana*	DQ849300	M. Lambauer 0177 (GZU)
29	*Rinodina immersa*	DQ849301	M. Lambauer 0129 (GZU)
30	*Rinodina interpolata*	AF250809	M263
31	*Rinodina jamesii*	DQ849303	H. Mayrhofer 10810 (GZU)
32	*Rinodina lecanorina*	AF540545	H. Mayrhofer 13.120 (GZU)
33	*Rinodina lepida*	AY143413	Trinkaus 137
34	*Rinodina luridata*	DQ849304	H. Mayrhofer 12122 (GZU)
35	*Rinodina luridescens*	AJ544183	B42835
36	*Rinodina metaboliza*	MT260864	20080224 (XJU-L)
37	*Rinodina milvina*	GU553299	KW 63379
38	*Rinodina mniaroea*	KX015689	Spribille 20101 (GZU)
39	*Rinodina mniaroea*	KX015691	V. Wagner, 15.07.06/1 (GZU)
40	*Rinodina mniaroea*	KX015692	Spribille 20391 (GZU)
41	*Rinodina moziana*	DQ849307	H. Mayrhofer 6729 (GZU)
42	*Rinodina moziana* var. *moziana*	DQ849305	M. Lambauer 0214 (GZU)
43	*Rinodina nimisii*	AJ544184	B42685
44	*Rinodina obnascens*	AJ544185	B42477
45	*Rinodina oleae*	DQ849308	M. Lambauer 0178 (GZU)
46	*Rinodina oleae*	GU553301	GZU 000272565
47	*Rinodina olivaceobrunnea*	AF540547	J. Romeike 2.090300 (GOET)
48	*Rinodina orculata*	DQ849309	H. Mayrhofer 15754 (GZU)
49	***Rinodina orientalis***	**MW832807**	**BDNA-L-0000284**
50	***Rinodina orientalis***	**MW832808**	**BDNA-L-0000653**
51	***Rinodina orientalis***	**MW832809**	**BDNA-L-0000774**
52	*Rinodina oxydata*	DQ849313	H. Mayrhofer 11406 (GZU)
53	*Rinodina plana*	AF250812	E34
54	*Rinodina pyrina*	AF540549	P. Bilovitz & H. Mayrhofer 483 (GZU)
55	*Rinodina ramboldii*	DQ849315	G. Rambold 5094 (M)
56	*Rinodina reagens*	DQ849316	M. Lambauer 0218 (GZU)
57	*Rinodina roboris*	MK811851	O-L-206765
58	*Rinodina roscida*	DQ849317	S. Kholod plot515 (GZU)
59	***Rinodina salicis***	**MW832810**	**BDNA-L-0000558**
60	***Rinodina salicis***	**MW832811**	**BDNA-L-0000560**
61	*Rinodina septentrionalis*	GU553303	GZU 000272561
62	*Rinodina sheardii*	MK778639	J. Malicek 10238
63	*Rinodina sheardii*	MK778640	J. Vondrak 15298 (PRA)

No.	Species	ID (ITS)	Voucher
64	*Rinodina sophodes*	AF540550	P. Bilovitz 968 (GZU)
65	*Rinodina teichophila*	GU553305	GZU 000272659
66	*Rinodina trevisanii*	KX015684	de Bruyn s.n. 2011 (GZU)
67	*Rinodina tunicata*	AF540551	H. Mayrhofer 13.749 & R. Ertl (GZU)
68	*Rinodina turfacea*	AF224362	Moberg 10422
69	*Rinodina vezdae*	DQ849318	H. Mayrhofer 15757 (GZU)
70	***Rinodina zeorina***	**MW832812**	**BDNA-L-0000642**
71	***Rinodina zeorina***	**MW832813**	**BDNA-L-0000646**
72	***Rinodina zeorina***	**MW832814**	**BDNA-L-0000650**
73	***Rinodina zeorina***	**MW832815**	**BDNA-L-0000651**
74	***Rinodina zeorina***	**MW832816**	**BDNA-L-0000668**
75	***Rinodina zeorina***	**MW832817**	**BDNA-L-0000933**
76	*Rinodina zwackhiana*	AF540552	H. Mayrhofer 13.848 (GZU)
77	*Rinodinella controversa*	AF250814	M281
78	*Rinodinella dubyanoides*	AF250815	E29
	Overall	**78**	

DNA sequences which were generated in this study, i.e., two new species such as *Rinodina salicis* and *R. zeorina*, and another compared species, *R. orientalis*, are presented in bold. All others were obtained from GenBank. The species names are followed by GenBank accession numbers and voucher information. ITS, internal transcribed spacer; Voucher, voucher information.

ing alone in a single clade. Several species such as *R. mniaroea* (Ach.) Körb., *R. roscida* (Sommerf.) Arnold, *R. bischoffii* (Hepp) A. Massal., *R. luridata* (Körb.) H. Mayrhofer, Scheid. & Sheard, *R. metaboliza* Vain., *R. albana* (A. Massal.) A. Massal., *R. afghanica* M. Steiner & Poelt, *R. zwackhiana* (Kremp.) Körb., *R. calcarea* (Hepp ex Arnold) Arnold, *R. immersa* (Körb.) J. Steiner, *R. tunicata* H. Mayrhofer & Poelt, *Rinodinella controversa* (A. Massal.) H. Mayrhofer & Poelt, and *R. dubyanoides* (Hepp) H. Mayrhofer & Poelt, are situated close to the new species; this particular clade lacks statistical support (bootstrap value of 58 and a posterior probability of 0.75). *Rinodina zeorina*, the other new species, was located in a clade with *R. sheardii* Tønsberg, represented by a bootstrap value of 89 and a posterior probability of 0.88 (not shown) for the branch (Fig. 3).

Taxonomy

Rinodina salicis **B.G. Lee & J.-S. Hur sp. nov.**
No: MB839186
Fig. 4

Diagnosis. *Rinodina salicis* differs from *R. excrescens* by olive-gray thallus with smaller areoles without blastidia, contiguous apothecia, the absence of pruina on disc, paler disc color, wider ascospores in the *Pachysporaria*-type, and the absence of secondary metabolites.

Type. South Korea, Gangwon Province, Gangneung, Seongsan-myeon, Eoheul-ri, a forested wetland, 37°43.61'N, 128°48.13'E, 212 m alt., on bark of *Salix koreensis* Andersson, 02 June 2020, B.G.Lee & H.J.Lee 2020-000358 (holotype: BDNA-L-0000558; GenBank MW832810 for ITS); same locality, on bark of *Salix koreensis*, 02 June 2020, B.G.Lee & H.J.Lee 2020-000360, with *Caloplaca gordejevii* (Tomin) Oxner, *Lecanora* sp., and *Phaeophyscia* sp. (***paratype*****:** BDNA-L-0000560; GenBank MW832811 for ITS).

Thallus corticolous, crustose, minutely bullate, some developing to conglomerate and continuous, rarely lobulated, thin, grayish-green to olive green, margin indeter-

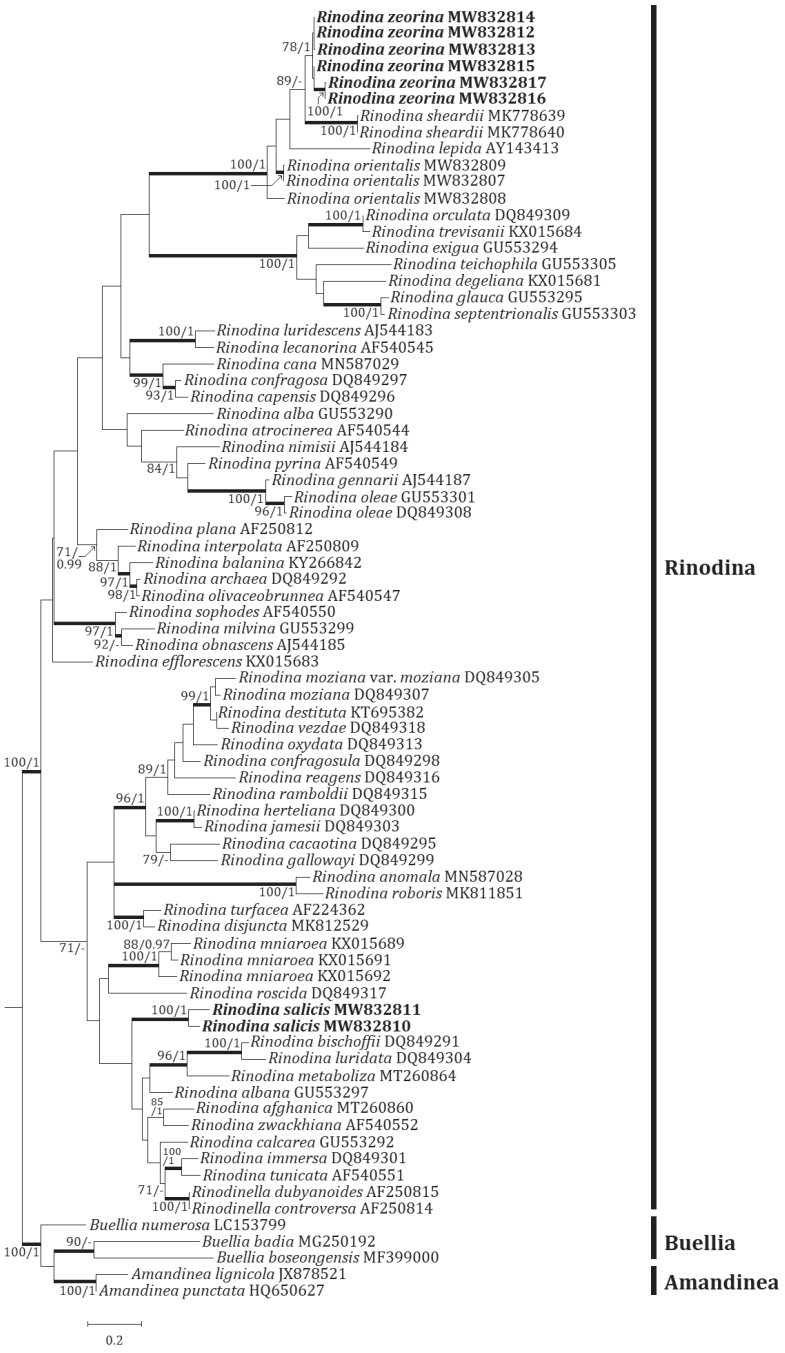

Figure 3. Phylogenetic relationships among available species in the genus *Rinodina* based on a maximum likelihood analysis of the dataset of ITS sequences. The tree was rooted with the sequences of the genera *Amandinea* and *Buellia*. Maximum likelihood bootstrap values ≥ 70% and posterior probabilities ≥ 95% are shown above internal branches. Branches with bootstrap values ≥ 90% are shown as fatty lines. Two new species, *R. salicis* and *R. zeorina* are presented in bold as their DNA sequences were produced from this study. All species names are followed by the Genbank accession numbers.

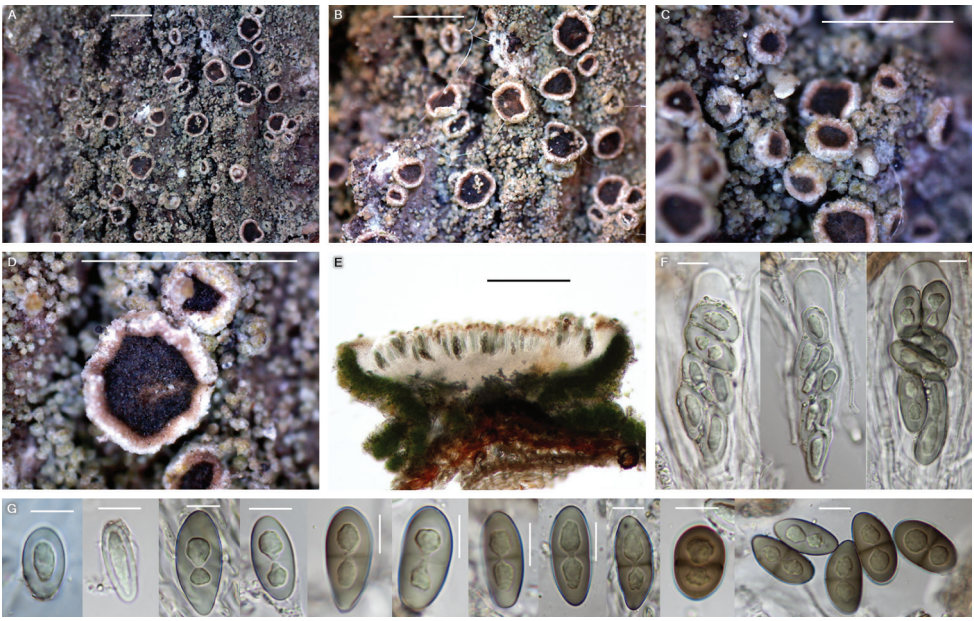

Figure 4. *Rinodina salicis* (BDNA-L-0000558, holotype) in morphology **A–D** habitus and apothecia. Thallus olive-gray composed of tiny areoles and non-pruinose apothecia **E** well-developed amphithecium and algal layer extending to the base **F** asci clavate with eight spores **G** ascospores simple in the beginning and developed 1-septate, *Pachysporaria*-type II, rarely *Physcia*-type at mature. Scale bars: 1 mm (**A–D**); 200 µm (**E**); 10 µm (**F, G**).

minate, vegetative propagules absent, areoles 0.1–0.2 mm diam., 85–90 µm thick; cortex hyaline, 10 µm thick, cortical cells 5–9 µm diam.; medulla 60–65 µm thick, intermixed with algal cells, without crystals (PL–); photobiont coccoid, cells globose, 5–15 µm. Prothallus absent.

Apothecia abundant, rounded, often contiguous, emerging on the surface of thallus and sessile when mature, constricted at the base, 0.2–1.3 mm diam. Disc flat, not pruinose, pale brown or dark brown from early stages, 220–260 µm thick; margin persistent, prominent, generally entire or somewhat flexuous, a little crenulate, thalline margin concolorous to thallus but proper margin near disc distinctly pale brown. Amphithecium well-developed, with small crystals in both cortical layer and the algal-containing medulla, crystals extending to the base, not dissolving in K, 60–70 µm wide laterally, algal layers continuous to the base or solitary, algal cells 5–15 µm diam., cortical layer hyaline, 10–20 µm thick. Parathecium hyaline but light brown at periphery, 45–50 µm wide laterally and 70–80 µm wide at periphery. Epihymenium brown, not granular, pigment slightly paler in K but not diluted, 5–10 µm high. Hymenium hyaline, 70–90 µm high. Hypothecium generally hyaline, with pale yellow pigment, prosoplectenchymatous (irregular), 70–80 µm high. Oil droplets are present mainly in hypothecium and a little in hymenium. Paraphyses septate, anastomosing, 1–1.5 µm wide, simple or branched at tips, tips swollen, pigmented, epihymenium pigmented by paraphysial tips, 4.5–7.5 µm wide. Asci clavate, 8-spored, 68–90 × 20–25 µm (n

= 5). Ascospores ellipsoid, 1-septate, *Pachysporaria*-type II, rarely *Physcia*-type, Type A development, hyaline when young and light brown to brown in mature, 14–24 × 8–13.5 µm (mean = 18.2 × 10.5 µm; SD = 2.12(L), 1.19(W); L/W ratio 1.2–2.4, ratio mean = 1.7, ratio SD = 0.2; n = 105). Pycnidia not detected.

Chemistry. Thallus K–, KC–, C–, Pd–. Hymenium I+ purple-blue. UV–. No lichen substance was detected by TLC.

Distribution and ecology. The species occurs on the bark of *Salix koreensis*. The species is currently known from the type collections.

Etymology. The species epithet indicates the lichen's substrate preference, namely the substrate tree *Salix koreensis*.

Notes. The new species is similar to *R. excrescens* and *R. bullata* Sheard & Lendemer in having bullate thallus. However, the new species differs from *R. excrescens* by olive-gray thallus with smaller areoles without having blastidia, contiguous apothecia, the absence of pruina on disc, paler disc color, ascospore type, larger ascospore, and the absence of secondary metabolites (Sheard 1966; Sheard et al. 2012).

The new species is closer to *R. bullata* in having small bullate areoles without having blastidia. However, the new species differs from the latter by olive-gray thallus, contiguous and larger apothecia, proper margin with pale brown color, crystals present in both cortex and medulla in amphithecium, larger ascospores, K– reaction on thallus, and the absence of lichen substance (Sheard et al. 2012, 2017).

The new species is comparable to *R. granulans* Vain. as the latter represents thallus with minute areoles. However, the new species differs from the latter by thallus color, slightly smaller areoles without blastidia, abundance of apothecia without pruina, *Pachysporaria*-type II ascospores, K– reaction on thallus, and the absence of lichen substance (Giralt et al. 1994; Galanina et al. 2011). Reference Table 2 provides the key characteristics distinguishing *R. salicis* from the compared species above.

Table 2. Comparison of *Rinodina salicis* with closely-related species.

Species	***Rinodina salicis***	***Rinodina bullata***	***Rinodina excrescens***	***Rinodina granulans***
Thallus growth form	bullate without blastidia	bullate without blastidia	bullate with blastidia	bullate with blastidia, forming leprose crust
Areoles (mm in diam.)	0.1–0.2	0.1–0.15(–0.2)	up to c. 1.98	(0.1–)0.2–0.3(–0.5)
Thallus color	olive-gray	light gray	gray	gray to gray-brown
Apothecia (mm in diam.)	0.2–1.3	0.3–0.6	up to c. 1.26	up to 0.3
Apothecia contiguation	often contiguous	not contiguous	not contiguous	not contiguous
Apothecia abundance	abundant	abundant	abundant	very rare
Pruina	absent on disc	–	often present on disc	often present on disc
Disc color	pale to dark brown	brown	brown to black	reddish brown
Proper margin	pale brown	indistinct	–	indistinct
Crystals in amphithecium	present in medulla and cortex	present in cortex	–	present
Ascospore type	*Pachysporaria*-type II	*Pachysporaria*-type II	*Physcia*-type	*Physcia*-type to *Milvina*-type
Ascospores (µm)	14–24 × 8–13.5	14.5–16.5 × 8–9	17.5–19.5 × 8.5–9.5	18–25 × 10–14
Spot test	thallus K–	thallus K+ yellow	thallus K–	thallus K+ faint yellow
Substance	absent	atranorin	pannarin, (rarely zeorin)	pannarin
Reference	BDNA-L-0000558 (holotype), BDNA-L-0000560 (paratype)	Sheard et al. 2012, 2017	Sheard 1966; Sheard et al. 2012, 2017	Giralt et al. 1994; Galanina et al. 2011

The morphological and chemical characteristics of several species close to the new species are referenced from the previous literature. All information on the new species is produced from type specimens (BDNA-L-0000558 and BDNA-L-0000560) in this study.

Rinodina zeorina **B.G. Lee & J.-S. Hur sp. nov.**
No: MB839187
Fig. 5

Diagnosis. *Rinodina zeorina* differs from *R. hypobadia* by areolate, brownish thallus, apothecia without pruina, hyaline and wider parathecium, narrower paraphyses with hyaline and unswollen tips, longer and narrower ascospores with just angular to globose lumina, and the absence of pannarin.

Type. South Korea, North Gyeongsang Province, Bonghwa-gun, Seokpo-myeon, Mt. Cheongok, 37°01.89'N, 128°58.65'E, 1,104 m alt., on bark of *Quercus mongolica*, 16 June 2020, B.G. Lee & H.J. Lee 2020-000733, with *Biatora* sp., *Lecidella euphorea* (Flörke) Kremp., *Pertusaria multipuncta* (Turner) Nyl., and *Sagiolechia* sp. (***holotype*****:** BDNA-L-0000933; GenBank MW832817 for ITS).

Thallus corticolous, crustose, areolate, rimose to continuous, thin, light gray to light brownish gray, margin indeterminate or determinate with prothallus, vegetative propagules absent, 160–250 mm diam., 80–170 µm thick, areoles 0.1–0.5 mm diam.; cortex brown, 5–8 µm thick, with epinecral layer, hyaline, 3–7 µm thick; medulla 35–40 µm thick, intermixed with algal cells, without crystals (PL–); photobiont coccoid, cells globose, 5–9 µm. Prothallus absent or brownish black when present.

Apothecia abundant, rounded, erumpent in the beginning and sessile when mature, constricted at the base, 0.2–0.6 mm diam. Disc flat, not pruinose but epinecral debris shown in water, black to dark brown from early stages, 150–200 µm thick; margin persistent, prominent, generally entire or a little crenulate, concolorous to thallus. Amphithecium well-developed, with small crystals in the algal-containing medulla and particularly near the base, dissolving in K, 70–90 µm wide laterally, algal cells evenly distributed from periphery to base, 10–15 µm diam., cortical layer brownish, cortical cells granular, 2–3 µm diam., with epinecral layer, up to 5 µm thick. Parathecium hyaline but light brown at periphery, 5–10 µm wide laterally and 20–50 µm wide at periphery. Epihymenium red-brown, small granules not dissolving in K, 8–10 µm high. Hymenium hyaline, 90–95 µm high. Hypothecium brown with olive pigment in upper part, prosoplectenchymatous (irregular), 60–65 µm high. Oil droplets present a little in hypothecium. Paraphyses septate, anastomosing, 0.5–1 µm wide, simple or branched at tips, tips generally not swollen or little swollen, not pigmented, epihymenium pigmented by small granules, not by paraphysial tips, up to 1.5 µm wide. Asci clavate, 8-spored, 60–75 × 15–21 µm (n = 3). Ascospores ellipsoid, 1-septate, *Dirinaria*-type but lumina angular to globose, Type B development not detected, septum inflated a little or not, without a torus, hyaline when young and generally brown or dark brown in mature, 11–20 × 5–8.5 µm (mean = 15.4 × 7.1 µm; SD = 1.77(L), 0.70(W); L/W ratio 1.5–3.4, ratio mean = 2.2, ratio SD = 0.3; n = 105). Pycnidia raised, asymmetric, 175–225 µm wide. Pycnoconidia bacilliform, 3–4 × 0.5 µm.

Chemistry. Thallus K–, KC–, C–, Pd–. Hymenium I+ blue. UV–. Zeorin was detected by TLC.

Distribution and ecology. The species occurs on the bark of *Quercus mongolica*, *Tilia amurensis* Rupr., and *Maackia amurensis* Rupr. & Maxim. The species is currently known from a humid forest and a forested wetland of two mountainous sites.

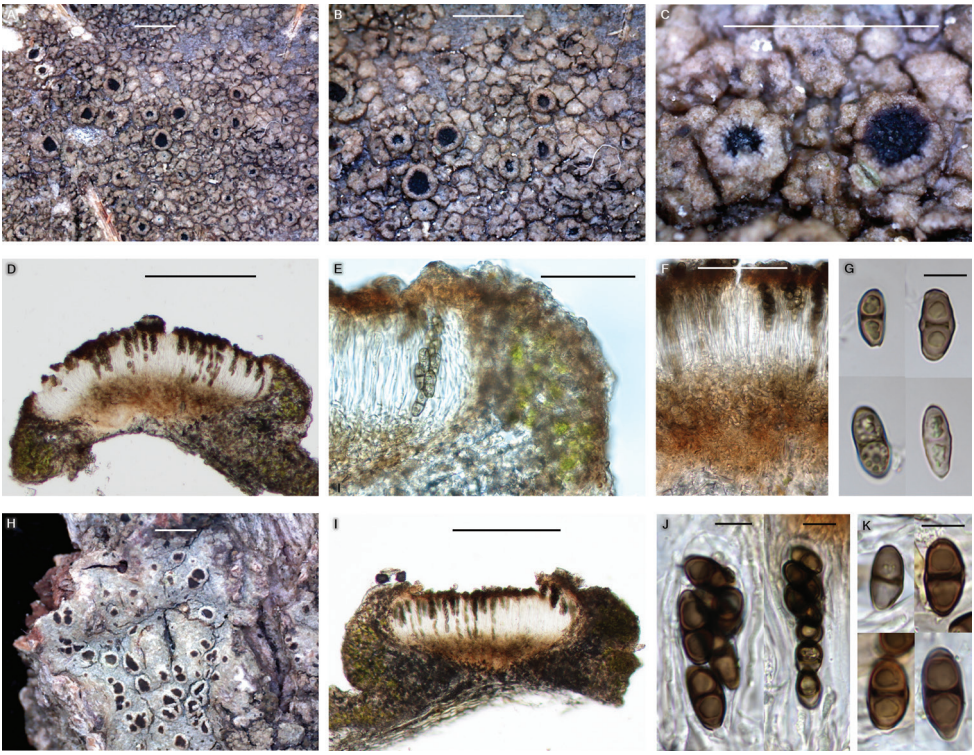

Figure 5. *Rinodina zeorina* (BDNA-L-0000933, holotype for **A–G**; BDNA-L-0000668 for **H–K**) in morphology **A–C** habitus and apothecia on bark of *Quercus mongolica*. Thallus brownish and areolate and non-pruinose apothecia **D** well-developed amphithecium and pigmented hypothecium **E** epihymenium with brown pigment which extending to the cortical layer of amphithecium. Parathecium light brown at periphery **F** hypothecium with light (olive-)brown pigment **G** ascospores 1-septate, *Dirinaria*-type but lumina angular to globose **H** habitus and apothecia on bark of *Tilia amurensis*. Thallus more grayish **I** apothecial section representing well-developed amphithecium and pigmented hypothecium **J** asci clavate with eight spores **K** ascospores 1-septate, *Dirinaria*-type but lumina angular to globose. Scale bars: 1 mm (**A–C**); 200 μm (**D**); 50 μm (**E, F**); 10 μm (**G**); 1 mm (**H**); 200 μm (**I**); 10 μm (**J, K**).

Etymology. The species epithet indicates that the lichen's substance, zeorin, is a major compound.

Notes. The new species is similar to *R. hypobadia*, *R. sheardii*, and *R.* sp. A in having a pigmented hypothecium. However, the new species differs from *R. hypobadia* by areolate, brownish thallus, apothecia without pruina, hyaline and wider parathecium, narrower paraphyses with hyaline and unswollen tips, longer and narrower ascospores with just angular to globose lumina, and the absence of pannarin (Sheard et al. 2017).

The new species differs from *Rinodina sheardii* by the absence of vegetative propagules, and *Dirinaria*-type ascospores in smaller size (Sheard et al. 2017).

The new species differs from *Rinodina* sp. A by wider parathecium, narrower paraphyses with swollen tips, smaller ascospores *Dirinaria*-type, and the absence of pannarin (Sheard et al. 2017).

Table 3. Comparison of *Rinodina zeorina* with closely-related species.

Species	***Rinodina zeorina***	***Rinodina hypobadia***	***Rinodina manshurica***	***Rinodina sheardii***	***Rinodina* aff. *oleae***	***Rinodina* sp. A**
Thallus growth from	areolate, rimose to continuous	rimose, not areolate	rimose, rimose-areolate	±areolate to ±continuous, sorediate	continuous, rimose-areolate	continuous to areolate
Thallus color	light gray to light brownish gray	light to dark gray	gray-brown	yellow, yellow-brown, or pale brown or greenish	(dark gray to olive-green)	dark gray to gray-brown
Pruina	absent, but epinecral debris shown in water	slightly pruinose	absent	absent	(absent)	–
Parathecium color	hyaline and light brown at periphery	red-brown	–	red-brown to brown	(hyaline to brownish)	–
Parathecium at periphery (µm)	20–50	10–20	c. 20	c. 30	(up to 30)	c. 25
Paraphyses (µm)	up to 1.5	2–2.5	2.0	2.0	(1–2)	3.0
Paraphysial tips	not or little swollen, not pigmented	3–4 µm, lightly pigmented	c. 3 µm, light pigmented	c. 3 µm	–	c. 4.5 µm, pigmented
Hypothecium color	brown with olive pigment	reddish or chestnut brown	hyaline	dilute brown to red-brown	hyaline	light brown
Crystals in amphithecium	present in medulla	present in both cortex and medulla	absent	present	–	present in medulla
Ascospore type	*Dirinaria*-type with angular-globose lumina	*Dirinaria*-type with *Physcia*- or *Physconia*-like lumina	*Dirinaria*-type, with *Physcia*-like lumina	*Pachysporaria*-type I	*Dirinaria*-type with *Physcia*-like lumina	*Pachysporaria*-type I
Ascospores (µm)	11–20 × 5–8.5	12.5–18.5 × 6.5–10	14–16.5 × 7.5–8.5	16–35 × 8–17	15.5–19 × 6.5–9.5	22–28.5 × 10.5–15.5
Pycnidia	175–225	up to 300	–	–	–	–
Pycnoconidia (µm)	3–4 × 0.5	3.5 × 1.0	–	–	(4–5 × 1)	–
Substance	zeorin	pannarin, zeorin	absent	zeorin	(absent)	pannarin, zeorin
Reference	BDNA-L-0000933 (holotype), BDNA-L-0000642, BDNA-L-0000646, BDNA-L-0000650, BDNA-L-0000651, BDNA-L-0000668	Sheard et al. 2017	Sheard et al. 2017	Tønsberg 1992; Sheard et al. 2017	Joshi et al. 2013; Smith et al. 2009; Sheard et al. 2017	Sheard et al. 2017

The morphological and chemical characteristics of several species close to the new species are referenced from the previous literature. All information on the new species is produced mainly from the type specimen (BDNA-L-0000933) in comparing with additional specimens (BDNA-L-0000642, BDNA-L-0000646, BDNA-L-0000650, BDNA-L-0000651, BDNA-L-0000668) in this study . The brackets in the column of *R.* aff. *oleae* are referenced from *R. oleae* as some information of *R.* aff. *oleae* is not mentioned in the reference.

The new species can be compared with *R. manshurica* and *R.* aff. *oleae* in having erumpent apothecia, small ascospores(<21 µm long) with swollen septum among corticolous species. However, the new species differs from *R. manshurica* by crystals present in the amphithecium, wider parathecium, narrower paraphyses without swollen tips, pigmented hypothecium, and longer and narrower ascospores (Tønsberg 1992; Sheard et al. 2017).

The new species is distinguished from *R.* aff. *oleae* by narrower ascospores, and pigmented hypothecium (vs. hyaline hypothecium) (Sheard et al. 2017). Reference Table 3 provides the key characteristics distinguishing *R. zeorina* from the compared species above.

The new species is compared further with other *Rinodina* species having the substance zeorin, *R. ascociscana* (Tuck.) Tuck., *R. buckii* Sheard, *R. efflorescens* Malme, *R. luteonigra* Zahlbr., *R. subalbida* (Nyl.) Vain., *R. subminuta* H. Magn., and *R. willeyi*

Sheard & Giralt. However, all of them are different from the new species because those species represent larger ascospores in *Physcia*- to *Physconia*-type for *R. ascociscana*; sorediate thallus, mostly light brown hypothecium and *Teichophila*-type ascospores and the presence of pannarin for *R. buckii*; sorediate thallus, colorless hypothecium, *Pachysporaria*-type ascospores and the presence of pannarin and secalonic acid A for *R. efflorescens*; colorless hypothecium, larger ascospores in *Pachysporaria*-type and the presence of thiomelin for *R. luteonigra*; larger spores in *Pachysporaria*-type and the presence of pannarin for *R. subalbida*; larger spores in *Physcia*-type for *R. subminuta*; sorediate thallus and the presence of pannarin for *R. willeyi* (Sheard et al. 2012, 2017).

Additional specimens examined. South Korea, Gangwon Province, Pyeongchang-gun, Daegwallyeong-myeon, Heonggye-ri, a forested wetland, 37°46.00'N, 128°42.33'E, 1,047 m alt., on bark of *Maackia amurensis*, 03 June 2020, B.G. Lee & H.J.Lee 2020-000442, with *Buellia disciformis* (Fr.) Mudd, *Buellia* sp., *Catillaria nigroclavata* (Nyl.) J. Steiner, *Lecanora megalocheila* (Hue) H. Miyaw., *Lecanora symmicta* (Ach.) Ach., *Lecidella euphorea*, and *Lambiella* cf. *caeca* (J. Lowe) Resl & T. Sprib. (BDNA-L-0000642; GenBank MW832812 for ITS); same locality, 37°46'0.02"N, 128°42'19.58"E, 1,047 m alt., on bark of *Maackia amurensis*, 03 June 2020, B.G. Lee & H.J.Lee 2020-000446 (BDNA-L-0000646; GenBank MW832813 for ITS); same locality, 37°46.00'N, 128°42.33'E, 1,047 m alt., on bark of *Maackia amurensis*, 03 June 2020, B.G. Lee & H.J.Lee 2020-000450 (BDNA-L-0000650; GenBank MW832814 for ITS); same locality, 37°46.00'N, 128°42.33'E, 1,047 m alt., on bark of *Maackia amurensis*, 03 June 2020, B.G. Lee & H.J.Lee 2020-000451 (BDNA-L-0000651; GenBank MW832815 for ITS); same locality, 37°46.00'N, 128°42.33'E, 1,047 m alt., on bark of *Tilia amurensis*, 03 June 2020, B.G. Lee & H.J.Lee 2020-000468, with *Amandinea punctata* (Hoffm.) Coppins & Scheid., *Bacidia* aff. *beckhausii* Körb., *Catillaria* sp., *Micarea prasina* Fr., *Phaeophyscia limbata* (Poelt) Kashiw., *Rinodina* cf. *oleae* Bagl., *Traponora* aff. *varians* (Ach.) J. Kalb & Kalb (BDNA-L-0000668; GenBank MW832816 for ITS).

Key to the species of *Rinodina* from the far eastern Asia (63 taxa)

Eleven more species have been recorded since Sheard et al. (2017), such as *Rinodina badiexcipula*, *R. colobinoides*, *R. convexula*, *R. herrei*, *R. laevigata*, *R. occulta*, *R. oxneriana*, *R. parasitica*, *R. tephraspis*, and two new species from this study (Kondratyuk et al. 2016, 2017; Yakovchenko et al. 2018; Galanina and Ezhkin 2019; Kondratyuk et al. 2020; Galanina et al. 2021). Particularly, *R. laevigata* of Aptroot and Moon (2014) was rejected by Sheard et al. (2017), but Galanina et al. (2021) confirmed the species in the far eastern Asia. This key includes all above species except for *R. convexula* because the species was just announced for a new record to Korea without any specific description for reference (Kondratyuk et al. 2020). *Rinodina confragosa* (Ach.) Körb., *R. milvina* (Wahlenb.) Th. Fr., and *R. olivaceobrunnea* C.W. Dodge & G.E. Baker were reported from Korea and Russian Far East (Kondratyuk et al. 2016; Galanina et al. 2021) as expected to occur (Sheard et al. 2017). All expected species are remained with an asterisk mark(*).

Overall, 63 taxa of *Rinodina* are currently recorded or expected to the far eastern Asia (Korea, Japan and Russian Far East).

1 Substratum rock.....**2**
– Substratum bark, wood, soil, decaying ground vegetation, bone or other lichens **17**
2 Thalli with vegetative propagules.....**3**
– Thalli lacking vegetative propagules.....**4**
3 Thallus effigurate, typically with isidia; when fertile spores belong to the *Physconia*-type; associated with seabird colonies; northern .....***R. balanina***
– Thallus not effigurate, vegetative propagules blastidia with budding soredia; spores *Pachysporaria*-type II; not coastal; southern..... ***R. placynthielloides***
4 Always maritime, typically on coastal rocks; spores *Dirinaria*-type....***R. gennarii***
– Generally inland or occasionally maritime; spores belonging to a different type **5**
5 Medulla orange, K+ red-violet; spores *Pachysporaria*-type I, ultimately developing satellite apical lumina..... ***R. cervina***
– Medulla not orange, not K+ red-violet; spores of various types but never developing apical lumina.....**6**
6 Thallus and apothecium margins K+ yellow, atranorin in cortex **7**
– Thallus and apothecium margins K–, atranorin absent.....**10**
7 Spores with angular lumina, walls thickened at septum and apices, *Physcia*-type; proper exciple hyaline throughout, or if lightly pigmented not aeruginose (N–); thalline margin never pigmented.....**8**
– Spores with 'hourglass'-shaped lumina, *Mischoblastia*-type; proper exciple typically aeruginose at periphery (N+ red under microscope); thalline margin often becoming pigmented **9**
8 Apothecia 0.1–0.3 mm diam., hymenium 80–100 µm high, hypothecium 65–135 µm high, asci 75–80 × 16–19 µm, spores 17–27 × 8–13 µm.....***R. confragosa***
– Apothecia 0.6–1.5 mm diam., hymenium 55–85 µm high, hypothecium 10–55 µm high, asci 45–50 × 13–20 µm, spores 11–16 × 5–9 µm.....***R. occulta***
9 Thallus plane; spores averaging <21 µm in length, rarely swollen at septum ....***R. oxydata***
– Thallus verrucose; spores averaging >21 µm in length, often swollen at septum when mature.....***R. moziana*** (syn. *R. destituta*)
10 Spores elongately ellipsoid, l/w ratio c. 2.0, *Pachysporaria*-type....***R. cinereovirescens***
– Spores broadly ellipsoid, l/w ratio <2.0, belonging to various types **11**
11 Spores >20 µm long at maximum, *Teichophila*-type, often swollen at septum, more so in KOH.....**12**
– Spores <20 µm long, never swollen at septum, belonging to another type **13**
12 Spores 18.5–25 × 10–12.5 µm.....***R. tephraspis***
– Spores 20–32 × 11–19 µm..... ***R. teichophila***
13 Spores with broad pigmented band around septum, *Bischoffii*-type....***R. bischoffii****
– Spores lacking a broad pigmented band around septum, belonging to another type.....**14**
14 Spores with *Physcia*-like lumina when immature, becoming rounded especially at the apices, lateral walls thin.....**15**
– Spores with rounded lumina from beginning, lateral walls relatively thick.....**16**

15 Thallus thick, dark brown; spores constricted at septum when mature, *Milvina*-type; secondary metabolites absent ..... ***R. milvina***
– Thallus thin, gray to light brown; spores *Physconia*-type; thalline margin C+ red (under microscope), gyrophoric acid in medulla ..... ***R. sicula***
16 Apothecial discs pruinose; spores *Pachysporaria*-type ..... ***R. compensata***
– Apothecial discs not pruinose; spores *Pachysporaria*- to *Milvina*-like .... ***R. kozukensis***
17 On soil, decaying ground vegetation, wood, bone or lichenicolous **18**
– Strictly corticolous or lignicolous **27**
18 Spores 1-septate **19**
– Spores 3-septate or submuriform **20**
19 Spores *Teichophila*-type ..... ***R. herrei***
– Spores *Physcia*-type, rarely with apical satellite lumina **21**
20 Spores strictly 3-septate, type B development (apical wall thickened prior to septum formation); secondary metabolites absent ..... ***R. conradii***
– Spores 3-septate at first, typically becoming submuriform, type A development (apical wall thickening after septum formation); deoxylichesterinic acid present . ..... ***R. intermedia***
21 Strictly lichenicolous, on *Aspicilia* or *Rhizocarpon* ..... ***R. parasitica***
– Generally not lichenicolous **22**
22 Sphaerophorin crystals in medulla (sometimes lichenicolous) ..... ***R. turfacea***
– Sphaerophorin lacking in medulla (never lichenicolous) **23**
23 Cortex K+ yellow or medulla orange, K+ red **24**
– Cortex reaction absent **25**
24 Thallus light gray; K+ yellow, atranorin in cortex ..... ***R. mniaroeiza****
– Thallus a shade of brown; medulla orange, K+ red, skyrin or other anthraquinones present ..... ***R. cinnamomea****
25 Spores averaging <23 µm in length ..... ***R. olivaceobrunnea***
– Spores averaging >23 µm in length **26**
26 Thallus and apothecia not pruinose; apothecial discs becoming convex, thalline margin then excluded; spores averaging 24.5–25.5 µm in length, l/w ratio 2.0–2.2 ..... ***R. mniaroea***
– Thallus and apothecia typically pruinose; apothecial discs plane or concave, not convex, thalline margin never excluded; spores averaging 30–32 µm in length, l/w ratio 2.2–2.5 ..... ***R. roscida***
27 Vegetative propagules present **28**
– Vegetative propagules absent **37**
28 Thallus typically golden yellow **29**
– Thallus a shade of gray or brown **30**
29 Thallus with small, dense isidia; very rarely with apothecia; spores *Pachysporaria*-type I ..... ***R. chrysidiata***
– Thallus with marginal, labriform soralia, sometimes becoming pustulate; frequently, but not always, with apothecia; spores *Physcia*-type ..... ***R. xanthophaea***
30 Phyllidia present ..... ***R. oxneriana***
– Blastidia or soredia present **31**

31 Thallus mainly blastidiate, blastidia 35–60 μm diam. ..... ***R. colobinoides***
– Thallus generally not blastidiate, but sorediate or sometimes blastidiate **32**
32 Blastidia present at margin, no substance, spores *Teichophila*-type ..... ***R. herrei***
– Soredia and/or blastidia present, atranorin or pannarin present, spores in various types **33**
33 Thallus light gray; soralia labriform at first, soredia whitish; K+, P+ yellow, cortical atranorin present, pannarin absent ..... ***R. subparieta*** (syn. *R. degeliana*)
– Thallus darker gray; soredia never whitish; K–, P+ cinnabar, atranorin absent, pannarin present **34**
34 Thallus usually of convex to bullate areoles; blastidia often present, sometimes breaking into soredia; zeorin typically absent, when fertile pannarin also in epihymenium ..... ***R. excrescens***
– Thallus never consisting of bullate areoles; soredia always present; zeorin typically present, pannarin never in epihymenium **35**
35 Soredia typically yellowish, secalonic acid A present; spores *Physcia*-type when fertile, averaging <20 μm in length ..... ***R. efflorescens***
– Soredia never yellowish, secalonic acid A absent; spores not *Physcia*-type, averaging >20 μm in length **36**
36 Thallus minutely verrucose, verrucae central on areoles, quickly forming raised soralia, later spreading over thallus surface; soredia >40 μm diam.; spores *Teichophila*-type ..... ***R. buckii***
– Thallus with plane areoles, soredia developing marginally on areoles, never raised centrally on verrucae, later spreading over thallus surface; soredia <40 μm diam.; spores *Pachysporaria*-type I ..... ***R. willeyi***
37 Ascospores 3-septate or submuriform **38**
– Ascospores 1-septate, rarely with satellite apical cells **39**
38 Spores strictly 3-septate, type B development (apical wall thickened prior to septum formation); secondary metabolites absent ..... ***R. conradii***
– Spores 3-septate at first, becoming submuriform, type A development (apical wall thickening after septum formation); deoxylichesterinic acid present ..... ***R. intermedia***
39 Thallus brightly pigmented; xanthone present, UV+ orange **40**
– Thallus a shade of gray or brown; xanthone absent, UV– **41**
40 Thallus citrine, thiomelin present; spores averaging 31.0–34.5×16.0–17.5 μm, *Pachysporaria*-type I; not sorediate; subtropical, Tsushima Island, Japan ..... ***R. luteonigra***
– Thallus golden yellow, secalonic acid A present; spores averaging 23.5–28.5×2.0–15.0 μm, *Physcia*-type; frequently sorediate; temperate, widely distributed ..... ***R. xanthophaea***
41 Thallus K+ yellow or P+ cinnabar, atranorin or pannarin present **42**
– Thallus K–, P–, both atranorin and pannarin absent **49**
42 Thallus K+ yellow, atranorin present, pannarin absent **43**
– Thallus P+ cinnabar, pannarin present, atranorin absent **45**
43 Spores averaging >33 μm long, *Pachysporaria*-type I ..... ***R. megistospora***
– Spores averaging <33 μm long, *Physcia*- or *Physconia*-type **44**

44 Spores averaging >26 µm long, strictly *Physcia*-type; never sorediate; distribution limited to coastal foreshores ..... ***R. macrospora***
– Spores averaging <26 µm long, *Physcia*- to *Physconia*-type; most frequently sorediate; distribution inland..... ***R. subparieta*** (syn. *R. degeliana*)
45 Hypothecium pigmented dark reddish brown; spores *Dirinaria*-type, (12–)14–16.5(–18)× (6.5–)7.0–8.5(–9.5) µm, lightly pigmented..... ***R. hypobadia***
– Hypothecium never strongly pigmented; spore type otherwise..... **46**
46 Spores averaging <20 µm in length, *Physcia*-type; thallus becoming bullate, often with minute blastidia ..... ***R. excrescens***
– Spores averaging >20 µm in length, not *Physcia*-type; thallus sometimes verrucate but never bullate or blastidiate **47**
47 Thallus persistently plane; epihymenium lacking crystals, P–; spores averaging >29 µm ..... ***R. tenuis*** (syn. *R. adirondackii*)
– Thallus becoming verrucate; epihymenium with or without crystals, P+ or P–; spores averaging <29 µm **48**
48 Epihymenium typically possessing pannarin crystals, P+ cinnabar; spores lacking apical canals; widely distributed in Japan and adjacent mainland..... ***R. subalbida***
– Epihymenium lacking pannarin crystals, P–; spores with very obvious apical canals; Cheju Island, Korea ..... ***Rinodina* sp. A**
49 Spores 16 per ascus ..... ***R. polyspora***
– Spores 4–8 per ascus **50**
50 Medulla with sphaerophorin crystals, PL+ **51**
– Medulla lacking sphaerophorin crystals, PL– **52**
51 Thallus dark gray, typically dark brown; areoles becoming contiguous, plane, 0.40–0.55 mm wide; spores averaging 26.5–27.5 × 13.5–14.5 µm..... ***R. badiexcipula***
– Thallus light gray, sometimes brownish; areoles remaining discrete, convex, 0.20–0.30 mm wide; spores averaging 23.0–25.5 × 11.5–13.5 µm .... ***R. cinereovirens***
52 Spores swollen at septum, more so in KOH, type B development (apical wall thickening prior to septum formation), *Dirinaria*-type **53**
– Spores not swollen at septum, even in KOH, type A development (apical wall thickening after septum formation), various types..... **59**
53 Spores averaging >21 µm long..... ***R. endospora***
– Spores averaging <21 µm long..... **54**
54 Spores lacking wall thickening at maturity (septal and apical thickenings may be present briefly in immature spores) **55**
– Spore lumina *Physcia*-like, with persistent apical wall thickening..... **56**
55 Thallus gray to ochraceous, rugose, areoles to 0.7 mm wide; apothecia to 0.8 mm in diam., discs plane, never convex; spores averaging 15.5–18.0 × 8.0–8.5 µm, l/w ratio 1.9–2.1 ..... ***R. mongolica***
– Thallus gray, never ochraceous, continuous to rimose; apothecia to 0.30–0.50 mm in diam., discs often becoming convex; spores averaging 12.5–13.5 × 5.5–6.0 µm, l/w ratio 2.1–2.4 ..... ***R. pyrina****
56 Apothecia not erumpent; spores averaging 17.5–21.5 × 9–11 µm.... ***R. metaboliza***
– Apothecia erumpent; spores smaller **57**

57 Hypothecium pigmented with brown, spores 11–20 × 5–8.5 μm, zeorin present ..... ***R. zeorina***
– Hypothecium colorless, spores 15.5–18 × 8–9 μm, no substance **58**
58 Spores averaging 15.5–16.0 μm in length..... ***R. manshurica***
– Spores averaging 16.5–18.0 μm in length..... ***R.* aff. *oleae***
59 Spores averaging >22 μm in length..... **60**
– Spores averaging <22 μm in length..... **61**
60 Margins of apothecia often radially cracked; spores *Physcia*- to *Physconia*-type .... ***R. ascociscana*** (syn. *R. akagiensis*, *R. melancholica*)
– Margins of apothecia not radially cracked; spores *Pachysporaria*-type I .... ***R. dolichospora***
61 Spores *Pachysporaria*-type II ..... ***R. salicis***
– Spores *Physcia*- or *Physconia*-type **62**
62 Spores *Physcia*- to *Physconia*-type, some lumina becoming rounded at apices, at maturity thin-walled **63**
– Spores strictly *Physcia*-type, apical walls remaining thick **67**
63 Thallus dark brown, spores darkly pigmented at maturity, torus prominent; oro-arctic to coastal **64**
– Thallus a shade of gray, sometimes brownish, spores typically pigmented at maturity, torus present but not prominent; boreal..... **66**
64 Thallus inconspicuous; apothecia mostly crowded, typically broadly attached .... ***R. olivaceobrunnea****
– Thallus of dispersed or contiguous areoles; apothecia mostly dispersed, narrowly or broadly attached **65**
65 Ascospores 20–21.5 × 10–11.5 μm, thallus well-developed, flat, scurfy or thick rugose areolate, apothecia broadly attached in the beginning then becoming narrow and even stipitate, discs convex when mature ..... ***R. sibirica***
– Ascospores 18.5–19.5 × 8.5–9.0 μm, thallus poorly developed, evanescent, thin or scabrid, sometimes areolate, apothecia broadly attached to thallus, discs typically flat ..... ***R. laevigata***
66 Thallus thick, rugose, areolate; apothecia crowded, discs persistently plane, thalline margins persistent..... ***R. archaea****
– Thallus thin, plane, continuous or rimose-areolate; apothecia dispersed, discs becoming convex, often excluding thalline margin ..... ***R. trevisanii****
67 Spores averaging >18 μm long, zeorin present ..... ***R. subminuta***
– Spores averaging <18 μm long, zeorin absent **68**
68 Apothecia erumpent at first, discs often becoming strongly convex; spores with lightly pigmented tori at maturity ..... ***R. orientalis***
– Apothecia never erumpent, discs persistently plane; spores with very dark, prominent tori at maturity **69**
69 Apothecia crowded, broadly attached; thalli associated with leaf scars or other mesic microhabitats; areoles plane, contiguous, to >0.2 mm in diam. ..... ***R. freyi***
– Apothecia mostly scattered, narrowly attached; thalli typically in more xeric microhabitats; areoles convex, scattered, to 0.2 mm in diam. ..... ***R. septentrionalis***

Acknowledgements

This work was supported by a grant from the Korean Forest Service Program through the Korea National Arboretum (KNA-202003127AF-00) for the forested wetland conservation of Korea.

References

Aptroot A, Moon KH (2014) 114 new reports of microlichens from Korea, including the description of five new species, show that the microlichen flora is predominantly Eurasian. Herzogia 27(2): 347–365. https://doi.org/10.13158/heia.27.2.2014.347

Bouckaert RR, Drummond AJ (2017) bModelTest: Bayesian phylogenetic site model averaging and model comparison. BMC evolutionary biology 17(1): e42. https://doi.org/10.1186/s12862-017-0890-6

Bouckaert R, Vaughan TG, Barido-Sottani J, Duchêne S, Fourment M, Gavryushkina A, Heled J, Jones G, Kühnert D, De Maio N, Matschiner M, Mendes FK, Müller NF, Ogilvie HA, du Plessis L, Popinga A, Rambaut A, Rasmussen D, Siveroni I, Suchard MA, Wu CH, Xie D, Zhang C, Stadler T, Drummond AJ (2019) BEAST 2.5: An advanced software platform for Bayesian evolutionary analysis. PLoS Computational Biology 15(4): e1006650. https://doi.org/10.1371/journal.pcbi.1006650

Bungartz F, Giralt M, Sheard JW, Elix JA (2016) The lichen genus *Rinodina* (Physciaceae, Teloschistales) in the Galapagos Islands, Ecuador. The Bryologist 119(1): 60–93. https://doi.org/10.1639/0007-2745-119.1.060

Edler D, Klein J, Antonelli A, Silvestro D (2019) raxmlGUI 2.0 beta: a graphical interface and toolkit for phylogenetic analyses using RAxML. bioRxiv. https://doi.org/10.1101/800912

Elix JA (2011) Australian Physciaceae (Lichenised Ascomycota). Australian Biological Resources Study, Canberra. Version 18 October 2011. http://www.anbg.gov.au/abrs/lichenlist/PHYSCIACEAE.html

Elix JA, Edler C, Mayrhofer H (2020) Two new corticolous species of *Rinodina* (Physciaceae, Ascomycota) from New Zealand. Australasian Lichenology 86: 95–101.

Ekman S (2001) Molecular phylogeny of the Bacidiaceae (Lecanorales, lichenized Ascomycota). Mycological Research 105: 783–797. https://doi.org/10.1017/S0953756201004269

Galanina IA, Ezhkin AK (2019) The genus *Rinodina* in the Kuril Islands (Russian Far East). Turczaninowia 22(4): 5–16. https://doi.org/10.14258/turczaninowia.22.4.1

Galanina IA, Yakovchenko LS, Tsarenko NA, Spribille T (2011) Notes on *Rinodina excrescens* in the Russian Far East (Physciaceae, lichenized Ascomycota). Herzogia 24(1): 59–64. https://doi.org/10.13158/heia.24.1.2011.59

Galanina IA, Ezhkin AK, Yakovchenko LS (2018) *Rinodina megistospora* (Physciaceae) in the Russian Far East. Novitates Systematicae Plantarum non Vascularium 52(1): 133–139. https://doi.org/10.31111/nsnr/2018.52.1.133

Galanina IA, Yakovchenko LS, Zheludeva EV, Ohmura Y (2021) The genus *Rinodina* (Physciaceae, lichenized Ascomycota) in the Magadan Region (Far East of Russia). Novitates

Systematicae Plantarum non Vascularium 55(1): 97–119. https://doi.org/10.31111/nsnr/2021.55.1.97

Giralt M (1994) Key to the corticolous and lignicolous species of the genus *Rinodina* present in the Iberian Peninsula and Balearic Islands. Bulletin de la Socie'te linne'enne de Provence 45: 317–326.

Giralt M (2001) The lichen genera *Rinodina* and *Rinodinella* (lichenized Ascomycetes, Physciaceae) in the Iberian Peninsula. Bibliotheca Lichenologica 79: 1–160.

Giralt M, Mayrhofer H, Obermayer W (1994) The species of the genus *Rinodina* (lichenized Ascomycetes, Physciaceae) containing pannarin in Eurasia with a special note on the taxonomy of *Rinodina granulans*. Mycotaxon 50: 47–59.

Giralt M, Mayrhofer H, Sheard JW (1995) The corticolous and lignicolous sorediate, blastidiate and isidiate species of the genus *Rinodina* in southern Europe. The Lichenologist 27(1): 3–24. https://doi.org/10.1017/S0024282995000041

Grube M, Arup U (2001) Molecular and morphological evolution in the Physciaceae (Lecanorales, lichenized Ascomycotina), with special emphasis on the genus *Rinodina*. The Lichenologist 33(1): 63–72. https://doi.org/10.1006/lich.2000.0297

Hall TA (1999) BioEdit: A User-Friendly Biological Sequence Alignment Editor and Analysis Program for Windows 95/98/NT. Nucleic Acids Symposium Series 41: 95–98.

Joshi S, Kondratyuk SY, Crişan F, Jayalal U, Oh SO, Hur JS (2013) New additions to lichen mycota of the Republic of Korea. Mycobiology 41(4): 177–182. https://doi.org/10.5941/MYCO.2013.41.4.177

Kaschik M (2006) Taxonomic studies on saxicolous species of the genus *Rinodina* (lichenized Ascomycetes, Physciaceae) in the Southern Hemisphere with emphasis in Australia and New Zealand. Bibliotheca Lichenologica 93: 1–162.

Kondratyuk S, Lőkös L, Tschabanenko S, Haji Moniri M, Farkas E, Wang X, Oh SO, Hur JS (2013) New and noteworthy lichen-forming and lichenicolous fungi. Acta Botanica Hungarica 55(3–4): 275–349. https://doi.org/10.1556/ABot.55.2013.3-4.9

Kondratyuk SY, Lőkös L, Halda JP, Upreti DK, Mishra GK, Haji Moniri M, Farkas E, Park JS, Lee BG, Liu D, Woo JJ, Jayalal RGU, Oh SO, Hur JS (2016) New and noteworthy lichen-forming and lichenicolous fungi 5. Acta Botanica Hungarica 58(3–4): 319–396. https://doi.org/10.1556/ABot.58.2016.3-4.7

Kondratyuk SY, Lőkös L, Halda JP, Roux C, Upreti DK, Schumm F, Mishra GK, Nayaka S, Farkas E, Park JS, Lee BG, Liu D, Woo JJ, Hur JS (2017) New and noteworthy lichen-forming and lichenicolous fungi 6. Acta Botanica Hungarica 59(1–2): 137–260. https://doi.org/10.1556/034.59.2017.1-2.7

Kondratyuk SY, Lőkös L, Oh SO, Kondratiuk TO, Parnikoza IY, Hur JS (2020) New and Noteworthy Lichen-Forming and Lichenicolous Fungi, 11. Acta Botanica Hungarica 62(3–4): 225–291. https://doi.org/10.1556/034.62.2020.3-4.3

Kumar V, Ngangom R, Nayaka S, Ingle KK (2021) New species and new records in the lichen genus *Rinodina* (Physciaceae) from India. Taiwania 66(2): 193–202. https://doi.org/10.6165/tai.2021.66.193

Lendemer JC, Sheard JW, Thor G, Tønsberg T (2012) *Rinodina chrysidiata*, a new species from far eastern Asia and the Appalachian Mountains of North America. The Lichenologist 44(2): 179–187. https://doi.org/10.1017/S0024282911000764

Lendemer JC, Hoffman JR, Sheard JW (2019) *Rinodina brauniana* (Physciaceae, Teloschistales), a new species with pseudoisidia from the southern Appalachian Mountains of eastern North America. The Bryologist 122(1): 111–121. https://doi.org/10.1639/0007-2745-122.1.111

Malme GO (1902) Die Flechten der ersten Regnell'schen Expedition. II. Die Gattung *Rinodina* (Ach.) Stiz. Bihang til Konghga Svenska Vetenskaps-Akademiens Handlingar 28(111, 1): 1–53. https://doi.org/10.5962/bhl.part.9812

Matzer M, Mayrhofer H (1996) Saxicolous species of the genus *Rinodina* (lichenized Ascomycetes, Physciaceae) in southern Africa. Bothalia 26(1): 11–30. https://doi.org/10.4102/abc.v26i1.683

Mayrhofer H (1983) The saxicolous species of *Rinodina* in New Zealand. The Lichenologist 15: 267–282. https://doi.org/10.1017/S0024282983000407

Mayrhofer H (1984a) Die saxicolen Arten der Flechtengattungen *Rinodina* und *Rinodinella* in der Alten Welt. Journal Hattori Botanical Laboratory 55: 327–493.

Mayrhofer H (1984b) The saxicolous species of *Dimelaena*, *Rinodina* and *Rinodinella* in Australia. Nova Hedwigia 79: 511–536.

Mayrhofer H, Poelt J (1979) Die saxicolen Arten der Flechtengattung *Rinodina* in Europa. Bibliotheca Lichenologica 12: 1–186.

Mayrhofer H, Moberg R (2002) *Rinodina*. Nordic Lichen Flora 2: 41–69.

Mayrhofer H, Obermayer W, Wetschnig W (2014) Corticolous species of the genus *Rinodina* (lichenized Ascomycetes, Physciaceae) in southern Africa. Herzogia 27: 1–12. https://doi.org/10.13158/heia.27.1.2014.1

Morse CA, Sheard JW (2020) *Rinodina lecideopsis* (Teloschistales, Physciaceae) a new endemic species from the central United States related to *R. bischoffii*. The Bryologist 123(1): 31–38. https://doi.org/10.1639/0007-2745-123.1.031

Nadyeina O, Grube M, Mayrhofer H (2010) A contribution to the taxonomy of the genus *Rinodina* (Physciaceae, lichenized Ascomycotina) using combined ITS and mtSSU rDNA data. The Lichenologist 42(5): 521–531. https://doi.org/10.1017/S0024282910000186

Orange A, James PW, White FJ (2001) Microchemical Methods for the Identification of Lichens. The British Lichen Society, London.

Poelt J (1965) Zur Systematik der Flechtenfamilie Physciaceae. Nova Hedwigia 9: 21–32.

Rambaut A (2014) FigTree v1.4.2. Edinburgh: University of Edinburgh. http://tree.bio.ed.ac.uk/software/figtree

Resl P, Mayhofer H, Clayden SR, Spribille T, Thor G, Tønsberg T, Sheard JW (2016) Morphological, chemical and species delimitation analyses provide new taxonomic insights into two groups of *Rinodina*. The Lichenologist 48(5): 469–488. https://doi.org/10.1017/S0024282916000359

Schwarz G (1978) Estimating the dimension of a model. Annals of Statistics 6: 461–464. https://doi.org/10.1214/aos/1176344136

Sheard JW (1966) A revision of the lichen genus *Rinodina* in Europe and its taxonomic affinities. PhD thesis, University of London, England.

Sheard JW (2004) *Rinodina*. In: Nash III TH, Ryan BD, Diederich P, Gries C, Bungartz F (Eds) Lichen Flora of the Greater Sonoran Desert Region, Vol. II. Lichens Unlimited, Tempe, 467–502.

Sheard JW (2010) The Lichen Genus *Rinodina* (Ach) Gray (Lecanoromycetidae, Physciaceae) in North America, North of Mexico. NRC Research Press, Ottawa, 246 pp.

Sheard JW (2018) A synopsis and new key to the species of *Rinodina* (Ach.) Gray (Physciaceae, lichenized Ascomycetes) presently recognized in North America. Herzogia 31(p1): 395–423. https://doi.org/10.13158/heia.31.1.2018.395

Sheard JW, Mayrhofer H (2002) New species of *Rinodina* (Physciaceae, lichenized Ascomycetes) from western North America. The Bryologist 105(4): 645–672. https://doi.org/10.1639/0007-2745(2002)105[0645:NSORPL]2.0.CO;2

Sheard JW, Lendemer JC, Spribille T, Thor G, Tønsberg T (2010) Further contributions to the genus *Rinodina* (Physciaceae, Lecanoromycetidae): two species new to science and a new record for the Canadian High Arctic. Herzogia 25(2): 125–143. https://doi.org/10.13158/heia.25.2.2010.125

Sheard JW, Knudsen K, Mayrhofer H, Morse CA (2011) Three new species of *Rinodina* (Physciaceae) and a new record from North America. The Bryologist 114(3): 453–465. https://doi.org/10.1639/0007-2745-114.3.453

Sheard JW, Ezhkin AK, Galanina IA, Himelbrant D, Kuznetsova E, Shimizu A, Stepanchikova I, Thor G, Tønsberg T, Yakovchenko LS, Spribille T (2017) The lichen genus *Rinodina* (Physciaceae, Caliciales) in north-eastern Asia. The Lichenologist 49(6): 617–672. https://doi.org/10.1017/S0024282917000536

Smith CW, Aptroot A, Coppins BJ, Fletcher A, Gilbert OL, James PW, Wolseley PA (2009) The lichens of Great Britain and Ireland. The British Lichen Society, London.

Stecher G, Tamura K, Kumar S (2020) Molecular Evolutionary Genetics Analysis (MEGA) for macOS. Molecular Biology and Evolution 37(4): 1237–1239. https://doi.org/10.1093/molbev/msz312

Tønsberg T (1992) *Rinodina sheardii*, a new lichen species from northwest Europe and northwest North America. The Bryologist 95(2): 216–217. https://doi.org/10.2307/3243437

Wedin M, Baloch E, Grube M (2002) Parsimony analyses of mtSSU and nITS rDNA sequences reveal the natural relationships of the lichen families Physciaceae and Caliciaceae. Taxon 51(4): 655–660. https://doi.org/10.2307/1555020

White TJ, Bruns T, Lee S, Taylor JW (1990) Amplification and direct sequencing of fungal ribosomal RNA genes for phylogenetics. PCR protocols: a guide to methods and applications 18(1): 315–322. https://doi.org/10.1016/B978-0-12-372180-8.50042-1

Wijayawardene NN, Hyde KD, Al-Ani LKT, Tedersoo L, Haelewaters D, Rajeshkumar KC, Zhao RL, Aptroot A, Leontyev DV, Saxena RK, Tokarev YS, Dai DQ, Letcher PM, Stephenson SL, Ertz D, Lumbsch HT, Kukwa M, Issi IV, Madrid H, Phillips AJL, Selbmann L, Pfliegler WP, Horváth E, Bensch K, Kirk PM, Kolaříková K, Raja HA, Radek R, Papp V, Dima B, Ma J, Malosso E, Takamatsu S, Rambold G, Gannibal PB, Triebel D, Gautam AK, Avasthi S, Suetrong S, Timdal E, Fryar SC, Delgado G, Réblová M, Doilom M, Dolatabadi S, Pawłowska JZ, Humber RA, Kodsueb R, Sánchez-Castro I, Goto BT, Silva DKA, de Souza FA, Oehl F, da Silva GA, Silva IR, Błaszkowski J, Jobim K, Maia LC, Barbosa FR, Fiuza PO, Divakar PK, Shenoy BD, Castañeda-Ruiz RF, Somrithipol S, Lateef AA, Karunarathna SC, Tibpromma S, Mortimer PE, Wanasinghe DN, Phookamsak R, Xu J, Wang Y, Tian F, Alvarado P, Li DW, Kušan I, Matočec N, Mešić A, Tkalčec Z, Maharachchikumbura SSN, Papizadeh M, Heredia

G, Wartchow F, Bakhshi M, Boehm E, Youssef N, Hustad VP, Lawrey JD, Santiago ALCMA, Bezerra JDP, Souza-Motta CM, Firmino AL, Tian Q, Houbraken J, Hongsanan S, Tanaka K, Dissanayake AJ, Monteiro JS, Grossart HP, Suija A, Weerakoon G, Etayo J, Tsurykau A, Vázquez V, Mungai P, Damm U, Li QR, Zhang H, Boonmee S, Lu YZ, Becerra AG, Kendrick B, Brearley FQ, Motiejūnaitė J, Sharma B, Khare R, Gaikwad S, Wijesundara DSA, Tang LZ, He MQ, Flakus A, Rodriguez-Flakus P, Zhurbenko MP, McKenzie EHC, Stadler M, Bhat DJ, Liu JK, Raza M, Jeewon R, Nassonova ES, Prieto M, Jayalal RGU, Erdoğdu M, Yurkov A, Schnittler M, Shchepin ON, Novozhilov YK, Silva-Filho AGS, Gentekaki E, Liu P, Cavender JC, Kang Y, Mohammad S, Zhang LF, Xu RF, Li YM, Dayarathne MC, Ekanayaka AH, Wen TC, Deng CY, Pereira OL, Navathe S, Hawksworth DL, Fan XL, Dissanayake LS, Kuhnert E, Grossart HP, Thines M (2020) Outline of Fungi and fungus-like taxa. Mycosphere 11(1): 1060–1456. https://doi.org/10.5943/mycosphere/11/1/8

Yakovchenko LS, Davydov EA, Paukov A, Frisch A, Galanina I, Han JE, Moon KH, Kashiwadani H (2018) New lichen records from Korea–I. Mostly arctic-alpine and tropical species. Herzogia 31(2): 965–981. https://doi.org/10.13158/heia.31.2.2018.965

Zheng XJ, Ren Q (2020) Three *Rinodina* species new to China. Mycotaxon 135(1): 195–201. https://doi.org/10.5248/135.195

MycoKeys 87: 183–204 (2022)
doi: 10.3897/mycokeys.87.76125
https://mycokeys.pensoft.net

RESEARCH ARTICLE

A peer-reviewed open-access journal
MycoKeys
Launched to accelerate biodiversity research

Emending *Gymnopus* sect. *Gymnopus* (Agaricales, Omphalotaceae) by including two new species from southern China

Ji-Peng Li[1,2], Vladimír Antonín[3], Genevieve Gates[4], Lu Jiang[5], Tai-Hui Li[1], Yu Li[2], Bin Song[1], Chun-Ying Deng[6]

1 *State Key Laboratory of Applied Microbiology Southern China, Guangdong Provincial Key Laboratory of Microbial Culture Collection and Application, Institute of Microbiology, Guangdong Academy of Sciences, Guangzhou, Guangdong 510070, China* **2** *Engineering Research Center of Chinese Ministry of Education for Edible and Medicinal Fungi, Jilin Agricultural University, Changchun, Jilin 130118, China* **3** *Department of Botany, Moravian Museum, Zelný trh 6, Brno CZ-659 37, Czech Republic* **4** *Tasmanian Institute of Agriculture, Private Bag 98, Hobart, Tasmania 7001, Australia* **5** *Shenzhen Wildlife Conservation Division, Shenzhen, Guangdong 518048, China* **6** *Guizhou institute of biology, Guizhou Academy of Sciences, Guiyang, Guizhou 550009, China*

Corresponding authors: Tai-Hui Li (mycolab@263.net), Yu Li (yuli966@126.com)

Academic editor: R. H. Nilsson | Received 4 October 2021 | Accepted 30 January 2022 | Published 4 March 2022

Citation: Li J-P, Antonín V, Gates G, Jiang L, Li T-H, Li Y, Song B, Deng C-Y (2022) Emending *Gymnopus* sect. *Gymnopus* (Agaricales, Omphalotaceae) by including two new species from southern China. MycoKeys 87: 183–204. https://doi.org/10.3897/mycokeys.87.76125

Abstract

Based on phylogenetic analyses, some newly studied Chinese mushroom specimens were found to represent two distinct species within the genus *Gymnopus*. Along with *G. fusipes* (sect. *Gymnopus*) they form a distinct clade with high support, although their macromorphological characters seem to be closer to members of *Gymnopus* sect. *Levipedes* or sect. *Vestipedes* (*Collybiopsis*). When examined in detail, their micromorphological characters, especially the type of pileipellis, support them as new members of *G*. sect. *Gymnopus*. Therefore, two new species, *G. omphalinoides* and *G. schizophyllus*, and the emended circumscription of sect. *Gymnopus* are proposed in this paper. Detailed morphological descriptions, colour photos, illustrations of the two new species, morphological comparisons with similar taxa and the molecular-phylogenetic analyses of the combined nrITS and nrLSU data are presented. A key to the known species of *G*. sect. *Gymnopus* is also presented.

Keywords

Morphology, new taxa, phylogeny, taxonomy

Introduction

Gymnopus (Pers.) Roussel sect. *Gymnopus* is a monotypic section and its type species, *Gymnopus fusipes* (Bull.) Gray, also typifies the genus (Antonín and Noordeloos 2010). The sectional name, therefore, was proposed automatically. Formerly, *G. fusipes* was placed in *Collybia* (Fr.) Staude sect. *Striipedes* (Fr.) Quél. as *C. fusipes* (Bull.) Quél. (Singer 1986). Based on morphology, several species, in fact, several sections, were moved from *Collybia* to *Gymnopus*, a genus that was defined mainly based on American and European material (Antonín et al. 1997). Since then, the character of the pileipellis, especially the terminal cells, has become a significant factor in the delimitation of the sections within the genus. After undergoing a series of revisions, *Gymnopus* sensu lato (s.l.) was restricted as a monophyletic genus (*Gymnopus* sensu stricto (s. str.)) that comprised four sections. The other three sections are *G.* sect. *Androsacei* (Kühner) Antonín & Noordel, sect. *Impudicae* (Antonín & Noordel.) Antonín & Noordel. and sect. *Levipedes* (Quél.) Halling (Oliveira et al. 2019).

Morphologically, the current circumscription of *G.* sect. *Gymnopus* was adopted from Clémençon (1981) as *Collybia* sect. *Striipedes*. As a monotypic section, its circumscription is dominated by its type species which is characterised by a fleshy pileus, fusoid stipe with a distinct pseudorrhiza and a pileipellis made up of inflated, irregular, often coralloid elements, similar to the *Dryophila*-type structure (Antonín and Noordeloos 2010; Oliveira et al. 2019). It stands in stark contrast to other sections. Many studies published in recent years with an emphasis on *Gymnopus* reported or described species from the other sections, and discussions relating to the type species or *G.* sect. *Gymnopus* were hardly addressed. Wilson and Desjardin (2005) and Mata et al. (2007) noted that *G. fusipes* and members of *G.* sect. *Levipedes* share a similar pileipellis and that the type species of the genus mainly differs in the stipe with a pseudorrhiza. Besides, only *Collybia subsulcatipes* A.H. Sm. was considered a probable member of *G.* sect. *Gymnopus* based on morphology (Antonín and Noordeloos 1997, as *Collybia sulcatipes* A.H. Smith). It is characterised by a smooth or longitudinally grooved to subsulcate stipe with a long pseudorrhiza (Smith 1944). Nevertheless, whether this species belongs to this section is difficult to confirm because of the lack of molecular data.

Phylogenetically, Mata et al. (2004) reported on the phylogenetic position of *G. fusipes* and showed that it forms a distinct clade that is closely related to *Setulipes androsaceus* (L.) Antonín and always among other clades dominated by *Gymnopus* taxa. Wilson and Desjardin (2005) also produced a similar phylogenetic result. As the species typified the genus, these results had repercussions on the generic relationships. Hence, *S. androsaceus* was transferred to *Gymnopus* (Mata et al. 2004) and was designated as the type species of *G.* sect. *Androsacei* (Noordeloos and Antonín 2008). Subsequently, Oliveira et al. (2019) used a multi-gene phylogenetic analysis to restrict the concept of genus *Gymnopus* and to further confirm that *G.* sect. *Androsacei* is the closest group to *G.* sect. *Gymnopus*. However, there was no update on the phylogenetic nature of *G.* sect. *Gymnopus* due to the lack of new material.

In this study, two new species of *G.* sect. *Gymnopus* are described based on morphology and phylogenetic analysis. Detailed morphological descriptions, colour photos, illustrations of the species, morphological comparisons with similar taxa and molecular-phylogenetic analyses of combined nuclear ribosomal internal transcribed spacer (nrITS) and nuclear ribosomal large subunit (nrLSU) data are presented. An emended circumscription and a key to the species of *G.* sect. *Gymnopus* are provided.

Material and methods

Abbreviations

For Latin names: ***G.*** = *Gymnopus*; ***Ma.*** = *Marasmius*; ***Mi.*** = *Micromphale*; ***My.*** = *Mycetinis*; ***P.*** = *Paragymnopus.*

For phylogenetic analysis: **ML** = Maximum Likelihood; **BI** = Bayesian Inference; **BP** = Bootstrap Proportions; **PP** = Posterior Probability.

For collection locality: **FNNR** = Fanjingshan National Nature Reserve; **MC** = Maguan County; **MR** = Meizihu Reservoir; **TFP** = Tianluhu Forest Park; **WSA** = Wutongshan Scenic Area; **YNNR** = Yunkaishan National Nature Reserve.

For climate: **AAT** = average annual temperature; **AAR** = average annual rainfall; **MST** = major soil type; **MMMM** = mid-subtropical mountain moist monsoon; **SEM** = subtropical eastern monsoon; **SM** = subtropical monsoon; **SSM** = south subtropical monsoon; **SSO** = south subtropical oceanic.

For soil type: **B** = brown; **DBS** = dark brown soil; **La** = laterite; **LRS** = lateritic red soil; **MSMS** = mountain shrub meadow soils; **MRS** = mountain red soil; **RS** = red soil; **YBS** = yellow brown soil; **YS** = yellow soil.

Specimen collection and drying treatment

Nine collections from China were examined in this study: one came from the Guizhou Province (Tongren City), three collections from the Yunnan Province (one from Pu'er City and two from Maguan County) and five collections from the Guangdong Province (one from Guangzhou City, one from Shenzhen City and three from Xinyi City). The exact localities and their environmental characteristics are shown in Table 1. The fresh basidiomata of each collection were wrapped in separate mesh bags and dried in an electric drier operated below 50 °C. Dried collections were deposited in the Fungarium of Guangdong Institute of Microbiology, China (**GDGM**), Fungarium of the Herbarium of Kunming Institute of Botany, Chinese Academy of Sciences (**KUN-HKAS**) or Herbarium Mycology of Jilin Agricultural Science and Technology University (**HMJU**). The herbarium abbreviations follow Thiers (2021).

Table 1. The environmental characteristics of localities for each collection.

Locality	Climate	Average annual temperature	Average annual rainfall	Major soil type	References
FNNR	MMMM	16.9 °C	1351 mm	YS	Xiao et al. 1998; Zhong et al. 2011
MC	SEM	16.9 °C	1345 mm	La, LRS, RS, YS, YBS, BS, DBS	Zhao 2007
MR	SM	17.8 °C	1514.6 mm	La, LRS, RS	Tao 2002, 2006
TFP	SSM	22 °C	1725 mm	LRS	Huang and Li 2006; Kong et al. 2013
WSA	SSO	22.4 °C	1948.4 mm	LRS, RS, MSMS	Xv et al. 2009; Zhou et al. 2011
YNNR	SSM	18 °C	2300–2600 mm	LRS, MRS, YS	Huang (1998); Li et al. 2021b

Morphological studies

Fresh basidiomata were photographed and used for macromorphological descriptions. The colours are coded from Kornerup and Wanscher (1978). The ecology of the specimens is presented below. Lamellae were counted where 'L' refers to the number of full-length lamellae and 'l' refers to the number of lamellulae tiers.

Micromorphological structures were observed via a ZEISS Axio Lab. A1 microscope based on the hand-made sections of dried basidiomata mounted in 5 % KOH on a glass slide. When necessary, Congo Red solution was used as a stain and Melzer's reagent was used to test amyloid or dextrinoid reactions. For the various microscopic structures, 'n' refers to the number of measured elements. For basidiospores, 'E' represents the quotient of length and width in any one spore, and 'Q' represents the mean of E values. Basidiospore measurements do not include apiculus and are presented as '(a)b–c(d)', where 'b–c' represents the minimum of 90 % of the measured values and 'a' and 'd' represent the extreme values. The main body (sterigmata or excrescences not included) of basidia, basidioles, pleurocystidia and cheilocystidia were measured (if present).

DNA extraction, amplification and sequencing

Genomic DNA was extracted from dried tissue via a Magen HiPure Fungal DNA Kit (Magen Biotech Co., Ltd., Guangzhou) Fungal DNA Kit as in Li et al. (2021a). The nrITS (the nuclear ribosomal internal transcribed spacer) region and the nrLSU (nuclear ribosomal large subunit) gene were amplified by the polymerase chain reaction (PCR) technique using the primers ITS5 and ITS4 (nrITS; White et al. 1990), and LR0R and LR5 (nrLSU; Vilgalys and Hester 1990; Cubeta et al. 1991), respectively. A common PCR programme was used for amplification of both markers and is given below: 4 min at 95 °C; 35 cycles of 45 s at 95 °C, 45 s at 53 °C, 60 s at 72 °C; 10 min at 72 °C. Amplified products were used for Sanger dideoxy sequencing performed by Beijing Genomics Institute (BGI). The newly generated sequences were assembled from two overlapping reads and trimmed via BioEdit v.7.0.9 (Hall 2011). Before depositing in GenBank (Sayers et al. 2021; Table 2), quality control was done following the methods in Nilsson et al. (2012).

Phylogenetic analyses

Representative species and their sequences were selected to cover all sections of *Gymnopus* s. str. based on recent publications (Mata et al. 2004; Petersen and Hughes 2016; Oliveira et al. 2019; César et al. 2020). In addition, four sequences annotated as *Marasmius otagensis* were added to the matrix following an unpublished phylogenetic tree provided by Dr Jerry Cooper (Landcare Research, New Zealand). Two species of *Mycetinis* Earle were selected as the outgroup according to the phylogenetic results of Oliveira et al. (2019), Li et al. (2021a) and Li et al. (2021b). Our two-marker dataset, composed of ITS1-5.8S-ITS2-LSU sequences, was partitioned and used for the phylogenetic analyses. The samples NEHU MBSRJ48, HAKS 107312 and SFSU:DED 8209 have only ITS sequences available, and their LSU data were treated as missing data in the dataset. Information on sequences used in the phylogenetic analysis of this study is shown in Table 2. Sequences of each marker (nrITS and nrLSU) were aligned using MAFFT v.7.313 (Katoh and Standley 2013), applying the L-INS-I strategy, and manually concatenated and adjusted in BioEdit v.7.0.9 (Hall 2011). The combined dataset comprised four partitions (ITS1, the 5.8S gene, ITS2 and the LSU gene) and was analysed in the Maximum Likelihood (ML) and Bayesian Inference (BI) methods. The ML analysis was performed in RAxML v.8.2.10 (Stamatakis 2014), and the BI analysis was performed in MrBayes v.3.2.6 (Ronquist et al. 2012). The optimal substitution model for BI analysis was chosen by Modelfinder (Kalyaanamoorthy et al. 2017) using the Bayesian Information Criterion (BIC). The ML analysis was conducted using the GTRGAMMA substitution model, applying rapid bootstrap algorithm, with 5000 replicates. The BI analysis was implemented using two runs with four chains each for ten million generations sampling every hundredth generation. The average standard deviation of split frequencies was examined to make sure that the value was below 0.01. After discarding the first 25 % of trees as burn-in, a 50% majority rule consensus tree was generated from the remaining trees. Convergence of the MCMC chains was visualised in Tracer v. 1.7.1 (Rambaut et al. 2018) and examined manually. The tree files were viewed and edited in FigTree v1.4.3 (Rambaut 2009). The multiple sequence alignment and the ML and BI tree files were deposited in TreeBASE as Study ID 28774 (https://www.treebase.org).

Table 2. Information on DNA sequences used in the phylogenetic analyses. Newly generated sequences are highlighted in bold and type specimen is marked with an asterisk (*).

Taxon name	ITS	LSU	Collection No.	Locality	Reference
Agaricales sp.	AB859204	AB859204	Sw2-1	Japan	GenBank
G. adventitius nom. prov.	KY026760	KY026760	SFSU:DED8813	Not given	Petersen and Hughes (2016)
G. alliifoetidissimus	MT023348	MT017526	GDGM 76695	China	Li et al. (2021a)
G. androsaceus	KY026750	KY026750	CULTENN5609	USA	Petersen and Hughes (2016)
G. androsaceus	MH857175	MH868714	CBS 240.53	France	Vu et al. 2019
G. androsaceus	MH857174	MH868713	CBS 239.53	France	Vu et al. 2019
G. androsaceus	KY026748	KY026748	CULTENN5021h2	Canada	Petersen and Hughes (2016)
G. androsaceus	KY026663	KY026663	TENN:F-59594	Russia	Petersen and Hughes (2016)

Taxon name	ITS	LSU	Collection No.	Locality	Reference
G. atlanticus	KT222654	KY302698	URM 87728	Brazil	Coimbra et al. (2015)
G. aurantiipes	AY263432	AY639410	SFSU:AWW118	Indonesia	Wilson et al. (2004)
G. brunneiniger	MT232388	MW187069	XAL: Cesar50	Mexico	César et al. (2020)
G. brunneodiscus	MH589973	MH589988	BRNM 714974	South Korea	Ryoo et al. (2020)
G. cremeostipitatus	KF251071	KF251091	BRNM 747547	South Korea	Antonín et al. (2014)
G. densilamellatus	KP336685	KP336694	BRNM 714927	South Korea	Ryoo et al. (2016)
G. dryophiloides	MH589967	MH589985	BRNM 781447	South Korea	Ryoo et al. (2020)
G. dryophilus	DQ241781	AY640619	TENN:F-57012	Not given	Matheny et al. (2006)
G. dysodes	KY026666	FJ750265	TENN:F-61125	USA	Hughes and Petersen (2016)
G. foetidus	KY026739	KY026739	TENN:F-69323	USA	Hughes and Petersen (2016)
G. frigidomarginatus nom. prov.	KY026648	KY026648	TENN:F-55679	USA	Hughes and Petersen (2016)
G. fusipes	AY256711	AY256711	TENN:F-59300	Austria	Mata et al. (2004)
G. fusipes	KY026727	KY026727	TENN:F-69254	Slovakia	Hughes and Petersen (2016)
G. fusipes	AY256710	AY256710	TENN:F-59217	France	Mata et al. (2004)
G. impudicus	LT594119	LT594119	BRNM 714849	Czech Republic	Ryoo et al. (2016)
G. inflatotrama nom. prov.	KY026619	KY026619	TENN:F-48143	USA	Hughes and Petersen (2016)
G. inflatotrama nom. prov.	KY026744	KY026744	TFB 4529	USA	Hughes and Petersen (2016)
G. inflatotrama nom. prov.	KY026640	KY026640	TENN:F-53490	USA	Hughes and Petersen (2016)
G. inflatotrama nom. prov.	KY026632	KY026632	TENN:F-51233	USA	Hughes and Petersen (2016)
G. inusitatus	JN247553	JN247557	BCN:SCM B-4058	Spain	Antonín et al. (2012)
G. iocephalus	DQ449984	KY019630	TENN:F-52970	USA	Mata et al. (2007)
G. irresolutus	MF100973	Unavailable	SFSU:DED 8209	São Tomé	Desjardin and Perry (2017)
G. montagnei	DQ449988	AF261327	JMCR 143	Not given	Mata et al. (2007)
G. neobrevipes	MH673477	MH673477	TENN:F-14505	USA	Petersen and Hughes (2019)
G. novae-angliae nom. prov.	KY026745	KY026745	CULTENN4975	USA	Hughes and Petersen (2016)
G. novomundi nom. prov.	KY026759	KY026759	SFSU-DED5097	USA	Hughes and Petersen (2016)
G. ocior	KY026678	KY026678	TENN:F-65135	Belgium	Hughes and Petersen (2016)
G. omphalinoides sp. nov.	**MW134044**	**MW134730**	*GDGM 78318	China	This study
G. omphalinoides sp. nov.	**MW134047**	**MW134733**	HMJU 00506	China	This study
G. omphalinoides sp. nov.	**MW134040**	**MW134726**	GDGM 44411	China	This study
G. omphalinoides sp. nov.	**MW134045**	**MW134731**	GDGM 78483	China	This study
G. omphalinoides sp. nov.	**OK087326**	Unavailable	KUN-HKAS 107312	China	This study
G. pallipes	MW582856	**OK087327**	GDGM 81513	China	Li et al. (2021b) and this study
G. portoricensis	KY026627	KY026627	TENN:F-50999	Puerto Rico	Hughes and Petersen (2016)
G. schizophyllus sp. nov.	**MW134041**	**MW134727**	GDGM 76287	China	This study
G. schizophyllus sp. nov.	**MW134042**	**MW134728**	GDGM 77038	China	This study

Taxon name	ITS	LSU	Collection No.	Locality	Reference
G. schizophyllus sp. nov.	**MW134043**	**MW134729**	*GDGM 77165	China	This study
G. schizophyllus sp. nov.	**MW134046**	**MW134732**	KUN-HKAS 96494	China	This study
G. similis	KP336690	KP336697	BRNM 714981	South Korea	Ryoo et al. (2016)
G. spongiosus	KY026686	KY026686	TENN:F-65912	USA	Hughes and Petersen (2016)
G. subsupinus	KM975399	KM975375	PDD:96595	New Zealand	GenBank
G. talisiae	KT222655	KX958401	URM 87730	Brazil	Coimbra et al. (2015)
Ma. androsaceus	JN943605	JN941145	Sara Landvik:NN008037	Sweden	Antonín et al. (2014)
Ma. androsaceus	AF519893	AF519891	MUCL35155	Not given	Klonowska et al. (2013)
Ma. otagensis	MT974597	MT974601	PDD:106823	New Zealand	GenBank
Ma. otagensis	MT974600	MT974602	PDD:113265	New Zealand	GenBank
Mi. foetidum	KP877447	Unavailable	NEHU.MBSRJ.48	India	Borthakur and Joshi (2016)
My. alliaceus	KY696752	KY696752	TENN:F-55630	Russia	Petersen and Hughes (2017)
My. scorodonius	KY696748	KY696748	TENN:F-53474	USA	Petersen and Hughes (2017)
Pa. perforans	KY026625	KY026625	TENN:F-50319	Sweden	Petersen and Hughes (2017)

Results

Phylogenetic results

A BLAST search of nrITS sequences revealed that a sequence annotated as "*Micromphale foetidum*" (KP877447) was the most similar (7–8 different sites or more than 98.16% similarity) to the two new species described in this study.

The combined dataset comprised 113 sequences including 58 nrITS and 55 nrLSU. The alignment is 1,716 bases long, of which 1,263 are constant sites, 139 are variable and parsimony-uninformative sites and 314 (18 %) are parsimony-informative sites. The best-fit model for each partition applied in the BI analysis was HKY+F+I+G4 (for the nrITS1, nrITS2 and nrLSU markers) and K2P (for the nr5.8S gene). ML and BI analyses produced nearly identical topologies and only the ML phylogram is presented (Fig. 1). The ML-BP and BI-PP support values are shown above and below the branches, respectively.

In the generated phylogenetic tree (Fig. 1), *Gymnopus* s. str. formed a strongly supported clade (BI-PP/ML-BP = 1.00/100 %). Inside this clade, four samples from China (GDGM 76287, 77038, 77165 and KUN-HKAS 96494) of one morphospecies and five samples from China (GDGM 44411, 78318, 78483, KUN-HKAS 107312 and HMJU 00506) of the other morphospecies grouped in two different lineages implying two distinct species within *Gymnopus* s. str. The nine samples from China along with a sample from India (NEHU MBSRJ48) formed a single clade with high support (BI-PP/ML-BP = 1.0/88 %). This clade and two samples from New Zealand (PDD: 106823, 113265) grouped in one clade as sister to *G. fusipes* (*G.* sect. *Gymnopus*). Furthermore, they formed a distinct group as a monophyletic clade with high support (BI-PP/ML-BP = 1.00/98 %).

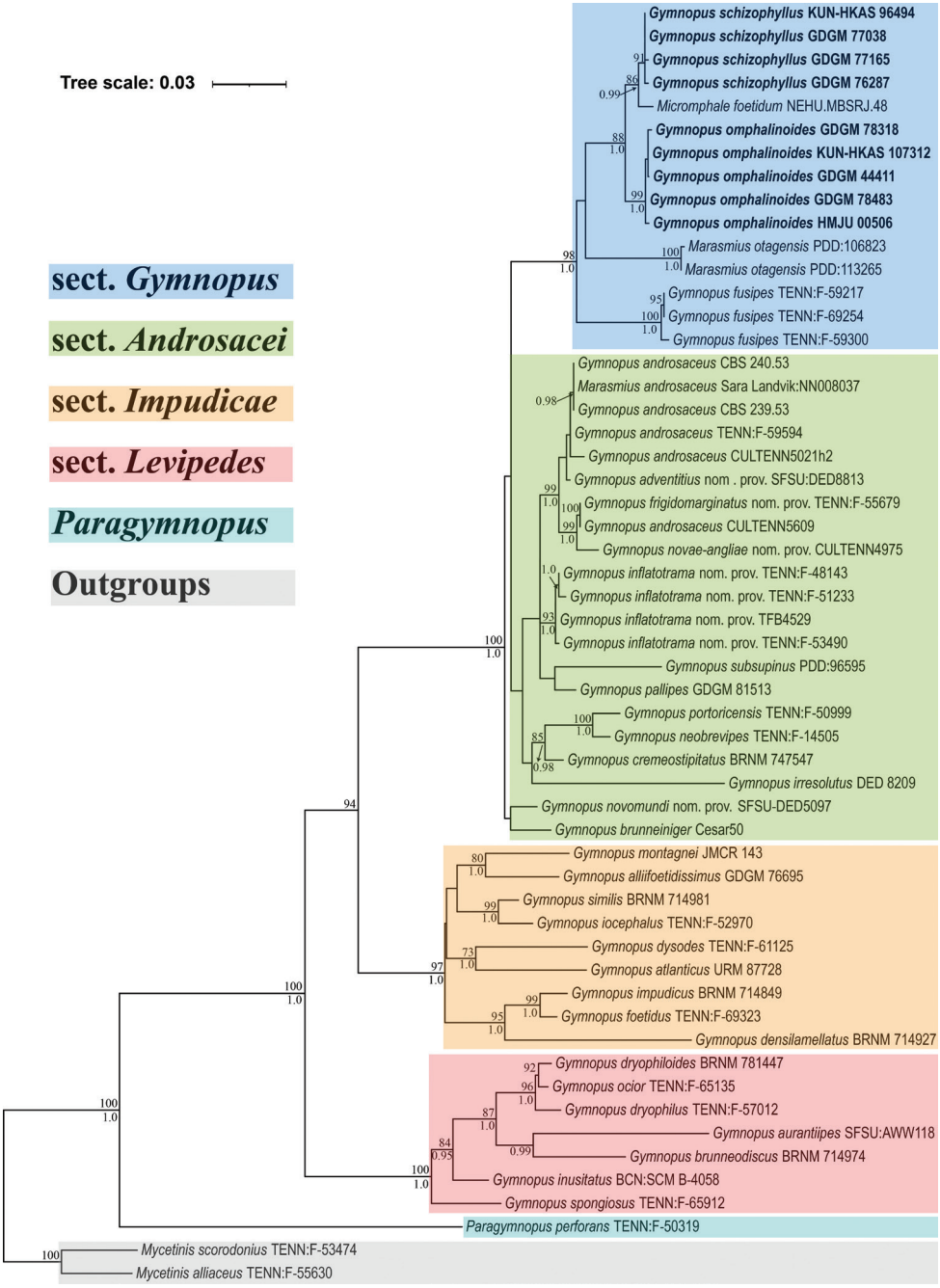

Figure 1. Phylogram generated by ML analysis of the combined dataset (ITS1-5.8S-ITS2-LSU region). ML-BP ≥ 70 % and BI-PP ≥ 0.95 are shown above and below the branches, respectively.

Taxonomy

Gymnopus omphalinoides **J.P. Li, T.H. Li & Y. Li, sp. nov.**
MycoBank No: 837641
Figs 2, 3

Typification. China, Guangdong Province, Shenzhen City, Wutongshan Scenic Area, 16 September 2019, H. Huang, L.Q. Wu & N. Zhan (GDGM 78318, holotype!).

Etymology. The epithet '*omphalinoides*' (Lat.) refers to the omphalinoid or *Omphalina*-like basidiomata of the new species.

Diagnosis. Differs from *G. volkertii* Murrill in its striate or grooved pileus and smaller basidiospores (4.0–5.5 × 2.5–3 μm). Basidiomata mainly gregarious on decayed wood in broadleaf forest; pileus disc reddish orange to dark brown becoming paler with age; lamellae broad, adnate and ventricose; stipe glabrous.

Description. Basidiomata omphalinoid, collybioid or gymnopoid. Pileus 10–40 mm broad, membranous, hemispheric when young, becoming convex, plano-convex to applanate, generally umbilicate to sometimes slightly depressed at the centre, inflexed then straight or reflexed at margin, with a marginal zone often undulating with age, glabrous, radially striate or grooved towards the margin, orange (6B7) or reddish orange (7B7) to brown (7D8) overall when young, somewhat reddish orange (7B7) or dark brown (7F8), then paler towards the margin, white or pale orange (6A3) to light brown (6D4), often greyish orange (6B4) to dark brown (6F8) at the disc. Lamellae adnate, broad, ventricose to broadly ventricose, white when fresh, sometimes with greyish red (7B4) to brown (7E7) tint somewhere, margin entire to split and sometimes grooved, L = 12–17, l = 3–5. Stipe 10–30 mm long, 2–4 mm thick in the middle, central, cylindrical, or compressed, with dense basal mycelium when young that disappears when old, hollow, fibrous, glabrous, slightly longitudinally striate when old, rooting deep in the substrate, but eventually attaches to the stump, dull white to greyish red (7B4) when young, soon darker towards the base, white to reddish orange (7A7) at apex, finally entirely dark brown (7F8). Odour not distinctive.

Basidiospores [n=80] (3.5–) 4.0–5.5 (–6.0) × 2.5–3 (–3.5) μm (average= 4.63 × 2.93 μm, E = 1.33–1.83 (–2), Q=1.58), obovoid, ellipsoid to subellipsoid, sometimes amygdaliform. Basidia [n=20] 17–31 × 3–5 μm, clavate, 4-spored. Basidioles [n=20] 17–32 × 4–5.5 μm, clavate, cylindrical. Lamellar edge sterile. Cheilocystidia [n=20] 17–32 × 4–10 μm, irregularly clavate, sphaeropedunculate or almost so, with tendency to be inflated, with or without finger-like apical projection(s) or more or less diverticulate elements. Pileipellis a cutis composed of cylindrical, thin-walled hyphae, up to 12.5 μm wide, smooth or with scattered diverticula, hyaline to slightly brownish; *Rameales*-like structures present, rare to abundant; terminal cells short, broad, mostly inflated, vesiculose or pyriform to cystidioid (clavate), obtuse and sometimes diverticulate, mixed with a few irregularly branched, slightly coralloid elements and some resembling *Dryophila*-type structures. *Stipitipellis* a cutis composed

Figure 2. Basidiomata of *Gymnopus omphalinoides* **a** GDGM 78483 **b** GDGM 78318 holotype! (with magnifying slightly longitudinally striate stipe) **c** KUN-HKAS 107312 **d, e** GDGM 44411 **f** HMJU 00506. **a** photographed by M. Zhang **b** photographed by L.Q. Wu, **c** photographed by X.H. Wang **d, e** photographed by J.P. Li **f** photographed by J.Z. Xu. For a detailed display, the slightly longitudinally striate stipe is magnified in **b**, and the split lamellar edge is magnified in **e, f**. Scale bars: 1 cm.

of cylindrical, slightly thick to thick-walled, smooth, non-dextrinoid, parallelly arranged hyphae, up to 12 μm wide, with or without *Rameales*-like structure. Caulocystidia absent. Clamp connections present.

Ecology. Saprotrophic, gregarious or in small clusters, usually rooting around the roots and stumps in broadleaf forests.

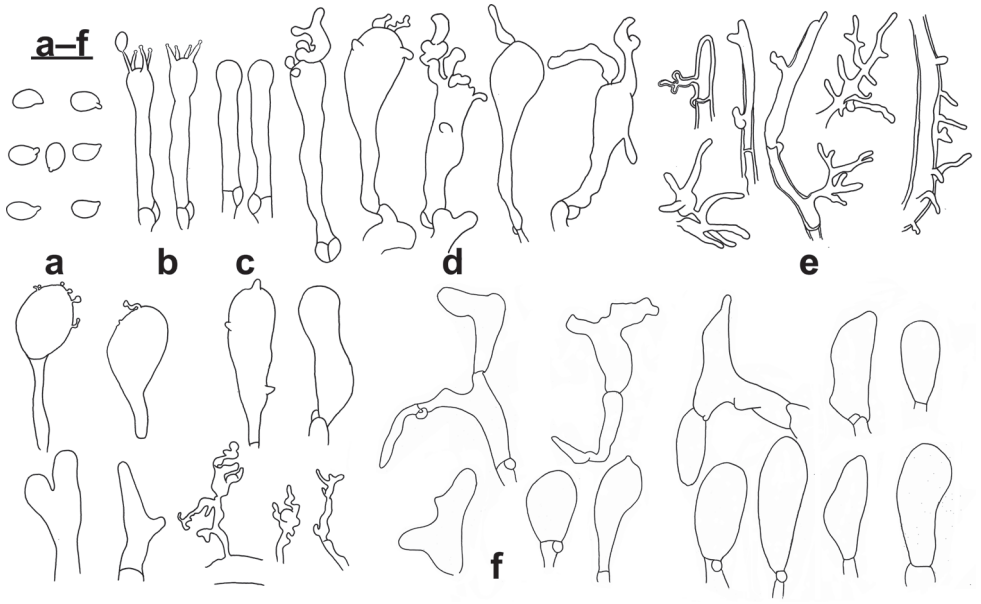

Figure 3. Microscopic features of *Gymnopus omphalinoides* (GDGM 78318, holotype!) **a** Basidiospores **b** Basidia **c** Basidioles **d** Cheilocystidia **e** Stipitipellis **f** terminal elements of the pileipellis. Drawing by J.P. Li. Sale bars: 10 μm (**a–d**), 20 μm (**e, f**).

Additional specimens examined. China, Guangdong Province, Guangzhou City, Tianluhu Forest Park, longitude and latitude not recorded, alt. not recorded, 4 April 2019, T.H. Li, W.Q. Deng, J.Y. Xu & J.P. Li (GDGM 44411); Guizhou Province, Tongren City, Fanjingshan National Nature Reserve, 27°48'33"N, 108°44'45"E, alt. 640 m, 14 July 2019, J.Z. Xu (HMJU 00506); Yunnan Province, Pu'er City, Meizihu Reservoir, 22°45'0"N, 100°58'48"E, alt. 1300 m, 19 September 2019, M. Zhang, T. Li & J.Y. Xu (GDGM 78483); Yunnan Province, Maguan County, Nanlao Village, 23°03'21"N, 104°31'12"E, alt. 1190 m, 5 August 2017, X.H. Wang (KUN-HKAS 107312).

Remarks. *Gymnopus omphalinoides* is a very distinct species due to its generally omphalinoid basidiomata, by a membranous and striate or grooved, reddish brown to brown pileus that becomes paler with age, by the broad, adnate, ventricose lamellae that are sometimes split to grooved at the edge, and by a pileipellis often with scattered cystidioid (clavate) or vesiculose to pyriform terminal elements. Collection GDGM 78318 is characterised by having cheilocystidia with more or less finger-like apical projection(s) and by a pileipellis with scattered *Rameales*-like structures, but the collection GDGM 44411 differs in its cheilocystidia with diverticulate elements and pileipellis with more *Rameales*-like structures.

Among the known species of *Gymnopus* with a striate or grooved pileus and ventricose lamellae, *G. bisporus* (J. Carbó & Pérez-De-Greg.) J. Carbó & Pérez-De-Greg., *G. dentatus* Murrill, *G. discipes* (Clem.) Murrill, *G. dysosmus* Polemis & Noordel., *G. fuscotramus* Mešić, Tkalčec & Chun Y. Deng, *G. pubipes* Antonín,

A. Ortega & Esteve-Rav. and *G. volkertii* are similar to the new species. However, *G. bisporus*, belonging to sect. *Levipedes*, has a brown to reddish brown pileus and larger basidiospores (9.0–11 × 4.5–5.5 μm), and true cheilocystidia are absent (Antonín and Noordeloos 2010); *G. dentatus* has a dentate pileus margin, a white stipe and larger basidiospores (7–8.5 × 6–7 μm), growing on lawns (Murrill 1916); *G. discipes* has free lamellae and a white stipe arising from a hypogaeous disk (Murrill 1916); *G. dysosmus*, sect. *Impudicae*, has garlic-smelling basidiomata, dark greyish brown lamellae, larger basidiospores (8.0–11 × 3.3–4.5 μm), and caulocystidia (Antonín and Noordeloos 2010); *G. fuscotramus*, belonging to sect. *Vestipedes* [= *Marasmiellus fuscotramus* (Mešić, Tkalčec & Chun Y. Deng) J.S. Oliveira], has abundant rhizomorphs, larger basidiospores (8.2–9.6 × 3.7–4.4), and pale grey-brown lamellar and pileus trama (Mešić et al. 2011); *G. pubipes*, sect. *Levipedes*, has deeply emarginate to adnexed lamellae and an entirely pubescent stipe with numerous caulocystidia (Antonín and Noordeloos 2010); and *G. volkertii* has a umbonate and estriate pileus, adnexed lamellae, and larger basidiospores (8.2–9.6 × 3.7–4.4 μm), growing on lawn (Murrill 1916).

***Gymnopus schizophyllus* J.P. Li, T.H. Li & Y. Li, sp. nov.**
MycoBank No: 837642
Figs 4, 5

Typification. China, Guangdong Province, Xinyi City, Yunkaishan National Nature Reserve, 22°17'08"N, 111°12'47"E, alt. 1453 m, 26 July 2019, B. Song, H.S. Wen & J.P. Li (GDGM 77165, holotype!).

Etymology. The epithet "*schizophyllus*" (Lat.) refers to the split edge of lamellae which is not so common in the genus.

Diagnosis. Differs from *G. omphalinoides* in its more or less depressed to slightly umbilicate pileus and more often split lamellar edge. Basidiomata mainly gregarious on decayed wood in broadleaf forest; pileus often pale orange to light brown; lamellae, adnate and generally split at the edge; stipe glabrous.

Description. Basidiomata gymnopoid or collybioid. Pileus 10–20 mm broad, membranous, hemispherical when young, then convex, with slightly inflexed margin, expanding to plano -convex , with a depressed disc, undulating at the margin, glabrous, radially striate or grooved towards the margin, often pale orange (6A3) to light brown (6D8), darker at the centre, sometimes to dark brown (6F8), white to light brown (6D8) towards the margin. Lamellae adnate, linear to arcuate, sometimes furcate to branched or venose, generally split at the edge, dull white to brownish orange (7C7), pale at the edge, sometimes with brown (7E8) to dark brown (7F8) tints somewhere, L = 10–20, l = 3–4. Stipe 11–21 mm long, 0.8–1 mm thick in middle, central, cylindrical, straight or sometimes curved, insititious, hollow, fibrous, glabrous, rooting deep in the substrate, but eventually attaches to the stump, white to orange-white (6A2) at first, slightly darker at base, then darker towards the apex, finally entirely light brown (7D8) to brown (7E8). Odour not distinctive.

Figure 4. Basidiomata of *Gymnopus schizophyllus* **a** GDGM 77038 **b** GDGM 76287 **c** GDGM 77165 holotype! **d** KUN-HKAS 96494 **a, c** photographed by J.P. Li **b** photographed by H.S. Wen **d** photographed by S.H. Li. For a detailed display, the split lamellar edge is magnified in a. Scale bar: 1 cm.

Basidiospores [n=80] 4–6 (–6.5) × 2.5–3 (–3.5) µm (average = 4.90 × 2.93 µm, E = (1.29–) 1.33–2.00 (–2.20), Q = 1.68) or [n=20] 6.5–8 × 2.5–3 µm (average = 7.35 × 2.86 µm, E = 2.17–3.2, Q = 2.65), obovoid, ellipsoid to subellipsoid, sometimes amygdaliform. Basidia [n=20] 15–32 × 4–6 µm, clavate, 4-spored, rarely 1–3-spored. Basidioles [n=20] 17–27.5 × 4–6.5 µm, clavate, cylindrical. Lamellar edge sterile. Cheilocystidia [n=20] 20–43 × 4.5–9 µm, irregularly clavate, tending to inflated, with finger-like apical projection(s) or more or less diverticulate elements. Pileipellis a cutis composed of thin-walled, cylindrical hyphae up to 18 µm wide, smooth or with scattered diverticula, hyaline to slightly greyish; *Rameales*-like structures present but very few; terminal elements short, broad, mostly inflated, vesiculose or pyriform to cystidioid (clavate), obtuse and sometimes diverticulate, mixed with a few irregularly branched elements, some resembling *Dryophila*-type structures. Stipitipellis a cutis composed of cylindrical hyphae, up to 19 µm wide, thin- to thick-walled, smooth, non-dextrinoid, diverticulate, parallelly arranged. Caulocystidia absent. Clamp connections present.

Ecology. Saprotrophic, gregarious or in small clusters, usually rooting around roots and stumps in broadleaf forests.

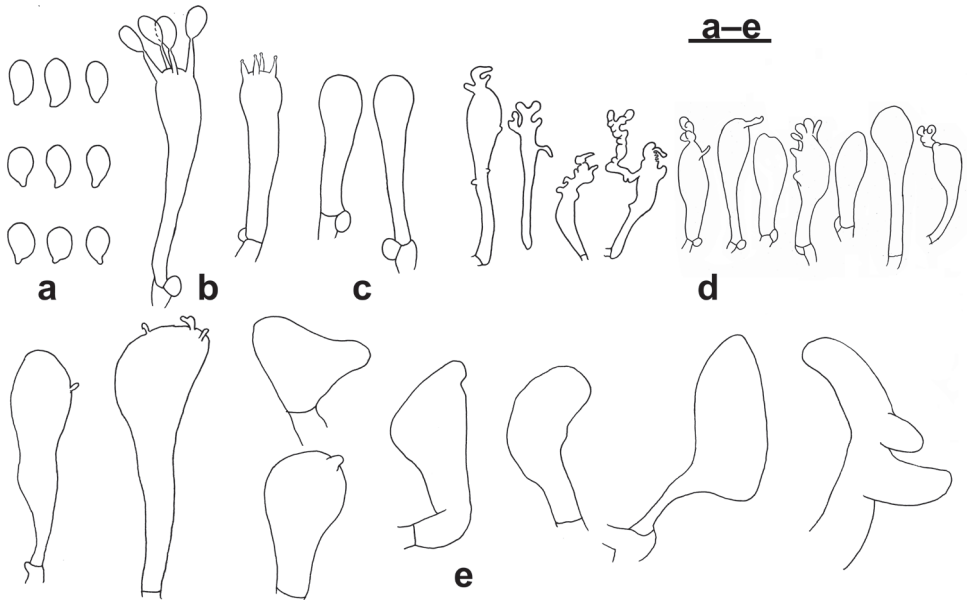

Figure 5. Microscopic features of *Gymnopus schizophyllus* (GDGM 77165, holotype!) **a** Basidiospores **b** Basidia **c** Basidioles **d** Cheilocystidia **e** terminal elements of the pileipellis. Drawing by J.P. Li. Scale bars: 10 μm (**a–c**), 20 μm (**d, e**).

Additional specimens examined. China, Guangdong Province, Xinyi City, Yunkaishan National Nature Reserve, 22°17'10"N, 111°12'50"E, alt. 1450 m, 26 July 2019, B. Song, H.S. Wen & J.P. Li (GDGM 77038); Guangdong Province, Xinyi City, Yunkaishan National Nature Reserve, 22°17'06"N, 111°12'51"E, alt. 1450 m, 29 May 2019, B. Song, H.S. Wen & J.P. Li (GDGM 76287); Yunnan Province, Maguan County, Laojunshan Moutain, 22°56'49"N, 104°32'44"E, alt. 1960 m, 11 August 2016, X.H. Wang (KUN-HKAS 96494).

Remarks. *Gymnopus schizophyllus* is a very distinct species by the orange to brown pileus that becomes paler with age; by the lamellae with generally split edge; by the two sizes of basidiospores: 1) 4–6 (–6.5) × 2.5–3 (–3.5) μm from the usual 4-spored basidia and 2) a few larger basidiospores up to 8 μm long from the 1–3-spored basidia; and by a pileipellis often with scattered cystidioid (clavate) or vesiculose to pyriform terminal elements.

Morphologically, among the known species of *Gymnopus* with a striate or grooved pileus and similarly sized basidiospores, *G. discipes*, *G. expallens* (Peck) Murrill, *G. fusipes* (Bull.) Gray, *G. micromphaloides* R.H. Petersen & K.W. Hughes, *G. oculatus* Murrill, *G. omphalinoides*, *G. pseudomphalodes* (Dennis) J.L. Mata, *G. purpureicollus* (Corner) A.W. Wilson, Desjardin & E. Horak, *G. sepiiconicus* (Corner) A.W. Wilson, Desjardin & E. Horak and *G. subflavescens* Murrill are similar to the new species. However, *G. discipes* has a subfleshy pileus with a wide umbo, free and ventricose lamellae and a white stipe (Murrill 1916); *G. expallens* has basidiomata with a distinct

odour, a hygrophanous pileus, adnexed and ventricose lamellae, and a broad stipe up to 4 mm (Murrill 1916); *G. fusipes* has a fleshy pileus and a fusoid stipe with pseudorrhiza (Antonín and Noordeloos 2010); *G. micromphaloides*, sect. *Vestipedes* [= *Collybiopsis micromphaloides* (R.H. Petersen & K.W. Hughes) R.H. Petersen], has adnexed and ventricose lamellae, a scurfy-vestured stipe, and strongly encrusted hyphae of the pileipellis (Petersen and Hughes 2014); *G. oculatus* has a white pileus in general, nearly free lamellae and a whitish pruinose, larger stipe (Murrill 1916); *G. omphalinoides* generally has a deeply umbilicate pileus, broad, adnate and ventricose lamellae; *G. pseudomphalodes* has a cream pileus and regularly cylindrical cheilocystidia (Dennis 1961); *G. purpureicollus* has a hygrophanous pileus, subfree to adnate lamellae with a decurrent tooth and a lamellar edge without cheilocystidia (Wilson et al. 2004); *G. sepiiconicus*, sect. *Levipedes*, has hyphae with annular incrustations in the stipitipellis (Wilson et al. 2004); and *G. subflavescens* has white basidiomata overall, crowded lamellae and small, globose basidiospores (Murrill 1916).

Discussion

According to the phylogenetic results, the two new species could be taken to represent a new section within *Gymnopus* s. s.tr., a new subsection of *Gymnopus* sect. *Gymnopus* or a new member of *G.* sect. *Gymnopus*. Suppose the two new species and samples from India represent a new section or subsection? In that case, the samples from New Zealand may occupy a taxonomic position at the same level due to their phylogenetic relationship. Thus, given the three alternative systematic interpretations for the two new species and the monophyletic group they form, we argue that the morphological features and evidence from the molecular data strongly support the two new species as members of *G.* sect. *Gymnopus*.

Morphologically, the taxonomic placement of *G. omphalinoides* and *G. schizophyllus* can be correlated with the pileipellis features, particularly its terminal cells. After comparison, the two new species with glabrous stipe and at least the part of *Dryophila*-like structures in pileipellis are easily confused with species within the *G.* sect. *Levipedes* (Fr.) Halling (Antonín and Noordeloos 2010). However, the new species have additional inflated and broad pileipellis terminal elements and are only distantly related to that section. *Gymnopus* sect. *Androsacei* and *G.* sect. *Gymnopus* are included in a strongly supported clade, indicating they are close. But *G.* sect. *Androsacei* has rhizomorphs, dextrinoid trama (at least in the stipe apex) and a pileipellis mixed with broom cells (Antonín and Noordeloos 2010). Furthermore, *G.* sect. *Androsacei* does not form a distinct monophyletic clade neither in this study nor in Oliveira et al. (2019), César et al. (2020), and so forth. This issue needs to be addressed in future studies. Currently, known species with molecular data are very few, which perhaps could explain this topologic structure. Additionally, a phylogenetic tree based on more genetic markers might provide an improved result. Besides, *G.* sect. *Impudicae* is characterised by basidiomata with distinctive odour and often inconspicuous cheilocystidia (Antonín

and Noordeloos 2010). These divergent morphological features reflect the non-trivial phylogenetic distance from the two new species. Unexpectedly, the two new species have a membranous pileus and non-fusoid stipe devoid of pseudorrhiza, contrary to the traditional circumscription of *G.* sect. *Gymnopus* in macro-morphology. However, the molecular phylogenetic results reveal that the clade they form is the most closely related group to *G.* sect. *Gymnopus* except for the two samples from New Zealand. After examining the micromorphological structures intensively, the synapomorphy eventually came to the surface. Cheilocystidia of both newly described species are versiform diverticulated cells and generally agree in size and shape with those of *G. fusipes* (Fig. 6). Also, the pileipellis, composed of inflated elements with some resembling *Dryophila*-type structures, is similar to *G. fusipes* and follows the key rule for sectional delimitation in *Gymnopus* s. str. [for a detailed macro- and micromorphological description of *G. fusipes* see Antonín and Noordeloos (1997, 2010)]. Besides, the two new species lack a typical *Rameales*-type pileipellis and any well-developed caulocystidia, in contrast to *G.* sect. *Vestipedes* which is already a part of *Collybiopsis* (Antonín and Noordeloos 2010; Oliveira et al. 2019; Petersen and Hughes 2021). Furthermore, the original *G.* sect. *Perforantia* is currently considered a distinct genus – *Paragymnopus* – whose members usually have non-glabrous stipe and lack cheilocystidia (Petersen and Hughes 2016; Oliveira et al. 2019).

As the characteristic of the pileipellis is a significant factor for sectional delimitation in *Gymnopus*, the features in macro-morphology are second. The current sectional concept was summarised based on features from one species, *G. fusipes*. That means the single known species circumscribes the current knowledge at the sectional level. This is also why only minor divergence in micro-morphology occurs between *G.* sect. *Gymnopus* and the two new species. Following the indication from phylogenetic results and similarity of micro-morphology, thus, an emended and improved concept of *G.* sect. *Gymnopus* is proposed herein by including *G. omphalinoides* and *G. schizophyllus*.

A very interesting and unusual characteristic is a splitting lamellar edge in both newly described species. What advantage such split lamellar edge could confer is difficult to surmise, but Antonín and Herink (1999) described the same characteristic in *Gymnopus luxurians* (Peck) Murrill [recently *Collybiopsis luxurians* (Peck) R.H. Petersen]. They proposed that this may be a reaction to specific climatic conditions (the higher humidity, the better hymenium development) because it was most distinct in the collections from greenhouses, botanic gardens and tropical Africa.

Borthakur and Joshi (2016) provided a nrITS sequence and a few morphological characteristics of the collection NEHU MBSRJ48 annotated as *Micromphale foetidum* which comes from a subtropical forest of Northeast India, quite similar to *G. schizophyllus*. However, the sequence is quite different from the sequences more well-recognised for the current *Gymnopus foetidus* (Sowerby) P.M. Kirk. It likely represents an incorrectly determined ITS sequence in GenBank like several others as argued by Nilsson et al. (2006) and Hofstetter et al. (2019). The specimen has a depressed to umbilicate pileus, a glabrous stipe and similarly sized basidiospores (5.2 × 2.88 μm). The nrITS sequence is highly similar to that of *G. schizophyllus*, implying they are possibly conspecific. The collection from India clearly belongs in *G.* sect.

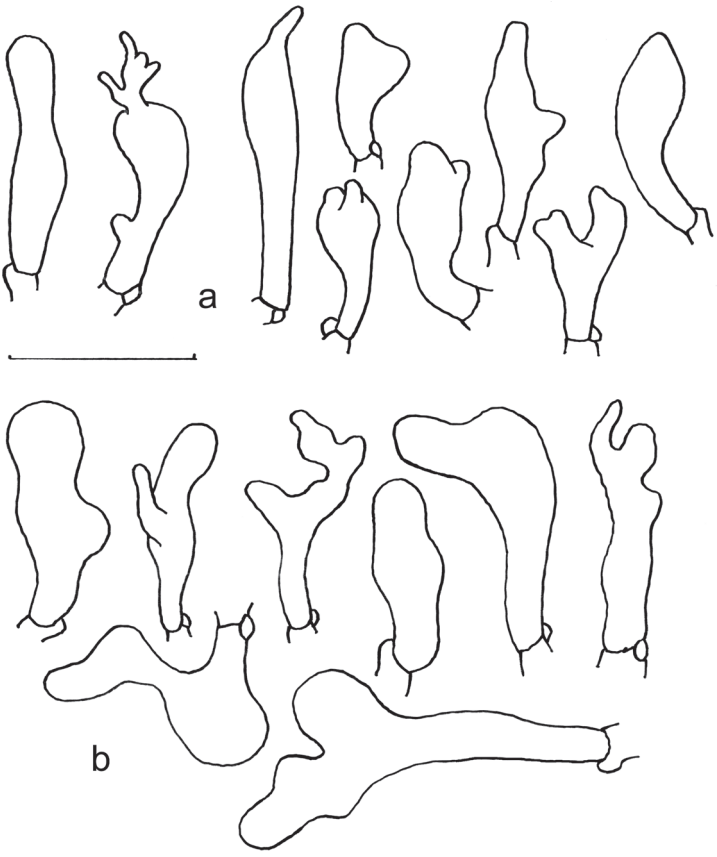

Figure 6. *Gymnopus fusipes* (Mokrá near Brno, place called Nad dlouhým (Sivický les forest), 18 June 2002, A. Vágner, BRNM 670783) **a** Cheilocystidia **b** Pileipellis terminal cells. Drawings by V. Antonín. Scale bar: 20 μm.

Gymnopus. The collections from New Zealand, named as *Marasmius otagensis*, are characterised by a depressed to umbilicate pileus, glabrous stipe and a pileipellis with broad, mostly inflated terminal elements (according to photos from Dr. Jerry Cooper). The phylogenetic placement indicates that this is another member of *G.* sect. *Gymnopus*.

***Gymnopus* sect. *Gymnopus*, emend.**

Emended circumscription. Pileus membranous or fleshy; stipe smooth or slightly to deeply sulcate-striate, with a well-developed or reduced pseudorrhiza; spore print white to pale ochraceous; cheilocystidia versiform, clavate, fusoid, tending inflated, sometimes with more or less finger-like apical projection(s), or diverticulate elements; pileipellis a cutis, or this transitioning to a trichoderm, with broad terminal elements, mostly inflated, mixed with irregularly branched elements and some resembling

Dryophila-type structures; no dextrinoid or cyanophilous structures; rooting in the substrate, frequently on roots or stumps.

Type species. *Gymnopus fusipes* (Bull.) Gray

Other currently recognised species. *G. omphalinoides* J.P. Li, T.H. Li & Y. Li, *G. schizophyllus* J.P. Li, T.H. Li & Y. Li

A key to species of *Gymnopus* sect. *Gymnopus*

1 Pileus fleshy; stipe with a distinct pseudorrhiza ..... ***G. fusipes***

– Pileus membranous; stipe without a pseudorrhiza but rooting in the substrate **2**

2 Pileus generally deeply umbilicate; lamellae broad, adnate and ventricose ..... ***G. omphalinoides***

– Pileus more or less depressed; lamellae adnate, linear to arcuate ..... ***G. schizophyllus***

Acknowledgements

Grateful thanks are due to Prof. Xiang-Hua Wang (Kunming Institute of Botany, CAS, Kunming, China) for providing specimen(s), sequences, suggestions and photographs, Dr Jerry Adrian Cooper (Landcare Research, New Zealand) for providing sequences and photographs, Dr Rolf Henrik Nilsson (University of Gothenburg, Gothenburg, Sweden) for improving our work, Dr Ji-Ze Xu (Jilin Agricultural Science and Technology University, Jilin, China) for providing specimens and sequence data, Dr Md Iqbal Hosen, Prof. Wang-Qiu Deng, Dr Chao-Qun Wang (Guangdong Institute of Microbiology, Guangzhou, China) and Xiao-Ya An (Shenyang Agricultural University, Shenyang, China) for providing suggestions, Dr Ming Zhang, Mr. Ting Li, Mr. Juan-Yan Xu, Mr. Hao Huang, Mr. Li-Qiang Wu, Mr. Ning Zhan, Mr. Hua-Shu Wen (Guangdong Institute of Microbiology, Guangzhou, China), Prof. Shu-Hong Li (Yunnan Academy of Agricultural Sciences, Kunming, China) for hunting collection(s). This work was supported by the National Natural Science Foundation of China (Nos. 31750001, 31970016), the Science and Technology Planning Project of Guangdong Province, China (2019B121202005, 2018B030320001, 20070617627078), the government procurement project of Shenzhen, China (SZCG2019191412), China Agriculture Research System (CARS-20), the government procurement project of China (ZX2021-FJC083), Projects of Science and Technology Programs of Guizhou Province ([2019]2451, [2019]4007-2), GDAS' Special Project of Science and Technology Development (Grant No. 2019GDASYL-0104011), and the Project of Comprehensive Scientific Investigation of Dalingshan Forest Park in Dongguan (441901-2021-08594). The studies of V.A. were made possible by the support provided to the Moravian Museum by the Ministry of Culture of the Czech Republic as part of its long-term conceptual development program for research institutions (DKRVO, ref. MK000094862).

References

Antonín V, Finy P, Tomšovský M (2012) Taxonomy of the *Gymnopus inusitatus* group and the new *G. inusitatus* var. *cystidiatus* from Hungary. Mycotaxon 119: 291–299. https://doi.org/10.5248/119.291

Antonín V, Halling RE, Noordeloos ME (1997) Generic concepts within the groups of *Marasmius* and *Collybia sensu lato*. Mycotaxon 63: 359–368.

Antonín V, Herink J (1999) Notes on the variability of *Gymnopus luxurians* (Tricholomataceae). Czech Mycology 52: 41–49. https://doi.org/10.33585/cmy.52103

Antonín V, Noordeloos ME (1997) A monograph of *Marasmius*, *Collybia* and related genera in Europe. Part 2: *Collybia*, *Gymnopus*, *Rhodocollybia*, *Crinipellus*, *Chaetocalathus* and additions to *Marasmiellus*. Libri Botanici 17: 1–256.

Antonín V, Noordeloos ME (2010) A monograph of marasmioid and collybioid fungi in Europe. IHW Verlag, Eching, 478 pp.

Antonín V, Ryoo R, Ka KH (2014) Marasmioid and gymnopoid fungi of the Republic of Korea. 7. *Gymnopus* sect. *Androsacei*. Mycological Progress 13: 703–718. https://doi.org/10.1007/s11557-013-0953-z

Borthakur M, Joshi SR (2016) Micrographical analysis of growth deformities in common pathogens induced by voucher fungi from India. Journal of Microscopy and Ultrastructure 4: 203–210. https://doi.org/10.1016/j.jmau.2016.04.001

César E, Montoya L, Bandala VM, Ramos A (2020) Three new marasmioid-gymnopoid rhizomorph-forming species from Mexican mountain cloud forest relicts. Mycological Progress 19: 1017–1029. https://doi.org/10.1007/s11557-020-01608-1

Clémençon H (1981) Compendium of gill fungi. I. *Collybia*. Zeitschrift für Mykologie 47(1): 5–25.

Coimbra VRM, Pinheiro FGB, Wartchow F, Gibertoni TB (2015) Studies on *Gymnopus* sect. *Impudicae* (Omphalotaceae, Agaricales) from Northern Brazil: two new species and notes on *G. montagnei*. Mycological Progress 14: e110. https://doi.org/10.1007/s11557-015-1131-2

Cubeta MA, Echandi E, Abernethy T, Vilgalys R (1991) Characterization of anastomosis groups of binucleate *Rhizoctonia* species using restriction analysis of an amplified ribosomal RNA gene. Phytopathology 81: 1395–1400. https://doi.org/10.1094/Phyto-81-1395

Dennis RWG (1961) Fungi venezuelani: IV. Kew Bulletin 15(1): 67–156. https://doi.org/10.2307/4115784

Desjardin DE, Perry BA (2017) The gymnopoid fungi (Basidiomycota, Agaricales) from the Republic of São Tomé and Príncipe, West Africa. Mycosphere 8(9): 1317–1391. https://doi.org/10.5943/mycosphere/8/9/5

Hall T (2011) BioEdit: an important software for molecular biology. GERF Bulletin of Biosciences 2(1): 60–61.

Hofstetter V, Buyck B, Eyssartier G, Schnee S, Gindro K (2019) The unbearable lightness of sequenced-based identification. Fungal Diversity 96(1): 243–284. https://doi.org/10.1007/s13225-019-00428-3

Huang H (1998) Study on the hydrologic effect of the forest ecological system in Guangdong Xinyi county. Journal of Guangxi Teachers College (Natrual Science Edition) 15(02): 9–15. [in Chinese] https://doi.org/10.16601/j.cnki.issn1001-8743.1998.02.002

Huang JB, Li JL (2006) Phytocoenology of natural *Etythrophloeum fordii* forest in Tianluhu Forest Park. Forestry Construction 01: 15–18. [in Chinese]

Kalyaanamoorthy S, Minh BQ, Wong TKF, von Haeseler A, Jermiin LS (2017) ModelFinder: fast model selection for accurate phylogenetic estimates. Nature Methods 14: 587–589. https://doi.org/10.1038/nmeth.4285

Katoh K, Standley DM (2013) MAFFT Multiple sequence alignment software version 7: Improvements in performance and usability. Molecular Biology and Evolution 30(4): 772–780. https://doi.org/10.1093/molbev/mst010

Klonowska A, Gaudin C, Ruzzi M, Colao MC, Tron T (2003) Ribosomal DNA sequence analysis shows that the basidiomycete C30 belongs to the genus *Trametes*. Research in Microbiology 154(1): 25–28. https://doi.org/10.1016/S0923-2508(02)00005-0

Kong B, Cao HL, Ma L, Wu LF, Chen C, Huang ZL (2013) Community characteristics of the Fengshui-wood of Erythrophleum Fordii in Guangzhou. Tropical Geography 33(03): 307–313, 332. [in Chinese] https://doi.org/10.6023/cjoc201208035

Kornerup A, Wanscher JH (1978) Methuen handbook of colour. 3th edn., London: Methuen, 243pp.

Li JP, Li Y, Li TH, Antonín V, Hosen MI, Song B, Xie ML, Feng Z (2021a) A preliminary report of *Gymnopus* sect. *Impudicae* (Omphalotaceae) from China. Phytotaxa 497(3): 263–276. https://doi.org/10.11646/phytotaxa.497.3.5

Li JP, Song B, Feng Z, Wang J, Deng CY, Yang YH (2021b) A new species of *Gymnopus* sect. *Androsacei* (Omphalotaceae, Agaricales) from China. Phytotaxa 52(1). https://doi.org/10.11646/phytotaxa.521.1.1

Mata JL, Hughes KW, Petersen RH (2004) Phylogenetic placement of *Marasmiellus juniperinus*. Mycoscience 45: 214–221. https://doi.org/10.1007/S10267-004-0170-3

Mata JL, Hughes KW, Petersen RH (2007) An investigation of Omphalotaceae (Fungi: Euagarics) with emphasis on the genus *Gymnopus*. Sydowia 58: 191–289.

Matheny PB, Curtis JM, Hofstetter V, Aime MC, Moncalvo JM, Ge ZW, Yang ZL, Slot JC, Ammirati JF, Baroni TJ, Bougher NL, Hughes KW, Lodge DJ, Kerrigan RW, Seidl MT, Aanen DK, DeNitis M, Daniele GM, Desjardin DE, Kropp BR, Norvell LL, Parker A, Vellinga EC, Vilgalys R, Hibbett DS (2006) Major clades of Agaricales: a multilocus phylogenetic overview. Mycologia 98: 982–995. https://doi.org/10.3852/mycologia.98.6.982

Mešić A, Tkalčec Z, Deng CY, Li TH, Pleše B, Ćetković H (2011) *Gymnopus fuscotramus* (Agaricales), a new species from southern China. Mycotaxon 117: 321–330. http://dx.doi.org/10.5248/117.321

Murrill WA (1916) North American Flora. Volume 9. The New York Botanical Garden, New York, 542 pp.

Nilsson RH, Ryberg M, Kristiansson E, Abarenkov K, Larsson K-H, Kõljalg U (2006) Taxonomic reliability of DNA sequences in public sequence databases: a fungal perspective. PLoS ONE 1(1): e59. https://doi.org/10.1371/journal.pone.0000059

Nilsson R, Tedersoo L, Abarenkov K, Ryberg M, Kristiansson E, Hartmann M, Schoch C, Nylander J, Bergsten J, Porter T, Jumpponen A, Vaishampayan P, Ovaskainen O, Hallenberg N, Bengtsson-Palme J, Eriksson K, Larsson K, Larsson E, Kõljalg U (2012)

Five simple guidelines for establishing basic authenticity and reliability of newly generated fungal ITS sequences. MycoKeys 4: 37–63. https://doi.org/10.3897/mycokeys.4.3606

Noordeloos ME, Antonín V (2008) Contribution to a monograph of marasmioid and collybioid fungi in Europe. Czech Mycology 60: 21–27. https://doi.org/10.33585/cmy.60103

Oliveira JJS, Vargas-Isla R, Cabral TS, Rodrigues DP, Ishikawa NK (2019) Progress on the phylogeny of the Omphalotaceae: *Gymnopus* s. str., *Marasmiellus* s. str., *Paragymnopus* gen. nov. and *Pusillomyces* gen. nov. Mycological Progress 18: 713–739. https://doi.org/10.1007/s11557-019-01483-5

Petersen RH, Hughes KW (2014) New North American species of *Gymnopus*. North American Fungi 9(3): 12–22. https://doi.org/10.2509/naf2014.009.003

Petersen RH, Hughes KW (2016) *Micromphale* sect. *Perforantia* (Agaricales, Basidiomycetes); expansion and phylogenetic placement. MycoKeys 18: 1–122. https://doi.org/10.3897/mycokeys.18.10007

Petersen RH, Hughes KW (2017) An investigation on *Mycetinis* (Euagarics, Basidiomycota). MycoKeys 24: 1–138. https://doi.org/10.3897/mycokeys.24.12846

Petersen RH, Hughes KW (2019) Two additional species of *Gymnopus* (Euagarics, Basidiomycotina). MycoKeys 45: 1–24. https://doi.org/10.3897/mycokeys.45.29350

Petersen RH, Hughes KW (2021) *Collybiopsis* and its type species, *Co. ramealis*. Mycotaxon 136(2): 263–349. https://doi.org/10.5248/136.263

Rambaut A (2009) FigTree 1.2.2. http://tree.bio.ed.ac.uk/software/figtree/

Rambaut A, Drummond AJ, Xie D, Baele G, Suchard MA (2018) Posterior summarization in Bayesian phylogenetics using Tracer 1.7. Systematic Biology 67(5): 901–904. https://doi.org/10.1093/sysbio/syy032

Ronquist F, Teslenko M, van der Mark P, Ayres DL, Darling A, Höhna S, Larget B, Liu L, Suchard MA, Huelsenbeck JP (2012) MrBayes 3.2: efficient Bayesian phylogenetic inference and model choice across a large model space. Systematic Biology 61: 539–542. https://doi.org/10.1093/sysbio/sys029

Ryoo R, Antonín V, Ka KH, Tomšovský M (2016) Marasmioid and gymnopoid fungi of the Republic of Korea. 8. *Gymnopus* section *Impudicae*. Phytotaxa 286(2): 75–88. https://doi.org/10.11646/phytotaxa.286.2.2

Ryoo R, Antonín V, Ka KH (2020) Marasmioid and gymnopoid fungi of the Republic of Korea. 8. *Gymnopus* Section *Levipedes*. Mycobiology 48(4): 252–262. https://doi.org/10.1080/12298093.2020.1769541

Sayers EW, Cavanaugh M, Clark K, Pruitt KD, Schoch CL, Sherry ST, Karsch-Mizrachi I (2021) GenBank. Nucleic Acids Research 49(D1): D92–D96. https://doi.org/10.1093/nar/gkaa1023

Singer R (1986) The Agaricales in Modern Taxonomy (4th edn.). Koeltz Scientific Books, Koenigstein, 981 pp.

Smith AH (1944) Interesting North American agarics. Bulletin of the Torrey Botanical Club 71(4): 390–409. https://doi.org/10.2307/2481312

Stamatakis A (2014) RAxML version 8: a tool for phylogenetic analysis and post-analysis of large phylogenies. Bioinformatics 30(9): 1312–1313. https://doi.org/10.1093/bioinformatics/btu033

Tao C (2002) Study of the Community characteristics of forest vegetations in Meizi Lake Scenic Spot of Simao Region,Yunnan Province. Master Thesis, Southwest University, Chongqing, China. [in Chinese]

Tao C (2006) Study of the species diversity of forest in Meizi lake scenic spot. Journal of Yunnan Normal University 26(5): 57–60. [in Chinese]

Thiers B (2021 [continuously updated]) Index Herbariorum. A global directory of public herbaria and associated staff. New York Botanical Garden's Virtual Herbarium. http://sweetgum.nybg.org/science/ih

Vilgalys R, Hester M (1990) Rapid genetic identification and mapping of enzymatically amplified ribosomal DNA from several *Cryptococcus* species. Journal of Bacteriology 172: 4238–4246. https://doi.org/10.1128/jb.172.8.4238-4246.1990

Vu D, Groenewald M, de Vries M, Gehrmann T, Stielow B, Eberhardt U, Al-Hatmi A, Groenewald JZ, Cardinali G, Houbraken J, Boekhout T, Crous PW, Robert V, Verkley GJM (2019) Large-scale generation and analysis of filamentous fungal DNA barcodes boosts coverage for kingdom fungi and reveals thresholds for fungal species and higher taxon delimitation. Studies in Mycology 92: 135–154. https://doi.org/10.1016/j.simyco.2018.05.001

White TJ, Bruns T, Lee S, Taylor J (1990) Amplification and direct sequencing of fungal ribosomal RNA genes for phylogenetics. In: Innis MA, Gelfand DH, Sninsky JJ, White TJ (Eds) PCR Protocols: A Guide to Methods and Applications. Academic Press, New York, 315–322. https://doi.org/10.1016/B978-0-12-372180-8.50042-1

Wilson AW, Desjardin DE (2005) Phylogenetic relationships in the gymnopoid and marasmioid fungi (Basidiomycetes. Euagarics clade). Mycologia 97: 667–679. https://doi.org/10.3852/mycologia.97.3.667

Wilson AW, Desjardin DE, Horak E (2004) Agaricales of Indonesia. 5. The genus *Gymnopus* from Java and Bali. Sydowia 56(1): 137–210.

Xiao ZF, Sommar J, Lindqvist O, Tan H, He JL (1998) Atmospheric mercury deposition on Fanjing Mountain Nature Reserve, Guizhou, China. Chemosphere 36(10): 2191–2200. https://doi.org/10.1016/S0045-6535(97)10191-6

Xv JX, Feng ZJ, Wang DY, Liu YJ, Xiao H, Xv SS (2009) Investigation on Vegetation Types of Wutongshan Provincial Scenic Spot in Shenzhen. Journal of Fujian Forestry Science and Technology 36(02): 154–161. [in Chinese]

Zhang MK, Mao XL, Qiu ZT, Yang LY (2018) Genetic Characteristics and Taxonomic Classification of Vertical Soils in the Fanjingshan Mountain. Chinese Journal of Soil Science 49(4): 757–766. [in Chinese] https://doi.org/10.19336/j.cnki.trtb.2018.04.01

Zhao SX (2007) Evaluation of Forest Resources Status and Thinking of Forestry Development in Maguan County. Inner Mongolia Forestry Investigation and Design 30(01): 34–37. [in Chinese]

Zhong YP, Shu GY, Yan LH (2011) Analysis of Fanjingshan Mountain's influence on local climate. Journal Of Guizhou Meteorology 35(6): 25–28. [in Chinese]

Zhou WJ, Shi ZY, Wang W (2011) Temporal and spatial patterns of soil respiration in subtropical forests of eastern China. Chinese Journal of Plant Ecology 35(7): 731–740. [in Chinese] https://doi.org/10.3724/SP.J.1258.2011.00731